Glutathione conjugation of herbicides and fungicides in plants and fungi:: functional characterization of glutathione transferases from phytopathogens

David Bryant

Glutathione conjugation of herbicides and fungicides in plants and fungi; functional characterization of glutathione transferases from phytopathogens.

Thesis submitted for the degree of
Doctor of Philosophy
at the University of Durham

by

David Bryant BSc hons (Plymouth)
Department of Biological & Biomedical Sciences
University of Durham

September 2004

Abstract

The aim of this research was to determine the relative importance of glutathione *S*-transferase (GST) mediated herbicide and fungicide detoxification in wheat plants and to functionally characterise GSTs cloned from phytopathogenic fungi. Wheat seedlings treated with and without safeners were used for *in vivo* and *in vitro* pesticide metabolism studies with the herbicide fenoxaprop-P-ethyl and the fungicide fluquinconazole, which are both known to undergo glutathione conjugation. Fenoxaprop-P-ethyl underwent rapid detoxification by this route and the rates of metabolism were enhanced in safener treated wheat. In contrast, fluquinconazole was poorly metabolised with only a small proportion detoxified by glutathionylation irrespective of whether or not the plants were safener treated. Subsequent studies confirmed that whereas fenoxaprop was a substrate for wheat GSTs, fluquinconazole was not. Similarly, when a diverse range of systemic and contact fungicides was tested, none were found to undergo conjugation mediated by wheat GSTs, even though several compounds underwent conjugation with glutathione in alkaline conditions. Metabolite profiling by HPLC-MS established that the alternative thiol present in wheat, hydroxymethyl glutathione, was used in addition to glutathione in fenoxaprop detoxification. The *S*-conjugates were then further metabolised by peptidases and glucosyl- and malonyl transferases to yield polar derivatives such as the cysteinyl-malonyl-glucosyl derivative. This rapid processing was in contrast to that determined in herbicide-susceptible and herbicide-resistant black-grass, where the glutathione derivative was the major metabolite of fenoxaprop.

Using an informatics approach, GSTs in *Magnaporthe griseae* and *Phytophthora infestans* were identified cloned and then expressed in *E. coli*, with the pure enzymes assayed for glutathione-dependent activities. *Mg*GSTX1 of

Magnaporthe griseae was found to be a member of a novel class of GSTs (termed xi class) and was shown to function as a thioltransferase, with a specific activity of 50.4 ± 3.4 nKat mg^{-1} protein. Unusually, the catalytic mechanism of thiol transfer was insensitive to the alkylating agent iodoacetamide, indicating that free cysteines were not involved in catalysis. *Mg*GSTX1 did not conjugate any of the experimental xenobiotics tested with GSH.

The theta class GST *Pi*GSTT1 cloned from *P. infestans* exhibited glutathione peroxidase activity and readily detoxified fungitoxic oxylipins produced by potato as antimicrobial defence by potato through the action of lipoxygenases. Using anti-sera raised against the purified recombinant protein, immunoblotting experiments revealed expression of *Pi*GSTT1 in the *in vitro* cultured fungus as well as during colonisation of potato. *Pi*GSTT1 did not demonstrate GSH conjugating toward any of the xenobiotic substrates tested including herbicides and fungicides. Based on the sequences of GSTs identified in this study an extension of the existing classification system is suggested to include the GSTs of fungal phytopathogens

Declaration & Statements

This work has not been previously submitted for any degree and is not being concurrently submitted for any other degree.

Acknowledgments

I would like to extend my thanks and appreciation to Professor Robert Edwards for accepting me as his student, making this work possible and for his valuable guidance, support and encouragement throughout and beyond the research of this Ph.D. I would also like to thank Dr Ian Cummins for helping me find my feet and for advising and patiently teaching me the lab based skills necessary for the completion of this thesis. The help and advice of Dr David Dixon and Dr Mark Skipsey on many molecular biology matters was also greatly appreciated.

I would like to thank Dr Ron Croy for raising the antisera used in this project and the advice and mass spectrometry training given by Dr Mike Jones was a great contribution to many aspects of this work. My thanks also go to Dr Elizabeth O'Neill of Bayer Crop Science, Lyon, France for all her help during my visit. For funding this project, thanks are extended to the BBSRC and Bayer Crop Science.

To all my family and friends, thank you for all the support and love you have shown me throughout my life. I love you all and know I could not have done it without you. To my wife Kez, cariad fy mywyd, thanks for all your love and support and for having to live with a cross between Dr Jekyll, Mr. Hyde and Zebedee over the first few months of our married life.

Abbreviations

13- (*S*)HPOT	(9*Z*,11*E*,15*Z*)-13-hydro(pero)xy-9,11,15-octadecatrienoic acid
5-(*S*)HPTE	5-hydroperoxyeicosatetraenoic
9,16-(*S*)diHPOT	(10*E*,12*Z*,14*E*)-9,16-dihydro(pero)xy-10,12,14-octadecatrienoic acid
16-(*S*)HPOT	(10*E*,12*Z*,14*E*)-9-hydroxy,16-hydro(pero)xy-10,12,14-octadecatrienoic acid
9-(*S*)HPOT	(10*E*,12*Z*)-9-hydro(pero)xy-10,12-octadecatrienoic acid
9-(*S*)HOT	(10*E*,12*Z*,15*Z*)-9-hydroxy-10,12,15-octadecatrienoic acid
ABC	ATP binding cassette
AEC	anion exchange chromatography
AMV	avian myeloblastosis virus
ARE	antioxidant responsive element
AS	antisense
ASLOX	antisense lipoxygenase
ATP	adenosine triphosphate
bp	base pairs
CA	colneleic acid (8*E*,1'*E*,3'*Z*,6'*Z*)-9-(1',3',6'-nonadienoxy)-8-nonenoic acid
CDNB	1-chloro-2,4-dinitrobenzene
CnA	colnelenic acid (8*E*,1'*E*,3'*Z*,6'*Z*)-9-(1',3',6'-nonatrienoxy)-8-nonenoic acid
Da	Daltons
DCOFs	dicarboscimide fungicides
DDT	1,1,1-trichloro-2,2-bis-(4'-chlorophenyl)ethane

DEPC	diethyl pyrocarbonate
DES	divinyl ether synthase
DES	divinyl ether synthase
DNA	deoxyribonucleic acid
dNTP	any deoxynucleoside (5'-)triphosphate
DTT	1,4-dithio-DL-threitol
EDTA	ethylenediaminetetraacetic acid
ESI-TOF-MS	electrospray ionisation time of flight mass spectrometry
Cb-cys	fenoxaprop-cysteinyl conjugate
Cb-cys-glc	fenoxaprop-csyteinyl-glucosyl conjugate
Cb-cys-glc-mal	fenoxaprop-csyteinyl-glucosyl-malonyl conjugate
Cb-cys-glu	fenoxaprop-csyteinyl-γ-glutamyl conjugate
Cb-GSH	fenoxaprop-glutathione conjugate
Cb-HmGSH	fenoxaprop-hydroxymethyl glutathione conjugate
GPOX	glutathione peroxidase
GSH	glutathione
GSNO	*S*-nitrosoglutathione
GSSG	oxidised glutathione
GST	glutathione *S*-transferase (E.C 2.5.1.18)
hGSH	homoglutathione
HIC	hydrophobic interaction chromatography
HmGSH	hydroxymethyl glutathione
HPLC	high performance liquid chromatography
HPLS	hydroperoxide lyase
IPTG	isopropyl-beta-D-thiogalactopyranoside

kbp	kilobase pairs
KP	potassium phosphate
LB	(Luria-Bertani medium)
LBA	(Luria-Bertani medium Agar)
LC-MS	liquid chromatography mass spectrometry
LN_2	liquid nitrogen
LOX	lipoxygenase (E.C. 1.13.11.12)
MES	2-Morpholinoethanesulphonic acid
mRNA	messenger ribonucleic acid
MW	molecular weight
N_2	nitrogen
NADPH	nicotinamide adenine dinucleotide phosphate
o-DNB	*o*-dinitrobenzene
PAGE	polyacrylamide gel electrophoreisis
PAU	peak area units
PCR	polymerase chain reaction
PDA	potato dextrose agar
PDB	potato dextrose broth
PMSF	phenylmethylsulphonyl fluoride
POX	peroxygenase
PUFA	polyunsaturated fatty acid
RACE	rapid amplification of cDNA ends
RNA	ribonucleic acid
RNAsin	RNAse inhibitor
$sddH_2O$	sterile double distilled water

sdH_2O	sterile distilled water
SDS	sodium dodecyl sulphate
TBS	tris buffered saline
TBST	tris buffered saline triton-X 100
Ttase	thiol transferase
UTR	untranslated region
XRE	xenobiotic responsive element

Table of contents

Chapter 1 Introduction.

1.1 Routes of pesticide detoxification; an overview

Organisms in the terrestrial environment are subject to ecological challenges, which may be the consequence of anthropogenic activities or abiotic and biotic insults. Stresses arising from anthropogenic activities include atmospheric pollution, heavy metal exposure from mining and sewage disposal and pesticide application from intensive farming practices. For example in Europe, plants are exposed to >3000 commercial compounds to improve crop productivity, 900 of which are pesticide products including herbicides, insecticides and fungicides (Hall *et al.*, 2001; Coleman *et al.*, 1997).

Substances that are foreign to biological systems and interact with the metabolism of organisms are termed xenobiotics (Smith, 2000). Of particular interest, in the area of crop protection, has been the metabolism of pesticides in plants, which has proved to be a major determinant of their activity in crop protection. In this respect, glutathione *S*-transferases (GSTs) are an important group of detoxifying enzymes, which catalyse the conjugation of hydrophobic compounds with the ubiquitous tripeptide glutathione (γ-Glu-Cys-Gly), thereby increasing their solubility. Conjugation, as defined by Hall *et al.*, (2001), is a metabolic process whereby an exogenous or endogenous natural compound is joined to a pesticide or its metabolite(s) facilitating compartmentalisation, sequestration, detoxification, and/or mineralization. Whereas GSTs have a well-known role in detoxifying herbicides (Edwards *et al.*, 2001; Cole & Edwards, 2000 Edwards 1996; Reichers *et al.*, 1996; Reade & Cobb, 1999; Hatton *et al.*, 1998; Cummins *et al.*, 1997; Hatton *et al.*, 1996; Hatton *et al.*, 1999; Edwards & Cole, 1996; Neunfeind *et al.*, 1997; Thom *et al.*, 2002), little is known with respect to their role in fungicide metabolism in crop plants.

Similarly the GSTs of crops and phytopathogenic fungi, which infect major crops have received little attention with respect to their roles in detoxifying fungicides.

1.2 Plant Metabolism of Xenobiotics

The physico-chemical properties of xenobiotics such as herbicides, which are highly lipophilic with typical octanol:water partioning coefficients $K_{ow} \approx 1 - 10^3$ and molecular mass <500 D, allows for their ready uptake by plants via penetration across the cuticle and access to the symplast (Kreuz *et al.*, 1996). Once entry to the cell has been gained, the xenobiotic may then exert its biological effect. In order to ameliorate toxicity, cellular detoxification occurs by chemical modification (transformation) of the compound, followed by sequestration and vacuolar compartmentalisation of metabolites (Coleman *et al.*, 1997).

Typically the overall process involves three phases of metabolism, although not all xenobiotics may be acted upon by all three. Detoxification in plants is similar to drug metabolism in man, with some notable differences. In phase I a functional group is introduced, or revealed in the lipohillic molecule. However, if a functional group is already present on the xenobiotic, or the compound contains an otherwise reactive moiety, phase one of detoxification may not be necessary. In phase II the phase I metabolite or reactive parent is conjugated with a polar bio-molecule, increasing the hydrophilicity and polarity of the compound in readiness for phase III, transport (Dutton, 1978). In plants the conjugated metabolite is transported into the vacuole in phase III, thereby removing it from the cytoplasm. An overview of plant enzyme classes involved in xenobiotic detoxification is presented in Table 1.1

Table 1.1 Plant enzymes involved in the detoxification of xenobiotics. With examples of pesticide substrates.

Enzyme class	Phase	Xenobiotic substrate
Cytochrome P450	1	Phenyl ureas, Sulphonyl ureas
Glutathione *S*-transferases	2	Fluorodifen, alachlor,atrazine, PCNB, Metolachlor, diclofluanid, fenoxaprop
Carboxylesterases	1	Aryloxyphenoxypropionate esters
O-Glucosyl transferases	2	Chlorinated phenols, imazethapyr, dicloprop, diclofop, bentazone
O-malonyl transferases	2	β-D-Glucosides of pentachlorophenol and diphenamid, flamprop 4-hydroxy-2,5-dichlorophenoxyacetic acid methazol.
N-Glucosyl transferases	2	Chlorinated anilines, chloramben, metribuzin, hymexazole, pyrazon, picloram.
N-malonyl transferases	2	Chlorinated anilines, *S*-cysteine conjugates EPTC, BPTC.

Adapted from Cole & Edwards 2000; Marrs1996; Sanderman 1992).

1.2.1 Phase I

Phase I detoxification results in the chemical activation of the xenobiotic, which although increasing hydrophilicity of the compound, primarily serves to create reactive sites by exposing or adding functional groups in preparation for Phase II metabolism. Esterases and amidases catalyse the hydrolysis of compounds. However the main detoxification enzymes in phase I are the cytochrome P-450

monoxygenases (Coleman *et al.*, 1997). Examples of cytochrome P450 monoxygenase reactions include aryl hydroxylation; alkyl hydroxylation and heteroatom release (Kreuz *et al.*, 1996). Although normally involved in detoxification, cytochrome P450s may enhance the toxicity of xenobiotics by forming cytotoxic reactive compounds. For example benzo(*a*)pyrene, B(*a*)P, a polycyclic aromatic hydrocarbon, undergoes cytochrome P450 mediated mono-oxygenation to B(*a*)P-7,8-diol-9,10-epoxide, which forms stable DNA adducts in animals the carcinogenicity and mutagenicity of which, has been extensively researched (Newbold and Brookes, 1976; Bartsch, 1996).

1.2.2 Phase II

Phase II detoxification results in the formation of water-soluble conjugates of phase I metabolites, through covalent linkage with endogenous hydrophillic molecules such as glucose, malonic acid and glutathione. These conjugations are catalysed by glucosyl, malonyl and glutathione *S*-transferases respectively (table 1.1) (Coleman *et al.*, 1997). Although glucosyl and malonyl transferases are not considered in depth here, the interested reader may refer to Cole & Edwards (2000) for an in depth discussion. Toxicity of the parent xenobiotic is further reduced by this step, however some conjugates, as is the case with *S*-glutathionylated metabolites, may cause product inhibition of the respective conjugating enzyme activity (Cole & Edwards, 2000; Coleman, 1997). Conjugation of herbicides with glutathione (GSH = γ-glu-cys-gly) in many cases is the basis of herbicide selectivity, whereby in crop species the xenobiotic is rapidly conjugated to glutathione as a result of elevated GST levels relative to slower detoxification in weed species (Figure 1.2.2A). However, enhanced toxicity of xenobiotics through GST mediated bioactivation has

also been reported. Shimuzu *et al.*, (1995) reported that the isourazole herbicide fluthiacemethyl was isomerised by plant GSTs to a triazolidine, a potent inhibitor of protophorinogen oxidase (Figure 1.2.2B). In animals, glutathione conjugation of ethylene di-bromide, an anti-knock additive in petrol, results in a sulphur mustard analogue containing a reactive episulphonium ion, which can alkylate DNA (Van Bladeren, 2000).

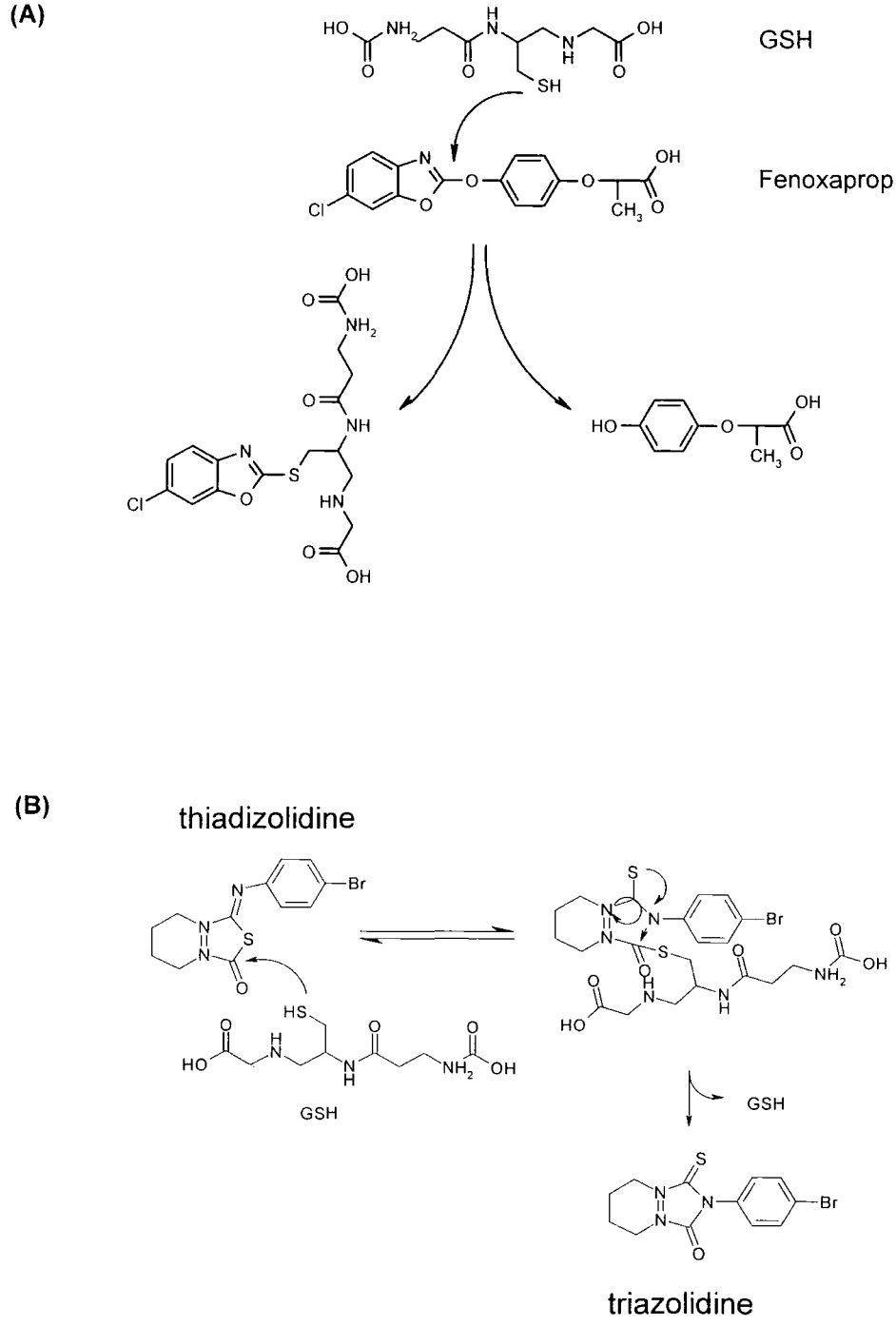

Figure 1.2.2 (A) GST mediated detoxification of the herbicide fenoxaprop by glutathione conjugation. Adapted from Tal *et al.*, (1993). (B) GST mediated isomerisation of a thiadizolidine pro-herbicde to the phytotoxic triazolidine. Taken from Edwards *et al.*, (2000).

1.2.3 Phase III

Phase III of the xenobiotic detoxification process involves vacuolar compartmentalisation of water soluble phase II products. The available evidence suggests that this is an ATP dependent process involving ATP Binding Cassette (ABC) transporters, which are present in the tonoplast and are related to the multidrug resistance proteins (MRPs) (Walczak & Dean, 2000). Conjugate transport across the vacuolar membrane is an active process, as in the cytosol (pH 7.4), the *p*K*a* of glutathione would result in the conjugate having a net negative charge. As such, non-ionic transport would not be feasible without the presence of ATP driven ABCs. Located in the tonoplast membrane is a Mg-ATP dependent glutathione conjugate transporter, which is highly efficient in transporting conjugates as compared with other electrogenic antiporters or driven by membrane potential dependent uptake (Coleman *et al.*, 1997). Vacuolar uptake of the natural products anthocyanin, medicarpin and cinnamic acid in the presence of glutathione (Walczak & Dean 2000; Marrs *et al.*, 1996; Li *et al.*, 1997) have all been attributed to ABC transporters (Theodoulou 2000; Rea *et al.*, 1998).

Once in the vacuole, glutathione conjugates have been reported to be processed by a carboxypeptidase, which catalyses the removal of glycine from the glutathione tripeptide (Wolf *et al.*, 1996). Recently, a phytochelatin synthase with such carboxypeptidase activity was purified from *Silene cucubalis* and the homologue being cloned from *A. thaliana* with resultant expression of the recombinant protein (Beck *et al.*, 2003). A membrane associated γgamma-glutamyl transpeptidase (γ-GTase) then removes the terminal glutamic acid leaving the *S*-cysteinyl derivative (Martin and Slovin 2000; Hall *et al.*, 2001; Edwards and Cole 2000; Coleman et al., 1997). Evidence, however, has also been demonstrated for the involvement of γ-

GTase activity in the processing of glutathione at the plasma membranes and in *Arabidopsis* a multigene-family of γ-GTases are present, whose proteins may have differing sub-cellular localisation and functions (Storozhenko *et al.*, 2002).

The final cysteinyl-conjugate may undergo transamination, yielding a thiolactic acid conjugate or malonylation mediated by malonyl transferases (Marrs, 1996). Malonylation in plants, which occurs in the cytoplasm, is analogous to the formation of mercapturic acids in mammals (Edwards and Cole, 2000; Cole, 1994; Dutton, 1978). In several plant species *N*-malonylcysteine conjugates of propachlor, metalochlor, butachlor, *S*-ethyl dipropylthiocarbamate (EPTC) and pentachloronitrobenzene (PCNB) have all been identified (Edwards and Cole, 2000; Marrs, 1996). In addition, glucosylated sulphur metabolites, derived from glutathione conjugates, have also been identified, which undergo subsequent conversion to sulphoxide and sulphonic acid derivatives (Edwards and Cole, 2000). In view of this processing system, it has been suggested that in plants, glutathione conjugates act as temporary non-toxic, transport storage metabolites of xenobiotics, which are then degraded to other polar conjugates (Coleman *et al.*, 1997). The metabolism of GSH-conjugated xenobiotics has been summarised in Figure 1.2.3.

Figure 1.2.3 Metabolism of glutathione conjugated xenobioitcs (X) in plants.

Adapted from Cole & Edwards 2000; Marrs 1996 and Tal *et al.*, 1993)

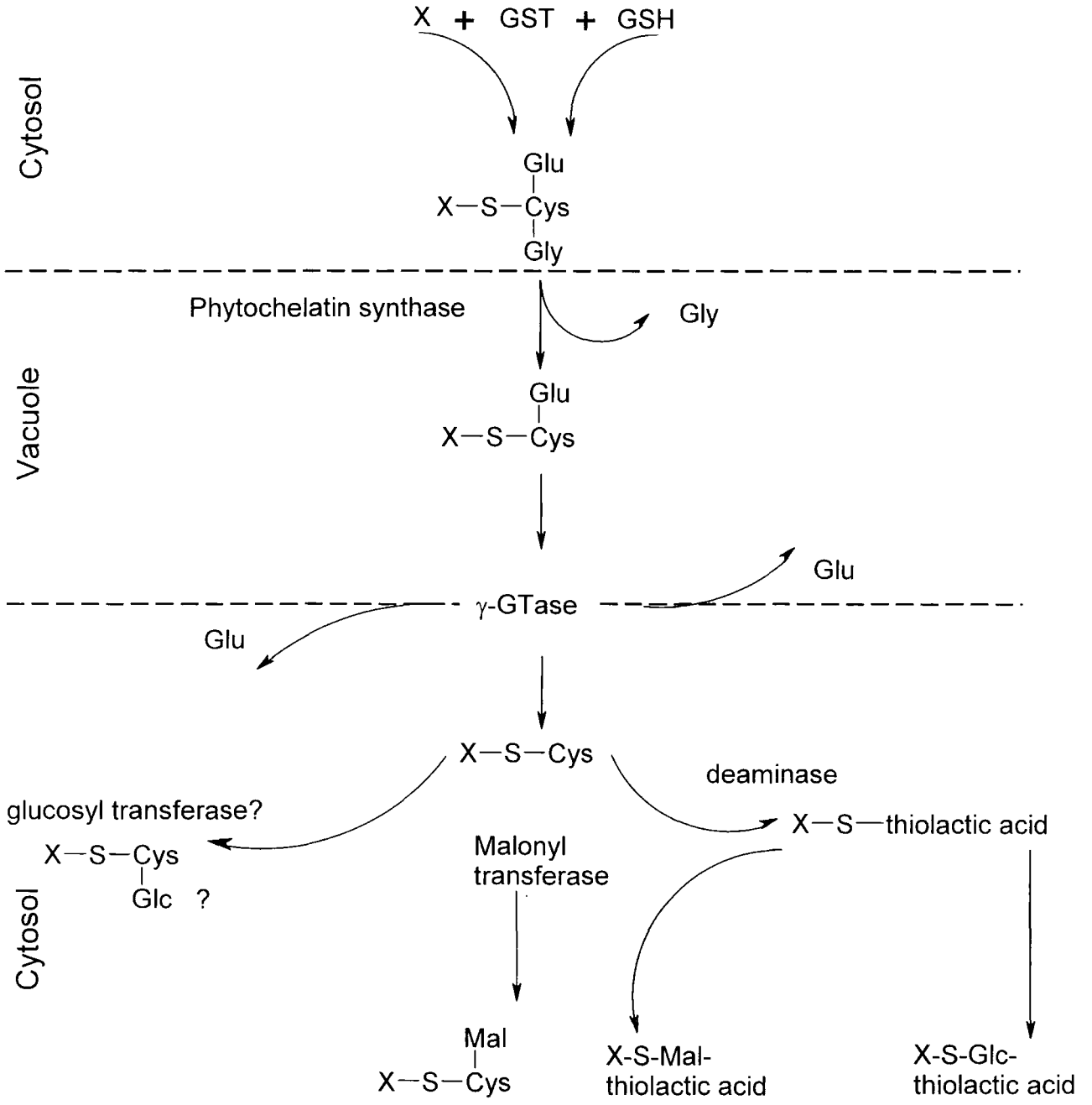

1.3. Glutathione *S*-Transferase Mediated Detoxification of Xenobiotics

The toxicological effects exerted on biological systems by xenobiotics can be cytotoxic or genotoxic. Cytoxicity may be the direct or indirect result of the xenobiotic disrupting normal metabolic activities of the cell, through enzyme inhibition, protein binding or oxidative stress resulting in cell death. Genotoxicity results from a xenobiotic directly exerting a damaging effect on DNA (Smith, 2000), with nucleic disruptions being inherited in subsequent generations. In both cases such detrimental effects are often due to reactive electrophilic sites in the foreign compound, which can accept electrons from a nucleophile to form a covalent bond. As such, these electrophilic centres are able to form covalent bonds with biological macromolecules that possess nucleophilic sites that are either electron rich, or have electrons in non-bonded pairs or in π bonds (Coleman *et al.*, 1997).

Reduced glutathione (GSH) is capable of undergoing spontaneous conjugation with compounds containing electrophillic centres. In particular, the nucleophillic thiolate anion of GSH can attack electrophillic substrates (X-Z) with concomitant displacement of a leaving group (Z) or more rarely take part in addition reactions (Kreuz *et al.*, 1996).

$$\text{X-Z} + \text{GSH} \longrightarrow \text{X-SG} + \text{HZ}$$

Following conjugation with glutathione, the water soluble X-SG is targeted to the vacuole for compartmentalisation and further processing. Schroder and Stampfl (1999) followed the intracellular transport of glutathionated conjugates of monochlorobimane, which are brightly fluorescing compounds, in onion cells. Prior to sequestration in the vacuole, these conjugates were shown to be transported to the

nucleus. Significantly, this conjugate, as well as conjugates of several other electrophilic xenobiotics, stimulated GST activity and the authors concluded that glutathione conjugates might act as signal molecules, which regulate GST activity. GSH conjugates may also regulate the transport of other metabolites. Thus, the vacuolar uptake of the rye flavone glucuoronide, luteolin 7-*O*-diglucuronyl-4'-*O*-glucuronide was found to be regulated by the relative concentrations of reduced glutathione and the GSH conjugate of dinitrobenzene (Klein *et al.*, 2000).

1.3.1 GST detoxification of herbicides

Plant soluble and microsomal GSTs were first reported to be present in maize seedlings with activity toward chloro *S*-triazine herbicides over 30 years ago (Frear, 1970). While investigating xenobiotic detoxification in lower plant species, Pflugmacher *et al.*, (2000), noted that considerable research has been directed toward the characterisation of soluble GST isoenzymes in crop plants in the last 20 years. The majority of interest has been directed to determining the importance of GST-mediated detoxification as a basis for herbicide selectivity. GSTs are certainly widespread in the plant kingdom and associated activities have been identified in mosses, trees and many weed species (Pflugmacher *et al.*, 2000). Thus, the taxonomic distribution of soluble and microsomal GST activities toward a range of model xenobiotics and the pesticides atrazine and fluorodifen was determined in 59 higher and lower plant species and four cell suspension cultures. High GST activities have been reported in marine macroalgae of the divisions *Chlorophyta*, *Phaeophyta* and *Rhodophyta* (Pflugmacher & Sandermann, 1998a, b). The authors concluded that marine macroalgae have the potential to remove xenobiotic pollution due to their biomass and GSTs as well as the additional presence of detoxifying cytochrome

P450 mono-oxygenases (Pflugmacher and Sandermann, 1998a) and glucosyltransferases (Pflugmacher & Sandermann, 1998b).

The agrochemical industry has funded considerable research into plant GSTs, as the understanding of plant xenobiotic detoxification mechanisms is pivotal to understanding herbicidal selectivity. In many cases, plants with higher titres of detoxifying enzymes, such as major crops, are less susceptible to herbicidal toxicity compared to weed species with lower contents of GSTs (Hoagland *et al.*, 2001). GST contents within cereal crop species can be further elevated through the application of safeners, a group of agrochemicals, which induce detoxifying enzymes (Davies and Casley, 1999). Safeners can therefore enhance selectivity by upregulating these GSTs in the crop over those in weeds by being applied prior to or in conjunction with herbicides.

The importance of GSTs in herbicide selectivity is most dramatically observed in metabolism-based resistance in weeds. Acquired tolerance to the herbicide atrazine, resulting from the enhanced conjugation of the herbicide to GSH, has been reported in velvetleaf, *Abutilon theophrasti* (Hall *et al.,* 2001; Anderson and Gronwald, 1991), a dicotyledonous weed of corn, soybean and other annually tilled crops. While in the weed black-grass, *Alopecurus myosuroides,* elevated GST and glutathione peroxidase activity has been shown to confer multiple herbicide resistance in this weed as compared with a susceptible biotype (Cummins *et al.*, 1999).

Through the use of genomics, McGonigle *et al.*, (2000), of Du Pont, identified and cloned 25 GST full length cDNA sequences from soybean and 42 GSTs from maize. Expression of 28 recombinant GSTs revealed 18 with herbicide detoxifying activity towards the substrate alachlor. Of those, 10 were from soybean. In contrast to

maize where glutathione is used by GSTs, the dominant thiol found in soybean is homoglutathione (hGSH; γ-Glu-Cys-β-Ala) with soybean GSTs preferentially using hGSH in the detoxification of diphenyl ether herbicides (Skipsey *et al.*, 1997). Overexpression of a recombinant soybean GST revealed that the substrate specificity for conjugating the diphenyl ether herbicides fomesafen and aciflurofen, was largely due to the preferential use of hGSH as a co-substrate rather than GSH (Skipsey *et al.*, 1997; McGonigle *et al.*, 2000).

Within the family Poaceae a further thiol is present, Hydroxymethyl glutathione, HmGSH (γ-Glu-Cys-Ser) where the terminal amino acid, glycine, is replaced with serine (Klapheck *et al.*, 1992). In wheat, GSH and HmGSH are present in approximately equal concentrations (Cummins *et al.*, 1997). The use of HmGSH in herbicide detoxification has not been demonstrated, but *in vivo* metabolism studies with wheat treated with the safener fenchlorazole ethyl, has shown an important role for GSTs in the detoxification of the herbicide fenoxaprop (Edwards and Cole, 1996). Cummins *et al.*, (1997) subsequently purified 4 GSTs from wheat with herbicide detoxifying activities toward fenoxaprop-P-ethyl, atrazine, metolachlor and fluorodifen.

In mammals glutathione *S*-transferases have been classified into alpha, mu, pi, sigma, theta and zeta classes based on immunological cross reactivity and sequence relatedness (Edwards *et al.*, 2000). Based on the original mammalian classification system, the theta class contains most non-mammalian GSTs and contains the closest relatives to the progenitor of all GSTs. Originally all plant GSTs were classified as theta, being divided into 3 main sub-types (Droog, 1997). Type I GST genes have 3 exons with the proteins exhibiting herbicide detoxifying activity; Type II genes have 10 exons and are much closer to mammalian zeta GSTs; while

type III GST genes contain two exons and are mainly auxin inducible. A Type IV GST was later identified in *Arabidopsis* which was more similar to the classical theta class (Edwards *et al.*, 2000). In view of the confusion in classifying the plant GSTs, the nomenclature based on the above criteria is now considered to be outdated. The convention for the revised GST classification system will be clarified in section 1.4.2.

1.3.2 Fungicides

Literature on the involvement of GSTs or glutathione conjugation in the metabolism of fungicides in plants is scant. Belonging to a group of *N*-trihalomethylthio compounds, Dichlofluanid is a contact fungicide used to prolong the storage of many crops including strawberries (Edwards & Cole, 2000). The initial metabolic step of this compound is to react with glutathione, resulting in scission of the sulphonyl bond and the formation of a fungitoxic sulphamide. The trihalomethylthio, which is also released, may also undergo dechlorination yielding antimicrobial thiophosgene and gaseous products including hydrogen sulfide, hydrogen chloride and carbonyl sulfide (Roberts and Hutson, 1999). The involvement of GSTs in these reactions is unclear and the reaction with glutathione may be the result of non-enzymic nucleophilic attack by the thiol. As mentioned previously (section 1.2) the fungicide pentachloronitrobenzene, PCNB, is also known to undergo glutathionylation (Edwards and Cole, 2000) as do the phenylamide fungicides. However, Oros and Komives (1991) concluded that sensitivity or tolerance to phenylamide pesticides was not regulated by the efficiency of GSH conjugation in the phytopathogen *Phytophthora infestans*. As such glutathione conjugation of fungicides mediated by fungal GSTs has not been reported and their potential involvement as a mechanism of resistance among fungal phytopathogens is largely unknown.

1.3.3 Insecticides

The use of insecticides in the control of agronomic pests and vectors of human disease has been a key strategy in both crop improvement and safeguarding human health. A major consideration to both the biomedical and agrochemical communities, has been the evolution of insect resistance to such pest control agents. Of particular interest has been the involvement of cytochrome P450s, esterases and GSTs associated with pesticide detoxification in acquired resistance to insecticides. For example, detoxification of the organophosphorous insecticides, diazinon, methyl-parathion and lindane through conjugation to GSH, has been demonstrated in the insecticide-resistant phenotype of the common housefly, *Musca domestica*, Cornell-HR (Wei *et al.*, 2001; Syvanen *et al.*, 1996). Recombinant *Md*GSTs-1, -2, -3, -4, -5 and -6 were shown to contribute to insecticide resistance in this strain, with protein sequence alignments indicating they belong to an insect specific class of GSTs.

As a secondary detoxification mechanism, insect GSTs are responsible for the *O*-dealkylation and *O*-dearylation of organophosphorous insectide metabolites in addition to the dehydrochlorination of organochlorines such as DDT (Hemingway *et al.*, 1991). In the latter reactions, GSTs utilise GSH as a cofactor rather than a co-substrate and this is regarded to be the most common mechanism of metabolism-based resistance to DDT (1,1,1-trichloro-2,2-bis-(4'-chlorophenyl)ethane) in mosquitoes (figure 1.3.3). DDT resistance in the West African mosquito, *Anopheles gambia*, has been attributed to GST mediated dehydrochlorinase acitivity, with GST expression showing both qualitative and quantitative differences to that seen in the susceptible phenotype (Prapanthadara *et al.*, 1993). Additionally a DDTase GST has been purified from the Thailand mosquito *A.dirus* (Prapathanda *et al.*, 1995). It has been suggested that where GST-mediated conjugation of primary insecticide

metabolites does occur, it often acts as a secondary resistance mechanism in concert with monoxygenase or esterase based resistance mechanisms (Hemmingway, 2000).

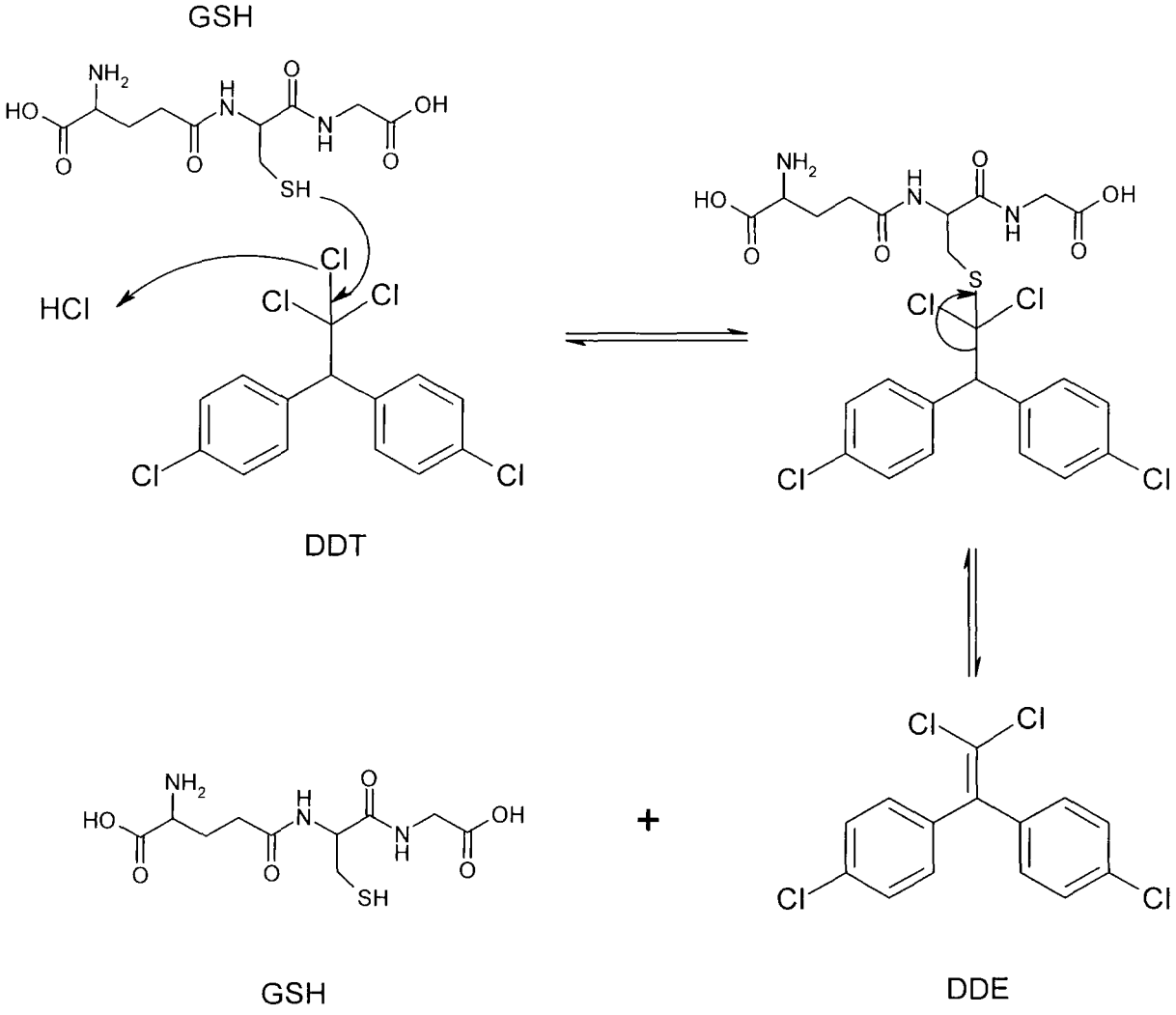

Figure 1.3.3. GST mediated dehydrochlorination of DDT (1,1,1-Trichloro-2,2-bis-(4'-chlorophenyl)ethane) to DDE (1,1-Dichloro-2,2-bis(4'-chlorophenyl)ethylene).

The brown plant hopper, *Nilaparvata lugens* is a devastating insect pest of rice. Recently Vontas *et al.*, (2001) demonstrated that GSTs, functioning as antioxidant defence agents, conferred resistance to pyrethroid insecticides in this invertebrate. In susceptible phenotypes exposure to pyrethroids was shown to deplete reduced glutathione, induce lipid peroxidation and result in protein oxidation. Pyrethroid resistant strains had elevated GST levels and showed reduced pyrethroid-induced lipid peroxidation and resulting mortality.

Contrary to the useful exploitation of GSTs as a basis of herbicide selectivity and herbicide resistance in crops, GSTs in insect strains have proven to be problematic. As has been seen with the evolution of GST-based herbicide resistance in weed species, such as black-grass, resistance based mechanisms can evolve in insect populations under the selective pressure of control methods utilising organophosphorous insecticides, DDT or pyrethroids. In turn, use of pyrethroid-impregnated bed nets, for control of malarial vectors, may also result in selection of mosquito phenotypes with multiple-resistant based mechanisms. Hemmingway *et al.*, (2002) noted that through exposure to DDT and pyrethroids multiple insecticide resistant strains of *A. gambia* have been selected in the field in East and West Africa. GST based insecticide resistance has been shown to be of major concern in insect pest control. Resistance mechanisms associated with this superfamily of detoxifying enzymes have been attributed to both direct metabolism of the insecticides rendering them non-toxic, or through amelioration of the cytotoxic effects of their action, such as counteracting lipid peroxidation, exerted by the agent.

1.4 GST family overview concentrating on nomenclature, classification and characterisation.

As a multi-functional superfamily of detoxification enzymes, plant GSTs have been subject to extensive research and review (Dixon *et al.*, 2002; Edwards *et al.*, 2001; Hall *et al.*, 2001; Sheehan *et al.*, 2001; Edwards *et al.*, 2000; Edwards & Cole, 2000; Marrs, 1996; Cole, 1994). Due to their ubiquitous nature, interest in their functional activities has also spanned the disciplines of biomedical, agrochemical, microbiological, and ecological research. The purpose of this section is not to provide a highly detailed review of all GSTs, their structure and function, but to establish the convention of nomenclature adopted and highlight similarities and differences between groups and their relatedness to one another (Table1.4.2 and Figure 1.4.17).

1.4.1 What makes a GST a GST?

An ancient and diverse protein family, GSTs exhibit common structural features including a hydrophobic binding domain (H-site) and the ability to bind glutathione (G-site). Greatest similarity between members of the GST family is observed in the GSH binding domain containing a motif of four highly conserved amino acids (Edwards *et al.*, 2000). Here, a catalytically essential tyrosine or serine (table 1.3.3) activates glutathione by lowering the pKa of the thiol group from around pH 9 to approximately pH 6, thus enhancing the rate of nucleophillic attack by the resulting thiolate anion toward electrophillic substrates at physiological pH (Dixon *et al.*, 2002; Sheehan *et al.*, 2001; Caccuri *et al.*, 1999). The H site is more variable, accounting for the broad range of endogenous and xenobiotic substrates utilised by this family of GSH dependent enzymes (Edwards, 2001).

Edwards *et al.*, (2000) suggest that although GSTs should be able to selectively bind GSH or natural homologues such as hGSH and HmGSH, sequence similarity and the ability to bind GSH alone were insufficient criteria for GST classification. Many proteins with related sequences, such as squid lens crystallin and elongation factor gamma proteins have evolved alternative functions and lost their ability to use GSH catalytically. Application of the dual classification of GSH binding and the ability to use GSH in conjugation reactions with electrophiles distinguishes GSTs from proteins with related sequences (Edwards *et al.*, 2000).

1.4.2 GST classification and nomenclature

Prior to the inclusion of GSTs sequenced from fungal species, this super-family of GSH-dependent enzymes had been subdivided into 13 classes based upon primary amino acid sequence alignments (Table 1.4.2). Sequences sharing over 40% identity are generally assigned to the same class (Chelvanayagam *et al.*, 2001), with sequences demonstrating less than 30% identity being assigned to separate classes (Sheehan *et al.*, 2001). Recently, a fourteenth grouping, gamma, composed of sequences from the basidiomycete *Cunninghammella elegans* was published (Cha *et al.*, 2002). As such, they represent the first bonafide fungal specific GST class. Although possible to plot these fungal sequences in relation to other GST classes, they shall at present be omitted and are discussed in greater depth in chapter 6.

The GST nomenclature developed for animal GSTs centres upon the Greek alphabet and makes use of species initials and subunit composition for full description (Edwards *et al.*, 2000). Italicised initials represent the source organism, followed by class letter and sub-unit composition. The latter numbering is based on gene organisation or order of discovery in organisms where complete genome

information is unavailable (Edwards et al., 2000). The need for digits is necessary due to the ability of some GSTs to form both homo and heterodimers with sub-units of the same class (Dixon *et al.*, 2002; Sheehan *et al.*, 2002: Dixon *et al.*, 2001; Edwards *et al.*, 2000; Dixon *et al.*, 1998). Figure 1.4.2 clarifies this system. The gene encoding each sub-unit adopts an italicised annotation e.g. *AtGstU1* encodes *At*GSTU1 (Landi, 2000; Edwards *et al.*, 2000).

The theta class θ, considered to be the closest progenitor to all eukaryotic GSTs originally included a heterogeneous grouping of non-mammalian GSTs. Edwards *et al.*, (2000) suggested that classification of plant GSTs in this primitive sub group were inappropriate. Revision of plant GST nomenclature has given rise to two plant specific groups Phi (F) and Tau (U) replacing type I and type III GST nomenclature respectively. In addition, both Zeta (Z), replacing type II and Theta (T) GSTs, replacing type IV have been adopted as plant classes which have homologues in animals (Edwards *et al.*, 2000). In the case of fungal GSTs, assigning classification has proved difficult due to limited sequence data available and has been further compounded through their assignment, based on weak amino acid identity, to the 'generic' theta-class (Pemble & Taylor, 1992; Tamaki *et al.*, 1999; Fraser *et al.*, 2002). Sequence analysis of the fungal GSTs shall be discussed later in chapter 6 to clarify the ambiguity of their classification. In summary, the current GST classes identified, with the exception of gamma, are alpha, mu, pi, sigma, zeta, beta, theta, delta, phi, lambda, tau, omega and kappa. The major activities of each class and whether or not each class has been crystallised and its structure solved is given in Table 1.4.2

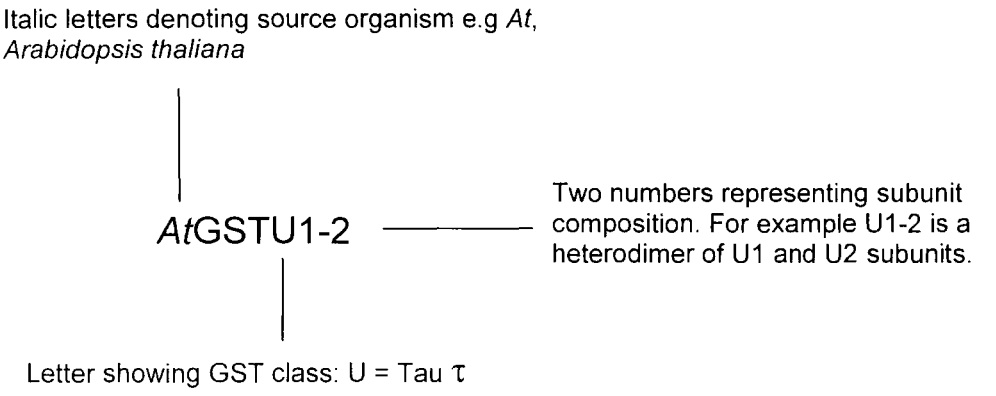

Figure 1.4.2 Nomenclature for *Arabidopsis* Tau class GST adapted from the mammalian system. Taken from Dixon *et al.*, 2002, Edwards *et al.*, 2000.

Table 1.4.2 Classification groupings and key features of the GST superfamily. Classes found in plants are highlighted in bold.

Class	Symbol	Abbreviation	Major activities	G-site catalytic residues	Crystal structure
Alpha	α	A	Steroid isomerase, GPOX, 4-HNE conjugation.	Tyrosine	Yes[1]
Beta	β	B	Ligandin	Cysteine	Yes[2]
Delta	δ	D	Organo-phosphate detoxification	Serine	
Kappa	K	K	Unknown		No
Lambda	λ	L	Thiol transferase	Cysteine	No
Mu	μ	M	Unknown	Tyrosine	Yes[3]
Omega	ω	O	Thiol transferase, DHAR	Cysteine	Yes[4]
Phi	ϕ	F	Ligandin, isomerase, conjugation, GPOX	Serine	Yes[5]
DHAR			Thiol transferase, DHAR	Cysteine	No
Pi	π	P	Retinoic acid isomerase, Jun N-terminal kinase inhibition	Tyrosine	Yes[6]
Sigma	σ	S	Prostaglandin synthesis	Serine	Yes[7]

Table1.4.2 continued

Tau	τ	U	Herbicide metabolism, GPOX, Anthocyanin transport	Serine	Yes[8]
Theta	θ	T	GPOX, dehalogenase	Serine	Yes[9]
Zeta	ζ	Z	Isomerase MAAI, dehalogenase	Serine	Yes[10]

(1) Sinning *et al.*, (1993), (2) Nishida *et al.*, (1998), (3) Ji *et al.*, (1992), (4) Board *et al.*, (2000), (5) Reinemer *et al.*, (1996), (6) Reinemer *et al.*, (1991), (7) Ji *et al.*, (1995), (8) Thom *et al.*, (2002), (9) Rossjohn *et al.*, (1996), (10) Thom *et al.*, (2001)

1.4.3 θ Theta Class (T)

Considered the closest progenitor to the ancestral GST, glutathione mediated reduction toxic of organic hydroperoxides by glutathione peroxidase activity has been demonstrated in theta class GSTs from animals to plants (Dixon *et al.*, 2001). Members of this class also possess dehalogenase activity toward dichloromethane resulting in the formation of formaldehyde (Blocki *et al.*, 1994). Compared to the alpha, mu and pi classes, theta GSTs, are inactive toward ethacrynic acid and have low activity toward, 1-chloro-2, 4-dinitrobenzene (CDNB), a commonly used GST substrate for gluathione conjugation (Landi, 2000, Sheehan *et al.*, 2002; Habig & Jackoby, 1974). *Arabidopsis At*GST1-1 was shown to have low activity towards CDNB (77 nKat mg^{-1}) with comparatively high glutathione peroxidase activity toward cumene hydroperoxide (210 nKat mg^{-1}) and the 13-(*S*)-HPOD of linoleic acid (230 nkat mg^{-1}) (Dixon *et al.*, 2001). Serine 11 appears to be a catalytically essential residue for the theta GSTs and is replaced in other classes by a tyrosine (alpha, mu and pi classes) and by cysteine (omega and beta classes) (Landi 2000; Sheehan *et al.*, 2002).

1.4.4 δ Delta Class (D)

The delta class GST are an insect specific subfamily closely related to the theta class and almost certainly share a common ancestral progenitor in recent evolutionary history (Chelvanayagam *et al.*, 2001) (Figure 1.4.17). Originally classified as class I GSTs, Chelvanayagam *et al.*, (2001) suggested the nomenclature be revised for insect classes I & II, to conform with the class system derived for mammalian and plant classes. Class I has been assigned the character delta and class II placed within class sigma (figure 1.3.16). In *Musca domestica*, *Md*GSTD3 transcript levels have been strongly associated with high-level resistance to organophosphate insecticides (Zhou and Syvanen, 1997). The delta GST genes lack introns but may contain 5' untranslated sequences. Based on the additional 5' sequence delta GST genes may be subject to alternative mRNA splicing resulting in multiple enzymes being produced, thereby having the potential to increase functional diversity (Sheehan *et al.*, 2002; Ketterer, 2001: Ranson *et al.*, 1998). For example, Jirajaroenrat *et al.*, (2001) cloned a single delta class GST gene from *Anopheles dirus*, which was transcribed to give 4 splice variants.

1.4.5 σ Sigma Class (S)

Sigma GSTs are associated with an endogenous role in prostaglandin synthesis with this class being identified in rat, man, chicken and mouse (Sheehan *et al.*, 2002). Prostaglandin H_2, PGH_2, is a short-lived intermediate in the synthesis of prostaglandin D_2, PGD_2, which in turn is derived from arachidonic acid. *Gallus gallus* sigma GSTs isomerise PGH_2 to PGD_2 in a glutathione dependent-reaction (Thomson *et al.*, 1998), bringing about the opening of the epidioxy bridge (figure 1.4.5). These

sigma class GSTs are distinct from the non-glutathione dependent prostaglandin isomerases. Campbell *et al.*, (2001) reported a nematode specific class of GSTs that appears closely related to sigma (figure 1.4.17). The authors noted a logical name could not be ascribed to these GSTs and as such, for the purpose of nomenclature were assigned as a sigma subfamily. Inclusive to this class, as determined by sequence alignments, are insect type II GSTs (Chelvanayagam *et al.*, 2001).

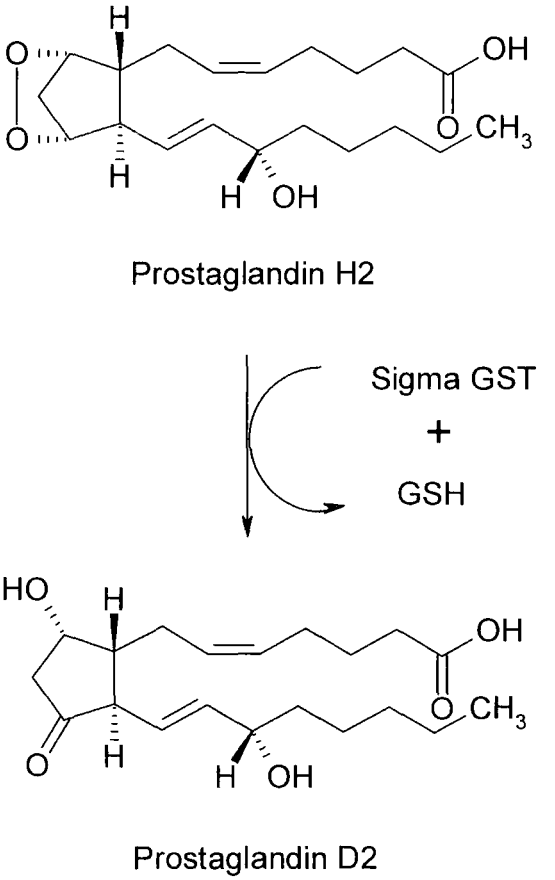

Figure 1.4.5 The glutathione-dependent conversion of prostaglandin H_2 to prostaglandin D_2 mediated by sigma class GSTs.

1.4.6 ϕ Phi Class (F)

Similar to the tau class, phi are a plant specific GST class previously designated type I. Present in the crops maize, soybean and wheat (McGonigle *et al.*, 2000; Dixon *et al.*, 1998), the role of these safener-inducible GSTs in herbicide metabolism in maize is well characterised (Edwards and Dixon., 2000). Tolerance of *Alopecurus myosuroides*, a weed of wheat crops, to multiple herbicides has also been correlated to high levels of phi GST expression (Cummins *et al.*, 1999). The recombinant *Am*GSTF1 had negligible herbicide conjugating activity, whilst exhibiting high glutathione peroxidase activity toward organic hydroperoxides. Immunoblots revealed expression of phi class GSTs exclusively in herbicide resistant black grass lines as opposed to susceptible populations. Tolerance of black grass to the cytotoxic effects of herbicides has been suggested to be the result of detoxification of organic hydroperoxides, facilitated by glutathione peroxidase activity mediated by phi class GSTs (Cummins *et al.*, 1999).

1.4.7 ζ Zeta Class (Z)

Zeta class GSTs are known to metabolise α-halo-acid, such as dichloroacetic acid a common contaminant of chlorinated drinking water (Dixon *et al.*, 2000). Enzyme activity, however, has been shown to undergo product inhibition as the carbonium-sulfonium intermediate forms an inactive covalent complex with the zeta GST (Anders *et al.*, 2001). Zeta GSTs function in endogenous metabolism as malelylacetoactate isomerases (MAAIs). MAAI, the fifth enzyme of the phenylalanine and tyrosine catabolic pathway, catalyses the penultimate step in tyrosine degradation, by the glutathione dependent *cis-trans* isomerisation of malelyacetoacetate (MAA) to fumarylacetoacetate (FAA) (figure 1.4.7). Despite low

sequence identity with other GSTs (<20%), the crystal structure of *At*GSTZ1 shows that this enzyme adopts the canonical fold characteristic of GSTs (Thom *et al.*, 2001; Polekihina *et al.*, 2001). Additionaly, a zeta class GST has been characterised in the fungus *Aspergillus niduans* (Fernández-Cañón and Peñalva 1998).

Maleylactetoacetate Fumarylacetoactate

Figure 1.4.7. The *cis-trans* isomerisation of malelylacetoactate to fumarylacetoacetate catalysed by zeta class GSTs. Taken from Edwards *et al.*, (2000)

1.4.8 τ Tau Class (U)

Originally classified as type III GSTs, this plant specific class have been reclassified Tau (Droog, 1997). Important physiological roles including intracellular signalling, vacuolar deposition of anthocyanins, responses to auxin and cytokinin hormones and determination of herbicide selectivity have all been associated with these enzymes (van der Zaal *et al.* 1991). In addition, both native and recombinant subunits of tau class GSTs from *Zea mays* have been shown to form functional heterodimers with activity toward herbicides (Dixon *et al.*, 1998; Dixon *et al.*, 1999). Safener-inducible Tau class GSTs active toward the herbicides fenoxaprop and

dimethenamid have been purified from *Triticum tauschii* (Riechers *et al.*, 1997), and bread wheat *T. aestivum* (Cummins *et al.*, 1997). Recently, the crystal structure of *Ta*GSTU4-4 in complex with *S*-hexylglutathione was determined to a resolution of 2.2A (Thom *et al.*, 2002). The tau GSTs are a diverse gene family and through the use of genomics McGonigle *et al.*, (2000) identified 20 tau GSTs in *Glycine max* and 17 in *Zea mays*.

1.4.9 α Alpha Class (A)

GST isoenzymes, belonging to the alpha class, are known to metabolise endogenous toxic substrates such as 4-hydroxynonenal (4-HNE) by glutathione conjugation. 4-HNE is a metabolite derived from the hydroperoxides of 6-omega polyunsaturated fatty acids including linoleic acid and arachidonic acid. In addition, the reduction of lipid hydroperoxides has been demonstrated within this mammalian specific GST grouping. In particular, experiments using recombinant *Hs*GSTA1-1 and *Hs*GSTA2-2 have implicated alpha class in playing a role in protection against phospholipid peroxidation and in the reduction of 5-hydroperoxyeicosatetraenoic (5-HPTE) acid, a key intermediate in leukotriene biosynthesis (Awasthi *et al.*, 2001).

1.4.10 μ Mu Class (M)

Mu class GSTs have been investigated for their potential in detoxifying reactive metabolites such as *o*-quinones, derived from catecholamine oxidation. GSH conjugation by class mu GSTs may contribute to the removal of reactive quinone metabolites, such as aminochrome, dopachrome noradrenochrome and adrenochrome, which may otherwise lead to damge of the central nervous system and the onset of schizophrenia and Parkinsons disease. Mu class GSTs have been

shown to be 200 to 4000 times more active toward these substrates than GSTs in either alpha, pi or theta classes (Hansson *et al.*, 1999; Beaz *et al.*, 1997; Segura-Aguilar *et al.*, 1997). Additionally mu class GSTs are believed to be involved in protecting cells against oxidative stress. It has been proposed that of the 4 allelic variants at the GST M1 locus, a null allele is present in about 50% of the human population, which may predispose individuals to greater risk from xenobiotics and cancer (Sheehan *et al.*, 2002).

1.4.11 π Pi Class (P)

Regarded as the most ubiquitously expressed GST in mammals (Henderson *et al.*, 1998), pi class has been demonstrated to catalyse the glutathione-dependent isomerisation of 13-*cis*-retinoic acid to 13-*trans*-retinoic acid, vitamin A (Sheehan *et al.*, 2002), and is implicated in susceptibility to colon carcinogenesis (Niitsu *et al.*, 2001). Overexpression of pi GSTs in rat liver preneoplastic nodules and human tumour cells made them more resistant to anticancer drugs (Wolf *et al.*, 2001). Following hepatic cytochrome P450 activation of drugs, pi GSTs have been found to have the highest capacity for conjugating reactive metabolites of acetaminophen (paracetamol) with glutathione. Surprisingly, studies of GST pi knock out mice revealed increased resistance to the cytotoxic effects of paracetamol compared to wild type mice. Wolf *et al.*, (2001) suggest paracetamol tolerance was associated with constitutive activation of N-jun kinase due to the absence of endogenous pi GST, which is a known inhibitor of this transcription factor. N-jun kinase is associated with cytoprotective mechanisms against oxidative stress, such as those mediated by paracetamol toxicity.

1.4.12 β Beta Class (B)

A bacterial-specific GST class, beta GSTs display immunological and structural properties, which distinguish them from other GST classes (Rossjohn *et al.*, 1998). Interestingly *Proteus mirabilis*, *Pm*GSTB1-1, has been shown bind a range of antibiotics although its endogenous function was unclear (Allocati *et al.*, 2001). Immunoblot analysis of *Pm*GSTB1-1 revealed that its expression remained unaffected by the exposure of the bacteria to rifampycin, tetracycline or cumene hydroperoxide, whereas CDNB and ampicillin elevated expression 3 – 4 fold. On this basis the authors suggest *Pm*GSTB1-1 may be involved in the metabolism of these compounds (Allocati *et al.*, 2001). Similar to the omega class, the three-dimensional structure of beta class GSTs reveals a conserved cysteine forming a mixed disulphide with the thiol of glutathione. As opposed to theta and delta class GSTs, beta GSTs have a close packed interface in the H-site lacking the V-shaped open hydrophobic interface associated with theta and delta GSTs (Sheehan *et al.*, 2002).

1.4.13 ω Omega Class (O)

Most human tissues express the omega GST, *Hs*GSTO1-1. The broad tissue range in which it is expressed differs from most other GSTs, suggesting a fundamental role in cellular metabolism. *Hs*GSTO1-1 exhibits dehydroascorbate reductase activity and characteristics of the glutaredoxins, namely activity as a glutathione dependent thiol transferase. The crystal structure has been deduced for this enzyme showing Cys 32 to be a catalytically important residue, which forms a mixed disulfide with glutathione. The presence of a large cleft between the sub-units and relatively polar H site has led to the hypothesis that this enzyme may dethiolate proteins which have been *S*-thiolated during oxidative stress (Board *et al.*, 2001).

Omega orthologues have been identified in rat, mouse, and the invertebrate *Caenorhabditis elegans* (Sheehan *et al.*, 2002).

1.4.14 K Kappa Class (K)

Identified in rat mitochondria as a single gene copy, with orthologues present in pig and human, kappa GSTs were originally designated to theta class prior to full-length cDNA sequence analysis. Lacking the SNAIL/TRAIL motif, among other structurally features, they are unique among the GST superfamily (Sheehan *et al.*, 2002; Pemble *et al.*, 1996). Due to a lack of homology with other GSTs, this class has been excluded from sequence homology and GST diversity shown in figure 1.4.17.

1.4.15 λ Lambda Class (L)

First identified in maize through their inducible expression following exposure to the safener *N*-(aminocarbonyl)-2-chlorobenzenesulphonamide (2-cbsu) (Hershey and Stoner, 1991) and representing somewhat of an enigma, lambda GSTs have, until recently, been regarded a cryptic class with respect to catalytic activity. Cloned from *Arabidopsis* (Dixon *et al.*, 2002), recombinant lambdas' have been shown to have putative roles in maintaining intracellular redox homeostasis, deduced from induction studies with chemical agents and oxidative stress. Lambdas' appear to be unusual from other GSTs in that they are functionally active monomers, being shown to have thiol transferase activity, whilst showing similarity to omega GSTs with a cysteine residue forming a mixed disulphide with glutathione at the active site. Of the two lambda genes identified in *Arabidopsis*, one was found to be chloroplast targeted, whilst the other was cytosolic (Dixon *et al.*, 2002).

1.4.16 Dehydroascorbate reductase (DHAR)

An undesignated class with respect to GST nomenclature, dehydroascorbate reductases, catalyse the glutathione-dependent reduction of dehydroascorbate to ascorbic acid (Dixon *et al.*, 2002). Although seemingly part of the GST superfamily (Figure 1.4.17), these enzymes have not been classified as such due to the well-characterised endogenous function and absence of conjugating activity. Similar to omega, beta and lambda an active site cysteine is a catalytically important residue of DHAR forming mixed disulfides with GSH.

1.4.17 Classification summary

The GSTs are a large and diverse superfamily of enzymes exhibiting broad range and in many cases overlapping substrate specificities. Conjugation, central to GST nomenclature is but one of several reactions mediated by these proteins. Endogenous roles include the reduction of organic hydroperoxides, isomerisation of physiological substrates, protein reactivation and the regulation of protein/protein signalling interactions as a cytoprotective mechanism against oxidative stress.

Clarification of plant-based nomenclature, through it being brought into line with that for mammalian GSTs, has produced the plant specific groupings tau and phi with distinct functions from the previously heterogeneous theta class. With fungal genomics still in its infancy, fungal GST groupings should be brought into line with the accepted nomenclature, (table1.4.2 and figure 1.4.17) to avoid confusion and assist in determining the roles of these enzymes in such a diverse protein family.

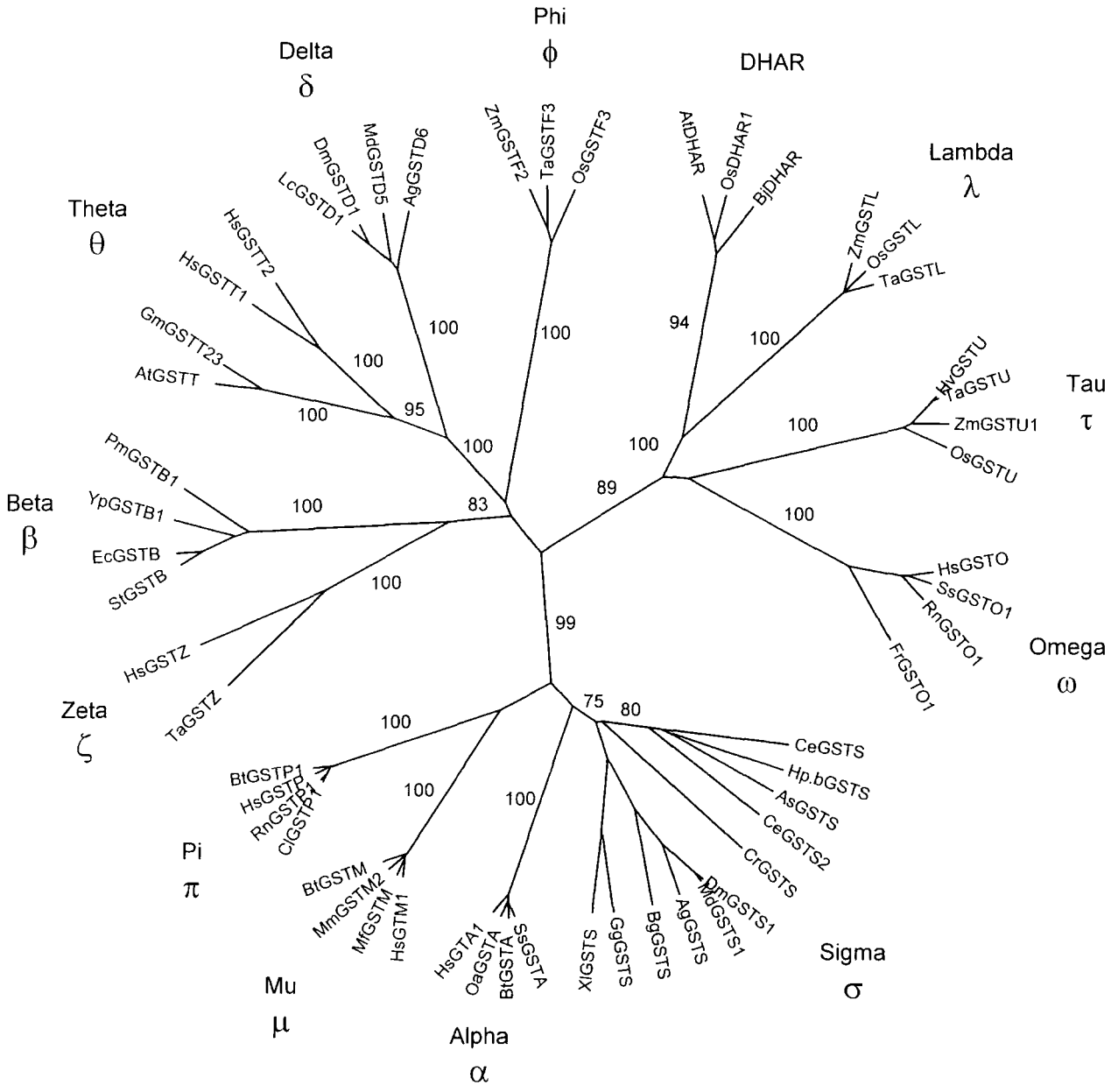

Figure 1.4.17 Dendogram showing the relationship between the main classes of glutathione *S*-transferase polypeptide amino acid sequences. Digits represent bootstrapped branch point confidence n = 100.

*At*DHAR, *Arabidopsis thaliana* Q8LB28; *Os*DHAR1, *Oryza sativa* AB037970; *Hs*GTA1, *Homo sapiens* P08263; *Ss*GSTA, *Sus scrofa* Q29057; *Oa*GSTA, *Ovis aries* Q9XS30, *Bt*GSTA, *Bos taurus*, Q28035; *Hs*GTM1, *H.sapiens* P09488; *Mf*GSTM, *Macca fascicularis* Q9TSM5; *Bt*GSTM *B.taurus* Q9NOV4; *Mm*GSTM2, *Mus musculus* P15626; *Bt*GSTP1, *B.taurus* P28801; *Hs*GSTP *H.sapiens* P09211; *Cl*GSTP1 *Cricetulus longicaudatus* P46424; *Rn*GSTP1 *Rattus norvegicus* P04906; *Hs*GSTO, *H.sapiens* U90313; *Rn*GSTO1, *Rattus norvegicus* Q9Z339; *Ss*GSTO1, *S.scrofa* Q9N1F5; *Fr*GSTO1, *Fugu rubripes* Q90XY6; *Zm*GSTL, *Zea mays* X58573; *Os*GSTL, *O.sativa* Q9M578; *Ta*GSTL, *Triticum aestivum* CAD29476; *Ta*GSTZ, *T.aestivum* O04437; *Hs*GSTZ, *H.sapiens* O43708; *Zm*GSTF2, *Z.mays* P46420; *Ta*GSTF3, *T.aestivum* CAD2946; *Oa*GSTF3 *O.sativa* Q9FUE0; *Zm*GSTU1, *Z.mays* O24595; *Hv*GSTU; *Hordeum vulgare*, Q9SES7; *Ta*GSTU, *T.aestivum* Q8RW02; *Os*GSTU, *O.sativa* O65032; *At*GSTT; *A.thaliana* AB010072; *Hs*GSTT1, *H.sapiens* P30711; *Hs*GSTT2, *H.sapiens* Q9HD76; *Gm*GSTT23, Q9FQD5; *Ag*GSTS, *Anopheles gambia* P46428; *Gg*GSTS, *Gallus gallus* O73888; *Cr*GSTS, *Chlamydomnas reinhardti* BQ825815; *Dm*GSTS1, *Drosophilla melongaster* Q9V7Y4; *As*GSTS *Ascarius sum* P46436; *Md*GSTS1, *Musca domestica* P46437; *Xl*GSTS, *Xenopus laevis* Q8JHA7; *Bg*GSTS *Blattella germanica* O18598; *Ce*GSTS, *Caenorhabditis elegans* CE14870; *Ce*GSTS2, *C.elegans* CE07825; *Hp.b*GSTS, Heligmosomoides polygyrus. Bakeri AF128959; *Pm*GSTB1, *Proteus mirabilis* U38482; *Yp*GSTB1, *Yersinia pestis* AAM85534; *St*GSTB, *Salmonella typhi* Q8Z6Q4; *Ec*GSTB, *Escherichia coli* P39100; *Md*GST5, *M.domestica* Q254450; *Lc*GSTD1, *Lucila cuprina* P42860; *Ag*GSTD6, *A.gambia* Q93113.

1.5 Pathogen-induced plant glutathione *S*-transferases

Evidence for the regulation and role of plant GSTs has not been restricted to research directed solely in the area of safening and GST-mediated herbicide detoxification in crop species. It has been shown that elevated GST transcripts accrue in a variety of plant species following infection with fungal plant pathogens.

Mauch and Dudler (1993) reported differential expression of three GSTs termed GST25, GST26 and GST29 in response to xenobiotics and pathogen attack in *Triticum aestivum* L. The authors found that mRNA transcripts of *GstA1*, the gene encoding phi class GST29, accumulated 2hr after inoculation with *Erysiphe graminis*, preceeding hyphal penetration of the host cell, which occurred after 10hr. In addition, phi *GstA1* was also induced in wheat plants by cell free extracts of autoclaved *E. graminis* spores, suggesting a soluble elicitor enhanced expression. In contrast, the herbicides paraquat, atrazine, metalochlor and alachlor did not induce GST29 but strongly enhanced GST25 and GST26 expression. Conversely, GST25 and GST26 were not induced by fungal elicitation. GST29 did not appear to directly confer resistance of wheat to the pathogens *E. graminis* F.sp. *hordei* or *E. graminis* F.sp. *tritici* but instead was believed to play a specific host defence role against general pathogen attack (Mauch & Dudler, 1993). Classified as a member of the phi class, *GstA1* showed 46-53% identity with maize *Zm*GSTF2, (accession P46420); wheat *Ta*GSTF3, (accession CAD29476) and rice *Os*GSTF3, (accession Q9FUE0). Further alignment with unclassified GSTs revealed greater identity 62-87%, toward other GSTs from rice, (accession Q9AS59); barley, (accession AF430069) and black-grass, (accession AJ010454).

Similarly Martini *et al* (1993) found a GST-like member of the *PRP*1 (pathogenesis related protein) gene family in potato (*Solanaceae tuberosum*). The

PRP1-1 transcripts accumulated following elicitation with *Phytopthora infestans* or filtrates of the fungus. Elevated mRNA levels did not accumulate when potato leaves were subject to heat shock at 40°C, illumination with white light or wounding. Again their findings indicate that hyphal penetration was not responsible for the enhanced transcription of *PRP1-1* suggesting signalling interplay between host and pathogen at the molecular level through soluble elicitors. The amino acid sequence of the PRP1 protein in potato shows high similarity to that of soybean heat shock protein HSP26 (*Taylor et al.* 1990). Further analysis of the *PRP1* gene has revealed the encoded product was a glutathione *S*-transferase (GST1), exhibiting 74 and 75% amino acid sequence identity to 3 auxin-inducible GSTs, accessions Q03663, Q03662 and Q03664, of tobacco (van der Zaal *et al.* 1991). Additionally, 65% identity is shared with a putative GST of tomato, Q9FT22. From the known GST classes, PRP1 shows greatest homology, 35–39%, with tau class GST sequences; accessions from maize *Zm*GSTU1; *Hordeum vulgare* Q9SE57; *Triticum aestivum* Q9RWO2; *Oryza sativa* O65032. Within the tau class, the above sequences share between 66-95% amino acid identity. Similarities with hormone inducible GSTs may suggest transcription of *PRP1-1* results from hormonal alterations occurring in the host plant during pathogenesis.

Employing Suppression Subtractive Hybridisation (SSH) to identify genes in potato leaves, which were enhanced during colonisation by *P .infestans*, Beyer *et al.*, (2001) identified a GST transcript, S1-11B. Transcript expression of S1-11B was found to be higher in susceptible Bintje plants than in control plants 48 h post inoculation with *P. infestans*. Significantly, co-regulated transcripts S2-3G, S1-12A & S2-12B also encoded enzymes of glutathione metabolism, detoxification and transport showing 68%, 60% and 45% amino acid sequence homology to a

Lycopersicon esculentum γ-glutamylcysteine synthetase, *A. thaliana At*MRP 3 ABC transporter and *L .japonicus* cytochrome P450 respectively. Each gene class encodes proteins, which are known to interact with the GST mediated detoxification pathway of xenobiotics. Thus, cytochrome P450s introduce functional epoxides and hydroxyl groups into molecular structures thereby facilitating electrophilic centres suitable for glutathione conjugation. Elevated expression of γ-glutamylcysteine synthetase would be required to elevate the glutathione pool required for conjugation and oxidative stress amelioration. The homologue of the *Arabidopsis At*MRP 3 ABC transporter, which is known to function X-SG transport, may be required for vacuolar deposition of GST conjugated products (Theodoulou 2000; Tommasini 1997; Tommasini 1998).

Upregulation of a further transcript, S1-9D, sharing homology to a WRKY transcription factor of *Arabidopsis*, was also observed in potato leaves colonised by *P. infestans*. WRKYs have been shown to be induced by plant pathogens (Eulgem *et al.*, 1999), and to regulate the expression of NPR1, NON-EXPRESSOR OF PR1, which interacts with a TGA/OBF bZIP transcription factor, which is known to control the expression of *GST6* in *Arabidopsis* (Lebel *et al.*, 1998; Chen and Singh, 1999). Similarly the bZIP transcription factors are known to fulfil roles in xenobiotic stress responses (Singh *et al.*, 2002). Collectively, these results show that during infection potato plants require the up-regulation of pathways normally associated with xenobiotic detoxification, which may be under the regulatory control of a pathogen inducible WRKY transcription factor.

Sharing 92% amino acid sequence homology to that of auxin-inducible *Nicotiniae tabaccum* tau class GST (Van der Zaal *et al.*, 1991; X56266), S1-11B also shared 88% and 77% identity to GST like sequences from *L. esculentum* (Q9SE30)

and *Glycine max* O49235 respectively. Similar to PRP1, placement of S1-11B in the tau class was based on sequence identity at the amino acid level. The Q9SE30 GST sequence of *L.esculentum* was of particular interest, Kampranis *et al.*, (2000) co-expressed the mammalian apoptosis inducer Bax in yeast with the tau class GST, BI-GST/PX, which had been isolated from tomato. Expression of Bax in plant and yeast cells results in the lethal phenotype, thought to be brought about through interaction of the protein and mitochondrial membrane. It has been speculated that interaction at this site results in the opening of a mitochondrial permeability transition pore, a multi-protein complex located between the inner and outer mitochondrial membrane, which results in the release of cytochrome C, and toxicity is related to disruption in oxidative processes. Consistent with a link between Bax induced apoptosis and oxidative stress, intracellular pools of GSH were diminished during Bax expression, as were total phospholipids. The authors found that when Bax was co-expressed with the tomato GST, the lethal phenotype was suppressed and the GSH pool and mitochondrial membrane potential maintained (Kampranis *et al.*, 2000).

Yu & Facchini, (2000) cloned and characterised a tau class GST from an opium poppy, *Papaver somniferum*, cell culture treated with a fungal elicitor prepared from *Botrytis cinerea*. In both cell cultures and developing seedlings, it was found that opium poppy contained a small family of highly conserved tau GSTs that were induced following elicitation. The authors suggested that tau GSTs played a role in the metabolism and translocation of hydroxycinamic acid-CoA esters and cell wall-bound secondary products, as part of a defence and developmental response. Of the pathogen inducible GSTs mentioned so far, the opium poppy GSTs showed very low homology to GSTs with other tau class enzymes. Conservation was most notable,

(56-60% sequence identity) between the *Ps*GST and tau class GSTs from *Gossypium hirsutum*, Upland cotton, Q9M6R4 *Arabidopsis* Q9FUS8 and Q94II0.

It is tempting to speculate that these alignment data may suggest the presence of pathogen-inducible orthologous GST sub classes. Similarly, intra-groupings of GSTs associated with specific functions/origins have been suggested for sigma class GSTs with respect to a nematode specific sub-grouping (Campbell *et al.*, 2002). From the sequence alignment analysis, summarised in Figure 1.5, it can be seen that pathogen elicited (PE) GSTs were placed in apparent discreet groupings within classes phi and tau. *Erysiphae graminis* inducible wheat GST29 was placed in-group PE1, *P. infestans* inducible potato PRP1 and S1-11B in-groups PE2 and PE3 respectively and *Papaver somniferum* elicitable GST in-group PE4. Formation of sub-unit heterodimers within a class (Dixon *et al.*, 1999), may serve to extend the diversity of GST substrate specificity thereby allowing challenges from both biotic and abiotic insults to be met.

It seems probable that complexities observed between groups are also underpinned by more subtle heterogeneity within GST classes. Elucidation of underlying endogenous roles of the GST superfamily of detoxification enzymes may ultimately provide an insight into the interactions occurring at the molecular level between plants and their environment.

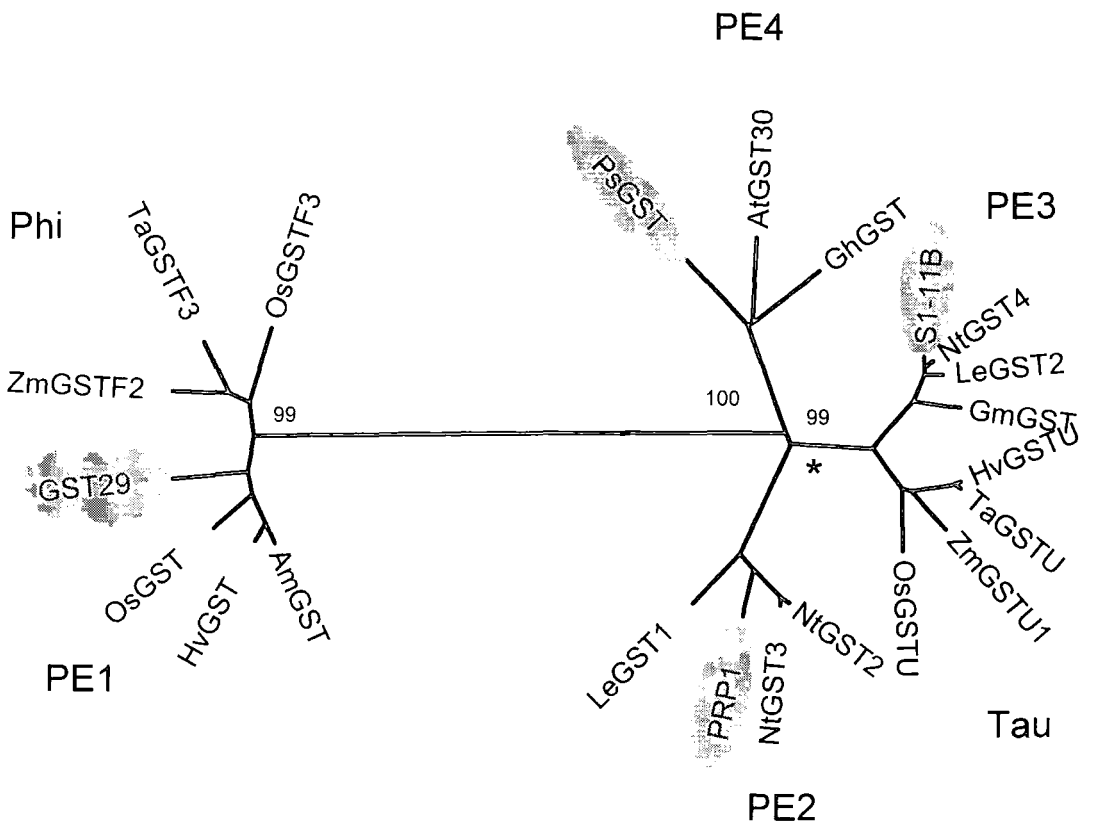

Figure 1.5 Alignment of pathogen elicited (grey shading), tau and phi class GSTs. Aligned sequences with greatest identity at the amino acid level have been clustered together. Class phi, 60-71% identity; class tau 66-95% identity; PE 1, 62-87% identity; PE2, 77-92% identity; PE3, 65-75% identity; PE4, 56-60% identity. *Am* = Black grass; *Hv* = *Hordeum vulgare*; *Os* = *Oryza sativa*; *Zm* = *Zea mays*; *Ta* = *Triticum aestivum*; *Ps* = *Papaver somniferum*; *At* = *Arabidopsis thaliana*; *Gh* = *Gossypium hirsutum*; *Nt* = *Nicotiniae tabaccum*; *Le* = *Lycopersicon esculentum*; *Gm* = *Glycine max*. Digits represent bootstrap branch point confidence, * represents branch point with low confidence.

Phytopathogens are not the only fungal representatives capable of eliciting GST gene transcription in plants. Nehls *et al.*, (1998) reported increased expression of a gene, *EgHypar*, in the roots of *Eucalyptus globulus* seedlings during ectomycorhizal development of *Pisolithus tinictorius*. The full length cDNA *EgHypar* encoded a protein of about 25.5kDa with 66% homology to plant auxin-induced tau GSTs and 68% amino acid identity to prp1-1. Furthermore, treatment of root cultures with cell-free extracts of *P. tinctorius* or indoles secreted by the symbiont including hypaphorine (tryptophan betaine), indole-3-acetic acid or 2,4-dichlorophenoxyacetic acid also resulted in upregulation of *EgHypar*. The authors noted that this was the first molecular evidence that gene transcription in a plant is upregulated by molecules produced by an ectomycorhizal mycobiont.

GST activity toward cinnamic acid was reported in cell cultures of the French bean *Phaseolus vulgaris* (Edwards and Dixon, 1991). It was shown that treatment with a fungal elicitor prepared from the cell walls of a bean fungal pathogen, *Colletotrichum lindemuthianum*, elevated GST activity toward cinnamic acid 2-3 fold. However, Dean and Devarenne (1997) provided evidence against the involvement of GSTs in conjugating cinammic acid and suggested that cytosolic ascorbate peroxidase enzymes led to the conjugation of cinammic acid instead. Interestingly, the induction of peroxidases by fungal elicitors is a well characterised part of the defence response and may account for the increased conjugating activity toward cinnamic acid (Dean & Devarenne, 1997).

Chick pea blight, *Asochyta rabei*, is an aggressive fungal pathogen, which attacks all aerial parts of the plant resulting in epinasty, water soaking and necrosis. These symptoms are associated with the production of Solanopyrone mycotoxins A & C in the fungus, which bring about membrane dysfunction of the host cells. Hamid

and Strange (2000) found that treatment of chickpea shoots with solanopyrone elevated GST levels 1.3 fold. Furthermore treatment of shoots with 150μg and 300μg of the safener dichlormid, a known GST inducer, resulted in shoots being 2.5 and 2.7 times less sensitive to solanopyrone. It was shown that when solanopyrone was incubated with GSH *in vitro* a conjugate was formed, which exhibited lower toxicity to chickpea cell cultures. However, *in vitro* or *in vivo* metabolism of solanopyrone A by chickpea GSTs was not demonstrated.

There is evidence that of the small number of diverse phytopathogenic and symbiotic fungi tested, all excrete compounds that elevate plant GST levels. In all cases it has been observed that hyphal penetration was not required to elicit such responses in host plants. The diversity of fungi eliciting GST expression includes *Erisyphae graminis* an obligate phytopathogen of wheat, *Botrytis cinerea* a mould causing fungus of fruit crops and the oomycete *Phytophthora infestans*, which causes late blight of potato. The latter is better classified among diatoms and algae rather than near ascomycetes and bascidiomycetes (Judleson, 1997). In addition, GST levels are also elevated during ectomycorhizal development in *E. globus* roots by the mycobiont *P. tinctorus*. It seems possible that glutathione *S*-transferases in plants may have endogenous roles for regulating production of antimicrobials during pathogenesis and symbiotic development or detoxifying phytotoxins produced by pathogenic fungi, which may be essential during the infection process (figure 1.5.1).

Figure 1.5.1 Generalised model of possible GST involvement during plant pathogen interaction. ARE, anti-oxidant responsive element; XRE, xenobiotic responsive element; WRKY, BZIP transcription factors.

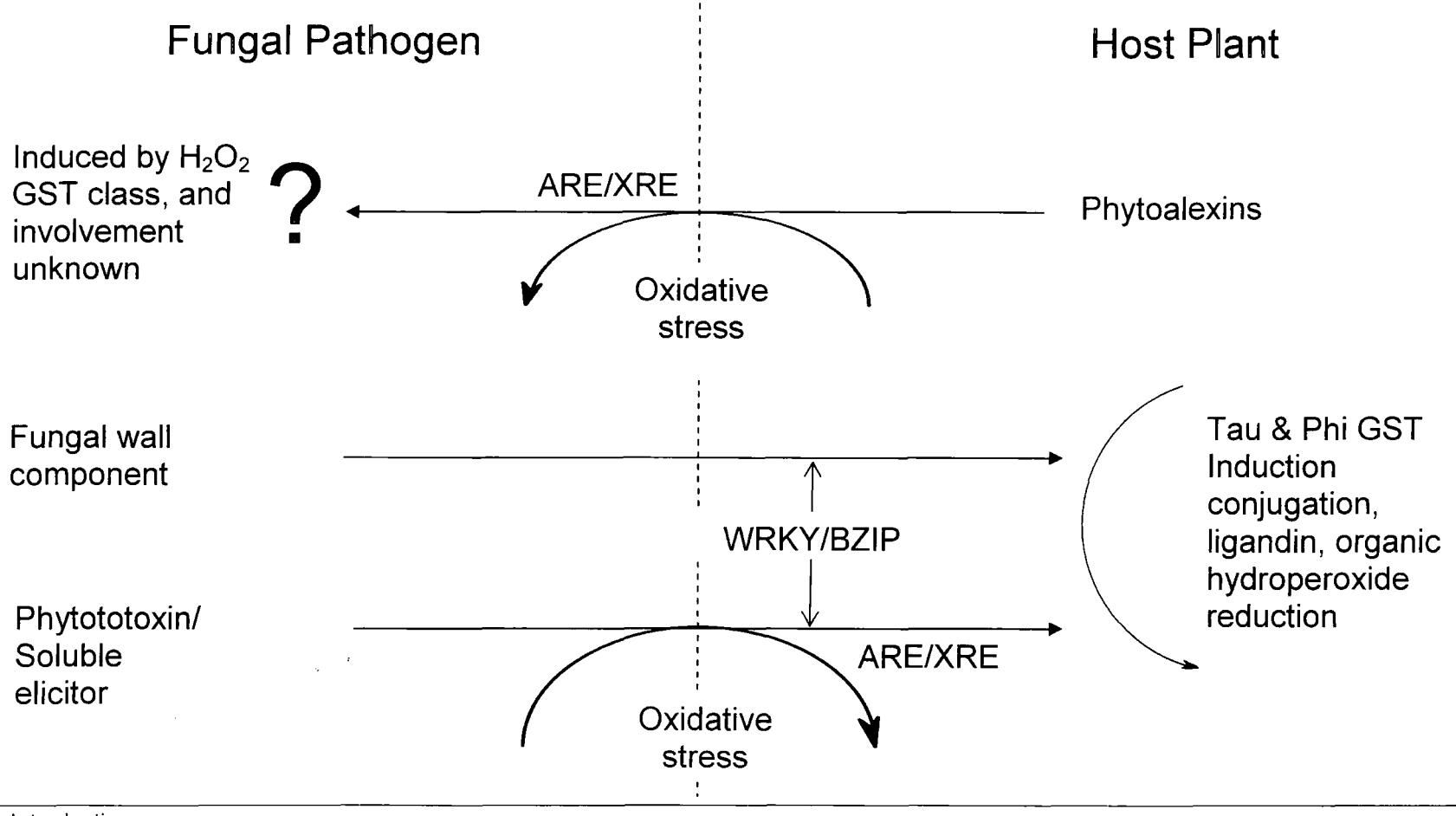

1.6 Fungal GSTs

The role of fungal glutathione *S*-transferases in pesticide and endogenous metabolism is poorly documented, with the evolutionary relationships of fungal GSTs in both saprophytes and pathogens being undefined. Several fungal GST sequences have been identified and cloned, though with the exception of GST-Y1 & GST-Y2 of *Issatchenkia orientalis* (Tamaki *et al.*, 1999), their function in xenobiotic detoxification remains largely unclear. The *Saccharomyces cerevisiae*, *Aspergillus nidulans* and *Neurospora crassa* genome sequencing projects have proved useful in identifying the diversity of fungal GSTs present. However, the lack of sequence information on GSTs in phytopathogens may be attributed, as suggested by Yoder and Turgeon (2001), to the slow speed of the fungal community to initiate genome wide sequencing projects. Recently genome sequencing databases for the agronomically important pathogens *Phytophthora infestans*, *Phytophthors sojae*, *Mycosphaerella graminicola*, *Magnaporthe grisea* and *Blumeria graminis* have become available, allowing advances in the understanding of the diversity of detoxification systems present in phytopathogenic fungi to be made.

There are several economic reasons for studying GSTs in phytopathogenic fungi. Considering the economic importance of crop disease, it is of interest to elucidate the detoxifying activity of GSTs toward fungicides in phytopathogenic fungi, in order to optimise the production of new and existing fungicides. Thus, rapid detoxification of fungicides by phytopathogens will reduce the efficacy of the pesticide. Characterising fungal GSTs may therefore assist in identifying a potential resistance mechanism toward fungicides. In addition a study of fungal GSTs may also uncover novel detoxifying activities and provide new insights into the evolution of the GST gene superfamily.

1.6.1 GSTs in Filamentous Fungi

In 1982, Wackett & Gibson demonstrated the presence of several GST activities in the filamentous fungi *Cunninghamella elegans*. Different ratios of activity toward the two substrates 1-chloro-2, 4-dinitrobenzene (CDNB) and *p*-nitrobenzyl chloride were obtained in different extracts, as were distinct thermal denaturation curves of GST activity. The activity of GSTs in *C. elegans* has since been found to be about 50% higher than previously reported with a specific activity of 20.8 nmol min^{-1} mg^{-1} protein determined with CDNB as the substrate (Zhang *et al.*, 1996). Recently Cha *et al.*, (2001) purified a glutathione *S*-transferase from *Cunninghamella elegans,* which had a specific activity toward CDNB of 2.162 μmol product formed min^{-1} mg^{-1} pure protein (table 1.6.4.1). Immunological studies revealed this GST bore no relationship to alpha, mu or pi class GSTs, although some cross-reactivity with antibodies raised to a theta GST was determined. The estimated Mr of the purified *C. ele*gans GST was 51 kDa with the subunit monomer being estimated at 27 kDa, confirming that the enzyme was a dimer. Following N-terminal sequencing, and cloning of the respective cDNA a new GST class, termed gamma, was identified in *C. elegans*, consisting of 2 distinct genes. The respective proteins, *Ce*GST1-1 and *Ce*GST2-2, were dimers with native masses of 59400 Da and 59800 Da and displayed specific activity toward CDNB of 2.04 and 0.075 umol min^{-1} mg^{-1} pure protein respectively. Placement of the fungal-specific gamma GSTs within the superfamily, as mentioned previously, shall be examined in chapter 6.

Zhang *et al.*, (1996) concluded that *C. elegans* would make a useful model organism for the study of xenobiotic metabolism. To date however, there has been little reported evidence for the formation of glutathione conjugated xenobiotics formed *in vivo* in fungal species. Furthermore, LCMS profiling of pesticide metabolism in 62

saprophytic and phytopathogenic fungal species spanning 24 genera, including *Cunninghamella*, has failed to identify *in vivo* glutathione conjugation toward a diverse range of xenobiotic pesticide substrates (Ramma, Bayer crop science *pers comm.*, 2002). Azerad (2000) noted that despite GSTs occurring in all fungi examined, albeit at low concentrations, the formation of thioethers of glutathione with endogenous or exogenous substrates has never been described. However, Tamaki *et al.*, (1991), reported that the yeast *Issatchenkia orientalis* detoxified *o*-dinitrobenzene (*o*-DNB) through conjugation to GSH, with the resulting processed *S*-(2-nitrophenyl)cysteine catabolite being released into the medium. Additionally, in the yeast *Saccharomycopsis lipolytica*, metabolism of the fungicide pentachlorophenol was shown to be initiated by GST mediated conjugation to GSH, which following subsequent processing the catabolised derivative was methylated by *S*-adenosylmethionine-dependent thiol methyltransferase and excreted from the cell (Hall *et al.*, 2001; Drotar & Fall, 1985). Thus, GST-mediated detoxification of xenobiotics in the majority of fungi tested has been shown to be a rare process, with conjugation being shown to operate in concert with catabolic and excretory mechanisms.

1.6.2 Induction of Fungal GSTs

Pemble & Taylor (1992) noted that in the yeast *Saccharomyces cereviseae*, the gene encoding the regulatory protein Ure2p had sequence similarity to that of the theta class GSTs of *Drosphila melonagaster* and maize. The Ure2p protein however did not demonstrate GST activity in *S. cereviseae* (Tamaki *et al.*, 1999). GST activity in the yeast *Isatchenkia orientalis* toward *o*-DNB, has been determined (Kumagai *et al.*, 1988). Sheehan & Casey (1992) confirmed these findings in the same strain of *I.*

orientalis, but not in other fungal species or other strains of *I. orientalis* where, *o*-DNB was not found to be an effective inducer of GSTs. Table 1.6.2 details the distribution of GST activities in crude yeast extracts toward *o*-DNB. Recently the expression of 2 yeast GSTs (Y-1 & Y-2) in *I. orientalis* were found to be induced by treatment with 200 μM *o*-DNB which caused an arrest in cell growth (Tamaki *et al.*, 1999). Both enzymes were previously shown to conjugate *o*-DNB with GSH *in vitro* (Tamaki *et al.*, 1989) and it was found that *o*-DNB in the medium reduced cell growth until it was apparently detoxified by conjugation with GSH. GST gene expression was shown to be elevated 3h after addition of the substrate. Tamaki *et al.*, (1999) suggested that cell growth was arrested as a result of the *I. orientalis* cells sensing xenobiotics, thus providing a mechanism by which mutations caused by these compounds can be prevented. Up regulation of the GSTs may then result in either primary detoxification or removal of cytotoxic products, such as organic hydroperoxides. Furthermore they postulate that GST Y1 & Y2 may be under the control of either a xenobiotic responsive element (XRE) or an anti-oxidant responsive element (ARE), which are known to be present in the 5' flanking region of many GSTs in animals (figure 1.5.1) (Rushmore *et al.*, 1990; Rushmore *et al.*, 1991).

The possibility that GSTs are elevated in fungi and yeast by the presence of mutagenic xenobiotics as a preventative/protective measure, appears to be supported by the work of Datta *et al.*, (1994) on *Aspergillus ochraceus*. Datta & Samanta (1992) first reported the characterisation of a novel microsomal GST in *A. ochraceus* whilst investigating the fate of xenobiotics in the environment. Subsequently it was determined that a further 3 distinct microsomal GSTs were found to be induced by a range of xenobiotics (Datta *et al.*, 1994). It was found that 100 μM Benzo-(a)-pyrene elevated GST specific activity 3 fold, 100 μM Gammexane

(benzene hexachloride) four fold, with 50 μM 3 methyl-cholanthrene having the greatest effect by increasing GST activity 7.9 fold from 53 nmoles min mg^{-1} to 419 nmoles min mg^{-1} protein. All of these inducers are known to be potent mutagens. It seems likely that expression of GSTs in *A. ochraceus* may also be under the control of either an XRE, or an ARE, (Rushmore *et al.*, 1990; Rushmore *et al.*, 1991) as suggested for GST-Y1 and GST-Y2 in *I. orientalis* by Tamaki *et al.*, (1999).

Table 1.6.2. Distribution of GST activity toward *o*-DNB in crude yeast protein extracts

Organism	Specific activity nmols min mg^{-1}
Issatenkia orientalis	1.58
Canidida vini	1.46
Canidida krusei	1.25
Schizosaccharomyces pombe	0.51
Pichia aganobii	0.32
Trichosporon cutaneum	0.31
Hansenula bimundalis	0.29
Hansenula jadinii	0.26
Hanseniaspora valbyensis	0.23
Saccharomycodes ludwigii	0.22
Hansenula wingei	0.20
Saccharomyces bisporus	0.17
Hansenula anomala	0.16
Saccharomyces chevalieri	0.15
Saccharomycopsis lipolytica	0.15
Pichia farinosa	0.14
Rhodotorula minuta	0.14
Hansenula silvicola	0.13
Pichia pseuodopolymorpha	0.13
Rhodotorula rubra	0.13
Saccharomyces uvarum	0.13

Data after Kumagi *et al.*, (1988) originally expressed in mU/mg, converted to nmoles min mg^{-1} crude protein, on the basis that one enzyme unit was defined as the amount of enzyme that produced 1 μmol of nitrite per minute.

1.6.3 GSTs in phytopathogenic fungi

GSTs, or their associated activities, have been identified in a number of fungal pathogens including *Alternaria alternata* (Dowd & Sheehan, 1993), *Fusarium oxysporum* f.sp *melonis* and *Rhizoctonia solani* (Cohen *et al*, 1986), *Phytophthora* spp., (Oros & Komives, 1991), *Botrytis cinerea* (Prins *et al.*, 1999) and the white rot fungus *Phanerochaete chrysosporium* (Dowd *et al.*, 1997). In addition Di Ilio *et al.*, (1993) have characterised a unique GST in the plant bacterial pathogen *Xanthomonas campestris* and designated this homodimer composed of 22 kDa sub-units as *Xc*-GST-4.5.

1.6.3.1 *Alternaria alternata*

Alternaria fungal pathogens are responsible for a number of diseases in wheat such as leaf blight caused by *Alternaria triticina*. Chlorotic, oval or eliptical lesions appear on the leaf surface, which develop and darken in colour at the borders of the lesions. In addition, other *Alternaria*-induced symptoms include black point, which results in a brown to black darkening of wheat pericarps at the germ end of the kernel with most economic seed losses resulting from seed discoloration. Some *Alternaria* spp., however, are saprophytes producing black moulds and are not technically fungal pathogens (http://wheat.pw.usda.gov/ggpages/wheatpests.html).

Dowd and Sheehan (1993) successfully purified a 20kDa monomeric GST from *Alternaria alternata*, having a low specific activity toward CDNB at 0.3 μmols min mg^{-1} pure protein and lacking activity toward other substrates (table 1.5.4.1). These results were comparable to the activities observed with purified GSTs isolated from the bacteria *Serratia marcescens* and *Proteus mirabillis* (*Pm*GST-7.3) with specific activity toward CDNB of around 0.16 μmols min mg^{-1} protein determined in

each case (Di Ilio *et al.,* 1991). The monomeric enzyme from *A. alternaria* is unusual as GSTs, with the exception of those in class lambda, had previously been found to occur as either homo or heterodimers. At present, no sequence data or further characterisation of the *A. alternaria* GST is available.

1.6.3.2 *Fusarium oxysporum*

A major health risk to both humans and livestock posed by fungal phytopathogens is illustrated by head blight caused by *Fusarium* spp. Grains infected by this pathogen accumulate the trichoethecene mycotoxin (Steyn & Stander, 1999), with consumption by pigs resulting in feed refusal, vomiting, gastrointestinal and dermal irritation or necrosis and immunological reactions (Matthies *et al.*, 1999). Furthermore, the trichoethecene nivanol has been shown to enhance Aflatoxin B_1 (AFB-1) induced hepatocarcinogenesis and liver cell cancerous foci in male rats (Ueno *et al.*, 1992).

GST activity was detected in *Fusarium oxysporum* fsp. *melonis* and *Rhizoctonia solani.* GST specific activities of preparations derived from the mycelia of *Fusarium* were determined toward CDNB and found to be 40-60 nmol min mg^{-1} protein (Cohen *et al.*, 1986). These activities were considerably lower than those obtained from *A. alternata.* However, the specific activities in *Fusarium* were derived from crude extracts and GSH affinity chromatography purified preparations were increased to 35.4 μmols min mg^{-1} protein (table1.6.4.1). These activities, are comparable to those determined for similarly processed GSTs from mammalian and insect sources. The purified GST preparations from *Fusarium* contained polypeptides with sub unit masses (25kDa) being similar to Mr 22-29 kDa plant, mammalian and insect GSTs (Cohen *et al.*, 1986).

1.6.3.3 *Botrytis cinerea*

The first reported GST cloned from a phytopathogenic fungus, *BcGST*, came from the grey mould *Botrytis cinerea*, a pathogen with broad host specificity (Prins *et al.*, 2000). The amino acid sequence was deduced and found to have high sequence homology with several GST like proteins found in other micro-organisms including *scherichi coli* Yfcg (44/57), *Burkholderia cepacia* (42/56), yeast Ure2 (36/55) and a putative GST from *Schizosaccharomyces pombe*. However, GST activity of the *GST1* gene product was not demonstrated. It was found that the *GST1* gene contained 2 introns with the open reading frame encoding a 254 amino acid protein. Initially it was postulated that *GST1* may play a role in detoxification of plant antimicrobials such as phytoalexins or hydrogen peroxide and function during pathogenesis. Transgenic disruptants failed to show any effect of disruption to *GST1* on virulence. However, elevated transcript levels of *Bc*GST in *B. cinerea* during the infection process and in response to 6 hr treatment with 5 mM hydrogen peroxide were reported. Expression of *Bc*GST was suggested to be under the control of a stress responsive element in the promoter region (Prins *et al.*, 2000).

1.6.3.4 *Phytophthora* spp.

Phytophthora spp. belong to the oomycete fungi, with *P. infestans* causing late blight of potatoes, the causal agent of the Irish potato famine during the 1840's (Judelson, 1997). Compared to other fungal classes, oomycetes bear little taxonomic resemblance to higher or true fungi. Thus they are separated from other fungi by phylogeny, cytology, physiology and genetics (Oros & Komives, 1991, Ingram, 1981; Burnett, 1987; Sansome, 1987 & Oros *et al.*, 1988). Recent phylogenetic studies based on small-subunit rRNA sequences have classed oomycetes closer to diatoms

and brown algae than to ascomycetes and basidiomycetes (Judelson, 1997; Forster *et al.*, 1990; Ilingworth *et al.*, 1991).

Oros and Komives (1991) studied the effect of the phenylamides ofurace, metolachlor, acetochlor, butachlor, dimethachlor, propachlor, CGA2921, metalaxyl, RE-26745, benalaxyl, furalaxyl, LAB-149202 on the GST activity of *Phytophthora* spp. using CDNB as a substrate. It was concluded that GST activity does not confer sensitivity or tolerance phenylamide pesticides in *Phytophthora* spp., However, GST activity toward CDNB was significantly increased in *P. infestans* following 24 h exposure to 1 mg mL^{-1} metalaxyl. GST conjugating activity toward these fungicides was not investigated.

1.6.4 Activities of GSTs in Fungi

Although *o*-DNB, as previously mentioned, can, in some instances, be an effective inducer of fungal GSTs, Kumagi *et al.*, (1984) reported very low specific activities of yeast GSTs toward this substrate (table 1.6.2). It can be seen that all specific activities are low, with the most appreciable activities found in *Canidida krusei*, *Canidida vini* and *Issatchenkia orientalis*, which were all lower than 1.6 nmol min mg^{-1}. It appears that the use of *o*-DNB would be better restricted to the induction of yeast and fungal GSTs than using this as a GST substrate for determining activities in crude extracts.

In contrast, the classic electrophillic GST substrate, CDNB, has been used to determine GST activity in a range of fungal phytopathogens as well as in yeast (table 1.6.4.1). In yeast, the GST activities with CDNB were more than 10 fold those observed with *o*-DNB. It is fair to note however, that the same fungal species were not used, therefore this is merely an illustrative point rather than a truly comparative

one. Table 1.6.4.1 details GST activity in a range of fungi, both in crude extracts and following purification. As can be seen the specific activities in crude extracts range from 3.8 nmol min mg^{-1} protein in *Phaenocrite chryosporium* to 57 nmol min mg^{-1} in *Aspergillus ochraceus*, demonstrating the highest activity recorded. Following purification activities are increased around 50 fold, with the exception of *Fusarium*. Here GST specific activities were increased 750 fold, indicating that the GSTs in this species are particularly amenable to isolation.

Table1.6.4.1 Distribution of glutathione *S*-transferase activities toward CDNB, found in crude extracts and subsequent purification from a range of fungal phytopathogens and two yeast species.

	Specific activity nmol min mg^{-1} protein	
Organism	Crude protein	Purified protein
Fusarium oxysporum	53	3540
A. ochraceus (C)	57	2850
A. ochraceus III	50.0	2690
A. ochraceus V	50.0	2600
A. ochraceus IV	50.0	2350
A. ochraceus II	50	2280
Cunninghamella elegans	12.6	2162
A. ochraceus VII	50.0	2110
A. ochraceus I	48.3	2008
A. ochraceus (B)	38.8	1938
M.circinelloides	9.6	1910
A. ochraceus (A)	31.2	1560
Mucor circinelloides	4.8	960
Rhizopus spp.	57	ND
Rhizoctonia solani	56	ND
Penicillium digitatum	56	ND
Chaeomium sp.	52	ND
Alternaria alternata	50	300
A. ochraceus VI	5.0	ND
A. niger	46	ND
Pythium spp.	30	ND
P. chryosporium	3.8	ND
Cunninghamella elegans	20.8	ND
Symbiotaphrina kochii	18.6	ND

Table 1.6.4.1 foot note, *Fusarium oxysporum, Rhizoctania solani*, *Alternaria alternata*, *Aspergillus niger*, *Chaeomium* sp.p., *Rhizopus* spp., and *Pythium* data after Cohen *et al.*, (1985). *Cunninghamella elegans* data after Zhang *et al.*, 1996 and *S.kochii* data after Shen & Dowd, 1991. *Mucor circenelloides* data after Dowd & Sheehan, 1999. *Phaenocryte chryosporium* data after Dowd *et al.*, 1997. *Aspergillus ochraceus* I-VII data after Datta & Samanta, 1992. *Aspegillus ochraceus* A-C data after Datta *et al.*, 1994. All data was originally expressed in mU/mg, converted to nmoles min mg, on the basis that one enzyme unit was defined as the amount of enzyme that produced 1μmol of product per minute at 25°C. ND = No data.

1.7 Aims and Objectives Associated with this programme

In this study the evidence for the detoxification of fungicides by glutathione conjugation and the potential involvement of fungal GSTs was examined. Initially the project was focused on fungicides used in wheat and the evidence for their glutathione mediated detoxification in the host plant and pathogen *Septoria tritici* (*Mycosphaerella graminicola*). Subsequently GSTs were identified and characterised in other fungal pathogens using a genomics led approach.

- To determine the importance of GSTs and GSH conjugation in the detoxification of fungicides.
- To compare the rates of GSH-mediated detoxification in wheat of the fungicide fluquinconazole with that of the herbicide fenoxaprop-P-ethyl, which is known to be metabolised by GSTs in this species.
- To identify GSTs in phytopathogens of wheat
- To identify GSTs in other phytopathogens
- To functionally characterise the activity and potential roles of fungal GSTs.

Chapter 2.0 Materials and Methods.

2.1 Reagents, antibodies and agrochemicals

Unless otherwise stated, all chemical reagents and antibodies were purchased from Sigma-Aldrich Company Ltd, Fancy rd, Poole, Dorset, BH12 4QH. Molecular biology reagents and enzymes were obtained from Promega UK Ltd. Agrochemicals (table 2.1) were kindly supplied by Bayer Crop Science, Lyon, France.

Table 2.1 The following agrochemicals were kindly supplied by Aventis Crop Science (now Bayer Crop Science, Lyon).

Common name	IUPAC	Chemical class	Mode of action	Spectum of activity
Fungicides				
Zoxamide	(*RS*)-3,5-dichloro-*N*-(3-chloro-1-ethyl-1-methyl-2-oxopropyl)-*p*-toluamide	Benzamide	Inhibition of nuclear division & disruption of the microtubule cytoskeleton	Oomycetes. *Plasmopora, Phytophthora, Pseudoperonospora*
Quinoxyfen	5,7-dichloro-4-quinolyl 4-fluorophenyl ether	Phenoxyquinolene	Alterion of signal recognition during the infection process	*Erysiphae spp.*
Fluazinam	3-chloro-*N*-(3-chloro-5-trifluoromethyl-2-pyridyl)-α,α,α-trifluoro-2,6-dinitro-*p*-toluidine	Pyridine	Uncoupling of mitochondrial respiration, and interaction with cellular thiols	*Botrytis cinerea, Peronospora, Ventura inequalis, Phytophthora infestans.*
Chlorothalanil	tetrachloroisophthalonitrile	Aromatic	Reacts with cellular thiols	Broad spectrum fungicide
Picoxystrobin	methyl (*E*)-3-methoxy-2-{2-[6-(trifluoromethyl)-2-pyridyloxymethyl]phenyl}acrylate	Stroburilin	Complex III of fungal respiration: ubiquinol oxidase, Qo site	Broad spectrum used on cereals only, *Septoria tritici, Rhyncosporium*
Azoxystrobin	methyl (*E*)-2-{2-[6-(2-cyanophenoxy)pyrimidin-4-yloxy]phenyl}-3-methoxyacrylate	Stroburilin	Inhibition of ubiquinone-cytochrome c redutase	Oomycete, Ascomycete, Deuteromycete and Basidiomycete class pathogens.
Cyazofamid	4-chloro-2-cyano-*N*,*N*-dimethyl-5-*p*-tolylimidazole-1-sulfonamide	Cyano-imidazole	Mitochondrial respiration inhibition, Qi site.	*Phytophthora, Plasmodiophora, Plasmopora, Pythium*

Table2.1 continued

Fluquinconazole	3-(2,4-dichlorophenyl)-6-fluoro-2-(1*H*-1,2,4-triazol-1-yl)quinazolin-4(3H)-one	Azole	Disruption of ergosterol biosynthesis through inhibition of 14 α-demethylase.	Ascomycetes, Deuteromucetes and Basidiomycetes
Ofurace	(*RS*)-α-(2-chloro-N-2,6-xylylacetamido)-γ-butyrolactone	Analide	Multiple sites of action	Oomycetes
Herbicides				
Ethofumesate	(*RS*)-2-ethoxy-2,3-dihydro-3,3-dimethylbenzofuran-5-yl methanesulfonate	benzofuranyl alkylsulfonate	Speculated to inhibit fatty acid biosynthesis	
Fenoxaprop-P-ethyl	(RS)-2-[4-(6-chloro-1,3-benzoxazol-2-yloxy)phenoxy]propionic acid	Aryloxyphenoxy propionic acid	Disruption of plant lipid synthesis by inhibition of acetyl CoA carboxylase (ACCase)	
Safeners				
Fenchlorazole ethyl	1-(2,4-dichlorophenyl)-5-trichloromethyl-1*H*-1,2,4-triazole-3-carboxylic acid			
Dichlormid	*N*,*N*-diallyl-2,2-dichloroacetamide			
Mefenpyr diethyl	(*RS*)-1-(2,4-dichlorophenyl)-5-methyl-2-pyrazoline-3,5-dicarboxylic acid			

2.2 Synthesis of reference metabolites

Pesticide standards (100 mg) (table 2.1) were individually dissolved in ethanol/acetonitrile (1:1 v/v) to a concentration of 10 mg mL^{-1}. To 100 μmoles of pesticide were added 100 μmoles reduced glutathione (GSH) dissolved in double distilled water (ddH_2O), with the pH being adjusted to pH 9.5 with triethyl amine. The volume was made up to 6 mL with ddH_2O and the mixture incubated for 36 hr at room temperature. The reaction mixture was adjusted to 20 mL with acetone and stored at –20°C for 24 h - 48 h. Conjugates were dried via a rotary evaporation with precipitate being resuspended in 1 mL methanol (Edwards *pers comm.*, 1999).

2.3. Analysis of metabolites

2.3.1 Thin layer chromatography of pesticides and their respective glutathione conjugates.

The presence of chemically synthesised *S*-glutathionylated pesticide conjugates was determined by thin layer chromatography (TLC). Of each methanolic preparation, 2 μL were independently applied to a Merck 20 x 20 cm silica gel 60 F_{254} TLC aluminium sheet, with 2 μL of each respective parent pesticide (10 mg mL^{-1}) run along side each reaction mix. The TLC plate was developed for 4 h - 6 h in butan-1-ol: acetic acid: ddH_2O (4:1:1). Pesticides and glutathione-conjugates were visualised by UV illumination, with conjugated reaction products staining positive after spraying with 0.3% (w/v) ninhydrin in acetone and brief heating with a hair dryer.

2.3.2 HPLC metabolite detection

After diluting the reference conjugates 1:2 with ddH_2O, 50 μl was injected onto a Phase Separations S502 reverse phase HPLC column and eluted using a mobile phase mixture of 1% phosphoric acid and an increasing proportion of acetonitrile. The flow rate was 0.8 mL $minute^{-1}$, run time was 40 minutes, with the change in absorbance of the eluant monitored at 264nm. The gradient over 0-36 minutes was 20-80 % acetonitrile, 36-42 minutes 80-100 % acetonitrile with a 3 minute wash from 42-45 minutes 100% acetonitrile. Following the wash the gradient was returned to 5% acetonitrile 95%, 1% phosphoric acid (Cummins *et al.*, 1999).

2.3.3 Electrospray mass spectrometry

Authentication of reference metabolites was confirmed on a Micromass LCT time of flight mass spectrometer. Glutathione conjugates (section 2.3) were diluted in methanol to a concentration of 100 μM, after assuming 100% conversion of the parent compound to the respective *S*-glutathionylated derivative. Samples were analysed by either direct infusion *via* a Hamilton syringe and automatic pump at 10 μL $minute^{-1}$ or following liquid chromatography using methanol/0.5% formic acid gradient, 0.2 mL minute flow rate, Phenomenex C18 50 mm x 2 mm ODS column. Signal optimisation was achieved with the electrospray source operating in positive or negative mode (analyte dependent), using settings of; cone voltage 30 V, desolvation temperature 120°C (10 μL $minute^{-1}$) or 200°C (0.2 mL $minute^{-1}$).

2.4. Plant material

Seeds of hexaploid wheat, *Triticum aestivum* L. cv. Hunter, were obtained from Plant Breeding International (Cambridge), while maize seeds, *Zea mays* L. cv. Pioneer 3394, and potato, *Solanum tuberosume* cv. *Bintje* were acquired from Bayer Crop Science, Lyon. Wheat and maize were maintained at 25°C under a 16–h photoperiod at a light intensity of 510 μmol m^{-2} s^{-1}. Maize and wheat seedlings were harvested at 10 days with roots and shoots frozen separately in liquid nitrogen and stored at –80°C. Tissues for *in vivo* metabolism studies were harvested fresh and used immediately.

2.4.1. Metabolism and safener studies

The wheat safeners fenchlorazole ethyl, mefenpyr diethyl or cloquintocet mexyl and the maize safener dichlormid were prepared as stock solutions of 10 mg mL^{-1} in acetone. Wheat seed was imbibed in the respective safener for 1 h in 10 mg L^{-1} after dilution with water of the acetone stock solutions. Control wheat seeds were imbibed with 0.1% (v/v) acetone in water. All imbibed seed was then sown on verimculite, watered when necessary with 0.1% (v/v) aqueous acetone or 10 mg L^{-1} of the relevant safener solution and maintained as described in section 2.4.

2.4.2 Metabolism Studies with ^{14}C Fluquinconazole and ^{14}C Fenoxaprop ethyl in ± Fenchlorazole ethyl Treated Wheat Shoots.

[^{14}C] fluquinconazole (1.1 mg 189 μCi, [U-^{14}C] fluquinconazole, specific activity 50 nCi nmol^{-1}) was dissolved in 945 μl acetone, to a final concentration of 4 mM. [U-^{14}C-phenyl] fenoxaprop-P-ethyl (1.3 mg 179 μCi, specific activity 50 nCi nmol^{-1}) was dissolved in 895 μl acetone giving a concentration of 4 mM [^{14}C] fenoxaprop-P-ethyl. Each pesticide (100 μl) was independently diluted with 900 μl acetone and then made up to 20 mL with ddH_2O giving a final concentration of 1 μCi mL^{-1} (20 μM) in each case. Each pesticide solution was dispensed into Eppendorf tubes in 1 mL aliquots. Two wheat shoots were placed in each Eppendorf tube and the top of the tube carefully sealed with Parafilm. Of the remaining 2 mL of each [^{14}C] pesticide, 10 μL of each labelled compound were added to a scintillation tube followed by 4 mL scintillation fluid to determine the administered dose. Radioactivity was quantified after correcting for quenching using an external standard source on a Packard 1600TR Liquid Scintillation Analyser. Wheat shoots were harvested in triplicate every 24 hr for 3 days, frozen in liquid N_2 and stored at –80°C. Radiolabelled metabolites of [^{14}C] pesticides were extracted from the foliage by homogenising 3 times in 2 mL methanol using a pestle and mortar. The slurry was centrifuged at 7000 x g 5 minutes and the supernatant decanted and made up to 6 mL with methanol and radio assayed by scintillation counting. The subsequent methanolic extract was concentrated under vacuum to 200 μL.

The concentrated extracts were analysed by thin layer chromatography using silica gel plates with butan-1-ol, acetic acid, water (4:1:1 v/v) as the mobile phase. Metabolites were identified by UV absorbance and their reaction with ninhydrin (0.3% w/v) after gentle heating with a hair dryer. Radioactivity was visualised using Kodak X-OMAT AR autoradiographic film. Radiolabelled positive spots were scraped from TLC plate in methanol (0.2 mL), prior to scintillation counting.

2.4.2.1 Radiochromatography

Resolution of metabolites of [^{14}C] fenoxaprop P-ethyl was achieved by injecting 20 μL (1:4 v/v dilution in methanol) a Beckman system Gold HPLC system using a Spherisorb 5U ODS1 C18 column (size 250 x 4.6 mm, particle size 5 μm) with the eluent monitored for UV absorbance at 264nm. The mobile phase consisted of 1% H_3PO_4, (buffer A) and CH_3CN (buffer B). Gradient conditions 0 - 0.5 min, 25% B; 0.5 min – 30.5 min, 25 – 60% B; 30.5 – 40.5 min, 60-100% B; 40.5 – 60.5 min, 100 % B; 0.8 mL min^{-1}. After flowing through the UV cell, the eluant was automatically mixed with Packard flo-scint A scintillation fluid at a ratio of 3:1, prior to entering the Beckman flow cell radio detector.

Isocratic separation was also used with the above system under the following conditions. 50 mM potassium phosphate buffer adjusted to pH 6.0 with glacial acetic acid, 12.5% acetonitrile, 35 minutes followed by 100% acetonitrile wash for 10 minutes.

2.4.3 LCMS fenoxpaprop ethyl glutathione conjugate profiling

Wheat shoots (4 g) treated with and without the safener cloquintocet mexyl were harvested at 10 days and cut into approximately 7.5 mm lengths, then incubated on an orbital shaker in 50 mL Murashige and Skoog basal medium containing 50 μM fenoxaprop-P-ethyl, at 100 rpm, at room temperature. Tissue was harvested at 12 h and 24 h, blotted dry and then frozen in liquid N_2 and stored at –80°C until required.

2.4.3.1 Metabolite extraction

Using sand as an abrasive, 2 g frozen tissue was homogenised in 8 mL of ice cold methanol in a cold pestle and mortar. The slurry was then centrifuged (3000 x g, 10 minutes, 4 °C) and the supernatant decanted and the pellet re-extracted twice in 8 mL ice cold methanol. The combined supernatants were then re-centrifuged as described.

2.4.3.2 Metabolite concentration

The methanolic supernatant was then taken to dryness under a constant stream of N_2 and the residue resuspended in 1-mL cold methanol on ice. After removing the precipitate by centrifugation at 12000 x g, the supernatant was retained and stored at –20°C until required.

2.4.3.3 Solvent partitioning of metabolites

Using a constant stream of N_2, 200 μL of methanolic concentrate was dried to completion and resuspended by vortexing in 200 μL ddH_2O to which 200 μL ethyl acetate was added. Following centrifugation, (12000 x g, 2 min) the upper ethyl acetate phase was removed and the aqueous phase repeatedly partitioned until the ethyl acetate phase was clear. Extraction in ethyl-acetate was necessary as a clean up step to remove excess chlorophyll and parent compound. The resulting polar metabolites were placed on ice in preparation for LC- PDAD-MS analysis.

2.4.3.4 LC- PDAD-ESMS

The clarified polar phase, (20 μL) was injected onto a Phenomenex Synergi Polar HPLC column (size 2 x 250 mm, particle size 4 μm, pore size 80 Angstrom) and eluted using a mobile phase composed of 0.5% formic acid with an increasing proportion of methanol. The integration time was 53 minutes and the gradient profile (0-2 minutes 5 % methanol, 5-42 minutes 5-100 % methanol with a 5 minute wash from 42 - 47 minutes 100% methanol. Following the wash the gradient was returned to methanol, 0.5% formic acid (5:95 v/v). The eluant was monitored by photodiode array detection (200-400nm) and electrospray ionisation mass spectrometry operating in the negative mode [M-].

2.5. Fungal cultures

2.5.1 Fungal culture media

2.5.1.1 *Septoria tritici* culture media

Liquid cultures were established in Potato Dextrose Broth (PDB) 24g L^{-1} dH_2O obtained from Sigma, which had been autoclaved for 20 minutes and allowed to cool. Cultures were also maintained on Potato Dextrose Agar prepared in the same way (PDA 39 g L^{-1}) at 12°C. Liquid cultures were maintained at room temperature, 180 rpm on a Thermo Sciences orbital shaker while solid cultures were maintained at 12°C.

2.5.1.2 *Phytophthora infestans* culture media

Cultures for protein extraction were grown in concentrated pea broth. Petit pois peas (Tesco; 300g) were boiled in 500 mL dH_2O in a microwave until soft then homogenised and sieved. The smooth puree and water was combined, with the volume adjusted to 1L with ddH_2O. The resulting broth was autoclave sterilised for 20 minutes. Pea agar was prepared in the same way with the addition of 1.5% (w/v) agar prior to autoclaving (O'Neill pers comm, Bayer Crop Science, 2002).

Fungal cultures for RNA extraction were grown in a dilute pea media. Peas 120 g L^{-1} dH_2O (Tesco) were autoclaved for 20 minutes, drained through 3 layers of mirra cloth, with the final volume adjusted to 1 L. The broth was then autoclaved for 20 minutes.

2.5.2 *Septoria tritici* (*Mycospaherella graminicola*)

Septoria tritici (*Mycospaherella grminicola*) *St*16 was kindly donated by Dr Tim-Joeseph-Horne, University of Bristol, Department of Biochemistry, School of Medical Sciences, University Walk, Bristol, BS8 1TD. Initial liquid cultures were established in PDB containing 10 μg mL^{-1} ampicillin, using an inoculum of 106 sporidia mL^{-1}. Cultures were maintained at 180 rpm on an orbital shaker, room temperature. Six individual 100 mL cultures were grown and the growth curve of *S.tritici* at 22°C determined over a 168 h period, with sampling every 24 h. Cell density was determined by a haemocytometer with the optical density of the media monitored at 600nm. Media was diluted to give an OD less than 1 and a serial dilution in PDB performed in triplicate, the OD 600nm recorded and the cells present counted using a haemocytomer. A standard curve was constructed and growth curve determined at OD 600nm according to the calibration obtained.

2.5.3 *Phytophthora infestans*

Bayer Crop Science kindly supplied virulent cultures of *P. infestans*. Cultures were initially maintained on pea agar. Liquid cultures were maintained in pea broth by inoculation of 5 – 10 pea agar plugs densely colonised by *P. infestans*, with shaking at 120 rpm, room temperature in the dark.

2.5.4 Culturing of *Phytophthora infestans* for total RNA extraction.

Mycelial cultures were maintained on pea agar in Petri dishes. Liquid cultures of 100 mL dilute pea media were inoculated with mycelial pea agar plugs (15 – 20 mm^2) and grown in darkness with constant shaking at 180 rpm, for 12 days on an orbital shaker at 23°C. Mycelia were either harvested or treated with experimental compounds and harvested by vacuum filtration, prior to freezing in liquid N_2 and storage at –80°C. Where required, media was retained and stored at –20°C.

2.5.5 Culturing of *Phytophthora infestans* for protein extraction

Cultures of *P.infestans* were grown for 7 days in concentrated pea media and harvested by vacuum filtration with extensive washing in 50 mM potassium phosphate buffer pH7, 1 mM EDTA, 0.4 M glucose. The fungi were then homogenised using a bead beater in 3 x 30 second bursts in 1-2 volumes 0.1M potassium phosphate pH7, 1 mM EDTA, 1 mM PMSF, 2 mM DTT, 3 x 30 seconds, 4°C. Homogenates were filtered, centrifuged (16,000 x g, 20 minutes, 4°C) and the supernatant adjusted to 80% with respect to ammonium sulphate. The protein precipitate was then collected following recentrifugation.

2.7 Cloning details

2.7.1 Bacterial culture media

All media was prepared as described in standard texts (Sambrook *et al.*, 1989).

2.7.1.1 Luria-Bertani liquid culture media (LB)

LB media composed of 1% (w/v) bacto-tryptone, 0.5% (w/v) bacto-yeast extract and 1% (w/v) NaCl was autoclaved for 20 minutes at 15 lb/sq. in^{-1}.

2.7.1.2 Luria-Bertani agar culture media (LBA)

LBA was prepared in the same way as LB but with 1.5% agar added prior to being autoclaved.

2.7.1.3 SOC Medium

1 L sddH_2O containing 2% (w/v) bacto-tryptone, 0.5% (w/v) bacto-yeast extract, 0.05% (w/v) NaCl, 2.5 mM KCl, with the pH adjusted to pH 7 with 5N NaOH, was autoclaved 20 minutes (15 lb/sq. in^{-1}). Following cooling sterile $MgCl_2$ and 0.22-micron filter sterilised glucose were added to a final concentration of 10 mM and 20 mM respectively.

2.7.2 Oligonucleotides

Table 2.7.2 PCR Primers used in this study were synthesised by MWG Biotech.

BAM H1 primer	5'-CGCGCGGGATCCGGATGAGCCTATTTCTTAGCATCAGC-3'
NCO1 primer	5'-CGCGCGCCATGGGAATCAAAACTGAC-3'
OG2	5'-GAGAGAGGATCCTCGAGTTTTTTTTTTTTTT-3'
OG9 Adapter primer	5'-CGCACTGAGAGAGGATCCTCGAG-3'
*Pi*23(2) NDE1 primer	5'-GTCATATGACCATCAAGCTCTACGCCAAC-3'
Primer 2	5'-GACACTGAGCACAAAGTGTCGTACC-3'
Primer 2b	5'-CGCGGTGGCGGCCGTTACTTACTTAGA-3'
Primer M.porthe_seq	5'-CTGCACAATATTTCAAGCTATAC-3'
*St*16 5' RACE 2	5'-CCCAGTGGGCGATGTCCGCGATGGT-3'
*St*16 5' RACE 3	5'-ATTCGATCTTCTCCGGGGCGTAGCG-3'
*St*16 5' RACE 4	5'-CTCGAGATCAATCCCAATGGCCGC-3'
*St*16 5' RACE adaptor	5'-CTTATACGGATATCCTGGCAATTCGGACTT-3'
*St*16 5' RACE adaptordT	5'-CTTATACGGATATCCTGGCAATTCGGACTTTTTTTTTTTTTTTT TT(AGC)-3'
*St*16dgP1	5'-AARAAYAC5CARAARGARCC5TGGTT-3'
*St*16dgP1b	5'-AARAAYGT5CARAARGARCC5TGGTT-3'
*St*16dgP2	5'-GC5GY5ACCCANCCCCARTG-3'

R = A or G; Y = C or T; 5 = Inosine

2.7.3 Isolation of total RNA

Total RNA was isolated from fungi essentially following the method of Gurr & McPherson (1992). Frozen, harvested mycelia were ground to a fine powder in a sterile pre-chilled pestle and mortar under liquid nitrogen. Equal volumes of extraction buffer, (8 M guanidine hydrochloride, 20 mM MES, pH7, 20 mM EDTA, 50 mM β-mercaptoethanol,) and a mixture of phenol:chloroform:isoamyl alcohol (25:24:1 v/v) were added per mL of powdered fungus. The preparation was then homogenised with two, ten second full speed bursts with a polytron, using a 7 mm probe, with cooling on ice. The slurry was then centrifuged (6000 x g, 20 minutes, 4°C) and the aqueous phase removed and re-extracted until the interface was clean using phenol:chloroform:isoamyl alchohol (25:24:1 v/v) followed by vortexing with an equal volume of chloroform isoamyl alcohol (24:1 v/v), and centrifugation (13000 x g, 5 minutes, 4°C).

To the final aqueous phase, 0.2 volumes of 1 M acetic acid and 0.7 volumes of –20°C ethanol were added and the sample stored over night at –20°C. Following centrifugation (13000 x g, 20 minutes, 4°C), the supernatant was decanted and the pellet washed with 400 µL 3M sodium acetate, pH 5.5, vortexed and centrifuged for 10 minutes. Washing was repeated until the pellet changed from being opaque to being translucent. After a final wash with 70% ethanol, the pellet was briefly air dried and resuspended in 20-30 µL, 0.1% DEPC-treated H_2O. Total RNA was quantified at OD 260 nm, given that 1 OD unit = 40 µg RNA. RNA quality was assessed comparing the ratio of OD260: 280 nm and by gel electrophoresis.

2.7.4 cDNA Synthesis

Total RNA (5 µg) was made up in 18 µL of sterile DEPC-treated H_2O and heated at 90°C, 5 minutes to denature RNA secondary structure. Following a brief centrifugation the sample was frozen in liquid N_2 and allowed to thaw on ice prior to the addition of 5 µL 5 x AMV RT buffer and 3 pmol OG2 primer (table 2.7.2). The volume was adjusted to 25 µL with sterile H_2O and primer annealing achieved by incubation on ice for 15 minutes. To the annealed primers/RNA, 24 µL of reaction mixture containing 10 U RNAsin, 5 µg BSA, 29.17 mM β-mercaptoethanol, 2.08 mM dNTP was added followed by 1 µL AMV reverse transcriptase. cDNA was then synthesised at 42°C, for 45 minutes and then samples were flash frozen in liquid N_2 and stored at –20°C.

2.7.5 PCR Methods

Each polymerase chain reaction (Mullis *et al.*, 1986; Mullis & Faloona 1987) contained 1 µL Taq polymerase, 4.56 µL 11 x buffer (494 mM Tris HCl pH 8.8, 123 mM ammonium sulphate, 50 mM $MgCl_2$, 0.53% (v/v) β-2-mercaptoethanol, 50 µM EDTA pH 8.0, 11.11 mM of each of the four dNTPs, 850 µg BSA), following the addition of template DNA the volume was adjusted to 50 µL with sterile H_2O. Products were then amplified on an appropriate programme (table 2.7.5).

Table 2.7.5 Polymerase Chain Reaction programmes

Programme A				
denaturation		15 cycles		1 cycle
94°C (mins)	94°C (mins)	55°C (mins)	72°C (mins)	72°C (mins)
2	0.5	0.5	1	10
Programme B				
denaturation		5 cycles		1 cycle
94°C (mins)	94°C (mins)	55°C (mins)	72°C (mins)	72°C (mins)
2	0.5	0.75	1	10
Programme C				
denaturation		30 cycles		1 cycle
94°C (mins)	94°C (mins)	55°C (mins)	72°C (mins)	72°C (mins)
0	0.5	0.75	1	10
Programme D				
denaturation	10 cycles decreasing annealing temperature 1°C per cycle			1 cycle
94°C (mins)	94°C (mins)	65°C – 55°C (mins)	72°C (mins)	72°C (mins)
2	0.5	0.5	1	10
Programme E				
denaturation		20 cycles		1 cycle
94°C (mins)	94°C (mins)	55°C (mins)	72°C (mins)	72°C (mins)
0	0.5	0.5	1	10

2.7.6 PCR product visualisation

Following a brief centrifugation, 2 μL of 6 x loading buffer (0.25% bromophenol blue, 0.25% xylene cyanol FF, 15% Ficoll Type 400; in sterile water) was added to 10 μL aliquots of each 50 μL PCR reaction mix. Products were loaded and separated by DNA gel electrophoreisis on a 0.8% TAE (4.84 g Tris-base, 1.09 g glacial acetic acid, 0.292 g EDTA L^{-1}) agarose gel containing 0.002% ethidium bromide at 140 V (Sambrook et al., 1989). To prepare the gel, agarose was melted in the requisite volume of TAE and allowed to cool to hand temperature, with ethidium bromide added and mixed with gentle swirling. A comb was added to the gel mould and the molten agarose poured in. Once set the comb was removed after the gel was placed in the electrophoresis tank and covered with TAE buffer; the gel was then run at 140V for 1h. Following electrophoresis DNA fragments were sized by comparison to 5 μL 1:10 dilution of BIORAD 1Kbp DNA ladder.

2.7.7 Phenol chloroform extraction of PCR products

Residual unincorporated bases and Taq polymerase were removed from the PCR products by 2 extractions in an equal volume of phenol chloroform pH 8, with the phases resolved by centrifugation and the aqueous phase retained (Skipsey *pers comm.* 2000).

2.7.8 Ethanol precipitation of PCR products

The PCR mix (30 μL) was treated with 20% (v/v) 3 M sodium acetate and 2.5 (v/v) of absolute ethanol with incubation on ice for 5 minutes. Samples were then centrifuged at full speed for 5 minutes. The decanted supernatant was discarded and the pellet washed with 100 μL 70% ethanol, followed by centrifugation for 5 minutes. All ethanol was then decanted and the DNA pellet dried for 5 minutes, 55°C (Skipsey *pers comm.* 2000).

2.7.9 Gel purification

Fluorescent bands of either plasmid or PCR products were identified on the UV transilluminator and cut from the gel following minimal exposure to UV. Gel slices were transferred to Eppendorf tubes and weighed. Three volumes of BioRad "Prep-a-gene" binding buffer were added to each gel slice and incubated at 55°C, with occasional mixing until the gel had dissolved. 10 μL of silica fines was added and vortexed thoroughly, followed by 5 minutes of mixing by hand. Samples were then centrifuged at maximum speed in bench top centrifuge for 5 minutes, with the resulting liquid decanted and discarded. The silica pellet was resuspended and washed twice with washing buffer, followed by 2 washes with 70% ethanol and centrifuged at maximum speed for 5 minutes. All of the ethanol was decanted and the pellet dried at 55°C prior to being resuspended in 10 μL sddH_2O.

2.7.10 Ligation of PCR products into pGEM-T easy vector

The DNA tube containing pGEM-T easy vector was briefly centrifuged to sediment the contents. The ligation mix contained 5 μL 2X rapid ligation buffer, 1 μL pGEM-T easy vector (50 ng), 3 μL gel purified PCR product (2.7.9), 1 μL T4 DNA ligase (3 Weiss units). The reaction was mixed by pipetting and incubated at 4°C over night.

2.7.11 Transformation of ligated vector into Epicurian *E.coli* XL10-Gold ultracompetent cells

XL10-Gold ultracompetent cells were thawed on ice and aliquoted into 2 100 μL lots. To each 100 μL aliquot of *E. coli* cells, 4 μL β-mercaptoethanol was added, gentle mixed and incubated on ice for 10 minutes. Following incubation either 2 μL of ligated pET11d, pET24a or pGEMT easy ligation mix containing the insert was added to one tube and 2 μL of the pET11d of pET24a self-ligation added to the remaining tube. Tubes were then incubated on ice for 30 minutes, heat pulsed for 30 seconds in a water bath (42°C) and placed back on ice for 2 minutes. 0.9 mL of pre-heated (42°C) SOC medium was then added followed by shaking at 225 rpm, 37°C for 1 hr. After centrifugation (1 minute, 140000 x g) the cells were resuspended in 100 μL SOC medium plated on to Petri dishes containing LB agar (Luria-Bertani medium, Sambrook *et al.*, 1989), containing 100 μg mL^{-1} of the requisite antibiotic added as a selective marker, using a sterile spreader. Plates were incubated overnight at 37°C.

2.7.12 Cloning of *StGSTX1* homologue fragment from *S. tritici*

Degenerate primers *St*16dgP1, *St*16dgP1b and reverse primer *St*16dgP2 were designed (table 2.7.2) to *Aspergillus* and *Botrytis* GST sequences. Primers *St*16dgP1 and *St*16dgP1b were used in combination with *St*16dgP2 and a fragment amplified from *S.tritici* cDNA using PCR programme A (table 2.7.5). Reaction products were separated on a 0.8% TAE agarose gel (2.7.6) gel purified (2.7.9), ligated into pGEMT easy (2.7.10) and then transformed into epicurean *E. coli* XL10-Gold (2.7.11). The plasmid was then prepped (2.7.19) and submitted for automated sequencing (University of Durham sequencing service). Following sequencing, the reaction was repeated using *St*16dgP1b and OG2 (table 2.7.2) and the amplification product separated, purified and sequenced as above.

2.7.12.1 5' prime RACE (Rapid Amplification of cDNA ends) of *StGSTX1* fragment

From the deduced sequence of the *S. tritici* GST homologue, primers were designed (table 2.7.2) for use in 5 prime RACE to determine the DNA sequence required to amplify the entire coding region. Primers *St*16 5' RACE adaptor and *St*16 5' RACE adaptor dT were generously donated by Dr. S. Casson, University of Durham.

2.7.12.2 cDNA synthesis for 5' RACE

cDNA was synthesised from *S. tritici* total RNA (2.7.3, 2.7.4) using primer St16 5' RACE 1 designed toward the 3' end of the sequence of the GST homologue (table 2.7.2) and AMV reverse transcriptase. Without gel purification, the cDNA was cleaned up using a BIORAD Prep-A-Gene DNA purification kit (2.7.9).

A poly A tailing reaction of the cDNA was performed by incubating, 17 μL cDNA, 2.5 μL dATP, 2.5 μL 10 x buffer 4, 2.5 μL sdH_2O at 94°C for 3 minutes, thereby denaturing cDNA secondary structure, followed by quenching on ice. To the reaction, 10 U of terminal transferase were added and incubated for 45 minutes on ice, followed by 15 minutes at 37°C. Terminal transferase was then heat inactivated at 70°C, 10 minutes.

2.7.12.3 5' PCR RACE 2

5' RACE PCR 2 was performed on the tailing reaction containing 4.5 μL 11 x buffer (2.7.5), 5 μL oligo dTTP adapter primer, 5 μL primer *St*16 RACE 2 (table 2.7.2), 5 μL template and 1 μL Taq polymerase all contained in 29.5 μL sddH_2O. Following heating at 94°C, 2 minutes, enrichment of oligo dTTP cDNA was achieved by 5 cycles of amplification using programme B (table 2.7.5). A PCR product was then amplified by PCR programme C (table 2.7.5).

2.7.12.4 Test PCR

A test PCR was performed using PCR programme A (see 2.7.5) extended to 30 cycles using primers *St*16 5' RACE 3 and *St*16 5' RACE 4 (table 2.7.2), containing 1 μL of a 1:20 dilution in sddH_2O of the PCR derived template (2.7.12.3).

2.7.12.2 5' PCR RACE2

5' PCR RACE2 was performed using PCR programme C using primers *St*16 5' RACE 3 and *St*16 5' RACE adaptor (table 2.7.2) containing 5 μL 1:20 dilution of the template PCR (2.7.12.3). Reaction products were separated on a 0.8% TAE Agarose gel (2.7.5), gel purified (2.7.9), ligated into pGEMT easy (2.7.10) transformed into epicurean *E. coli* XL10-Gold (2.7.11), plasmid prepped (Wizard, Promega) and submitted for automated sequencing to the University of Durham sequencing service.

2.7.13 Sequencing of 6E23 clone containing *Mg*GST insert from *Magnaporthe grisea.*

2.7.13.1 Vector

The *Mg*GST insert obtained from *Magnaporthe grisea* cDNA was supplied from Bayer Crop science (Lyon, France) in the p2.5 NW vector in *E.coli* clone 6E23.

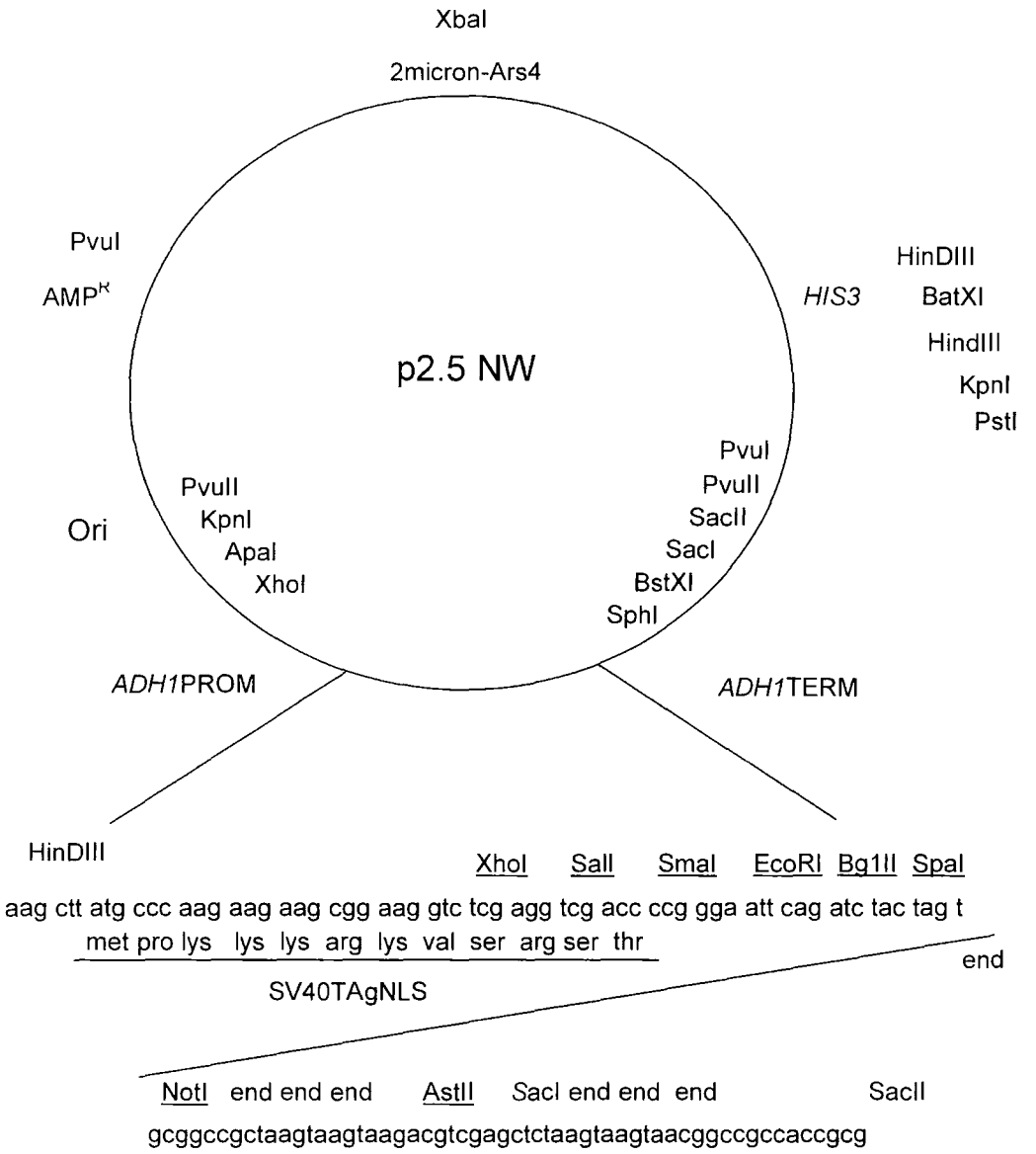

Figure 2.7.13.1 p2.5 NW vector detailing restriction sites, ampicillin marker, Ori, Autonomous Replicating Sequence, *ADH1* alcohol dehydrogenase promoter and cloning region.

2.7.13.2 Primer design

To determine the full sequence of the *M. grisea* *Mg*GST insert, the specific primer M.Porthe_seq (table 2.7.2) was designed to ATP synthase, which was also present in the p2.5NW vector, upstream of the *Mg*GST 5' coding region.

Following sequencing, using the M.porthe_seq primer, the *Mg*GST specific primer 2 was designed 461 base pairs from the beginning of the *Mg*GST coding sequence and used to sequence upstream. From the ATP synthase sequence data primer 2b was designed specific to the p2.5NW vector down stream from the poly A tail, functioning in reverse compliment.

From the determined sequence data a contig was constructed, with the deduced amino acid sequence sharing 65% sequence identity with *Bc*GST of *Botrytis cinerea* (accession Q9HF89) (Prins *et al.*, 2000).

2.7.13.3 Sub cloning *Mg*GST into pET11d expression vectors.

From the sequence data, primers were designed with engineered restriction sites to facilitate sub cloning into pET 11d. The combination of NCO1 and BAM H1 primers (table 2.7.2) generated a PCR product, which was sub-cloned into pET11d.

2.7.13.4 PCR generation of *Mg*GST with restriction sites

Each polymerase chain reaction (Mullis *et al.*, 1986; Mullis & Faloona 1987) contained 1 μL Taq polymerase, 4.56 μL 11 x buffer (see 2.7.5), 34.44 μL

sddH_2O, 2 μL 6E23 plasmid, 5 μL 10 μM NCO1 primer, 5 μL 10 μM BAM H1 primer. A negative control was conducted by replacing the primers with sddH_2O, ensuring PCR products were not the result of contamination.

2.7.14 PCR generation of *Pi*GSTT-1 with restriction sites

Both OG2 and OG9 primers (table 2.7.1) were generously donated by Dr David Dixon, University of Durham. *Pi*23(2) NDE1 primer was designed to the 5' sequence of the EST CON_003_02985 obtained from the *Phytophthora* Genome Consortium Database.

Each PCR reaction contained 1 μL Taq polymerase, 4.56 11 x buffer (2.7.5.4), 34.44 μL sddH_2O, 5 μL *P. infestans* cDNA, 5 μL 10 μM *Pi*23(2) NDE1 primer, 5 μL 10 μM OG9 adapter primer, which was complementary to the OG2 primer used to synthesise cDNA from *P. infestans* total RNA originally. A negative control was conducted consisting of 1 μg total RNA replacing cDNA, ensuring PCR products were not the result of genomic contamination.

2.7.14.1 Touch down PCR programme

A PCR amplification product of the theta class GST from *P.infestans* cDNA was obtained by touchdown PCR (programme D). The reaction mix was initially heated at 94°C 2 minutes followed by 10 cycles of 94°C 30 seconds, 65°C 30 seconds, 72°C 1 minute. In this regime, each subsequent cycle the annealing temperature was decreased by 1°C to enrich for template and reduce non-

specific amplification products. When the annealing temperature of 55°C was reached, a further 20 cycles on programme E (table 2.7.5), yielded a specific amplification product (Skipsey pers comm., 2000). Reaction products were separated on a 0.8% TAE Agarose gel (see 2.7.5) gel purified (see 2.7.9), ligated into pGEMT easy (see 2.7.10) and transformed into epicurean *E.coli* XL10-Gold (see 2.7.11).

2.7.14.2 Colony PCR identification of *PiGSTT1* insert positive colonies.

Individual colonies were picked, streaked onto a grided LB agar Petri dish containing 100 μg mL^{-1} kanamycin and dipped into individual PCR tubes containing 1 μL Taq polymerase, 4.56 11 x buffer, 34.44 μL sddH_2O, 5 μL 10 μM *Pi*23(2) NDE1 primer, 5 μL 10 μM OG9 adapter primer. The agar plate was incubated at 37°C overnight and colony PCR tubes were amplified under PCR programme A (table 2.7.5) through 25 cycles . PCR products were separated on a 0.8% TAE agarose gel (2.7.5). A PCR positive XL10-Gold colony was picked and grown in a 10 mL LB overnight culture at 225 rpm, 37°C containing 100 μg mL^{-1} kanamycin and plasmid prepped (see 2.7.19).

2.7.15 Digestion of PCR products

The ethanol-precipitated *Mg*GST pellet was resuspended in 16 μL sddH_2O to which 2 μL 10 x Promega Multicore reaction buffer and 1 μL of both *Nco*1 and *Bam*H1 restriction enzymes were added and incubated at 37°C overnight. 14 μL

of pGEMT-easy vector harbouring the *PiGSTT1* insert were restricted as described replacing enzymes with *Nde*1 and *Xho*1 using Promega 10 x reaction buffer D. Products were separated on a TAE gel (see 2.7.5) and purified (see 2.7.9).

2.7.16 Digestion of pET11d and pET24a expression vector

To a final volume of 20 μL were added 5 μL pET11d vector, 2 μL Promega 10 x Multicore reaction buffer, 9 μL sddH_2O and 1 μL of both N*co*1 and B*am*H1 restriction enzymes and incubated overnight at 37°C. pET 24a was restricted as described replacing enzymes with N*de*1 and X*ho*1 using Promega 10 x reaction buffer D. Products were separated on a TAE gel (see 2.7.5) and purified (see 2.7.9).

2.7.17 Ligation of PCR products into pET expression vectors

On a 0.8% TAE agarose gel (see 2.7.5), 2 μL of each digestion was visualised to determine relative ratio of vector to insert. These were visually quantified against 5 μL 0.3 mg mL^{-1} λ DNA marker.

Vector to insert ratio was standardised to 1:1 using sddH_2O. Ligations containing 4 μL pET11d, 4 μL insert, 1 μL 10 x ligase buffer and 1 μL DNA ligase were incubated overnight at 4°C. Self ligations of pET vectors were established in the same way replacing the insert with 4 μL sddH_2O.

2.7.18 Colony PCR of XL-10 pET transformants containing the recombinant GST insert

For *MgGST* screening, each reaction contained 1 μL Taq polymerase, 4.56 11 x buffer, 33.44 μL sddH_2O, 5 μL 10 μM NCO1 primer, 5 μL 10 μM BAM H1 primer. For *PiGSTT-1*, primers were replaced with Pi23(2) and OG2. Individual colonies were picked, streaked onto a grided LB agar Petri dish containing 100 μg mL^{-1} of the respective selectable marker and dipped into individual PCR tubes. The Petri dish was incubated at 37°C, while the PCR was run on programme A through 25 cycles.

2.7.19 Plasmid preparation of *E.coli* XL10 Gold containing GST inserts

A PCR positive XL10-Gold colony was picked and grown in a 10 mL LB overnight culture at 225 rpm, 37°C containing 100 μg mL^{-1} of the requisite antibiotic. A plasmid mini prep was performed in accordance with Promega Wizard(R) Plus miniprep DNA purification system instructions. The purified plasmid preparation was then sequenced for validation.

2.7.20 Transformation of *E.coli* BL21 with recombinant GSTs

Electrocompetent *E.coli* Bl21 were thawed on ice, transferred to a fresh electroporation cuvette and 1 μL of either pET11d or pET24a vector added and the cells electroporated in a BioRad electroporator set at 25 μF, 200Ω, 2.5 kv. SOC medium (950 μL) was then immediately added and the cells incubated at

37°C for 1 hour (Sambrook *et al.*, 1989). Cells were plated onto a LB agar Petri dish containing 100 μg mL^{-1} selectable marker and incubated overnight at 37°C. Colonies were screened by PCR for the presence of respective rGST sequences.

2.8 Expression and purification of recombinant GSTs from *E. coli* BL21

2.8.1 Expression of recombinant GSTs in *E. coli* BL21

PCR positive BL21 *E. coli* were selected from the agar grid and grown in a 10 mL LB culture containing 100 μg mL^{-1} selectable marker on an orbital shaker at 225 rpm, 37°C until the OD 600 nm was approximately 0.6. 1 mL of cells were harvested and the remaining cells induced by the addition of 1mM IPTG and grown for a further 2.5 hr. Harvesting was performed by centrifugation (3000 x g, 10 minutes, 4°C) using a Jouan BR4 bench top centrifuge.

2.8.2 PAGE analysis of *E.coli* BL21 soluble and insoluble fractions

Both the 1 mL and 9 mL batches of harvested cells were lysed by a 30 second sonication treatment after re-suspending in 0.5 mL 0.1 M Tris pH 7.5, 2 mM DTT, on ice. The soluble protein was then recovered in the supernatant after centrifugation (12,000 x g, 10 minutes, 4°C). The decanted supernatants were then standardised for loading on the basis of original culture volume. Thus, for the 1-mL harvest 12.5 μL of the lysate was added to 12.5 μL 2 x loading buffer (100 mM Tris HCl pH 6.8, 200 mM DTT, 4% SDS, 0.2% bromophenol blue, 20% glycerol), while 2.8 μL of the induced 9 mL culture added to 2.8 μL 2 x loading buffer making total volumes of 25 μL of uninduced and 5.8 μL induced protein to be applied to the gel. The insoluble fractions from the lysates were resuspended in 0.5 mL 0.1 M Tris pH 7.5, 2 mM DTT, and loaded at the same concentrations relative to the soluble lysates. Insoluble lysates were sonicated as above and

induced and non-induced samples were diluted 2 and 18 fold in re-suspension buffer respectively and diluted in 2 x loading buffer, prior to applying 5.8 μL and 25 μL of each respective sample to the gel. Samples were mixed and denatured in sample loading buffer on a heating block at 95°C, for 5 minutes and analysed on 12.5% SDS-PAGE run at 200V (Laemmli, 1970). The glass plates were then carefully removed and the gel washed 3 x 5 minutes in ddH_2O, stained 30 minutes in Gel Code Blue with 30 minutes de-staining in ddH_2O with continuous shaking.

2.8.3 Optimising soluble expression of recombinant GSTs through temperature regulation

E.coli BL21 cells containing pET11d harbouring the *Mg*GST insert were grown in 4 x 10 mL LB at 225 rpm, 37°C containing 100 μg mL^{-1} ampicillin until OD 600 was approximately 0.6. Each culture was then induced with 1 mM IPTG and grown under the following regimes.

10°C, 225 rpm, 16 hours; 22°C, 225 rpm, 16 hours; 30°C, 225 rpm, 16 hours; or 37°C, 225 rpm, 3 hours.

Cells were harvested and analysed by SDS PAGE as described above.

2.8.4 Glutathione affinity chromatography purification of *Mg*GST from BL21

E.coli BL21 cells expressing recombinant GST inserts were grown in 80 mL LB at 225 rpm, 37°C containing 100 μg mL^{-1} requisite antibiotic until OD 600

was approximately 0.6. The culture was then induced with 1 mM IPTG and grown for a further 16 hours (225 rpm 22°C). Cells were harvested by centrifugation (3000 x g, 10 minutes, 4°C) in a Jouan BR4 bench top centrifuge. Following resuspension in 20 mM Tris pH 7.5, 2 mM DTT, (Buffer A) the cells were lysed by 30 second sonication on ice. Clarification was achieved by centrifugation at 12,000 x g, 10 minutes, 4°C. An aliquot of the crude supernatant and the insoluble fraction were retained for PAGE analysis. The supernatant was then ammonium sulphate (80%) precipitated and stored at –20°C.

The protein pellets were allowed to thaw on ice and resuspended in 7 mL of buffer (A). A 5-mL Glutathione Sepharose affinity column (Pharamcia Bio-Tech) was equilibrated with 3 column volumes of buffer (A). The protein solution was then loaded at 1 mL a minute and washed with buffer (A) until no further protein was eluted. Buffer (A) + 10 mM reduced glutathione pH 7 was then applied to elute bound material. The flow through and fractions showing minor UV absorbing peaks were analysed by SDS PAGE (12.5% gels).

2.8.5 Hydrophobic interaction chromatography

Hydrophobic interaction chromatography was peformed on a BIO-RAD HRLC system with the eluant monitored for UV at 280nm. The 20 mL glutathione affinity column flow through containing recombinant *Mg*GST protein was equilibrated to 1 M $(NH_4)_2SO_4$ by the addition of an equal volume of 2 M $(NH_4)_2SO_4$. A 25 mL phenyl Sepharose column was equilibrated in 100% buffer A (1 M $(NH_4)_2SO_4$, 1 mM DTT, 50 mM potassium phosphate pH7.2). The protein

sample was applied to the column and separation was achieved using the following gradient at 2-mL min^{-1}. 0 - 10 minutes 100% A, 10 - 30 minutes linear increase to 100 % B, 30 to 45 minutes 100% B, 46 – 50 minutes 100% A. The gradient was halted at 40 minutes on 100% B (50 mM potassium phosphate, 1 mM DTT, pH 7.2) to ensure complete elution in the absence of salt. Then 10 mL 50% ethylene glycol in buffer B was used to wash the column to elute more hydrophobic proteins. Fractions were retained and analysed by 12.5% SDS PAGE.

2.8.6 Anion Exchange Chromatography

Following HIC, fractions containing recombinant rGST, were pooled and dialysed overnight against 2 L 20 mM Tris pH 7.2, 2 mM DTT , 4°C to remove residual salt. A 15mL Q-Speharose fast flow column packed at 4 mL $minute^{-1}$ was charged with 5 column volumes of Buffer B (20 mM Tris, 2 mM DTT, 500 mM NaCl) adjusted to either pH 7.2 or pH 7.8, which was one pH unit above the predicted pI, of pH6.2 or pH6.8, of the recombinant proteins *Mg*GSTX1 and *Pi*GSTT-1 respectively (http://ca.expasy.org/tools/pi_tool.html). The column was then equilibrated in 3 volumes of the respective buffer A (20 mM Tris, 2 mM DTT, pH 7.2 or pH 7.8) and the pH of the dialysed protein adjusted accordingly. The protein sample was then loaded onto the column at 2 mL $minute^{-1}$ and washed with buffer A until no further protein eluted. GSTs were then recovered using a 45 mL 0 – 100% buffer B gradient at 2 mL $minute^{-1}$, with individual 5 mL fractions analysed for GST related activity.

2.8.7 Protein concentration

During chromatography, GSTs were concentrated using a Vivascience vivaspin 20-mL centrifugation apparatus (10 kDa cut off) was used to concentrate the *Mg*GST by centrifugation for 13 minutes, 3000 x g, 4°C. Protein was quantified with Bio-Rad protein assay in accordance with the manufacturers instructions, using γ-globulin as a protein standard.

2.9 Investigation of substrate specificity

Recombinant GSTs were subjected to a range of biochemical analysis based on HPLC and spectrophotometric assays, the latter using a UnicaM Helios α instrument.

2.9.1 GST pesticide conjugation HPLC assays

Glutathione conjugating activity of the purified *Mg*GST toward a range of herbicides and fungicides was investigated including alachlor, metalochlor, atrazine, ofurace, fluorodifen, *S*-ethyl dipropyl thiocarbamate and fenoxaprop ethyl.

Duplicate enzyme assay containing 60 μL 0.2M Tris, pH8.5; 100 μL 100 μg protein mL^{-1}; 10 μL 20 mM pesticide in acetone; 20 μL reduced 100mM glutathione pH 7 were set up on ice and the reaction initiated by incubating for 1 hour at 30°C. Duplicate control assays were conducted by replacing the active protein sample with heat-denatured enzyme as well as replacing the pesticide

with solvent carrier only. Reactions were terminated on ice by the addition of 110 μL methanol (adapted after Edwards & Cole, 1996).

Resolution and quantification of glutathione-conjugated products was achieved using a Beckman system Gold HPLC with a Phenomonex Jupiter C18 column (150 x 4.6 mm, particle size 5 μm, pore size 300A). The UV absorbance of the eluate was monitored at 264nm. The mobile phase consisted of 1% H_3PO_4, (buffer A) and an increasing proportion of CH_3CN (buffer B). The gradient conditions were 0 - 0.5 min, 5% B; 0.5 min – 7.5 min, 5% to 100% B; 7.5 – 9.5 min, 100% B; 9.5 – 10.5 min, 100% to 5% B; 10.5 – 15 min, 5% B.

2.9.2. GST activity toward CDNB (1-chloro-2, 4-dinitrobenzene) assay

In a plastic cuvette 900 μL 0.1 M potassium phosphate buffer pH 6.5 and 25 μL 40 mM CDNB (dissolved in ethanol) were incubated at 30°C for 5 minutes. A 25 μL enzyme sample was then added followed by 50 μL 100 mM reduced glutathione pH 7 and after gentle mixing, the Δ 340nm was recorded over 30 seconds. Appropriate controls were conducted replacing enzyme sample with buffer. The enzymatic rate was calculated in nkat mg protein using the extinction coefficient 9.6 mM^{-1} cm^{-1} (Habig and Jackoby 1974).

2.9.3 GST activity toward α and β-unsaturated aldehydes using vinylpyridine and crotanaldehyde as substrates

In a plastic cuvette, 900 μL 0.1 M potassium phosphate buffer pH 6.5 and 10 μL 10 mM substrate dissolved in ethanol, were incubated at 37°C for 5 minutes. 100 μL of enzyme was added and the absorbance monitored for stability with vinylpyridine 248 nm and 230 nm for crotonaldehyde over 1 minute. The reaction was initiated with the addition of 10 μL 100 mM reduced glutathione pH 7 added and the decline in absorbance monitored at the appropriate wavelength over 1 minute. The non-enzymic rate was determined by replacing the enzyme solution for buffer.

2.9.4 GST activity toward ethacrynic acid

In a plastic cuvette, 900 μL 0.1 M potassium phosphate buffer pH 6.5 and 25 μL 8 mM ethacrynic acid dissolved in ethanol and 25 μL enzyme solution, were incubated at 30°C for 5 minutes. The reaction was initiated by the addition of 50 μL 100 mM reduced glutathione and the Δ 270 nm, 2 minutes at 30°C recorded. Conjugate formation was quantified using extinction coefficient 5 mM^{-1} cm^{-1}.

2.9.5 GST activity toward benzyl isothiocyanate (BITC)

In a plastic cuvette, 950 μL 0.1 M potassium phosphate buffer pH 7 was incubated at 30°C for 5 minutes, followed by the addition of 25 μL enzyme

solution and 10 μL 100 mM reduced glutathione pH 7. The reaction was initiated by the addition of 10 μL 16 mM BITC dissolved in dry CH_3CN, with mixing and Δ 274 nm monitored over 30 seconds. The chemical rate was determined by replacing the enzyme solution with buffer. The overall enzymatic rate was determined using the extinction coefficient 9.25 mM^{-1} cm^{-1}. (Kolm *et al.*, 1995).

2.9.6 GST mediated thiolysis activity toward 4-nitrophenyl acetate

In a plastic cuvette, 50 μL enzyme solution was mixed with 940 μL 200 μM 4-nitrophenyl acetate in 0.1 potassium phosphate buffer pH 7 at 30°C and the background Δ 400nm over 1 minute was determined to correct for hydrolysis due to non-glutathione dependent esterase activity. 10 μL 100 mM reduced glutathione pH 7 was then added and after mixing by inversion, the Δ 400nm monitored over 1 minute to establish the combination of enzymic and non enzymic GST mediated cleavage of the substrate. A control-replacing enzyme with buffer but including glutathione was carried out in parallel to determine the chemical rate in the presence of the thiol. The overall enzymatic rate was then determined using the extinction coefficient 15 mM^{-1} cm^{-1}.

2.9.7 Glutathione peroxidase activity toward cumene hydroperoxide

To a plastic 1mL cuvette were added 500 μL 0.25 M potassium phosphate buffer pH 7 containing 2.5 mM EDTA and 2.5 mM sodium azide, 100 μL 6 units mL^{-1} glutathione reductase in the 0.25 M potassium phosphate buffer

pH 7, 100 μL 10 mM reduced glutathione pH 7 and 100 μL 2.5 mM NADPH in 0.1% (w/v) $NaHCO_3$. After incubation at 37°C for 10 minutes, the cuvette was placed in a spectrophotometer and 100 μL of 12 mM cumene hydroperoxide and 100 μL protein sample added. The Δ 340 nm was determined for 2 minutes and the decline in absorbance due to non-enzymic processes determined by replacing the protein sample with buffer. Results were expressed as nKat mg^{-1} protein using the extinction co-efficient for NADP of 6200 M.

2.10 Biosynthesis and assay of (10*E*,12*Z*,15*Z*)-9-hydro(pero)xy-10,12,15-octadecatrienoic acid (9, (*S*)-HPOT).

2.10.1 Potato tuber protein extraction

Potato tuber var. Desiree was homogenised on ice in 2 volumes of extraction buffer 0.2 M Tris, 1 mM DTT, pH 7.4 using sand as an abrasive. The homogenate was filtered through 2 layers of Mirra cloth and centrifuged at 17,000 x g, 20 minutes, 4°C. The supernatant was decanted and the protein precipitated with 80% ammonium sulphate [561g L^{-1}]. Following centrifugation (17,000 x , 20 minutes, 4°C) the subsequent protein pellet was resuspended in 50 mM potassium phosphate buffer pH 6.4 and desalted via a PD-10 column into 3.5 mL of the same buffer.

2.10.2 Oxylipin assay

To 50 mL of pre-aerated 50 mM potassium phosphate buffer pH 6.4, 400 μL linolenic acid was added and incubated at 24°C for 10 minutes in the dark to minimise autocatalytic peroxidation. Under constant aeration, the reaction was initiated by adding a total of 142.6 mg of potato protein at 2-minute intervals to prevent rapid and complete denaturation of lipoxygenase. Incubation at room temperature was maintained for 1 h, and the reaction then terminated by acidification to pH 3 with glacial acetic acid. Following 15 minutes on ice, 15 mL of cold ethanol degassed with nitrogen was added and the mixture clarified by centrifugation (17,000 x g, 30 minutes, 4°C). The supernatant was then decanted into a clean opaque conical flask.

Two 500 mg Accu Bond C18 columns were washed under vacuum with 3 volumes of ethanol degassed with N_2 followed by 3 volumes of ddH_2O degassed with N_2. The supernatant was applied in equal 3.5 mL volumes to each column and the flow through discarded. Washing consisted of 20 mL ethanol degassed with N_2 with a subsequent 10 mL degassed ddH_2O. Residual water was removed and discarded by a final wash of 5 mL hexane . The linolenic acid hydroperoxide was then eluted from the column with 5 mL of methyl formate. The methyl formate eluates were pooled and dried to an oil like residue which was taken up in 0.5 mL methanol, which had been degassed with N_2. An aliquot, 20 μL was diluted 1:500 in methanol and the wavelength scanned 200 – 400 nm, with linolenic hydroperoxide quantified by the extinction coefficient ε = 25000 M cm^{-1} at 235 nm. The resulting products were stored under N_2 at –80°C.

2.10.3 Liquid chromatography electrospray mass spectrometry of oxylipins

Oxylipins were analysed on a Micromass LCT LC-MS operating in negative ionisation mode. Separation of reaction products was achieved on a C4 reverse phase column (2 x 50mm) at a flow rate of 0.2 mL minute methanol:water (A:B) gradient. 0 – 0.5 min, 5% A; 0.5 – 5 min, 5% to 100% A; 5 – 7 min, 100% A; 7 – 8 min 100% to 5% A; 8 – 13 min, 5% A.

The mass spectrometer was tuned using raffinose (50 μg mL^{-1}) and calibrated with sodium Iodide (200 ng μL^{-1}). Mass ions were obtained under the following parameters. Cone Gas Flow (L/hr) 5, desolvation Gas Flow (L/hr) 600, Polarity ES-, Capillary (V) 3000, Sample Cone (V) 20.0, RF Lens (V) 200, Extraction Cone (V) 6.0, Desolvation Temp (C) 120, Source Temp (C) 120.

2.11 2-D SDS PAGE and western blotting

2.11.1 Protein sample preparation

Phytophthora infestans control protein was desalted on a Pharmacia hi-trap column into 20 mM Tris pH 7.2, 1mM DTT. The sample was concentrated using a Micron Bio separations, Centricon centrifugal filter device at 3000 x g, 20 minutes, 4°C. Concentrated aliquots were precipitated with 80% ice cold acetone, placed on ice for 10 minutes and centrifuged at 12,000 x g, 5 minutes. Pellets were washed in 80% acetone and centrifuged as above. Pellets were then resuspended in 110 μL iso-electric focusing buffer containing 9 M urea, 2 M, thiourea, 4% CHAPS, 1% (w/v) DTT and 2% (v/v) pH 3 to pH 10 ampholytes (Fluka). An Immobiline 7cm, dry strip, pH 3 - pH10 was placed in the protein

solution in a re-swelling tray, covered with Drystrip cover fluid and allowed to re-hydrate overnight.

2.11.2 Electrophoresis 1: Iso-electric focusing

Following an overnight re-hydration, the isoelectric focusing strips were washed with ddH_2O, the acidic end aligned to the anode of the iso-electric focusing tray, secured with moist electro-focusing electrode strips and covered in Drystrip oil. Electrodes were connected and proteins sequentially focused at 500 V for 1h, followed by 1000 V 1hr and 3500 V 1h.

2.11.3 Electrophoresis 2: SDS PAGE

Strips were removed, extensively washed with ddH_2O, and equilibrated for 15 minutes in 50 mM Tris HCl pH 8.8, 6 M urea, 30% glycerol, 10% SDS, 100 mg DTT equilibration buffer containing a trace of bromophenol blue at room temperature. After equilibration the strip was well washed with ddH_2O and placed on top of a 12.5% SDS PAGE gel and covered with 0.1% low melting point agarose containing a trace of bromophenol blue. Once set SDS PAGE was performed in SDS electrophoresis buffer, 25 mM Tris, 192 mM glycine, 0.1% (w/v) SDS at 60 V, 10 minutes rising to 120 V, 1 h.

2.11.4 Western blotting

Hybond-P PVDF nylon membrane, approximately 10% larger than the gel was wetted in methanol for a few minutes and then equilibrated in cold transfer buffer, 15.9 mM Tris, 120 mM glycine (pH 8.1 – pH 8.4). The SDS PAGE gel was equilibrated in cold transfer buffer for 15 minutes. A transfer cassette and sponge pre-equilibrated in transfer buffer was assembled by sandwiching 3 mm paper followed by the PAGE gel, the PVDF membrane and the sponge in the locked cassette. Proteins were blotted across in cold transfer buffer containing an ice block, on a magnetic stirrer at 100 V, 1 h.

2.11.5 Immuno-detection

Following blotting, the membrane was rinsed in TBS (tris buffered saline, 10 mM tris, 150 mM NaCl, pH 7.4), then blocked for 1 h in TBS containing 3% (w/v) powdered milk. The anti-*Pi*GSTT1-serum was then added at a dilution of [1:10,000] and incubated with shaking overnight at 4°C. The membrane was washed for 2 x 20 minutes in TBST (Tris buffered saline Triton X-100, 10 mM tris, pH 7.4, 150 mM NaCl, containing 0.1% Triton X-100), followed by 1 x 20 minute wash in TBS. Secondary antibody (Sigma anti-rabbit alkaline phosphatase conjugate) was then added at a 1:5000 dilution in TBS containing 3% (w/v) milk powder and the membrane incubated for 1 h at room temperature with shaking and subsequent washing as above. Following a final rinse in 100 mM Tris pH 9.5, the blot was developed by adding 33 µL of both nitro blue tetrazolium (100 mg mL^{-1}), dissolved in 70% *N*,*N*,-dimethyl formamide and 5-Bromo-4 chloro 3-indolyl

phosphate (50 mg mL^{-1}) dissolved in *N*,*N*,-dimethyl formamide to 10 mL 100 mM Tris pH 9.5 with the reaction terminated by washing the blot with a large volume of dH_2O.

2.11.6 Silver staining of gels

The SDS PAGE gels were fixed by 2 x 15 minute washes each containing 40% ethanol 10% acetic acid and then incubated for 30 minutes in 30% ethanol containing 5% Na-thiosulphate, 830 mM sodium acetate and subsequently washed 3 x 5 minutes ddH_2O. Silver staining was achieved by a 20-minute equilibration in 14.7 mM silver nitrate followed by 2 x 1 minute ddH_2O washes, followed by Immersion in 200 mM sodium carbonate monohydrate containing 4.92 mM formaldehyde for 2 – 5 minutes. Finally, staining was terminated by immersion in 39 mM EDTA(Na_2) for 10 minutes.

2.12 Raising poly clonal anti-sera to r*Pi*GSTT1

Raising of anti-sera was conducted using Home Office approved, minimal severity procedures at the Department of Biological and Biomedical sciences, University of Durham. Animal welfare and blood letting was performed by animal house staff, Department of Biological and Biomedical Sciences, University of Durham. Harvesting of antisera was supervised by Dr. R Croy, University of Durham.

2.12.1 Pre-immune anti-sera harvesting

Two New Zealand white rabbits, NV29 and NV57 were bled from the ear, yielding approximately 10 mL each and incubated at 37°C, 2 h, to promote blood clot formation. Samples were stored on ice at 4°C overnight, and the sera were decanted off and centrifuged 5 minutes, 12,000 x g, room temperature. The supernatant was then decanted again and re-centrifuged. A few crystals of sodium azide were added to prevent bacterial growth.

2.12.2 Immunisation with recombinant *Pi*GSTT1-1

Recombinant *Pi*GSTT1 was purified to homogeneity (section 2.8.5, 2.8.6) to a concentration of 1 mg mL^{-1}, divided into 2 aliquots for raising antisera to native and denatured *Pi*GSTT1. To one aliquot, SDS was added to a final concentration of 1% (w/v) and heat-treated at 100°C, 10 minutes. For each protein solution, 1 mL, was independently added dropwise to 1mL tiremax Gold adjuvent while vortexing at maximum speed to aid emulsification. It was

necessary to repeatedly draw and expel the emulsion into the syringe for up to 15 minutes to ensure the formation of a stable emulsion. Each rabbit was administered 2 x 200 μL subcutaneous injections of native and denatured *Pi*GSTT1, which was then repeated intramuscularly. At four weeks a test bleed (20 mL) from an ear of each animal was performed and the serum tested for antigenic reactivity to recombinant *Pi*GSTT1, essentially as described in sections 2.8.5 and 2.8.6, using an antibody serial dilution from 1:500 – 1:10,000. Booster jabs were given six weeks post-immunisation using the previous method but replacing Titre-max Gold for Freunds incomplete adjuvant (courtesy of Dr R.Croy). Polyclonal antisera were harvested as described previously, stored at – 20°C and both animals subsequently released to good homes.

2.13 Bio-informatics

An initial database of protein sequences representing major GST classes were obtained with kind thanks from Dr David Dixon, Department of Biological and Biomedical Sciences, Durham, forming the basis of a GST sequence database compiled into DNA for Windows 2.5a (Dr D.P. Dixon 2002). Similarly putative and published plant and fungal GST protein sequences were downloaded from the European Bioinformatics Institute database (EBI) http://www.ebi.ac.uk/) forming the basis of a fungal and plant specific GST database. Multiple sequence alignments were performed by DNA for Windows using Clustal W (Thompson *et al.*, 1994). Web based protein and nucleic acid databases (PGCD - Phytophthora Genome Consortium https://xgi.ncgr.org/pgc/;

COGEME – Consortium for the Functional Genomics of Microbial Genomics - http://www.cogeme.man.ac.uk) were interrogated with plant and fungal GST sequences representing major GST classes (section 1.3). EST (Expressed Sequence Tagged) sequences showing homology to GSTs were identified, retrieved, trimmed to remove any vector sequence and stored in a customised DNA for Windows fungal GST database.

2.13.1 Fungal GST class analysis

Using GST protein sequences obtained from EBI, the relationship of GSTs within and between known GST classes was performed and the similarity to fungal GSTs determined using *PHYLogeny Inference Package* (PHYLIP 3.6. http://evolution.genetics.washington.edu/phylip.html). Protein sequences were initially compiled in DNA for Windows 2.5a (Dr D.P. Dixon 2002) using Clustal W (Thompson *et al.*, 1994) with the resulting sequence file (.seq) being converted to a PHYLIP file (.PHY) in Clustal W.

2.13.2 Alignment editing

The resulting .PHY file was imported into GeneDoc (Nicholas and Nicholas 1997) and gaps (-) at the beginning and end of each sequence in the alignment replaced for question marks to prevent false alignments being made based on gaps. All gaps within each sequence were not altered.

2.13.3 Bootstrapping

Subsequently, the .PHY file was opened in SeqBoot (Felsenstein 1991–2002) and bootstrapping (Felsenstein, 1985) performed on 100 replicates. Bootstrapping randomly introduces variation into the data set through duplication, removal and addition of amino acids without altering the size of the initial data set. Statistical analysis can be performed on the random variation gained from bootstrapping and so provide confidence weightings for branch nodes in the final analysis.

2.13.4 Estimation of distance

ProtDist was used to produce an amino acid-distance matrix on 100 multiple data sets and were analysed using the Jones-Taylor-Thornton matrix (1992). The resulting algorithm was analysed in Neighbour (Felsenstein 1991–2002) using UPGMA (Unweighted Pair Group Method using arithmetic Averages) option, which constructs a tree by successive (agglomerative) clustering using an average-linkage method of clustering. The data was then consolidated in Consense (Margush and McMorris, 1981). A phylogeny tree of the neighbour output was produced using Drawtree (Felsenstein 1990-2002) with the resulting tree being drawn in GhostScript and saved as a Word Meta File (.WMF).

2.13.5 Theoretical 3D molecular modelling of *Pi*GSTT-1 monomer

The predicted protein sequence of *Pi*GSTT-1 was submitted to Swiss-Model (http://swissmodel.expasy.org/) for theoretical molecular modelling based on alignments with GST theta class crystal structures within the database. The resulting PDB received, modelled on 24 sequences, was viewed in Deep View Swiss-PdbViewer (Guex and Peitsch, 1997) downloaded from (http://www.expasy.org/swissmod/SWISS-MODEL.html).

Chapter 3.0 Comparative Metabolism of Fenoxaprop-P-ethyl and Fluquinconazole in wheat.

3.1 Introduction

The use of agrochemicals in modern agriculture exposes both weed and crop species to a wide range of hydrophobic xenobiotic compounds, substances foreign to biological systems that can interact with an organisms' metabolism (Smith, 2000). Glutathione *S*-transferases (GSTs) are an important superfamily of detoxifying enzymes that increase water solubility of hydrophobic compounds via conjugation with the ubiquitous tripeptide glutathione. On the basis of sequence data 4 major plant GST groupings have been classified; Phi, Zeta, Tau and Theta (Edwards *et al.*, 2000).

The role played by plant glutathione *S*-transferases in detoxification of herbicides in crop plants forming the basis of herbicide selectivity has been subject to extensive research. In particular, *in vivo* metabolism of the post emergence herbicide fenoxaprop-P-ethyl by glutathione conjugation mediated by GSTs has been well characterised in *Triticum aestivum* (Cummins *et al.*, 1999; Edwards & Cole, 1996; Romano *et al.*, 1993; Tal *et al.*, 1993; Lefsrud & Hall, 1989). Fenoxaprop-P-ethyl exerts herbicidal activity, in susceptible weed species, through the inhibition of acetyl-CoA carboxylase in meristematic tissue thereby inhibiting the synthesis of fatty acids (Tal *et al.*, 1993). Additionally, *in vitro* metabolism studies with GSTs have been conducted with invasive weed species such as black grass, *Alopecurus myosuroides*. Thus, Cummins *et al.*, (1999) reported that GST activity may confer tolerance in black grass to multiple herbicides by playing a role in oxidative stress tolerance.

In contrast to herbicides, GST mediated detoxification of systemic fungicides in crop species has received little attention. The systemic fungicide fluquinconazole is fully translocated around the plant offering protection against phytopathogenic fungi such as *Venturia inaequalis* (Schnabel & Parasi, 1997) and *Fusarium* spp (Matthies

et al., 1999). Fungitoxic activity results from the triazol group of fluquinconazole competitively binding and inhibiting 14-α-demethylase, a key enzyme in the biosynthetic pathway of ergosterol, leading to the accumulation of eubricaol (O'Neil, *pers comm.*, 2001). Significantly, a consideration of the relative electrophilicity of this fungicide suggests that it may undergo glutathione conjugation as one route of detoxification (Briggs *pers comm.*, 2000).

In addition to the use of herbicides, crop protection is afforded by application of safeners, compounds responsible for up regulation of herbicide detoxifying enzymes in crop species, including GSTs (Davies and Casey, 1999). These have been central in enhancing herbicide selectivity through elevating herbicide metabolism in the crop but not in competing weeds. Frequently, the use of herbicide safeners and fungicides may overlap in agronomic systems with the consequences regarding fungicide detoxification remaining unknown. Presented here are a comparison and assessment of GST activity *in vitro* and *in vivo* mediated metabolism of fenoxaprop-P-ethyl and fluquinconazole in wheat seedlings ± treatment with the safener fenchlorazole ethyl.

3.2 Results

3.2.1 Electrospray mass spectrometry of herbicide and fungicide conjugate standards.

Fenoxaprop-P-ethyl

Glutathione conjugated pesticide standards of fenoxaprop-P-ethyl (figure 3.2.1) were prepared synthetically and authenticated by electrospray mass spectrometry. HPLC ESMS operating in the positive mode identified the glutathione and cysteine conjugates of fenoxaprop-P-ethyl as having respective masses of 459.16 and 273.76 (predicted masses 458 and 272 respectively). In addition the parent compound fenoxaprop P-ethyl and the bioactive metabolite fenoxaprop-P had respective masses of 375.3 and 403.28 (predicted masses 333 and 361 respectively). The elevated mass ions determined were consistent with a CH_3CN adduct being formed during ionisation of the parent ester and acids (figure 3.2.2.). Mass ions obtained reflect the stable isotope distribution of chlorinated compounds. The chemical structures of the metabolites, illustrated in figures 1a-1c, were in perfect agreement with masses derived by HPLC ESMS.

Nucleophilic attack by the thiolate anion of glutathione and cysteine cleaved the ether bond of fenoxaprop-P-ethyl with conjugation occuring on the chlorophenyl ring. Each of these thiol conjugates had an isotope distribution ratio corresponding to the presence of one chlorine atom with the isotopes ^{35}Cl and ^{37}Cl being present 3:1.

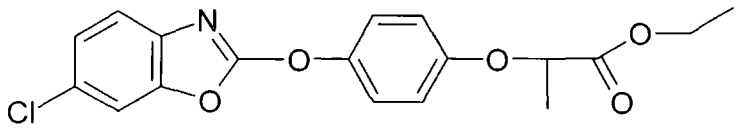

Figure 3.2.1A. Fenoxaprop P-ethyl Mw 361.78

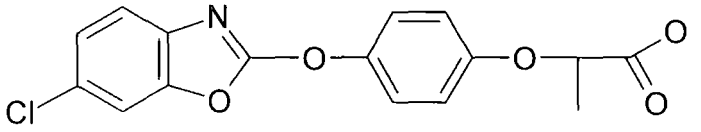

Figure 3.2.1B. Fenoxaprop P (R)-2-[4-(6-chloro-1,3-benzoxazol-2-yloxy)phenoxy]propionic acid.

Mw 333.73

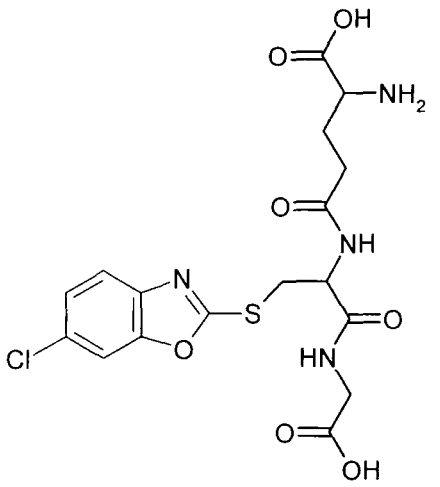

Figure 3.2.1 C. *S*-(6-chlorobenzoxazole-2y-l)-glutathione MW = 458.88

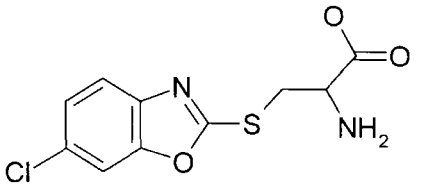

Figure 3.2.1D. *S*-(6-chlorobenzoxazole-2y-l)-cysteine Mw = 272.71

Figure 3.2.1.1 Fenoxaprop-P-ethyl respective authentic metabolites

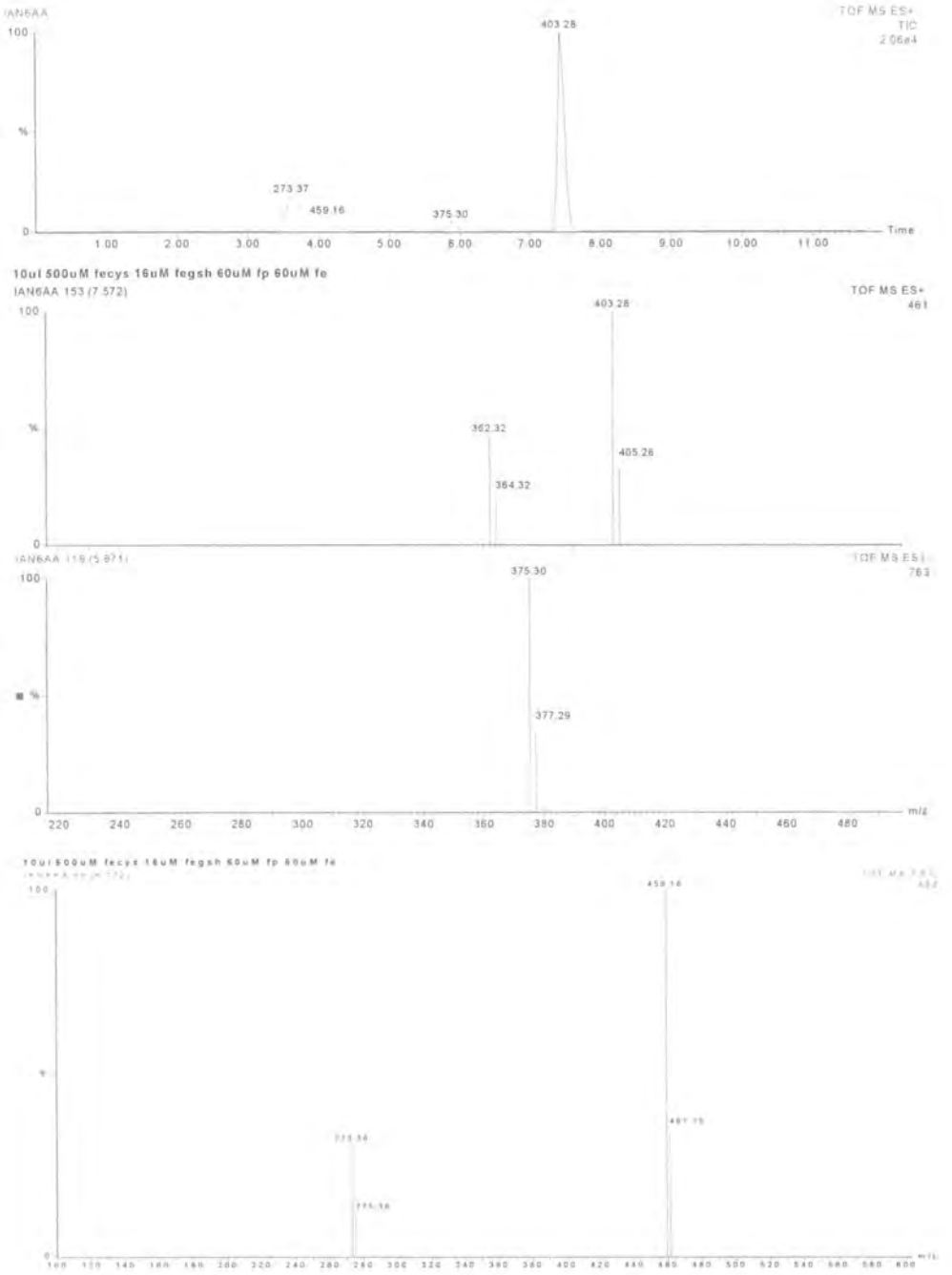

Figure 3.2.2. Chromatographic separation of fenoxaprop-P-ethyl and metabolite standards detailing respective masses determined by ES-MS operating in positive ionisation mode. The herbicide and its metabolites had masses of 403.28 = fenoxaprop-P-ethyl/CH_3CN adduct; 375.03 = fenoxaprop P/CH_3CN adduct; 459.16 = CB-GSH; 273.37 = Cb-cysteine respectively.

Fluquinconazole

The glutathione conjugate of fluquinconazole was prepared synthetically and authenticated by ESMS operating in the negative mode. The conjugate had characteristic isotopic masses of 612.43, 614.43 and 616.43 (figure 3.2.4). These are in agreement with the elucidated structural mass of this conjugate represented in figure 3.2.3b. Incubation of fluquinconazole with glutathione resulted in the nucleophilic displacement of the triazole, and substitution at carbon 2 of the quinazolin structure.

Figure 3.2.3 Fluquinconazole and glutathione conjugate

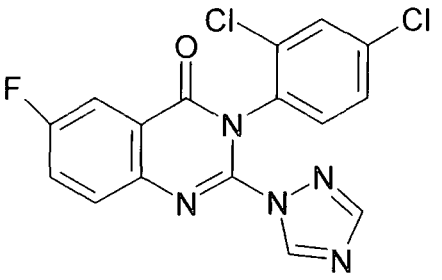

Fluquinconazole 3-(2,4-dichlorophenyl)-6-fluoro-2-(1H-1,2,4-triazol-1-yl)quinazolin-4(3H)-one

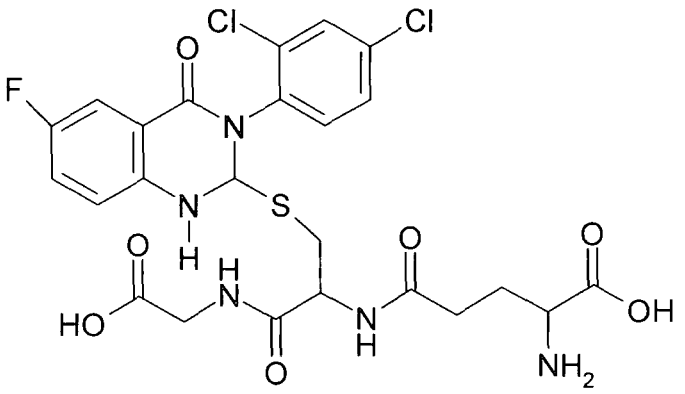

Fluquinconazole-glutathione conjugate Mw 616.46 *S*- (3-(2,4-dichlorophenyl)-6-fluoroquinazolin-4(3H)-one-glutathione.

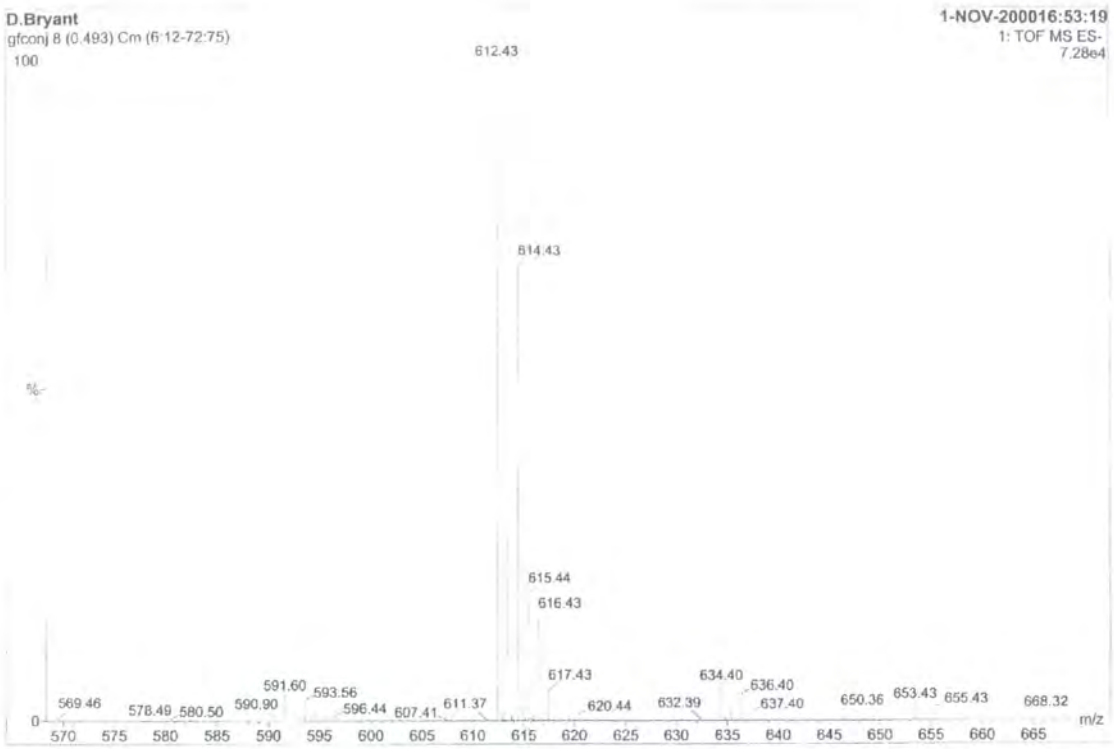

Figure 3.2.4 ESI-MS spectra of 60 μM fluquinconazole-GSH conjugate following nucleophilic displacement of the triazole moiety of fluquinconazole.

To determine whether or not wheat contained GSTs, which could conjugate fluquinconazole, crude extracts were prepared from the roots and shoots of wheat plants treated with a range of safeners, which are known to elevate detoxifying enzymes in this crop (Davies and Casely, 1999). The optimal source of GST activity toward CDNB was determined in the root extracts from plants treated with dichlormid (table 3.2.1) and this source was used to assay GST activity toward fenoxaprop-P-ethyl and fluquinconazole.

Table 3.2.1 Specific activity GSH conjugation toward CDNB using 10-day-old wheat seedlings, independently treated with 4 different safeners, as a GST enzyme source (n = 2).

Treatment	Tissue	nKat mg^{-1}	S.Error
Control	Shoot	1.44	0.043
Control	Root	4.37	0.210
Isoxadifen	Shoot	3.26	0.098
Isoxadifen	Root	7.96	0.404
Cloquincet mexyl	Shoot	4.10	0.074
Cloquincet mexyl	Root	10.68	0.221
Mefenpyr diethyl	Shoot	2.93	0.025
Mefenpyr diethyl	Root	13.54	0.540
Dichlormid	Shoot	3.32	0.206
Dichlormid	Root	23.32	0.368

3.2.2 HPLC pesticide assays

Assays determining the enzymic rate of conjugation toward fenoxaprop ethyl in *Triticum aestivum* have been previously developed (Cummins *et al.*, 1999) and the importance of glutathionylation in the detoxification of this compound well characterised in wheat (Tal *et al.*, 1993). For comparative purposes fluquinconazole was also investigated in wheat. In the first instance, the ability of crude protein preparations to catalyse the glutathionylation of fenoxaprop-P-ethyl and fluquinconazole was determined over a range of temperatures (figure 3.2.5)

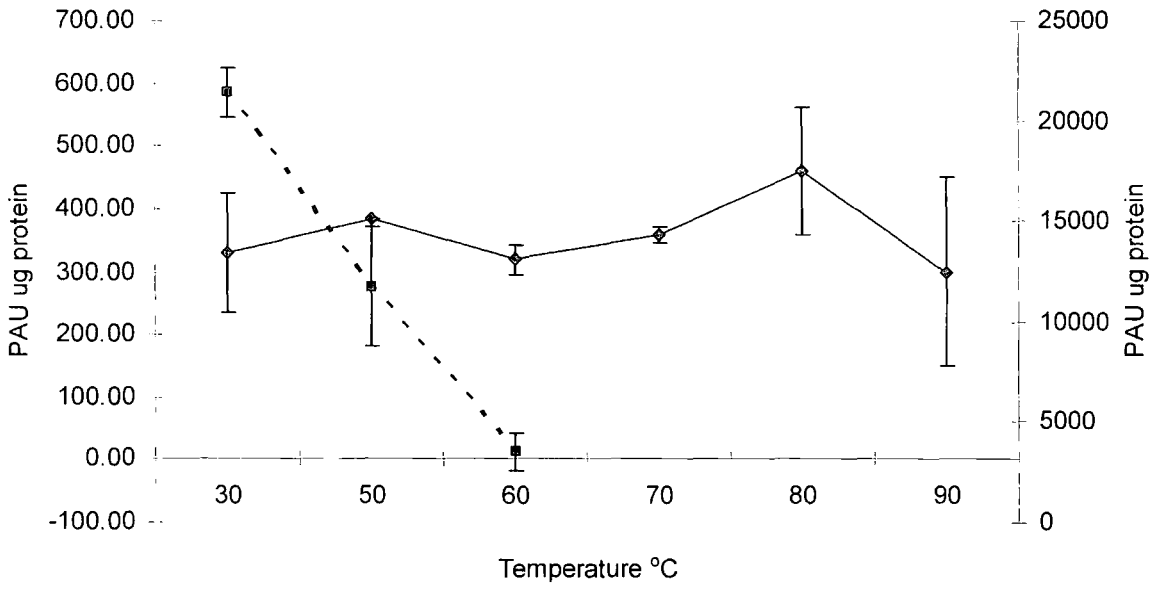

Figure 3.2.5 The effect of varying temperature on net enzymatic glutathione conjugation of fenoxaprop-P-ethyl (dashed line) and fluquinconazole (solid line) using dichlormid treated wheat root extract as a source of enzyme. Control samples contained boiled wheat root extract as a protein source and were deducted from the gross enzymic rate. Vertical bars represent standard deviation (n = 2).

The data in figure 3.2.5 show the effect of temperature on net GST conjugating activity toward fenoxaprop-P-ethyl, with enzyme activity, under standard assay conditions, being 584 PAU μg protein at 30°C while at 60°C no activity could be determined. Conjugating activity toward fluquinconazole remained unaffected by heat treatment with large standard errors being observed. The absence of a reduction in activity with an increase in temperature suggested that either the conjugation of glutathione to fluquinconazole was not protein catalysed or that the activity was due to a thermo stable GST whose catalytic activity was unaffected by temperature. As seen with the GST activity toward fenoxaprop-P-ethyl heat treatment also reduced activity toward CDNB resulting in total inhibition between 70° – 80°C (figure 3.2.6).

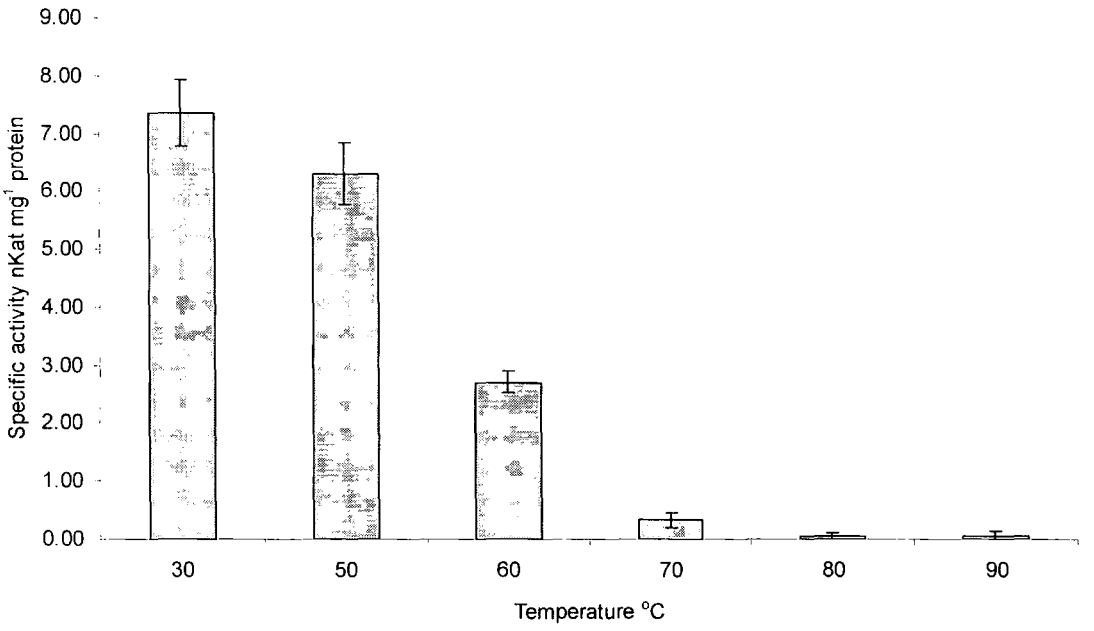

Figure 3.2.6. The effect of temperature on enzymic glutathione conjugation of CDNB using dichlormid treated wheat root as a source of enzyme. Vertical bars represent standard deviation (n = 2)

While the glutathione conjugation of fluquinconazole by extracts from wheat was unaffected by temperature, the presence of protein did appear to promote conjugate formation. Due to its hydrophobic nature, fluquinconazole was essentially insoluble in aqueous buffer and largely precipitated from solution on addition to the assay. It therefore seems that the apparent protein dependent "activity" observed at 30°C and higher temperatures is best explained by the protein in the mix acting as a carrier of the fungicide. Thus the protein may have had the effect of binding fluquinconazole and keeping it soluble in the aqueous phase where it could undergo chemically mediated *S*-conjugation with the water soluble glutathione. To test this possibility, increasing concentrations of γ-globulin were used in the assay and the effect on conjugate formation determined. The results demonstrated that as the non-catalytic γ-globulin was added in the range 0 – 80 μg protein that there was an increase in the glutathione conjugation of fluquinconazole (figure 3.2.6).

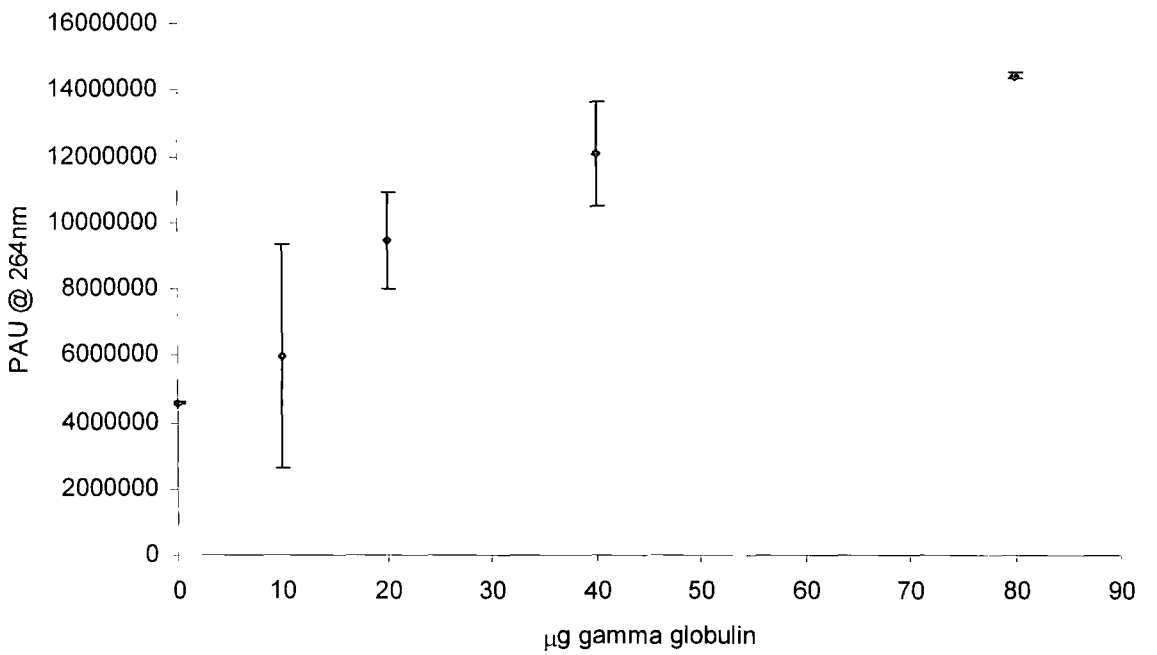

Figure 3.2.6. The effect of varying gamma globulin concentration on net non enzymic glutathione conjugation of fluquinconazole. Vertical bars represent standard deviation (n = 2)

3.2.3 *In vivo* metabolism of [^{14}C] fenoxaprop-P-ethyl and fluquinconazole in wheat shoots treated ± the safener fenchlorazole ethyl.

3.2.3.1 Fenoxaprop-P-ethyl metabolism *in vivo*

Previous studies have shown that treatment of *Triticum aestivum* with the safener fenchlorazole ethyl increased glutathione mediated detoxification of fenoxaprop-P-ethyl *in vivo* and that this was the major route of metabolism of this herbicide in this crop species (Tal *et al.*, 1993). The results of subsequent studies also showed an increase in apparent GST conjugating activity toward fenoxaprop in wheat shoots treated with safeners (Edwards and Cole, 1996).

Wheat shoots (10-day-old) treated with and without fenchlorazole ethyl were incubated with 20 μM [^{14}C] fenoxaprop-P-ethyl and the uptake and abundance of glutathione conjugated herbicide metabolites determined. The data in figure 3.2.3 demonstrate that glutathione conjugate formation was greatest in the safened shoots 48 h after the feed trial was initiated, with 27.8% of the recovered radioactivity being determined as the apparent GSH conjugated pesticide. Use of the safener fenchlorazole-ethyl elevated the accumulation of the GSH conjugated fenoxaprop as compared with non-safened plants by approximately 2 fold (figure 3.2.3). Of total radioactivity recovered in nmol equivalents, the GSH-fenoxaprop conjugate accounted for 27.78% [^{14}C] in extracts from the safener treated wheat and 13.4% in untreated wheat after 48 h (table 3.2.3.) After 48 h there was a decline in the concentrations of the conjugate in the safener treatment to a level similar to those observed in unsafened shoots by 72 h. Following glutathione conjugation the resulting metabolites are sequestered in the vacuole (Edwards *et al.*, 2000). The decrease in conjugate observed after 48 h may be explained by their subsequent

processing in the vacuole (Wolf *et al.*.1996; Martin and Slovin, 2000; Hall *et al.*, 2001; Edwards & Cole, 2000; Coleman *et al.*, 1997).

Interestingly, uptake of total radioactivity following dosing with [^{14}C] fenoxaprop-P-ethyl (figure 3.2.3.2) mirrored the formation of the conjugated metabolite between treated and untreated shoots (figure 3.2.3). Both uptake and conjugate formation were elevated at day 2 in safened wheat shoots as compared with untreated shoots with total radioactivity and conjugated herbicide then being indistinguishable in the two sets of extracts. Unsafened samples followed a more linear rate of uptake of radioactivity over time (figure 3.2.3.2).

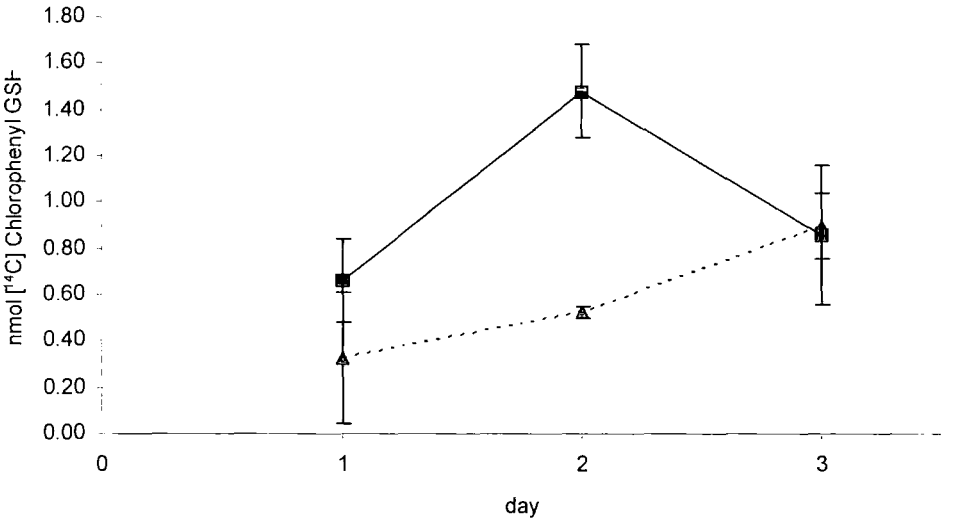

Figure 3.2.3 *In vivo* formation of [^{14}C] fenoxaprop glutathione-conjugated metabolite over a 3 day feed trial in 10-day-old wheat seedlings treated with (solid line) and without (dashed line) the safener fenchlorazole ethyl. Vertical bars represent standard deviation of the mean (n = 3).

Table 3.2.3 Net effect of the safener fenchlorazole ethyl on *in vivo* formation of fenoxaprop-GSH conjugate in 10 day old wheat seedlings.

	Total nmol radioactivity recovered in the shoots		Total nmol Cb-GSH conjugate present		% of dosed herbicide recovered as glutathione conjugate	
Day	-	+	-	+	-	+
1	3.31	3.33	0.32	0.7	9.7	21.0
2	3.89	5.40	0.52	1.5	13.4	27.8
3	4.97	5.30	0.89	0.9	17.9	17.0

N.B. -/+ denotes the absence or use of the safener fenchlorazole ethyl.

The apparent GSH conjugate of fenoxaprop-P-ethyl (Cb-GSH) (metabolite 2) (figure 3.2.3.1) accounted for 10% to 28% of the total radioactivity recovered from wheat shoots (table 3.2.3). A total of seven radioactive spots were identified by TLC (figure 3.2.3.1), indicating that the herbicide had undergone a series of chemical modifications. Metabolite 1, was counted as a single entity, however it appeared that there were 2 polar metabolites, which had seemingly co-chromatographed (figure 3.2.3.1). Metabolites 6 and 7 corresponded to the fenoxaprop following esterase cleavage of the ethyl group and the parent compound fenoxaprop-p-ethyl respectively. Both of the herbicide precursor and bioactive fenoxaprop were more rapidly metabolised in safened wheat shoots with 0.01 nmol [^{14}C] fenoxaprop-P-ethyl recovered at 24 h compared with 0.598 nmol of parent herbicide recovered from unsafened wheat shoots (tables 3.2.4 and 3.2.5). HPLC radio-chromatogrophy resolved fenoxaprop-P-ethyl, fenoxaprop free acid an unidentified product, the apparent GSH conjugate. In addition, the majority of radioactivity observed was in the

form of highly polar compounds, which were not retained on the C18 column and eluted with the injection peak (figure 3.2.3.3).

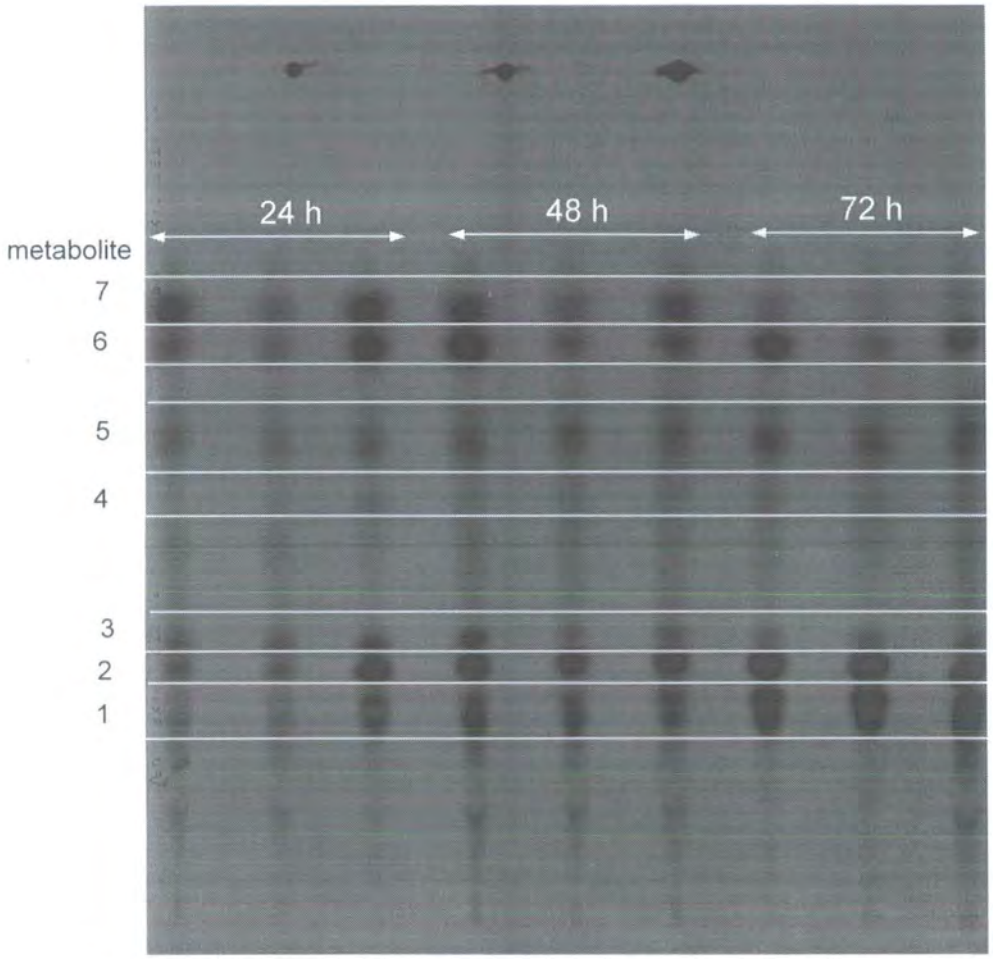

Figure 3.2.3.1 Autoradiogram of TLC separation using butan-1-ol: acetic acid: water (4:1:1) as the mobile phase of [^{14}C] metabolites of fenoxaprop-P-ethyl extracted from unsafened wheat seedlings incubated with the radio labelled herbicide for 24 h, 48 h and 72 h. Metabolites 7 and corresponded to the parent fenoxaprop-P-ethyl, and free ester fenoxaprop-P respectively and metabolite 2, corresponded to the apparent glutathionylated herbicide as determined by control TLC of authentic parent and authenticated metabolite standards.

Table 3.2.4. Distribution of nmols of [^{14}C] herbicide recovered from unsafened wheat shoots following TLC separation using butan-1-ol:acetic acid;HCl (4:1:1) as the mobile phase (n = 3).

spot	24 h		48 h		72 h	
7	0.598	± 0.200	0.454	± 0.098	0.167	± 0.042
6	0.419	± 0.143	0.260	± 0.116	0.473	± 0.152
5	0.181	± 0.022	0.256	± 0.020	0.296	± 0.009
4	0.057	± 0.006	0.095	± 0.011	0.083	± 0.008
3	0.180	± 0.040	0.197	± 0.050	0.183	± 0.023
2	0.324	± 0.163	0.524	± 0.015	0.894	± 0.083
1	0.141	± 0.085	0.348	± 0.076	0.594	± 0.101

Table 3.2.5. Distribution of nmols of [^{14}C] herbicide recovered from safened wheat shoots following TLC separation using butan-1-ol:acetic acid:HCl (4:1:1) as the mobile phase (n = 3).

spot	24 h		48 h		72 h	
7	0.010	± 0.001	0.017	± 0.006	0.014	± 0.001
6	0.394	± 0.031	0.244	± 0.001	0.242	± 0.102
5	0.057	± 0.008	0.072	± 0.014	0.071	± 0.014
4	0.076	± 0.043	0.299	± 0.016	0.217	± 0.046
3	0.160	± 0.036	0.217	± 0.020	0.177	± 0.030
2	0.658	± 0.105	1.477	± 0.117	0.859	± 0.173
1	0.127	± 0.027	0.654	± 0.036	0.542	± 0.065

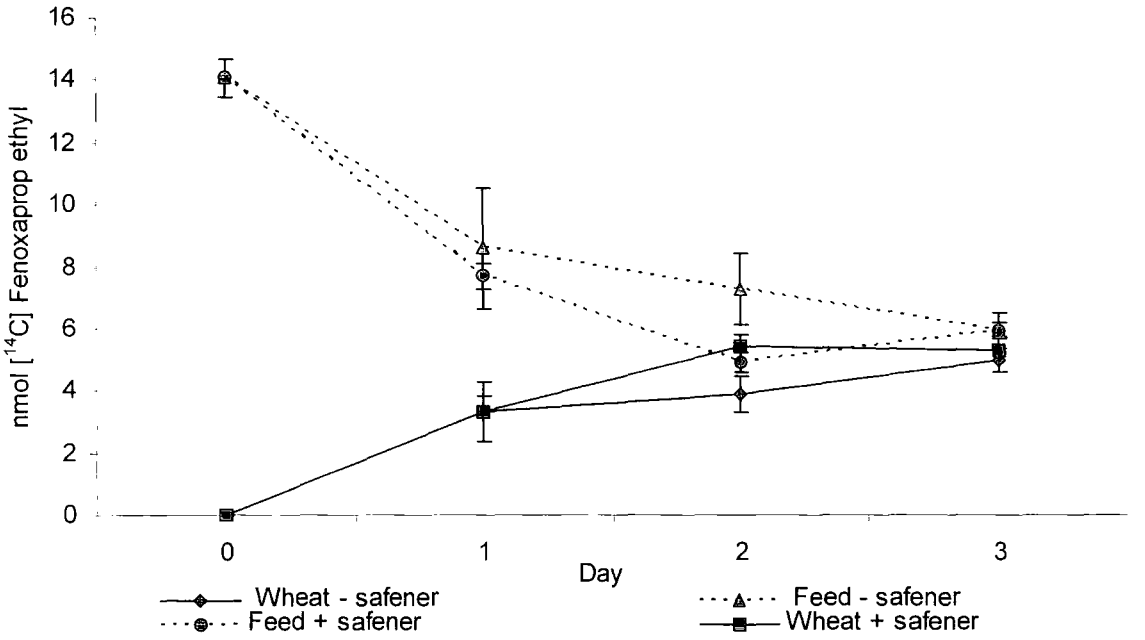

Figure 3.2.3.2 Uptake of radioactivity following dosing with [^{14}C] fenoxaprop-P-ethyl over a 3 day feed trial in ten-day-old wheat seedling shoots. Solid lines represent nmols [^{14}C] extracted from wheat shoots ± pre-treatment with the safener fenchlorazole ethyl. Dashed lines represent nmols [^{14}C] that remained in the feed solution the safener fenchlorazole ethyl. Triangular symbols represent nmol of fenoxaprop-P-ethyl remaining in the feed solution of unsafened plants and diamond symbols represent nmol remaining in the feed solution of safened plants. Square symbols represent nmol radioactive glutathione conjugate extracted from safened with nmol of radioactive glutathione conjugate extracted from unsafened shoots represented by diamonds on a solid line. Vertical bars represent standard deviation of the mean (n = 3).

Glutathione conjugate formation was also monitored by HPLC radio chromatography. The data in figure 3.2.3.3 demonstrate the formation of radioactive metabolites in fenchlorazole ethyl treated wheat shoots following 2 day incubation with [^{14}C] fenoxaprop ethyl. The major metabolites identified were the free acid fenoxaprop-P, formed following esterase cleavage of the ethyl group and a metabolite which, based on earlier reports was the glutathione conjugate (Tal *et al.*, 1993). In addition an unidentified metabolite was detected (3), which eluted just after the GSH conjugate. The majority of radioactivity was accounted for in the form of polar material (1), which may have resulted from metabolism of the conjugate to more polar derivatives. Interestingly, it can be seen that the radioactive glutathione conjugated metabolite (4) did not co-chromatograph identically with the synthesised Cb-GSH standard. *Triticum aestivum* has been shown to have two major thiols, glutathione (γGlu-Cys-Gly) and a homologue hydroxymethyl glutathione (HmGSH; γGlu-Cys-Ser) (Klapheck *et al.*, 1992). In light of the retention differences observed, it was hypothesised that the "glutathione conjugated metabolite" of fenoxaprop-P-ethyl formed *in vivo* in wheat may have possibly arisen from conjugation to HmGSH.

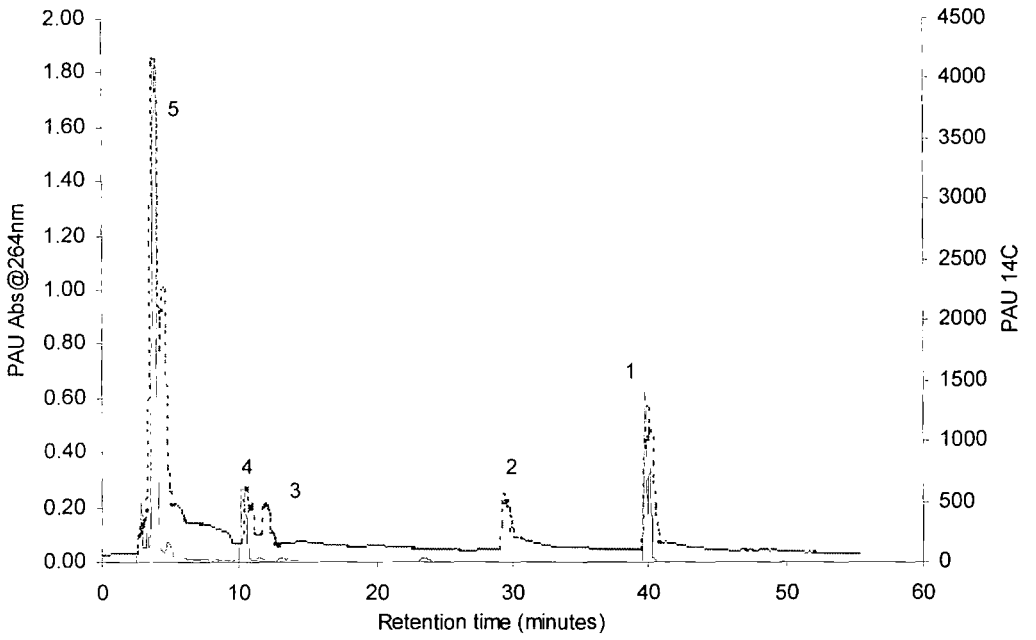

Figure 3.2.3.3. HPLC radio chromatographic separation of [^{14}C] fenoxaprop-P-ethyl and respective metabolites formed *in vivo* after 48h in ten-day-old fenchlorazole ethyl treated wheat shoots. Solid line represents UV absorbance at 264 nm, the dashed line the eluting radioactivity. (1) fenoxaprop-P-ethyl; (2) fenoxaprop-P; (3) unknown metabolite; (4) CB-GSH/CB-HmGSH; (5) Processed metabolites.

An isocratic HPLC chromatographic programme was developed to determine whether the *in vivo* conjugate and authenticated glutathione conjugate were the same. As can be seen in figure 3.2.3.4, the radioactive metabolite did not co-chromatograph with the authentic fenoxaprop-GSH conjugate. It was therefore possible that the *in vivo* metabolite was either a conjugate of HmGSH or was derived from post-synthetic modification of the glutathione conjugate by partial proteolysis. In

light of the hydroxyl group of serine increasing polarity of a potential conjugate, based on the retention time of unknown metabolite the latter hypothesis seemed more probable. However, these results suggest that the metabolite identified as the glutathione conjugate of fenoxaprop-P-ethyl in wheat (Tal *et al.*, 1993) was most likely another polar derivative of this herbicide.

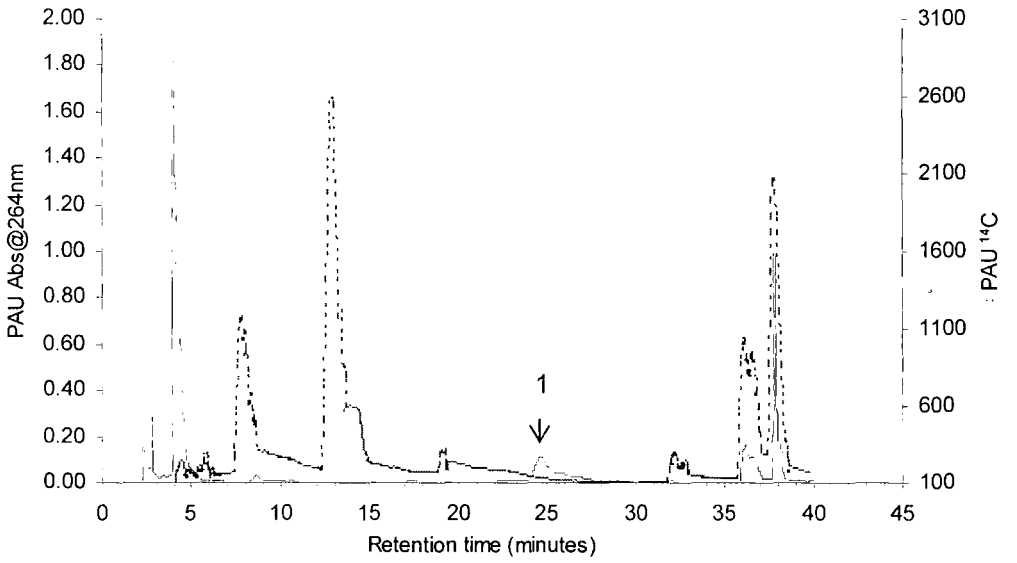

Figure 3.2.3.4 Isocratic co-chromatography of the authentic FEGSH cold standard and [^{14}C] metabolites of fenoxaprop ethyl formed *in vivo* at day 2 in 10 day old wheat plants treated with the safener fenchlorazole ethyl. 1 = authentic CB-GSH standard. UV absorbance shown with unbroken line and radioactivity shown with broken line.

in vivo metabolism of fluquinconazole in wheat

Although fluquinconazole was not a substrate for wheat GSTs, the compound did undergo non-enzymic glutathione conjugation. To determine the importance of glutathione mediated detoxification of the fungicide [^{14}C] fluquinconazole was fed to wheat plants, which had been treated with and without the safener fenchlorazole ethyl.

In contrast to the metabolism of fenoxaprop-P-ethyl the fungicide fluquinconazole did not undergo rapid metabolism in wheat (figure 3.2.3.5). A small quantity of glutathione conjugated metabolite was detected, but this accounted for only 0.26% of radioactivity taken up at day three, equating to 0.033 nmol equivalents of fluquinconazole, with no other metabolites being observed. It can be seen that fenchlorazole ethyl treatment did marginally enhance the formation of this metabolite, although due to the over lapping standard deviations of the data points this observation was not classed significant. The modest increase in glutathionylation of [^{14}C] fluquinconazole may have been due to safening treatment increasing glutathione content, thereby increasing the available GSH for spontaneous chemical conjugation of the fungicide. These data further confirm the inability of wheat GSTs to detoxify fluquinconazole. Although unmetabolised uptake of the systemic fungicide fluquinconazole followed a linear trend (figure 3.2.3.6), unlike fenoxaprop-P-ethyl uptake, which reached a plateau at 48 h. These data may suggest that the plateau effect observed with the uptake of fenoxaprop was a consequence of herbicidal tissue damage. Fluquinconazole, being a fungicide should not result in damage impeding uptake.

It was concluded that fluquinconazole was rare example of a xenobiotic, which appears to undergo non-enzymic spontaneous glutathione conjugation rather than

being detoxified by GSTs, albeit at a very slow rate. Considering glutathione conjugation of fluquinconazole leads to inactivation of the fungicide it seems fortuitous that detoxification by GSTs in wheat plants did not occur.

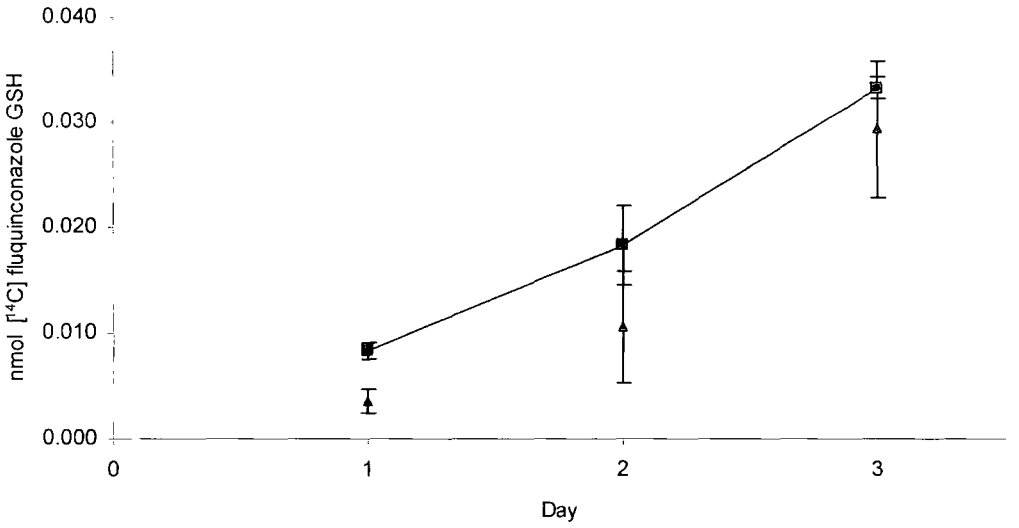

Figure 3.2.3.5. *In vivo* formation of [^{14}C] Fluquinconazole glutathione-conjugated metabolite over a 3 day feed trial in 10-day-old wheat seedlings treated with (solid line) and without (dashed line) the safener fenchlorazole ethyl. Vertical bars represent standard deviation of the mean (n = 3).

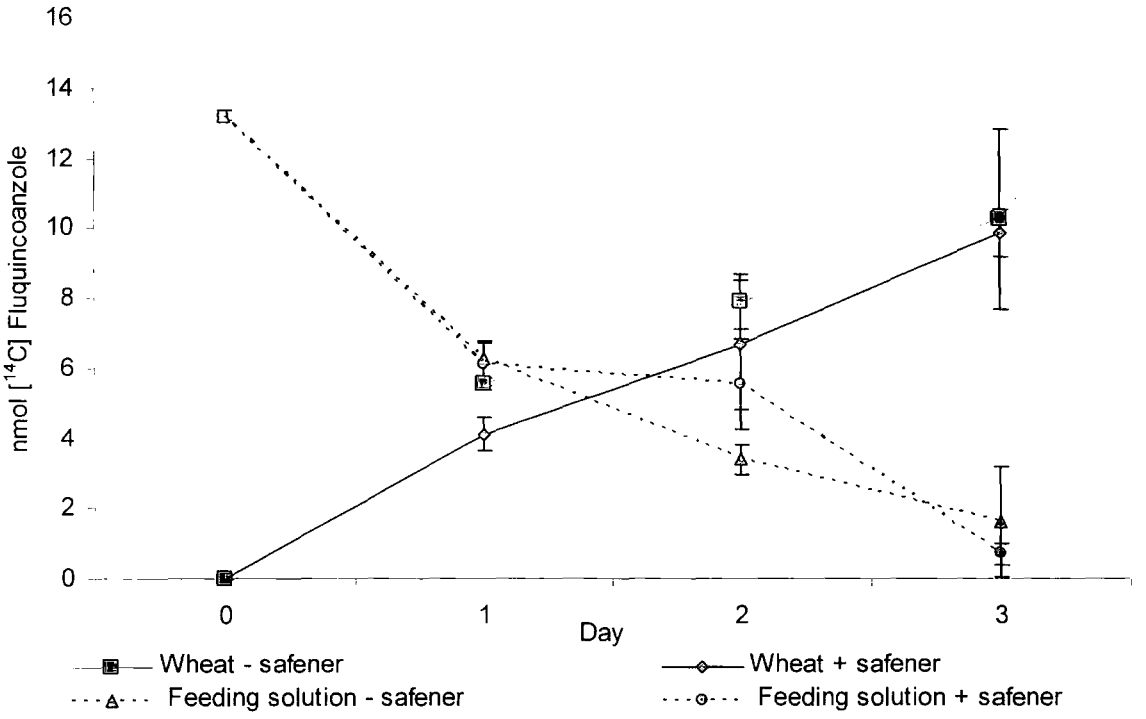

Figure 3.2.3.6. Uptake of [^{14}C] fluquinconazole over a 3 day feed trial in ten-day-old wheat seedling shoots. Solid lines represent nmols [^{14}C] extracted from wheat shoots treated ± the safener fenchlorazole ethyl. Dashed lines represent nmols [^{14}C] that remained in the feed solution ± the safener fenchlorazole ethyl. Triangular symbols represent nmol of fluquinconazole remaining in the feed solution of unsafened plants and square symbols on a dashed line represent nmol remaining in the feed solution of safened plants. Square symbols on a solid line represent nmol radioactivity extracted from unsafened shoots with nmol of radioactivity extracted from safened shoots represented by diamonds on a solid line. Vertical bars represent standard deviation of the mean (n = 3).

3.2.4 Profiling the metabolism of fenoxaprop-P-ethyl in wheat and blackgrass.

Since the metabolism studies carried out over 3 days failed to identify the major metabolites of fenoxaprop-P-ethyl in wheat plants, a more detailed study was carried out with the metabolites analysed by ES-LC-MS. In this case the feeding studies were carried out with unlabelled fenoxaprop-P-ethyl added to sectioned foliage of wheat or black grass.

Retention times of the authentic standards of fenoxaprop-P-ethyl, fenoxaprop and the respective glutathione and cysteine conjugates were established, for reference (figure 3.2.4). Each metabolite had an isotope distribution ratio corresponding to the presence of one chlorine atom (i.e. with the isotopes ^{35}Cl:^{37}Cl being present 3:1). In the case of the glutathione conjugate, a daughter ion fragmentation of the pyro-glutamate gave rise to an artefact of M+ 330, as determined from previous studies (Tal *et al.*, 1993). In the case of the parent herbicide sodium adducts of fenoxaprop and fenoxapro-P ethyl were observed with M+ 356 and M+ 384 respectively. In each case the combination of chlorine isotope distribution and partial fragmentation of the parent ion coupled to their retention time were useful tools in the identification of *in vivo* metabolites of fenoxaprop-P-ethyl formed *in vivo* in wheat and blackgrass.

Tissue incubated with 50 μM fenoxaprop-P-ethyl, was extracted with methanol, and the solvent concentrated under nitrogen prior to being extracted with ethyl acetate to remove the parent compound and non-polar contaminating metabolites. Subsequent LC-MS using a polar HPLC column (Tolstikov and Fiehn, 2002) for improved retention of polar metabolites aided the identification of the glutathione conjugate and a hydroxymethyl glutathione conjugate. Additionally a cysteinyl-*N*-glucosyl conjugate proposed to occur by Tal *et al.*, (1993) was also

identified by mass spectrometry as was the identification of a novel malonated derivative of this catabolite. Figure 3.2.4.2 details a total ion chromatogram of 10-day old safened wheat shoots following incubation with fenoxaprop-P-ethyl, while table 3.2.4 provides structure and retention time for each metabolite derived from the glutathione conjugation of fenoxaprop-P-ethyl. As a control, extracts from plants which had not been fed with fenoxaprop-P-ethyl did not contain any of these metabolites, which eluted between 16.85 – 39.57 minutes (figure 3.2.4.3).

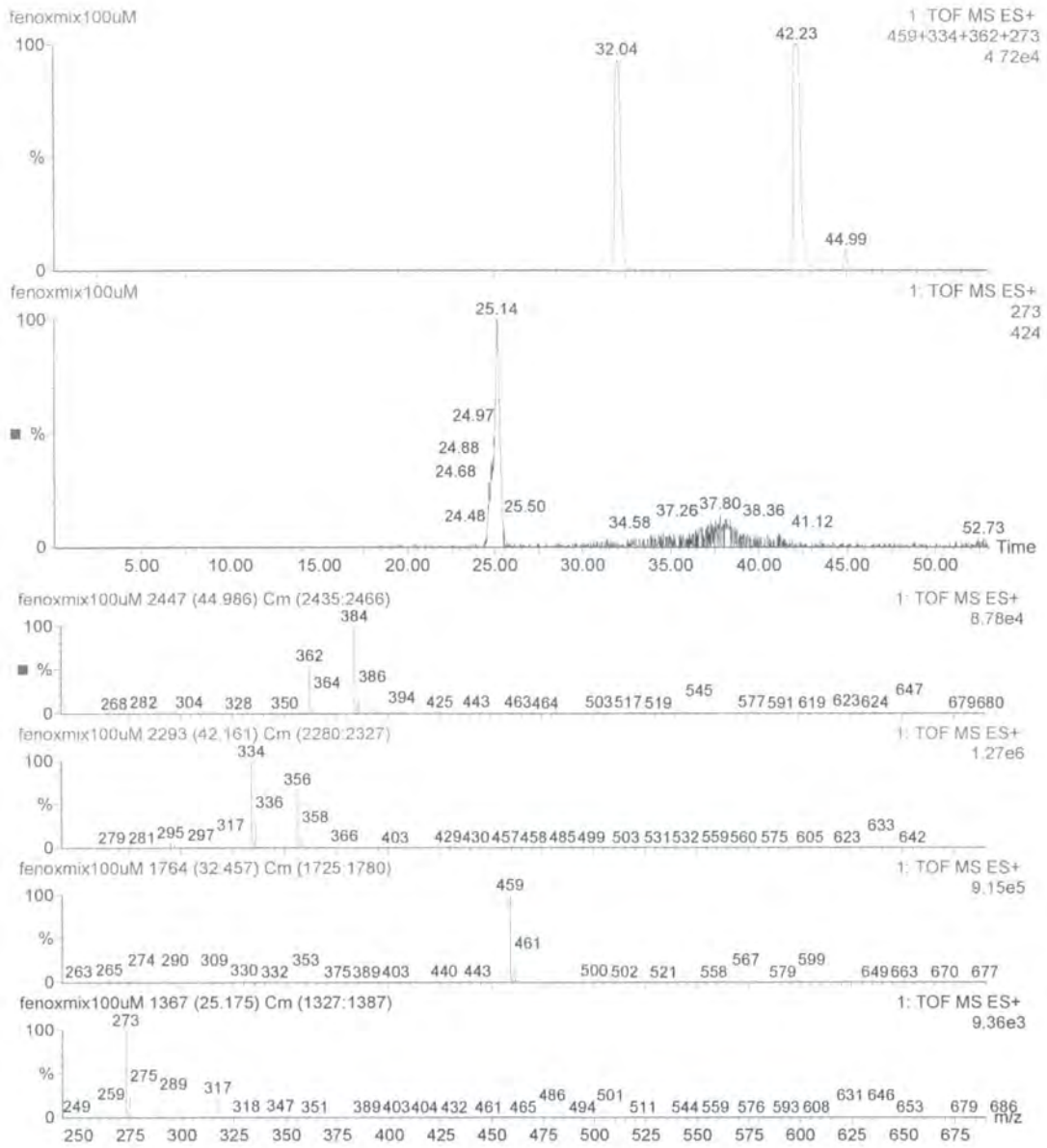

Figure 3.2.4 ES-MS total ionisation chromatogram operating in positive mode of fenoxaprop-P-ethyl (44.99 minutes; M+ 362), fenoxaprop (42.23 minutes; M+ 334), glutathione conjugate (32.04 minutes; M+ 459) and cysteine conjugate (25.14 minutes; M+ 273) authentic standards.

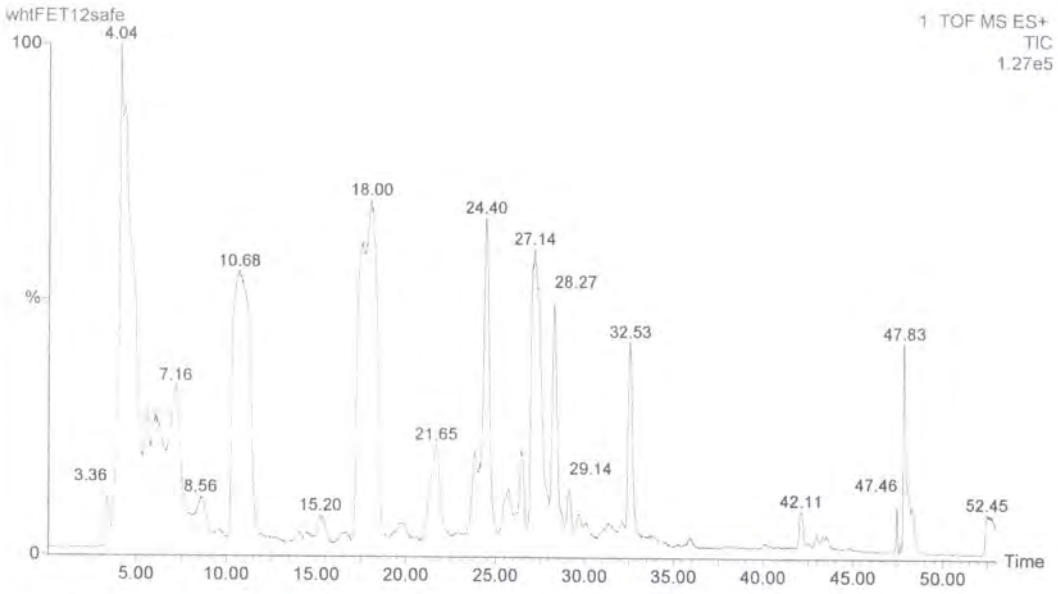

Figure 3.2.4.2. Total electrospray mass spectral ionisation chromatogram of 10-day-old safened wheat shoots treated with 50 μM fenoxaprop ethyl for 12 h following methanolic extraction, concentration and ethyl acetate extraction.

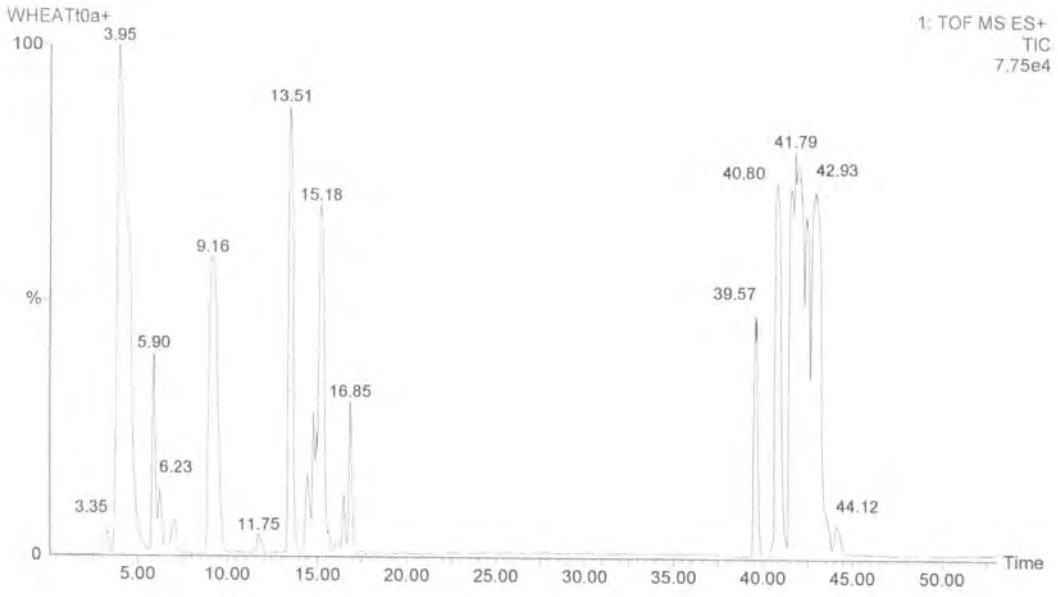

Figure 3.2.4.3. Total electrospray mass spectral ionisation chromatogram, operating in positive mode of 10-day-old safened wheat shoots following methanolic extraction, concentration and ethyl acetate extraction.

Table 3.2.4 Metabolites of fenoxaprop-P-ethyl identified by ES-LC-MS in wheat and black grass shoots. *not identified in blackgrass

Metabolite	Structure	Mass (M+)	Retention time (minutes)
S-(6-chlorobenzoxazole-2-yl)-cysteine-glutamic acid	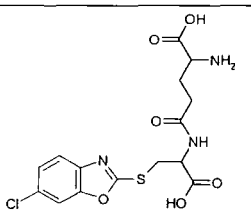	402	32.53
S-(6-chlorobenzoxazole-2-yl)-gluathione	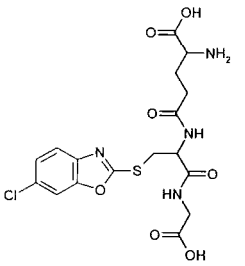	459	32.13
S-(6-chlorobenzoxazole-2-yl)-hydroxymethyl glutathione*	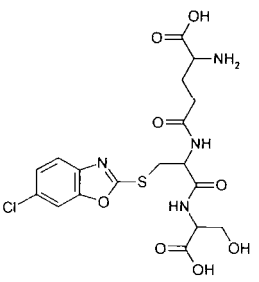	489	31.32
S-(6-chlorobenzoxazole-2-yl)-cysteine-glucose-malonic acid	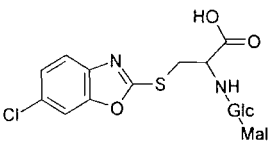	521	26.17
S-(6-chlorobenzoxazole-2-yl)-cysteine	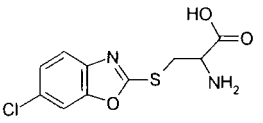	273	25.27
S-(6-chlorobenzoxazole-2-yl)-cysteine-glucose	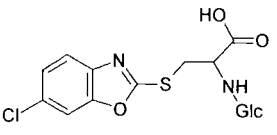	435	21.76

Interestingly, the peak at 32.53 minutes revealed M+ 402, 404 mass ions. The isotope distribution pattern of this conjugated catabolite, separation of 2 mass units, revealed that chlorine was present, confirming the presence of the chlorophenyl ring conjugated to the original glutathione moiety. Additionally, a mass ion of 273 was observed, with the respective chlorine distribution pattern, having been derived from the parent molecule by collision induced fragmentation. The daughter species observed was a result of the parent conjugate losing the pyro-glutamic acid during the ionisation procedure (Tal *et al.*,1993). It was concluded that this polar metabolite corresponded to the γ-Glu-Cys catabolite of the glutathione conjugate, resulting from carboxypeptidase cleavage of the tripeptide (figure 3.2.4.4). Recently purification of phytochelatin synthase from *Silene cubalus* and heterologous expression of phytochelatin synthase of *Arabidposis* have identified this enzyme as being responsible for carboxypeptidase cleavage (Beck *et al.*, 2003).

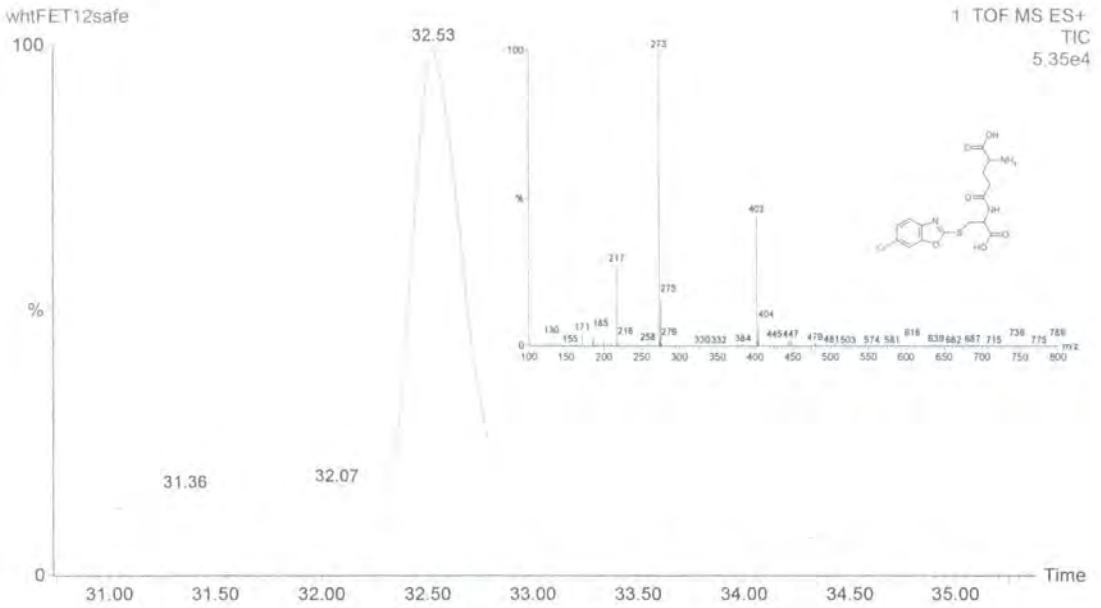

Figure 3.2.4.4 Chromatographic peak retention time 32.53 minutes, corresponding to Cb-Cys-Glu, the carboxy peptidase catabolite derived from hydrolysis of glycine from the glutathione conjugate of fenoxaprop-P-ethyl. Inset, the fragmentation pattern of Cb-Cys-Glu with the parent mass of M+ 402, Da and daughter ion of M+ 273 following fragmentation of the pyro glutamic acid. Both species exhibited isotope distribution patterns indicating the presence of one chlorine atom.

The glutathione conjugate was found to be slightly more polar than the γ-Glu-Cys derivative, having a retention time of 32.07-minute retention time, and was a minor metabolite in wheat (figure 3.2.4.5). Considering the close proximity and overlapping chromatography of these 2 conjugates, it seems probable that the anomaly observed in the chromatography between the authentic glutathione conjugate and the apparent [^{14}C] glutathione conjugate formed *in vivo* in wheat (figure 3.2.3.3), was the resulting product of carboxypeptidase cleavage of the glycine. The mass of M+ 459, 461 corresponded to the GSH conjugate containing a chlorine atom and the presence of a daughter ion at M+ 330 revealed the fragmentation of pyro-glutamic acid from the parent species.

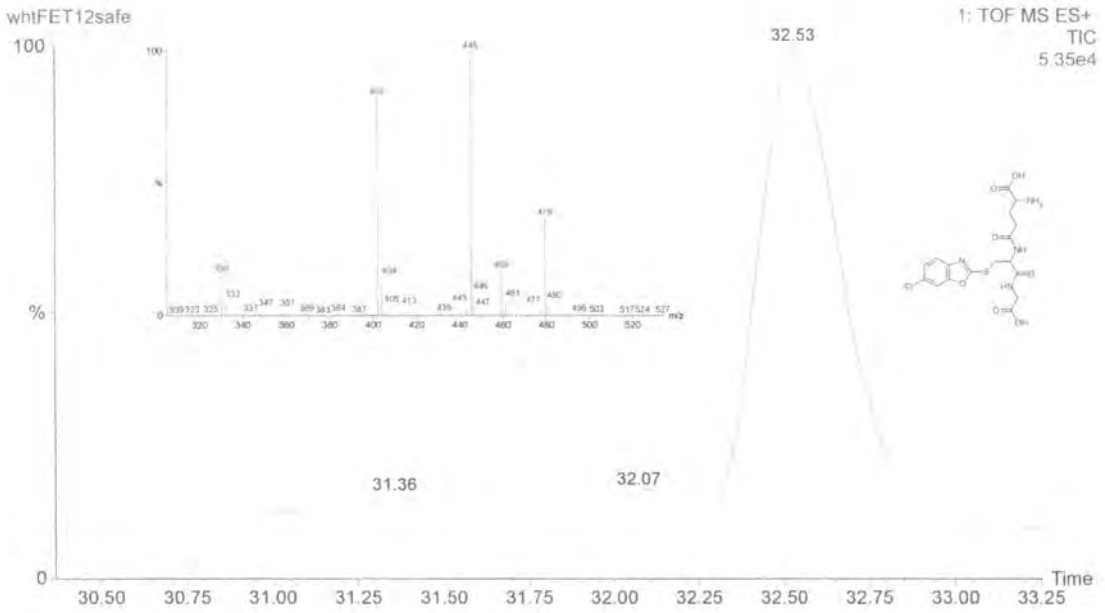

Figure 3.2.4.5 Chromatographic peak retention time 32.07 minutes, inset spectra of the parent glutathione conjugate of fenoxaprop-P-ethyl, M+ 459 and daughter ion M+ 330 following collision induced fragmentation of the pyro-glutamic acid Both species exhibited isotope distribution patterns indicating the presence of one chlorine atom. The conjugate catabolite Cb-Cys-Glu, M+ 402, remained visible due to a lack of chromatographic separation.

The presence of a glutathione homologue, hydroxymethyl glutathione (HmGSH), in wheat was reported by Klapheck *et al.*, (1991). Hydroxymethyl glutathione differs from glutathione in that the terminal glycine residue (γ-Glu-Cys-Gly) has been replaced by serine (γ-Glu-Cys-Ser), thereby increasing mass of the tripeptide from 307 Da (GSH) to 337 Da (HmGSH). Additionally, the hydroxyl group of serine has the effect of increasing the polarity of this tripeptide as compared with GSH. In accordance with these physico-chemical properties a hydroxymethyl glutathione conjugate of fenoxaprop was identified with a retention time of 31.36 minutes, which eluted approximately 30 seconds before the glutathione conjugate of fenoxaprop-P-ethyl (figure 3.2.4.6). The observed mass ion, M+ 489, was 30 Daltons heavier than the GSH-conjugate with the daughter ion of M+ 360 being present, resulting from the fragmentation of the parent compound. The hydroxymethyl glutathione conjugate identified in wheat treated with fenoxaprop-P-ethyl, accounted for the first example of this glutathione homologue being involved in herbicide detoxification. Significantly, equine liver GST was not found to use HmGSH as a substrate (Klapheck *et al.*, 1992) though the activities of wheat GSTs toward this thiol have not been determined.

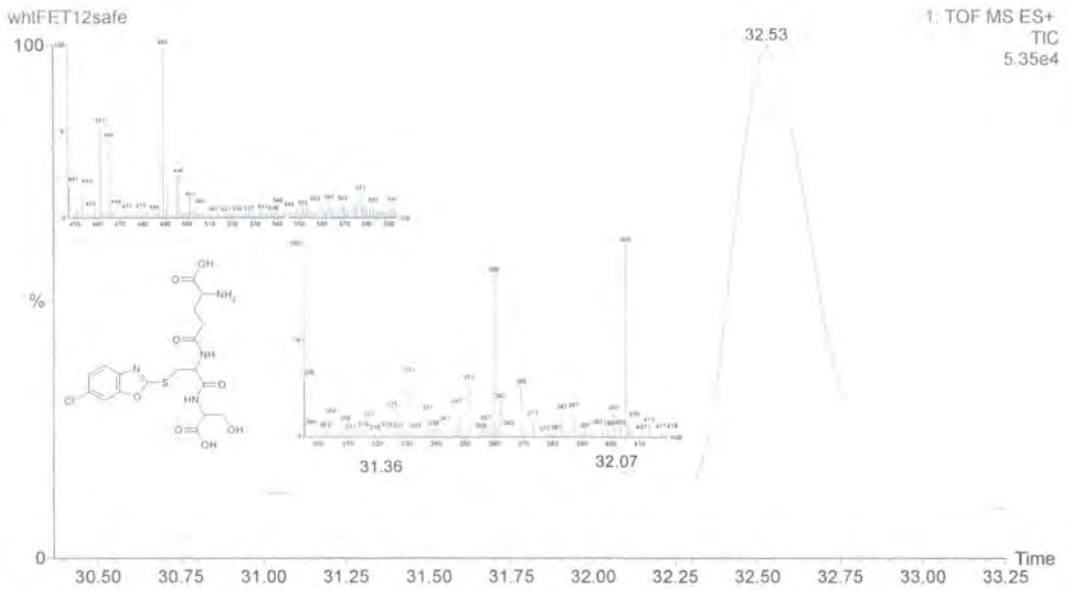

Figure 3.2.4.6 Chromatographic peak retention time 31.36 minutes, upper inset spectra of the parent hydroxymethyl glutathione conjugate of fenoxaprop-P-ethyl, M+ 489 and daughter ion M+ 360, lower spectra, following collision induced fragmentation of the pyro-glutamic acid. Both species exhibited isotope distribution patterns indicating the presence of one chlorine atom.

Following carboxy peptidase cleavage of the terminal glycine or serine residues, the fenoxaprop conjugate was then found to have undergone transpeptidase hydrolysis of γ-glutamic acid resulting in the formation of the cysteinyl derivative (figure 3.2.4.7). Single ion monitoring at M+273 identified a peak eluting at 25.27 minutes corresponding to the retention time of the authenticated cysteinyl conjugate of fenoxaprop-P-ethyl. As with the other conjugates, this compound exhibited the isotope distribution pattern common to molecules containing a chlorine atom. Although possible that fenoxaprop-P-ethyl was directly conjugated to cysteine, it is more likely to have arisen as a catabolite of the GSH or HmGSH conjugate (Martin & Slovin, 2000; Wolf *et al.*,1996).

A cysteinyl-glucosyl conjugate of fenoxaprop-P-ethyl was also identified, with a retention time of 21.76 minutes. Two species, M+273 Da and M+435 Da, were characterised, both with the corresponding isotope distribution pattern (figure 3.2.4.7). The mass difference of 162 Da, suggested that the 273 species was a fragmented daughter ion of a glucosylated cysteinyl conjugate of fenoxaprop. Tal *et al.*, (1993) reported an *in vivo* metabolite co-chromatographing with an authentic cysteinyl-glucosyl conjugate of fenoxaprop, which was resistant to acidic and β-Glucosidase hydrolysis. It was speculated that this metabolite was an *N*-glucoside conjugate of *S*-(6-chlorobenzoxazole-2-yl)-cysteine, where the glucose was attached to the primary amine of the benzoxazole moiety. The mass spectral data indicated that if the glucose, 180 Da, was *N* conjugated, it was likely to have been attached to the amine group of the cysteine residue, yielding a loss of 18 Da on ionisation resulting from the condensation of water. Linkage to the benzoxazole primary amine would have resulted in the loss of 17 daltons giving Cb-Cys-Glc with a mass of M+ 436 Da.

The Cb-Cys-Glc catabolite appeared to have undergone subsequent malonylation (figure 3.2.4.7). Thus, a mass ion of M+ 521, exhibiting the chlorine isotope distribution pattern, was observed in the chromatographic peak eluting with a retention time of 26.15 minutes. Again, a daughter fragmentation ion was observed at 273 with the respective chlorine isotope pattern. The mass difference of 248 corresponded to a 6 carbon sugar plus malonic acid, less 2 water molecules from condensation. The malonyl moiety may possibly have been conjugated to the sugar group, as the mass of M+359, corresponding to Cb-Cys-Mal, was not observed. Additionally if this was the case, the Cb-Cys-Glc fragment of M+435 may have been present, although it may be arguable that both the glucosyl and malonyl moieties were labile under the ionisation conditions used. Single ion monitoring for M+359 over the total ionisation chromatogram did not reveal a Cb-Cys-Mal species, suggesting that malonylation had occurred following glucosylation of the cysteinyl conjugate of fenoxaprop.

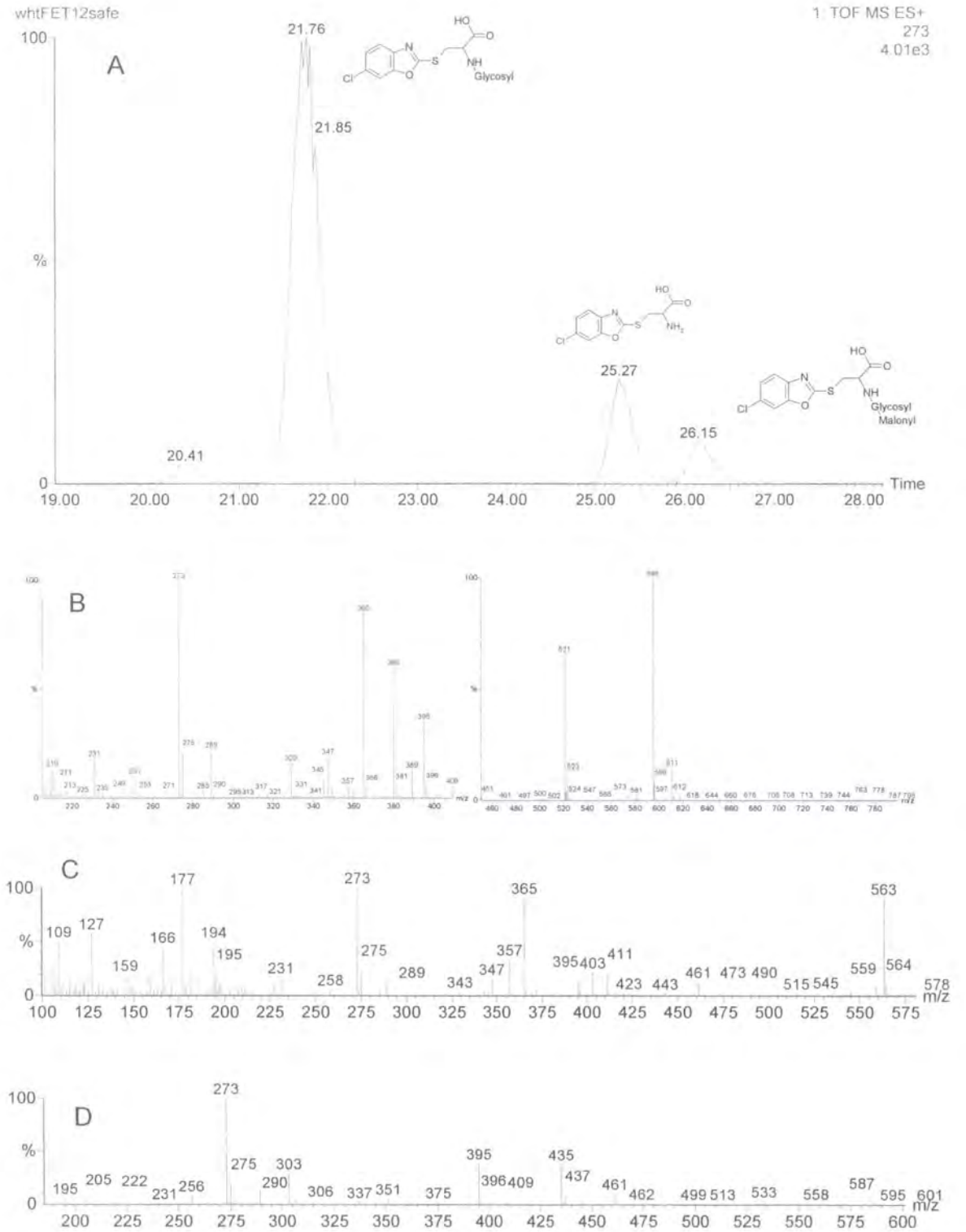

Figure 3.2.4.7 Full legend over leaf.

Figure 3.2.4.7 (A) Single ion monitoring chromatogram for the cysteinyl catobolite derived from the glutathione conjugate of fenoxaprop-P-ethyl, M+ 273. (B) Mass spectral summation of the chromatographic peak with a retention time of 26.15 minutes. M+ 521 corresponded to a Cb-cysteinyl-glucosyl-malonyl catabolite, with a collision induced fragmentation daughter ion observed, M+ 273 corresponding to Fenoxaprop-cysteinyl conjugate. (C) Summation of chromatographic peak, retention time 25.27 minutes. M+ corresponded to Cb-cysteinyl conjugate. (D) Mass spectral summation of the chromatographic peak with a retention time of 21.76 minutes. M+ 435 corresponded to a Cb-cysteinyl-glucosyl catabolite, with a collision induced fragmentation daughter ion being observed at M+ 273. All species exhibited isotope distribution patterns indicating the presence of one chlorine atom.

3.2.5 Metabolism of fenoxaprop-P-ethyl in herbicide susceptible (Rothamstead) and herbicide resistant (Peldon) biotypes of black-grass.

Herbicide resistant biotypes of *Alopecurus myosuroides* (black-grass), a competitive grass weed of winter wheat in Europe, have been shown to have evolved enhanced expression of detoxification enzymes, including GSTs, under the selective pressure of herbicide application (Hall *et al.*, 1997; Cummins *et al.*, 1999). As such, herbicide resistance has become problematic within biotypes of this weed species. Multiple herbicide resistance in black-grass peldon has been attributed to elevated metabolism as compared with the herbicide susceptible black-grass phenotype, Rothamstead. Black-grass Peldon was shown to have elevated glutathione peroxidase activities conferring tolerance to oxidative stress resulting from herbicide application in addition to GST mediated detoxification of the herbicide fenoxaprop-P-ethyl through conjugation with glutathione (Cummins *et al.*, 1999). In a parallel study to that of wheat, GST mediated detoxification of fenoxaprop-P-ethyl was examined in herbicide resistant (Peldon) and herbicide susceptible (Rothamstead) biotypes of black-grass, treated with and without the safener cloquintocet mexyl. Total ionisation chromatograms for black-grass have not been shown, but the metabolites have been comparatively quantified with those of wheat and summarised in the following figures.

Although identically treated with herbicide fenoxaprop-P-ethyl, the respective levels of glutathione conjugated fenoxaprop-P-ethyl identified in wheat and both biotypes of blackgrass differed greatly. Conjugate levels in safener treated wheat were maximal (9820 ion counts generated per 40 mg tissue), 12 h after herbicide treatment, whilst safened black grass peldon at 12 h, accumulated 12 fold higher concentration, (122300 ion counts generated per 40 mg of tissue) (figure 3.2.5). In wheat, safening had the effect of increasing GSH conjugate levels by 58% over

unsafened wheat shoots after 12-h incubation. However, after 24 h, concentration of the glutathione conjugate in safened shoots had reduced to 60% of that determined in the unsafened 12-h treated plants. The effect of GSH conjugate formation in the resistant, peldon, biotype of black grass did not appear to be altered in response to safening. However, glutathione conjugate levels were higher in the resistant shoots than those in the herbicide susceptible line. Safener treatment doubled the formation of glutathione conjugates in the herbicide susceptible plants, though considerable variation was seen in the unsafened extracts.

In contrast, summation of spectral data in the chromatographic peak, retention 32.53 minutes corresponding to the Cb-Cys-Glu catabolite derived from the glutathione conjugate of fenoxaprop-P-ethyl (figure 3.2.5.1), revealed major differences in the processing of xenobiotics between wheat and black grass. Comparatively, processing of the glutathione metabolite in wheat occurred at over 28 fold faster than determined in either herbicide resistant or susceptible biotypes of blackgrass. The highest levels of this catabolite were observed in safened wheat following 24 h incubation with fenoxaprop (612500 ion counts generated per 40 mg), while in black grass the highest level accrued in peldon (21425 ion counts per 40 mg), after a 12 h incubation. Considering the lower abundance of glutathione conjugate (figure 3.2.5) and higher accumulation of hydrolysed catabolite (figure 3.2.5.1) in wheat compared to black-grass, overall detoxification by conjugation was a more active process in *Triticum aestivum* than in the weed. The observed catabolic differences may be the result of higher phytochelatin synthase activites (Beck *et al.*, 2003) in wheat.

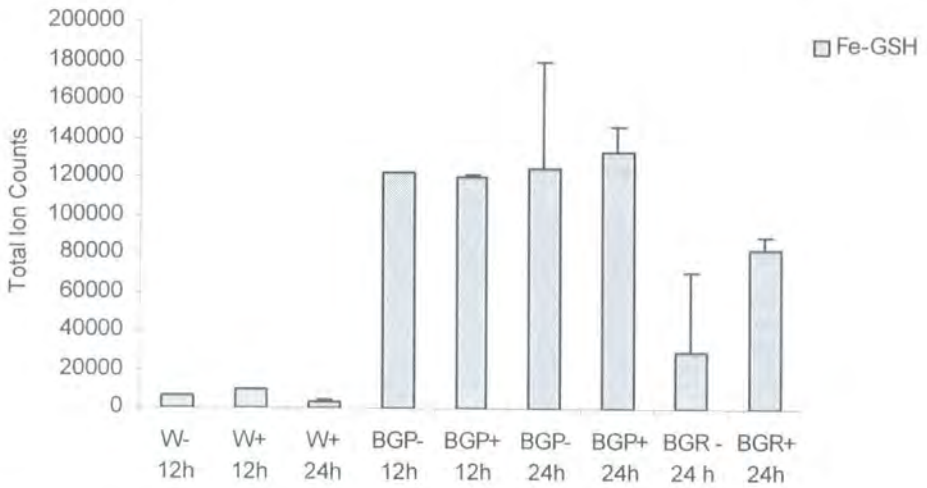

Figure 3.2.5 Comparison of the glutathione conjugate of fenoxaprop-P-ethyl in wheat (W) and black grass peldon (BGP) and Rothamstead (BGR) treated + - the safener cloquintocet mexyl following 12 h and 24 h incubation with 50 μM fenoxaprop-P-ethyl.

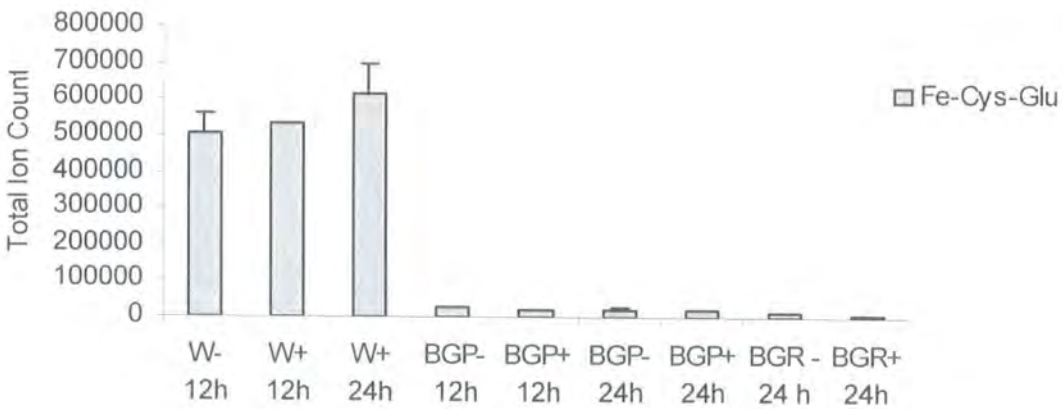

Figure 3.2.5.1 Comparison of the catabolite Cb-Cys-Glu derived from the glutathione conjugate of fenoxaprop ethyl in wheat (W) and black grass peldon (BGP) and Rothamstead (BGR) treated + - the safener cloquintocet mexyl following 12 h and 24 h incubation with 50 μM fenoxaprop-P-ethyl.

The hydroxy methyl glutathione conjugate of fenoxaprop was also identified in wheat, but not in either herbicide resistant (BGP) or susceptible black-grass (BGR) (figure 3.2.5.2). Thiol analysis of 20 day old wheat and 30 day black-grass has shown that both species contain both thiols, with GSH and HmGSH being present in wheat in approximately equimolar concentrations (Cummins *et al.*, 1997) (Table 3.2.5). Klapheck *et al.*, (1991), however report that in 10 day old wheat shoots the major thiol present was GSH in a ratio of 2.55:1 with hydroxymethyl glutathione. The ratio of the glutathione to hydroxymethyl glutathione conjugate of fenoxaprop-P-ethyl present in 10-day old unsafened wheat shoots incubated for 12 h approximately mirrored this observation, being 2.34:1 (table 3.2.5.1). Based on the relative abundance of the HmGSH conjugate in wheat, it is tempting to speculate that the GSTs in this species are capable of utilising HmGSH as a co-substrate in the detoxification of herbicides. GST mediated detoxification of fenoxaprop in wheat has been demonstrated with glutathione as a co-substrate both *in vivo* and *in vitro* (Cummins *et al.*, 1997; Edwards & Cole, 1996; Tal *et al.*, 1993). Assuming spontaneous HmGSH conjugation of fenoxaprop, the ratio of conjugates formed would have been expected to be proportionally low as compared with the GSH conjugates arising from enzyme mediated conjugation.

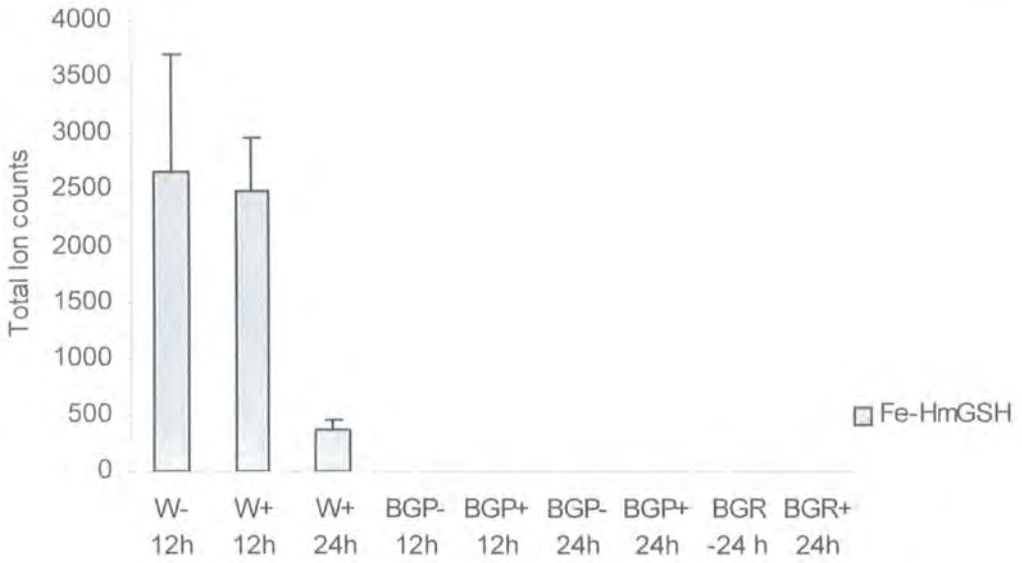

Figure 3.2.5.2 Comparison of the hydroxymethyl glutathione conjugate of fenoxaprop ethyl in wheat shoots (W) and black grass peldon (BGP) and Rothamstead (BGR) shoots treated + - the safener cloquintocet mexyl following 12 h and 24 h incubation with 50 μM fenoxaprop-P-ethyl.

Table 3.2.5 Thiol content in wheat and black grass shoot tissue

	Thiol content (nmol g^{-1} fresh weight)	
Species	Glutathione	Hydroxymethylglutathione
Wheat (10 day)	284 ± 37	111 ± 48
Wheat (20day)	121 ± 20	151 ± 33
Black grass (30day)		
Peldon	180 ± 14	29 ± 4
Rothamstead	106 ± 31	58 ± 17

Table adapted after Cummins *et al.*, (1997) Klapheck *et al.*, (1991)

Table 3.2.5.1 Respective levels of glutathione and hydroxymethyl glutathione conjugates of fenoxaprop-P-ethyl formed in 10-day old unsafened wheat shoots after 12 h exposure to 50 μM of the herbicide.

	total ionisation counts generated per 40 mg		
	GSH conjugate	HmGSH conjugate	Ratio of conjugates formed
12 h unsafened wheat shoots	6215	2661	2.34:1

Cb-HmGSH levels were not elevated in safener-treated plants after 12 h exposure to the herbicide. At 24 h the HmGSH, conjugate had decreased in safened plants by 86%. As with the glutathione conjugate, this decrease was probably due to processing to the γ-glu-cys derivative. Whether the formation of the HmGSH conjugate was spontaneous or catalysed by a GST remains unclear. As a result of the rapid processing of these tripeptide conjugates in wheat, the involvement of hydroxymethyl glutathione as a major or minor route of fenoxaprop ethyl detoxification remains unresolved. Further investigation of alternate thiol use in the metabolism of herbicides in wheat may uncover new information regarding GST substrate specificity and detoxification pathways within this crop species.

Tal *et al.*, (1993) identified a cysteine conjugate in wheat, possibly derived from catabolism of the glutathione conjugate of fenoxaprop-P-ethyl. The presence of this metabolite was confirmed in wheat and both biotypes of black grass. Safening had the effect of increasing cysteine conjugate levels by 150% over that of 12 h unsafened wheat, with levels greatly decreased after 24 h in safened shoots (figure 3.2.5.3). The data for black grass peldon appeared to show a relative increase in the formation of the cysteine conjugate as compared to susceptible plants, however the data were subject to large standard deviations. Overall, cysteine conjugate levels in

black grass Rothamstead were elevated 45% in response to safening, suggesting upregulation of γ-glutamyl transpeptidase activity.

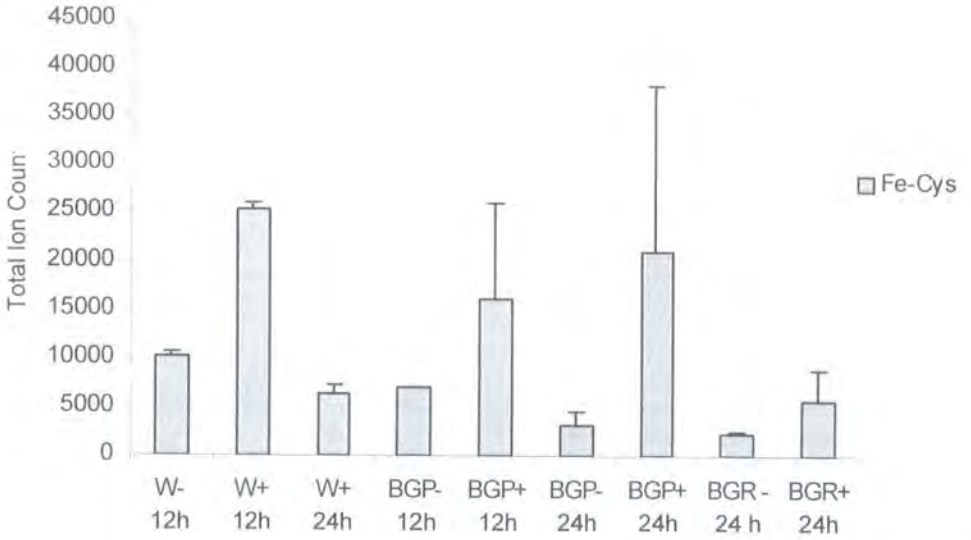

Figure 3.2.5.3 Comparison of the content of the cysteine conjugate of fenoxaprop ethyl derived from catabolism of GSH conjugates in wheat shoots (W) and black grass peldon (BGP) and Rothamstead (BGR) shoots treated + - the safener cloquintocet mexyl following 12 h and 24 h incubation with 50 μM fenoxaprop-P-ethyl.

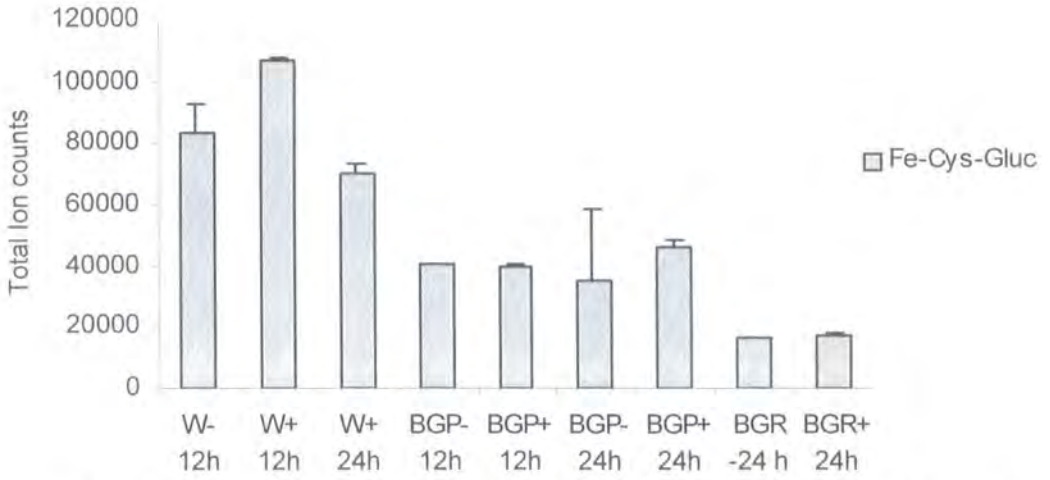

Figure 3.2.5.4 Comparison of the catabolite Cb-Cys-Gluc, derived from the glutathione conjugate of fenoxaprop ethyl in wheat shoots (W) and black grass peldon (BGP) and Rothamstead (BGR) shoots treated + - the safener cloquintocet mexyl following 12 h and 24 h incubation with 50 μM fenoxaprop-P-ethyl.

Confirming the proposition of Tal *et al.*, (1993), the *N*-glucoside of the cysteine conjugate of fenoxaprop was an abundant catabolite found in wheat and both species of blackgrass (Figure 3.2.5.4). Glucosylation of the cysteine catabolite suggested it had been transported from the vacuole into the cytosol for conjugation by a glucosyl transferase. In turn, this would indicate that a metabolic exchange occurred from cytosol to vacuole and back to the cytosol in the processing of glutathione conjugated xenobiotics in both grass species.

The speculative Cb-Cys-Glc-Mal metabolite was shown to increase in safened wheat and blackgrass peldon over 24h (figure 3.2.5.5). The increase in levels of this metabolite may suggest that following malonylation further processing of the conjugate became rate limiting. These remaining steps at present are unknown, but

may possibly involve incorporation of the herbicidal metabolite into bound residues. Further work on the detoxification of fenoxaprop-P-ethyl in wheat needs to be performed to accurately quantify the change in, and rate of conjugate formation and catabolism.

The identification of 2 novel metabolites derived from the GSH mediated detoxification of fenoxaprop-P-ethyl in wheat, has extended the current knowledge of xenobiotic detoxification in this major crop species (figure 3.2.5.6). Additionally, metabolite exchange between cytosol and vacuole may be inferred based on the known localisation of the respective enzymes and it is possible that these enzymes may also be responsive to safening. In this regard, it would be interesting to determine if the genes encoding the enzymes involved in the processing of glutathione conjugates were under common regulation with the proteins involved in synthesising and transporting these metabolites.

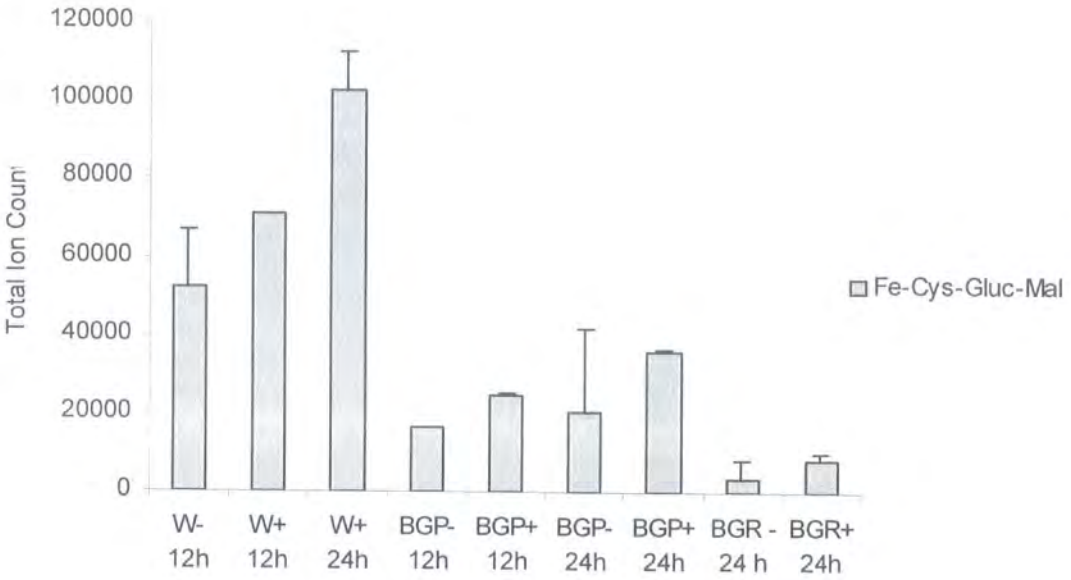

Figure 3.2.5.5 Comparison of the catabolite Cb-Cys-Glu-Mal, derived from the glutathione conjugate of fenoxaprop ethyl in wheat shoots (W) and black grass peldon (BGP) and Rothamstead (BGR) shoots treated + - the safener cloquintocet mexyl following 12 h and 24 h incubation with 50 μM fenoxaprop-P-ethyl.

Figure 3.2..5.6. Proposed pathway for the detoxification of fenoxaprop-P-ethyl in wheat. Solid and dashed lines indicate major and minor routes of detoxification respectively.

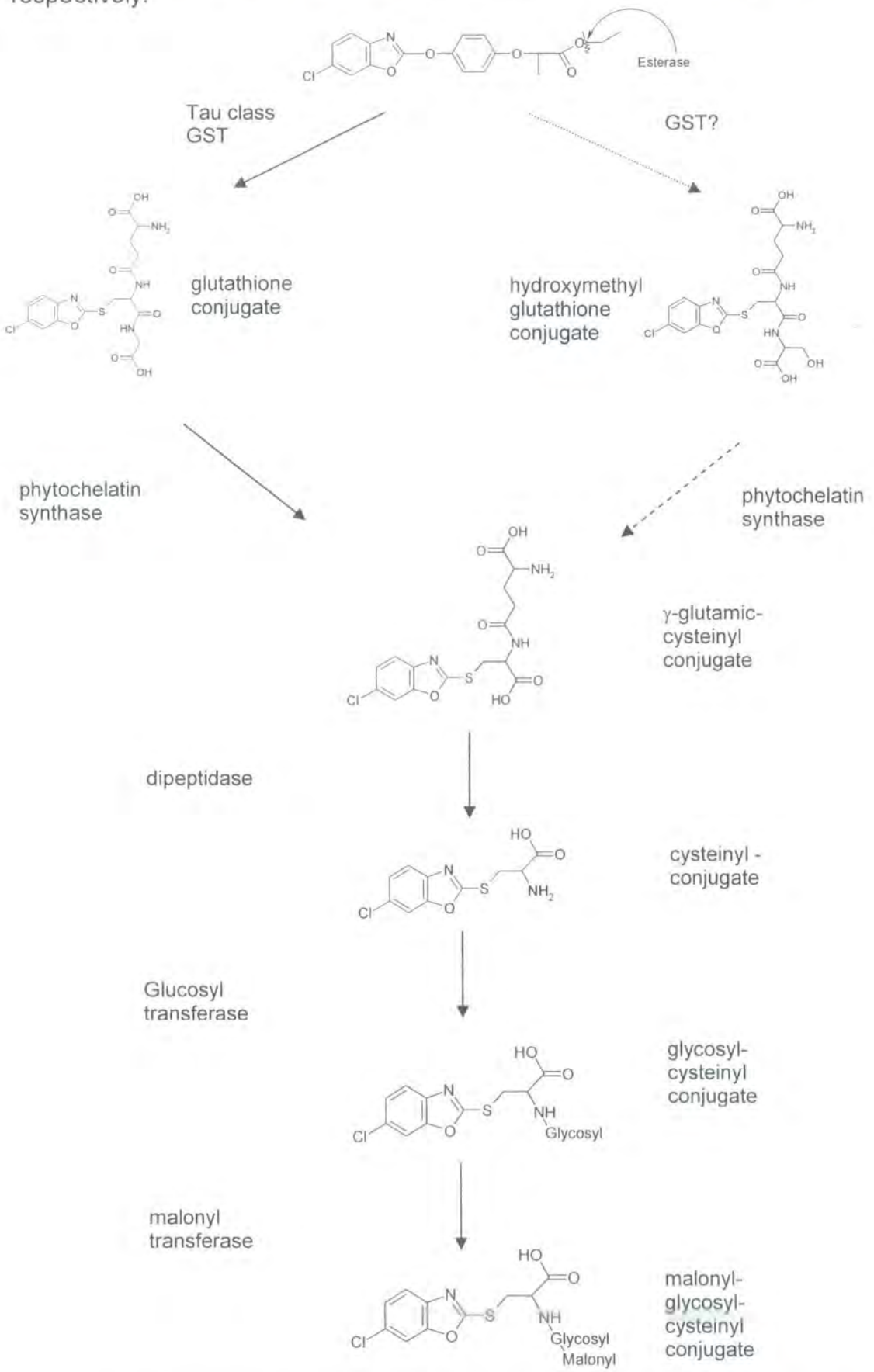

3.2.6 Chemical synthesis of fungicide glutathione conjugates

Table 3.2.6 Fungicides and herbicide tested for conjugation with glutathione

Name	Structure	Mass
Fenoxaprop-P-ethyl	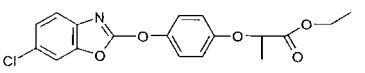	361.78
Fluquinconazole	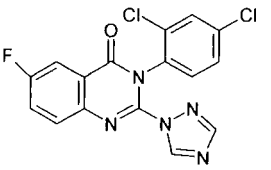	616.46
Zoxamide	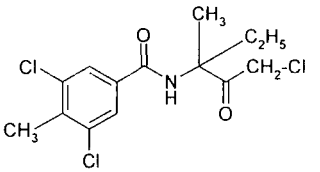	336. 645
Quinoxyfen	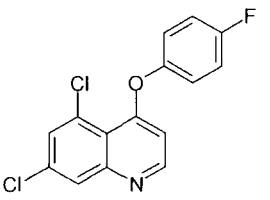	308.1385
Fluazinam	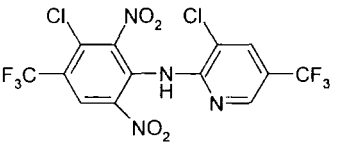	465.0951
Picoxystrobin	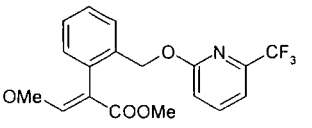	367.3246

Table 3.2.6 continued

Azoxystrobin	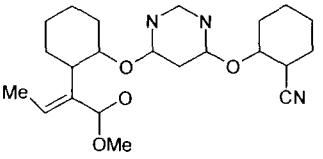	403.394
Cyazofamid	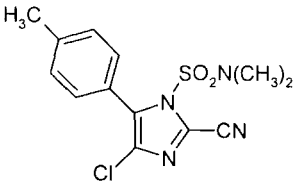	324.7907
Chlorothalanil	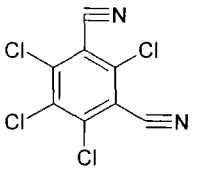	243

Following on from the metabolism studies of fenoxaprop-P-ethyl and fluquinconazole in wheat, a panel of fungicides (table 3.2.6) were tested for their ability to form glutathione conjugates *in vitro*. As with the GSH conjugates of fluquinconazole and fenoxaprop-P-ethyl, these were synthesised by incubating each fungicide with glutathione at pH 9.5 for 36 h and then analysing the reaction products by TLC and ES-MS. TLC identified UV and ninhydrin positive spots corresponding to putative glutathione conjugates of zoxamide, chlorothalanil, quinoxyfen and fluazinam (figures 3.2.6 and 3.2.6.1). However, the remaining fungicides were not found to have undergone glutathione conjugation. Of the conjugated fungicides, chlorothalinil and fluazinam appeared to have undergone multiple glutathione conjugation, with 2 polar UV/ninhydrin spots observed for each these pesticides (figure 3.2.6.1).

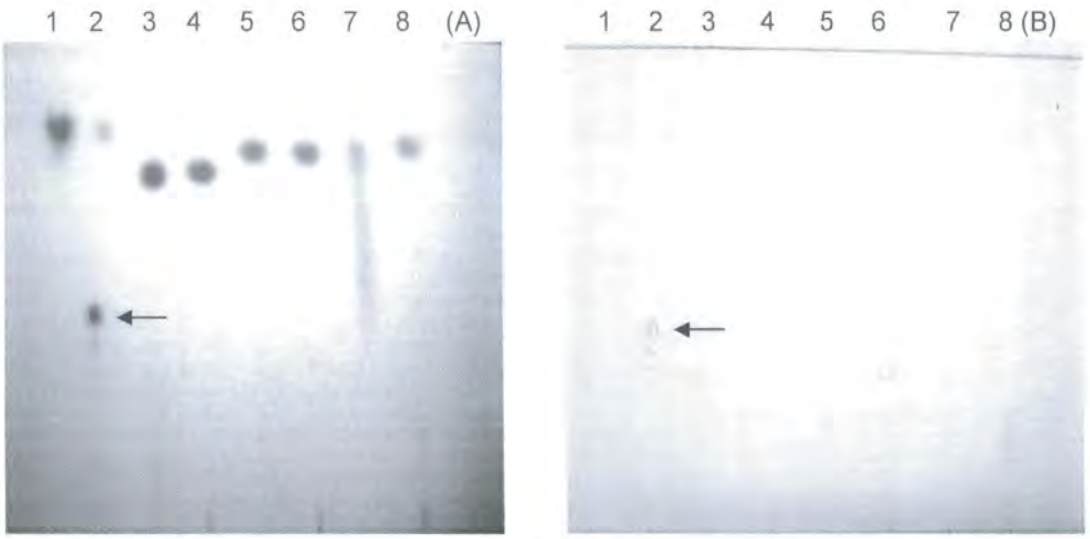

Figure 3.2.6 Examples of reaction product analysis for fungicide *S*-glutathionylation using TLC. Thin layer chromatography of 2 uL 100mM fungicides and respective incubation with glutathione. (A) UV visualisation (B) Ninhydrin derivatisation of conjugated fungicide. 1 = Zoxamide; 2 = Zoxamide + GSH; 3 = Azoxystrobin; 4 = Azoxystrobin + GSH; Picoxystrobin; 6 = Picoxystrobin + GSH; 7 = Cyazofamid; 8 = Cyazofamid + GSH. Putative conjugates are highlighted with an arrow.

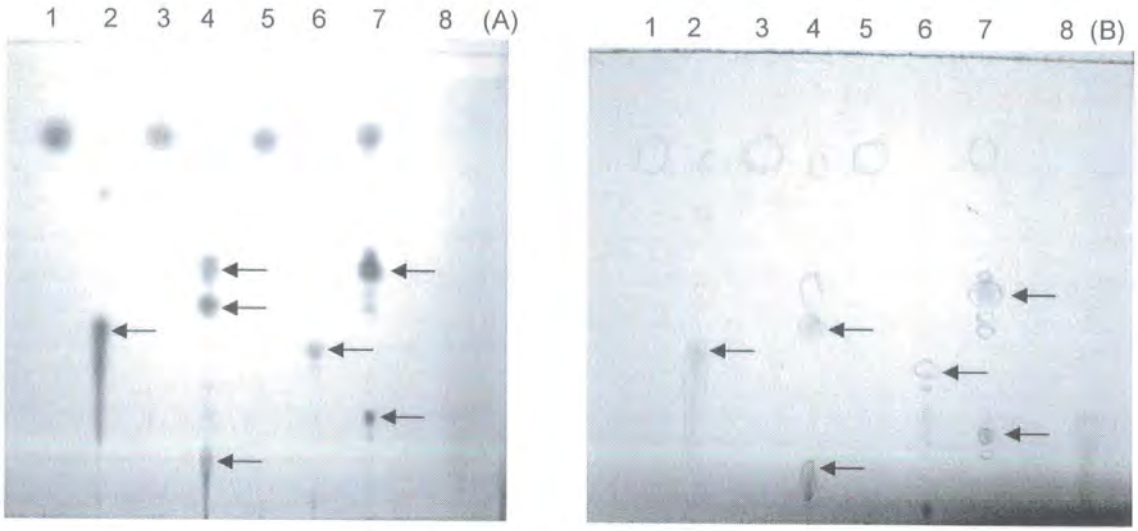

Figure 3.2.6.1 Examples of reaction product analysis for fungicide *S*-glutathionylation using TLC. Thin layer chromatography of 2 uL 100mM fungicides and respective incubation with glutathione. (A) UV visualisation (B) Ninhydrin derivatisation of conjugated fungicide. 1 = fenoxaprop-P-ethyl; 2 = fenoxaprop-P-ethyl + GSH; 3 = chlorothaonil; 4 = chlorothalanil + GSH; quinoxyfen; 6 = quinoxyfen + GSH; 7 = fluazinam + GSH; 8 = GSH. Putative conjugates are highlighted with an arrow.

Putative fungicide-glutathione conjugates were then further characterised by electrospray time of flight mass spectrometry operating in the negative mode. The parent compound of Zoxamide was identified having been hydrated with 2 molecules of H_2O, M- 372.04. The respective glutathione conjugate had the mass M- 605, which corresponded to the parent molecule having undergone glutathione substitution associated with dehalogenation (figure 3.2.6.2). Whilst not possible to identify the site of dechlorination, conjugation was suggested to have occurred at the 3 carbon of the ethyl group due to its potential reactivity (Briggs *pers comm.* 2002).

The glutathione conjugate of quinoxyfen, M-501.134, was found to be the result of cleavage of the bi-phenyl ether bond at carbon 4 resulting in the formation of

S-(5,7-dichloro-quinolin-4yl)-glutathione with concomitant displacement of the 4-fluoro-phenyl moiety (figure 3.2.6.3). The parent molecule was found to be recalcitrant to ionisation by ESMS.

Two glutathione conjugates of fluazinam were identified by ESMS, a mono, M- 734.123 and di-conjugate, M- 994. The mono conjugate appeared to be formed through substitution of the 3 carbon chlorine of the dinitrophenyl ring with the di-conjugate being formed through additional substitution of the nitro group at the 6 carbon of the dinitrophenyl ring (figure 3.2.6.4 & 3.2.6.5). The mono conjugate structure shown was based upon the 3 carbon having a greater $\delta+$ due to the proximity of an electron withdrawing nitro group at carbon 2 (table 3.2.6), resulting in this site being preferentially attacked by the thiolate anion of glutathione. It was speculated that the 6 carbon bond was similarly electrophilic, due to the proximity of a nitro group, allowing nucleophilic attack by the thiolate anion.

Hydrated mono-, M- 534.003, and di-, M- 805.119, -glutathione conjugates of chlorothalanil were identified with a dehydrated mono-conjugate, M- 489, being present (figure 3.2.6.6). Additionally, the parent chlorothalanil was also present in hydrated form, M- 260. These species may possibly have been a result of the ionisation conditions. The mass of the conjugates indicated that in both the mono and di glutathione conjugates chlorine had undergone substitution. However, from the structure of this tetra-chlorinated fungicide it was difficult to determine obvious sites of halogen substitution, the carbons shown to have undergone glutathione conjugation were purely speculative.

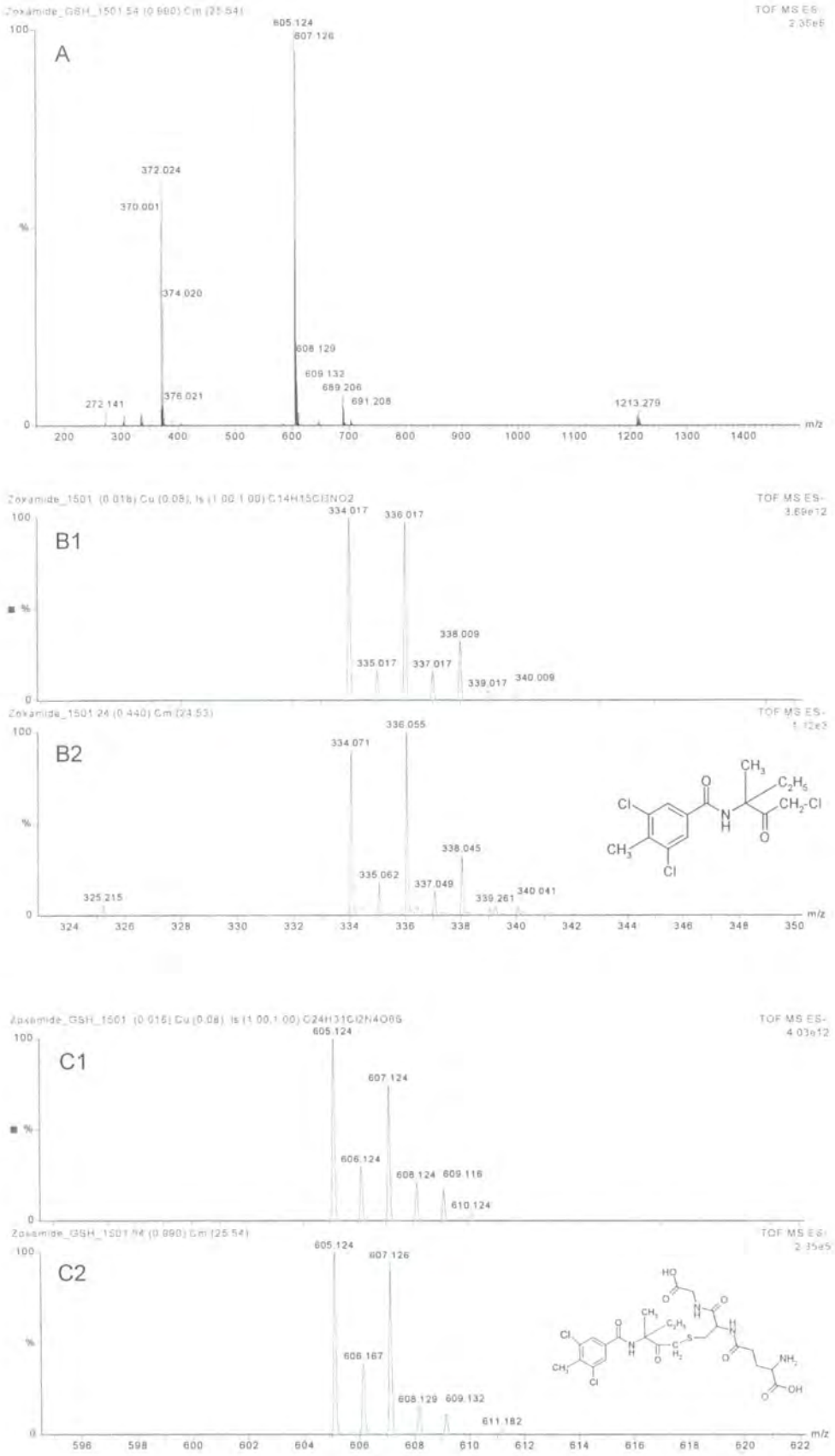

Figure 3.2.6.2 Legend over leaf

Figure 3.2.6.2 (A) ES-MS operating in negative mode direct infusion of 100 μM Zoxamide-GSH conjugate. M- 372.024 corresponded to zoxamide.$2H_2O$. M- 605.124 corresponded to Zoxamide-SG conjugate following substitution of the chlorine. (B1) Isotope distribution model for the molecular formula of Zoxamide. (B2) Isotope distribution of zoxamide. (C1) Isotope distribution model for the molecular formula of the zoxamide glutathione conjugate. (C2) Isotope distribution pattern of the zoxamide glutathione conjugate

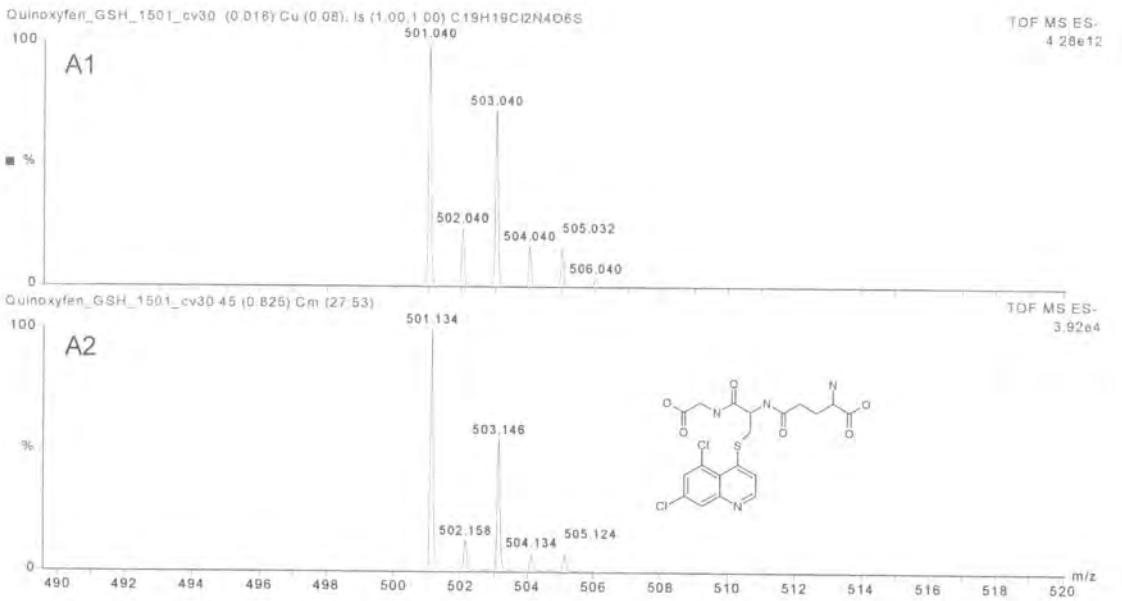

Figure 3.2.6.3 (A1) Isotope distribution model for the molecular formula of the Quinoxyfen glutathione conjugate. (A2) ES-MS operating in negative mode direct infusion of 100 μM Quinoxfen-GSH conjugate. M- 501.134 had the isotope distribution pattern corresponding to the glutathione conjugate of quinoxyfen following nucleophilic cleavage of the biphenyl ether bond (table 3.2.5).

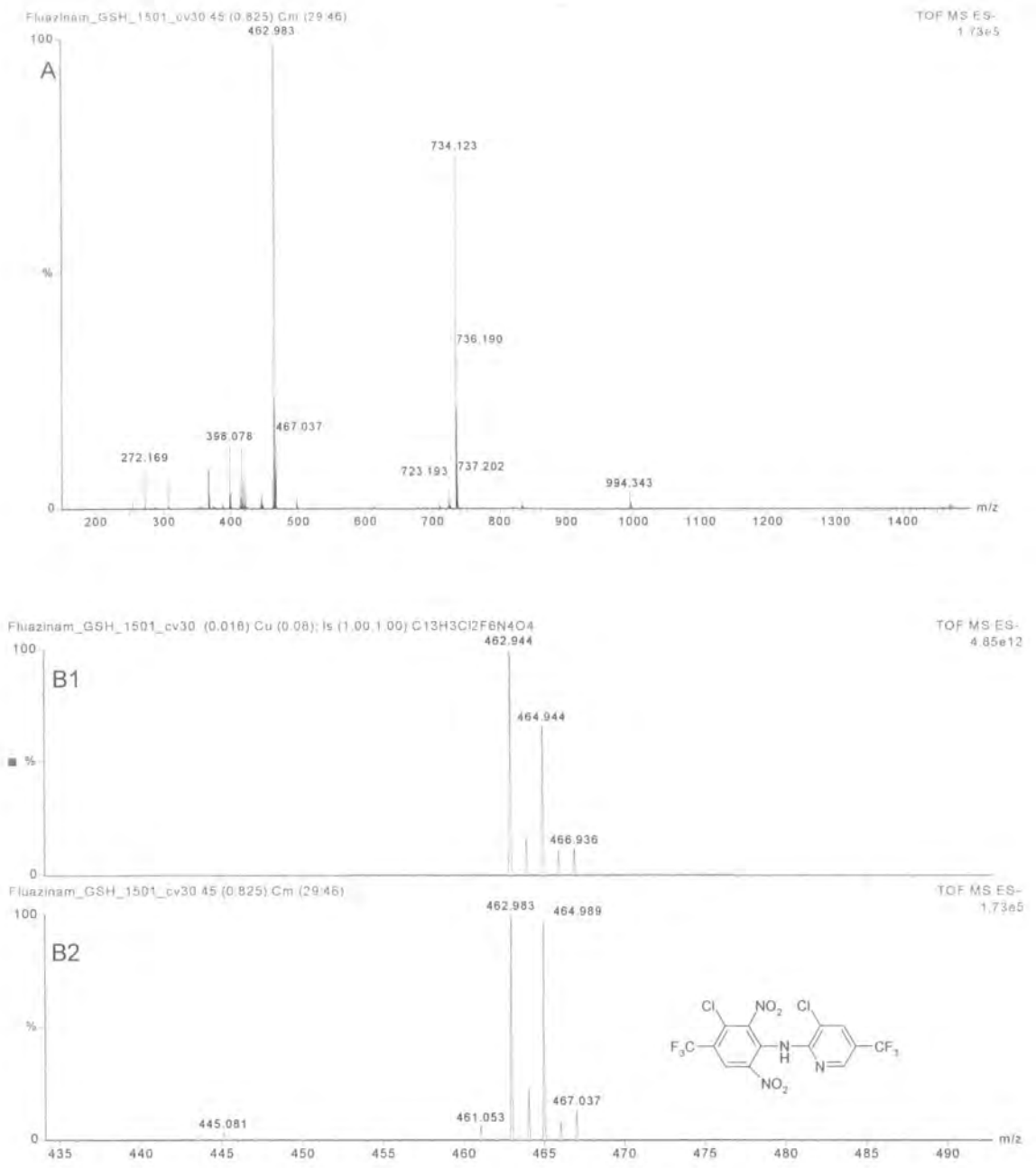

Figure 3.2.6.4 (A) ESMS spectra operating in negative mode of 100 uM of authentic fluazinam-glutathione conjugate synthesis following 36h incubation at room temperature. M- 462.983 corresponded to fluazinam, M- 734.123 corresponded to the glutathione conjugate Fluazinam-SG conjugate, M- 994.343 corresponded to the di-glutathione conjugate fluazinam-(SG_2). (B1) isotope distribution model of fluazinam molecular formula. (B2) The isotope distribution of fluazinam.

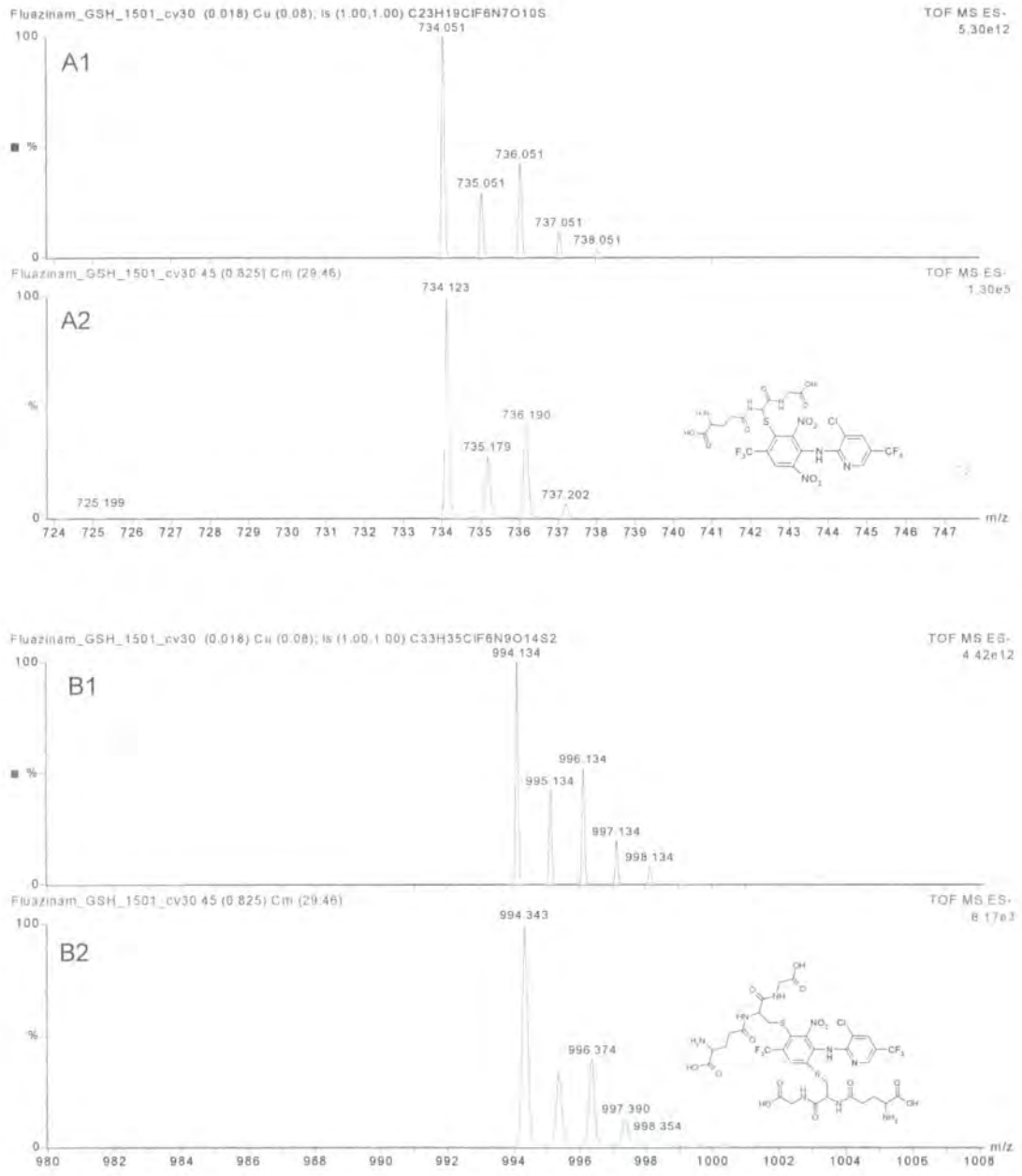

Figure 3.2.6.5 (A1) Isotope distribution model of the fluazinam glutathione conjugate following nucleophillic displacement of chlorine proximal to the nitro group. (A2) isotope distribution of the fluazinam-SG conjugate (B1) Isotope distribution model of the fluazinam glutathione conjugate following nucleophillic displacement of chlorine proximal to the nitro group and nucleophillic de-nitrosilation (B2) isotope distribution of the fluazinam di-glutathione conjugate.

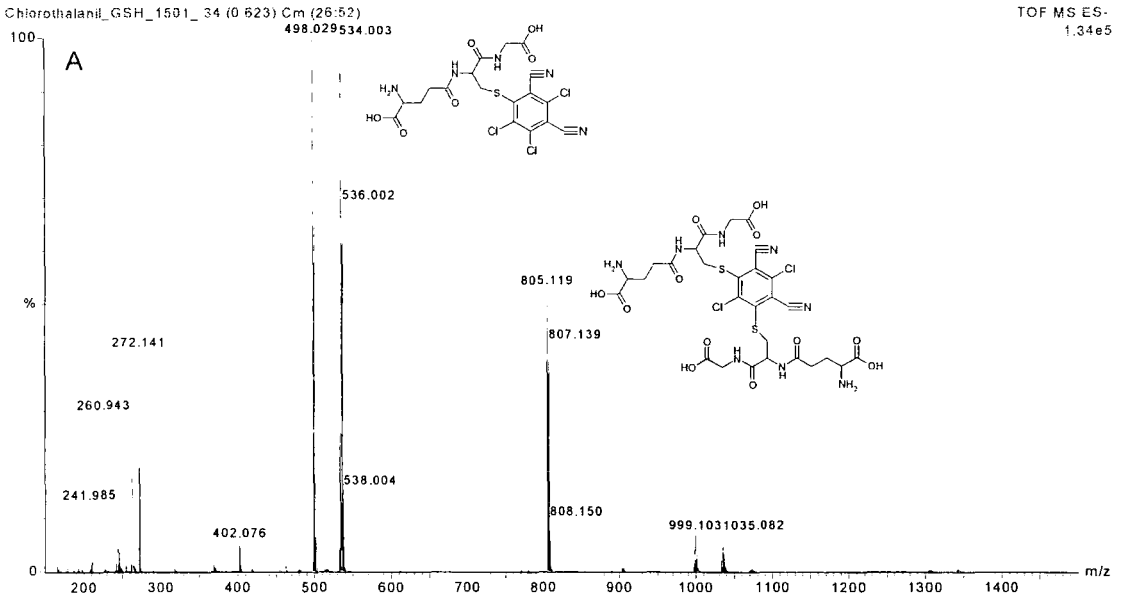

Figure 3.2.6.6 ESMS operating in negative mode of 100 μM glutathione chlorothalinil incubation after 36 h. M- 260 corresponded to hydrated chlorothalanil. M- 498.029 corresponded to the de-hydrated glutathione conjugate of chlorothalanil (M- 516), with M- 534 possibly arising from conjugate hydration. M- 805.119 corresponded to the hydrated di-glutathione conjugate of chlorothalinil (M-787).

Using dichlormid treated 10-day old wheat root as a crude source of GSTs the fungicides were incubated with the protein extract in the presence of GSH to determine whether or not glutathione conjugation could be enzyme catalysed. Using fenoxaprop-P and fenoxaprop-P-ethyl as positive controls, LC-ESMS was employed to identify conjugates. Based on the relative abundance of the GST mediated glutathione conjugates of fenoxaprop-P and fenoxaprop-P-ethyl present, dichlormid treated wheat root GSTs had specific activities of 24545 total ionisation counts min mg^{-1} protein and 9898 total ionisation counts min mg^{-1} protein to the respective substrates. These data indicated that wheat root GSTs had 2.5 times greater activity toward the bio-active free acid herbicde fenoxaprop-P over that of the ester fenoxaprop-P-ethyl. Furthermore they were in agreement with Tal *et al.*, (1993) who suggested that esterase activity was the first step in the metabolism of fenoxaprop-P-ethyl in wheat. Of the fungicide panel, none were found to have undergone GST mediated glutathione conjugation (table 3.2.6.2).

Table 3.2.6.2. Safened wheat root GST activities toward pesticide substrates, using boiled wheat root protein as a control enzyme source to compensate for spontaneous GSH conjugation of the pesticides.

Substrate	Specific activity TIC mg min^{-1}	
Fenoxaprop-P	24545	±7192
Fenoxaprop-P-ethyl	9898	±2038
Cyazofamid	nd	nd
Picoxystrobin	nd	nd
Azoxystrobin	nd	nd
Zoxamide	nd	nd
Quinoxyfen	nd	nd
Chlorothalanil	nd	nd

nd = not detected

Whilst wheat contained GSTs active in detoxification of fenoxaprop, of the panel of fungicides examined, none were found to have undergone enzyme mediated conjugation. Pesticide screening and trials may have played a large part in this observation. In order for efficacious treatment of crop diseases with fungicides, negligible activity by the host plant xenobiotic detoxification system may be essential to avoid pre-mature metabolism before reaching the target site in the invading pathogen.

Chapter 4.0 Cloning and Expression of a (ξ) Xi Class GST from *Magnaporthe grisea*.

4.1 Introduction

Arguably one of the most significantly important agronomic diseases in world agriculture is caused by the filamentous ascomycete *Magnaporthe grisea* (anamorph: *Pyricularia grisea*), the causal agent of rice blast. Annual rice crop losses attributed to this disease have been estimated sufficient to feed 60 million people (Zeigler 1994). Large ellipsoid leisions on the leaf surface characterise this disease, with infection in older plants spreading through to the panickle resulting in neck blast and complete crop loss (Talbot, 1995). Over 50 grass species are parasitized by strains of this fungus including wheat, barley, rice and millet crops (Talbot, 1995), with rice harvest losses reaching 30% annually (Talbot, 2003). The organism is so damaging that the Centres for Disease Control and Prevention have listed *Magnaprothe grisea* as a potential biological weapon (http://www-genome.wi.mit.edu/annotation/fungi/magnaporthe/).

Considerable research has focused on *M. grisea,* with the sequencing of its 7 chromosome 40 mbp genome recently completed and EST and genomic databases available for BLAST interrogation (table 4.1). As discussed in Chapter 1, sequence analysis of fungal GSTs has made placement within extant GST classes problematical with their relationship to plant and animal sequences being tenuous. EST analysis of *M. grisea*, performed by Bayer Crop Science, Lyon, identified a putative GST in the vector p2.5 NW, which appeared to be full-length, though the cDNA had only been partially sequenced. In this chapter the cloning and expression of this recombinant GST from *M. grisea* is reported and the respective enzyme purified and characterised. This GST belongs to a new grouping within this superfamily of detoxification enzymes, which has been termed the Xi class.

Table 4.1 *Magnaporthe grisea* genome databases

http://www-genome.wi.mit.edu/annotation/fungi/magnaporthe
http://cogeme.ex.ac.uk/search.html
www.fungalgenomics.ncsu.edu/

4.2 Results and Discussion

4.2.1. Sub cloning of *Mg*GSTX1 into the pET expression vector.

From contig sequence data of the GST insert in vector p2.5 NW, primers containing *BAMH1* and *NCO1* restriction sites were designed to the respective 3' and 5' regions of the coding sequence (see 2.7.13.2, table 2.7.2). The *MgGST* insert was amplified (table 2.7.5, programme A) and sub-cloned into the pET11d expression vector and used to transform *E. coli* XL10-Gold. Using primers directed to 3' and 5' regions of the sequence respectively (table 2.7.2). Colony PCR (table 2.7.5, programme E) revealed positive colonies harbouring inserts of the expected size of 855 base pairs (figure 4.2.1). A positive colony was then cultured overnight and the plasmid obtained used for transformation into *E.coli* BL21 electro competent cells.

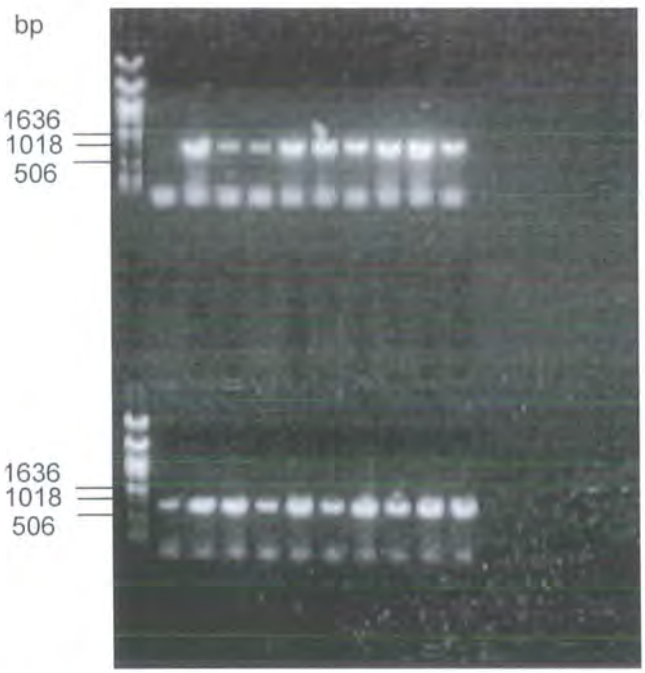

Figure 4.2.1 Colony PCR of independent colonies of pET11d *E.coli* XL10-Gold transformants containing the *MgGSTX1* insert grown overnight at 37°C. Inserts were detected using the combination of *BAM H1* and *NCO1* primers (table 2.7.2) directed to 3' and 5' regions of the sequence respectively. The observed PCR products were consistent with those previously determined by PCR programme E with and without plasmid template DNA.

Transformed bacteria were then re-assayed by colony PCR and a positive colony (figure 4.2.2) used to inoculate an LB agar plate, which was incubated overnight at 37°C. Colonies were harvested and plasmid DNA isolated by mini-prep, with bacterial stocks stored at -80°C in 15% glycerol.

Figure 4.2.2 Colony PCR (25 cycles, programme E) of pET11d *E. coli* BL21 transformant containing the *MgGSTX1* insert grown overnight at 37°C. Inserts were detected using the combination of *BAM H1* and *NCO1* primers (table 2.7.2) directed to 3' and 5' regions of the sequence respectively. Lane 1 = positive colony; 2 = control consisting of the PCR mix and primers only.

Prior to further analysis, purified pET11d plasmid preparations containing the *MgGST* insert were submitted to DBS Genomics for automated sequencing. The full coding sequence was obtained (Figure 4.2.3), respective amino acid sequence deduced and the molecular mass of the encoded polypeptide estimated at 28829 Daltons (Figure 4.2.4).

5' GCGCGCGGTACCCTTAGTTTTGACTG

ATGGGAATCAAAACTGACATTCACCTGTATACCACCGGTACGCCAAATGGCATC

AAGGTGTCTATCCTGCTCGAGGAGCTGGGCCTCGAGTACCAGGTGACCAAGAT

TGACATTATGAAGAACGTGCAAAAGGAGCAATGGTTCCTTGACATCAACCCCAA

CGGTCGCATCCCGGCATTGACCGACACTTTCACCGATGGCAAGCCCATCATTTT

GTTTGAGAGCGCCTCCATCATGCAGTACCTTGTGGCCCGTTATGACACTGAGCA

CAAAGTGTCGTACCCCCACGGTTCCAGGGAGCACTACCAGGTCCAGAACTGGG

TCTACTGGCAGATGGGCGGCCTTGGCCCCATGCAGGGTCAAGCGAACCACTTC

AGCCGCTACGCCCCGGAGAAGATCCAGTACGGCATTGACAGGTACCAAAACGA

GACCCGTCGTCTTTATGGCGTGATGGAGACGCAGCTCGCTAGCAACCCGTCCG

GATACCTTGTCGGTGATAAGGCGACCATCGCAGACTTTGCCTGCTGGGGATGG

GTAGCTGGTTACTCATGGTGTGGAATTGACATTGAGCCGTTCCCTCACTTGAAG

GCATGGCTCTGGAAGCTGAAGGAGAGACCTGGTCTTGACAAGGGTCGCAACGT

GCCTACTCCGCACACGGCTCTCGATCACGTTGGTAAGAGCCAGGAGGAGCTAG

ACAAGATGGCCGAGGAGTCGAGGAAGTGGATTCAGGCTGGCATGGCCGCTGAT

GCTAAGAAATAG-3'

Figure 4.2.3 Coding sequence of *Magnaporthe grisea MgGSTX1*. High lighted regions correspond to 5' NCO1 and BAMH1 primers for cloning into pET11d, 5' and 3' underlined bases correspond to the start and stop codons respectively.

MGIKTDIHLYTTGTPNGIKVSILLEELGLEYQVTKIDIMKNVQKEQWFLDINPNGRIPAL
TDTFTDGKTINLFESASIMQYLVDRYDTEHKVSYPHGSREHYQVQNWVYWQMGGL
GPMQGQANHFSRYAPEKIQYGIDRYQNETRRLYGVMETQLASNPSGYLVGDKATIA
DFACWGWVAGYSWCGIDIEPFPHLKAWLWKLKERPGLDKGRNVPTPHTALDHVG
KSQEELDKMAEESRKWIQAGMAADAKK

(Molecular mass 28829 Da)

Figure 4.2.4 Deduced amino acid sequence of *M. grisea* *Mg*GSTX1. Underlined amino acid residues 4-84 and 95-206 correspond to regions sharing homology with other GSTs. Underlined amino acid residues 220-227 were identified as a P-loop motif. These domains were identified through Interproscan.

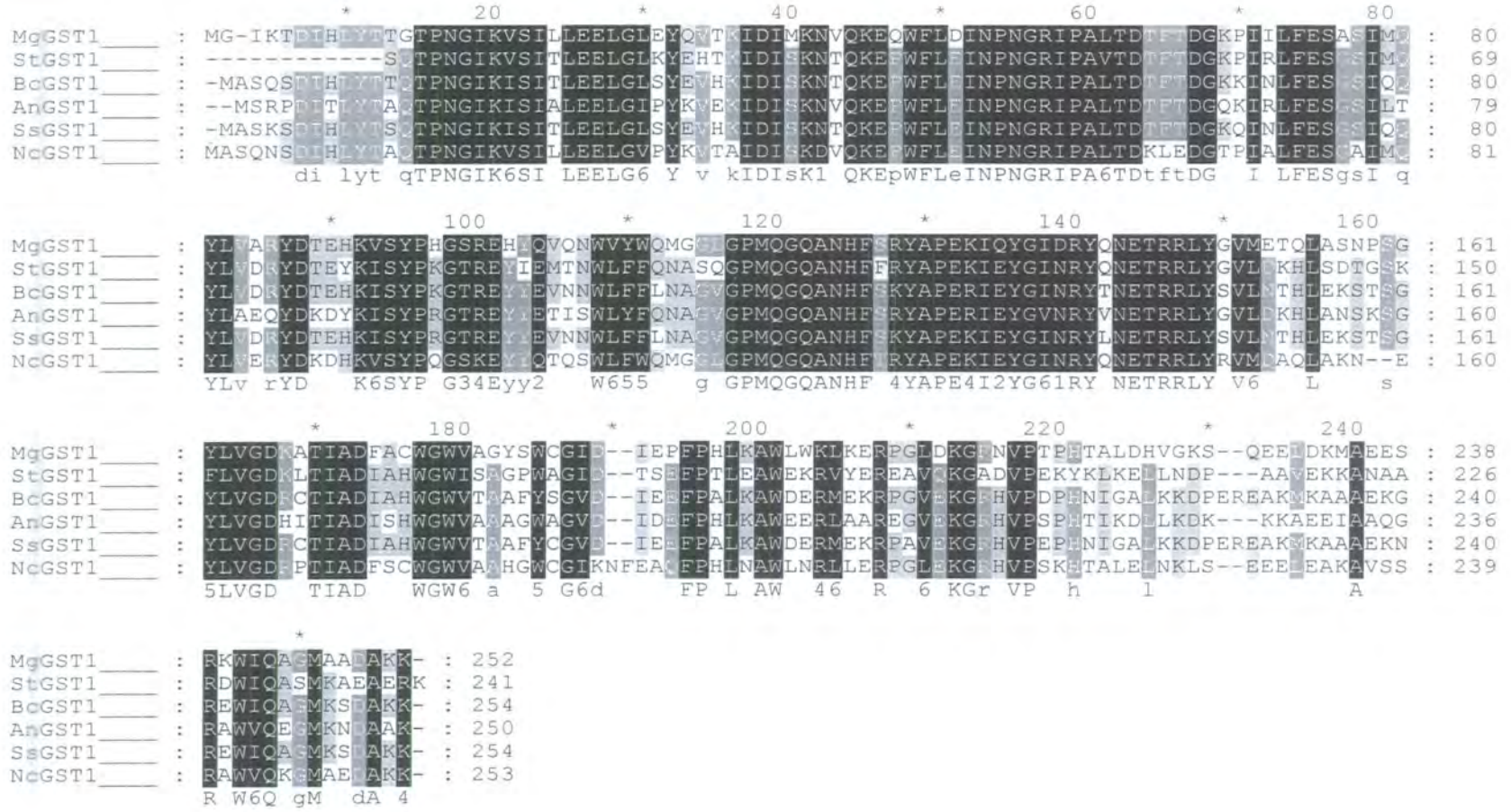

Figure 4.2.5 Multiple amino acid sequence alignment of sequences showing homology to *MgGSTX1* of *Magnaporthe grisea*. *St*GST1, partially cloned sequence from this study *Septoria tritici*; *Bc*GST1 (*Botrytis cinerea* Q9HF89); *An*GST1 (*Aspergillus nidulans* Q8NJZ8); *Nc*GST1 (*Neurospora crassa* EAA32029 hypothetical protein); *Ss*GST1 (AR123147 cloned from *Glycine max* infected with *Sclerotinium sclerotia*; see text 3.2.4 for explanation).

4.2.2 Sequence analysis of *Mg*GSTX1

Multiple sequence alignment of the *Mg*GSTX1 amino acid sequence cloned from the fungal pathogen *M. grisea* to GSTs from other fungal sources revealed striking similarities, with regions of homology being evident (figure 4.2.5). *Mg*GSTX1 shared 65% identity with *Bc*GST (Prins *et al.*, 2000) and 61% similarity with *GstA* from A*spegillus nidulans* (Fraser *et al.*, 2002). Additionally, 57% identity was shared with a partial *St*GST1 sequence (figure 4.2.5), which was cloned as an EST from *Septoria tritici* as part of this investigation (data not shown). Work on the *Septoria* GST was not pursued in favour of characterising the full *Magnaporthe* GST; clone kindly provided by Dr E. O'Neill, Bayer Crop Science (Lyon, France). Interestingly, the highest identity (96%) was observed between *Bc*GST and a putative GST isolated from soybean, the latter having been patented by McGonigle and O'Keefe of Dupont (patent. US 6168954). Initially, this observation suggested the presence of a GST family common to both plants and ascomycete fungi. On examination of the patent however, it was discovered that the cDNA was obtained from soybean plants infected with the phytopathogenic soybean stem rot fungus *Sclerotinium sclerotia*. Significantly, the homologous gene in *B. cinera* was also highly expressed during the infection of vine leaves (Prins *et al.*, 2000). It therefore seems likely that the Dupont patented soybean GST was actually derived from the infecting *S. sclerotia* cDNA and as such the "soybean" cDNA was reclassified as an *Ss*GST.

Recently an *MgGSTX1* homologue, *GstA*, was identified and cloned from *Aspergilllus nidulans* (accession AF425746). Through mutational studies GstA was shown to contribute to heavy metal and xenobiotic tolerance, though

paradoxically its expression conferred sensitivity toward the systemic fungicide carboxin, which is a succinate dehydrogenase inhibitor (Fraser *et al.*, 2002).

GstA was assigned to the theta class of GSTs on the basis that GST activity toward CDNB could not be detected in *A. nidulans* protein extracts and that other theta class GSTs also show no activity toward this substrate (Fraser *et al.*, 2002). However, sequence analysis does not support this classification as GstA did not contain the catalytically essential serine 11 common to all theta GSTs (Landi, 2000: Sheehan *et al.*, 2002), and only bore week amino acid identity to this class (17% - 20%). The strong conservation of amino acid sequence identity between *Mg*GSTX1 and homologues from other pathogenic and saprophytic fungal species, suggests these GST-like sequences actually belong to a unique class of fungal GSTs and as such they have been assigned the Greek letter Xi (ξ) to represent a suggested new grouping within the GST super family.

4.2.3 Interproscan database search of *Mg*GSTX1

Interrogation of the *M. grisea* *Mg*GSTX1 amino acid sequence by the Interproscan database search (http://www.ebi.ac.uk/interpro/scan.html) revealed the presence of 3 motifs within the predicted protein sequence. Amino acids 4 – 84 in the N-terminal domain contained a region with identity to GST sequences. The N-terminal domain contains catalytically essential residues for GSH activation (Nishida *et al.*, 1998). Between amino acids 95–206 blocks of conserved sequences matching 809 GST proteins (Interproscan search code IPR000521) were identified. In addition, an eight amino acid P-loop motif,

matching 3279 proteins (Interproscan search code IPR001687), was also found (figure 4.2.6).

Typically the P-loop binding motif is a glycine rich region forming a flexible loop between a beta-strand and an alpha loop, capable of interacting with one of the phosphate groups of either ATP or GTP (Detlef *et al.*, 2002). However, the P-loop sequence of *Mg*GSTX1, ALDHVGKS, is not glycine rich and as such there may be some speculation regarding it being a bonafide binding domain capable of conferring a novel activity to *Mg*GSTX1. Significantly, a P-loop binding domain was not found in either *Bc*GST or *Ss*GST.

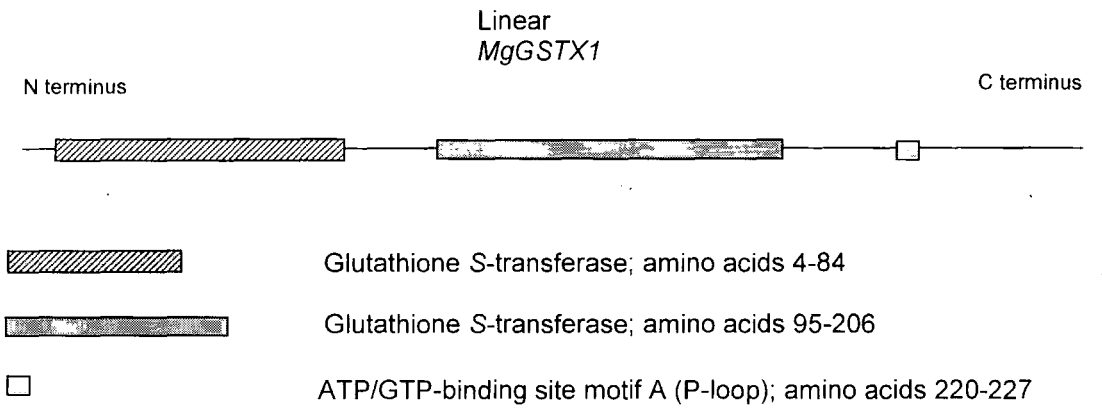

Figure 4.2.6 Linear schematic representation of the *MgGSTX1* amino acid sequence detailing domains found through Interproscan. The respective amino acid sequences are detailed by underlined regions in figure 4.2.4

4.3 Over expression and purification of recombinant *Mg*GSTX1

Analysis of recombinant *MgGSTX1* expression in *E. coli* BL21, mediated by vector pET11d, revealed the majority of the 29kDa protein was expressed in the insoluble fraction following IPTG induction (Figure 3.3.1 lane 4), with only a modest degree of expression observed also in the soluble protein fraction (Figure 4.3.1 lane 3).

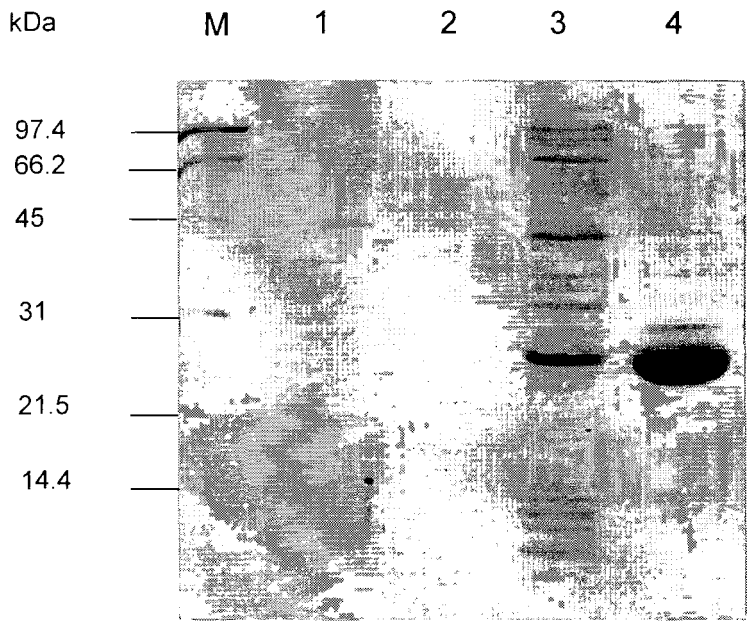

Figure 4.3.1 12.5% SDS PAGE of recombinant *MgGSTX1* following expression in *E. coli* BL21 using the vector pET11d. Bacteria were grown at 37°C prior to (lanes 1 and 2) and following induction with 1 mM IPTG Lanes 3 and 4). 1 = pET11d soluble; 2 = pET11d insoluble; 3 = pET11d induced soluble; 4 = pET11d induced insoluble; 4 = pET11d induced insoluble.

Rapid exponential growth of the bacteria following induction and the associated overproduction of *Mg*GSTX1 could provide a possible explanation for insoluble expression of recombinant enzyme. Thus it is likely that post-

translational processing utilising molecular chaparonins was saturated, resulting in the formation of insoluble aggregates of *Mg*GSTX1. In order to optimise *MgGSTX1* expression, the transformed bacteria were cultured at four temperature regimes following induction with IPTG. The hypothesis was to establish if by slowing *E. coli* BL21 growth it would be possible to obtain a greater proportion of *MgGSTX1* in the soluble form.

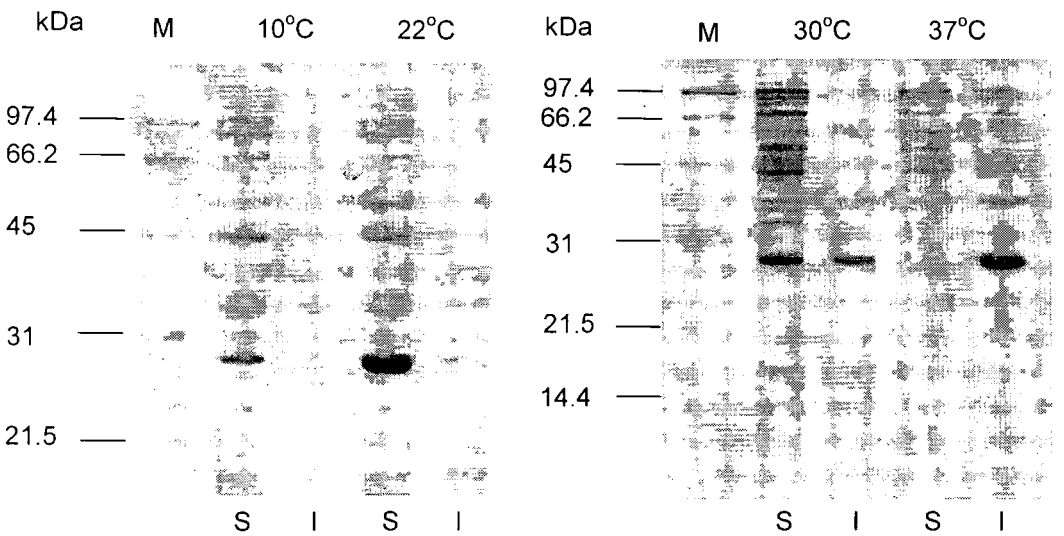

Figure 4.3.2 12.5% SDS PAGE of temperature regulated *Mg*GSTX1 expression pattern in *E.coli* BL21, pET11d vector following induction with 1 mM IPTG. S = soluble; I = insoluble.

Optimisation of the expression pattern of recombinant *Mg*GSTX1 in *E. coli* BL21 was achieved through temperature regulation following IPTG induction (figure 4.3.2). Cultures grown at 10°C, for 16 h expressed low levels of *Mg*GSTX1 in the soluble form and very low levels in the insoluble fraction. Following expression for 16 h at 22°C the majority of *Mg*GSTX1 remained in the soluble fraction, whereas 2.5 h at 30°C resulted in approximately even partitioning of

expression of the protein between soluble and insoluble fractions, with only insoluble expression being observed in the 2.5 h 37°C culture. Growth at 22°C for 16 h was ultimately selected as the optimal conditions for the soluble expression of *Mg*GSTX1 in *E. coli* BL21 resulting in good yield.

4.3.1 Glutathione affinity chromatography

Attempts to purify r*Mg*GSTX1 by glutathione affinity chromatography did not prove successful. With the protein showing no retention on the affinity matrix (figure 4.3.3).

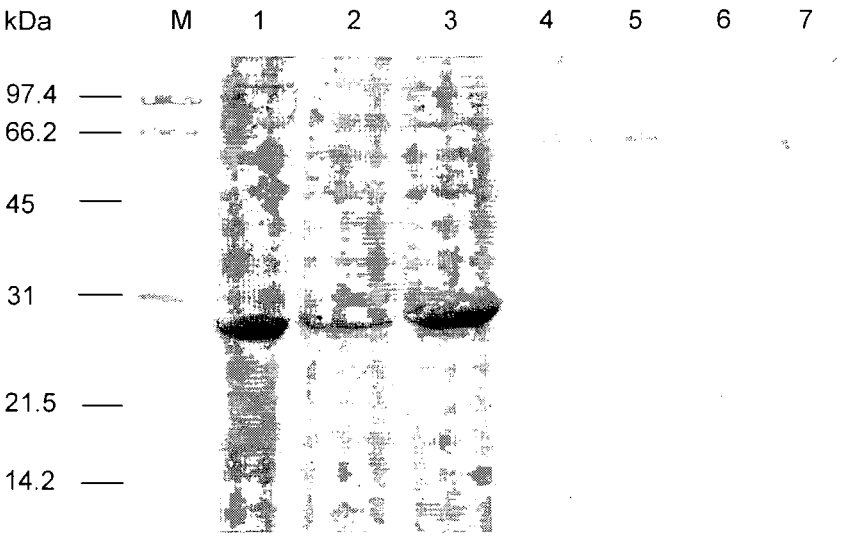

Figure 4.3.3 12.5% SDS PAGE of recombinant *MgGSTX1* following GSH affinity chromatography. 1 = crude lysate; 2 = desalted ammonium sulphate pellet; 3 = flow through; 4-7 fraction obtained after washing the column with 10 mM GSH.

4.3.2 Hydrophobic interaction chromatography

Crude lysates containing recombinant *Mg*GSTX1 were precipitated with 80% $(NH_4)_2SO_4$, stored at –20°C and desalted on a PD10 column into 2 mM potassium phosphate buffer pH 7 containing 1 M $(NH_4)_2SO_4$. Hydrophobic interaction chromatography was then employed to purify the recombinant protein. Five uv-absorbing peaks eluted from the phenyl Sepharose column (figure 4.3.4), which were analysed by SDS PAGE (figure 4.3.5). Peak one consisted of the unbound proteins and contained no recombinant *Mg*GSTX1, indicating hydrophobic interaction between the recombinant polypeptide and phenyl Sepharose column. *Mg*GSTX1 was then recovered after removing salt from the buffer in peaks 2 and 3 gradually eluting from the column during washing with 100% buffer B, while peak 4 being eluted as a sharp peak on addition of 50% ethylene glycol buffer B. Fractions containing recombinant *MgGSTX1* and the lowest level of contaminating protein (fractions 8 – 11 = peaks 2-3 figure 4.3.5) were pooled and concentrated to 5.26 mg protein mL^{-1} using a centrifugal concentrator. The protein was then stored at –20°C after adding an equal volume of glycerol.

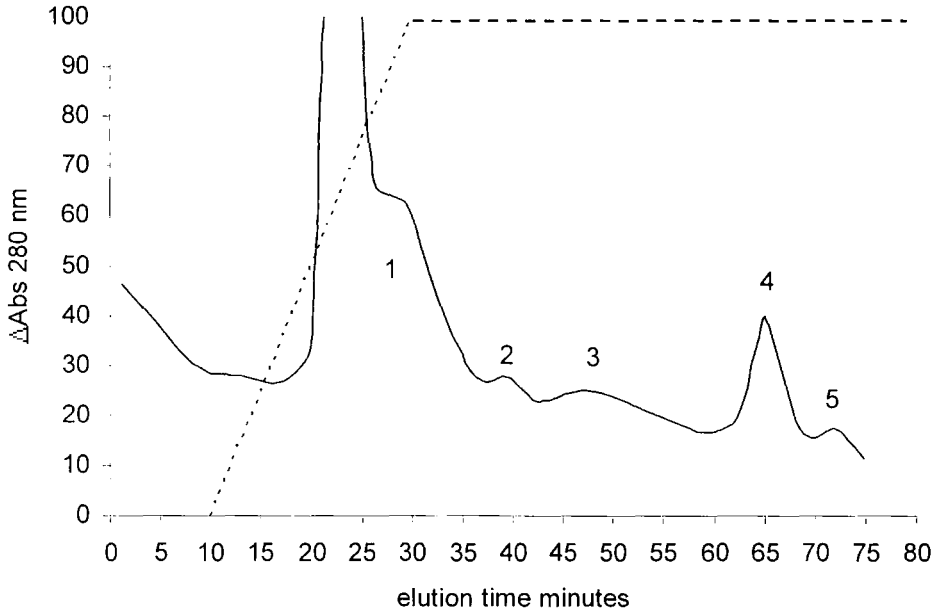

Figure 4.3.4 Purification of *Mg*GSTX1 by phenyl sepharose hydrophobic interaction chromatography with eluting protein being monitored for change in absorbance at 280 nm (solid line) as the percentage of elution buffer B (dashed line) was increased. Each numbered peak was analysed by SDS PAGE for the presence of the recombinant *Mg*GSTX1 polypeptide.

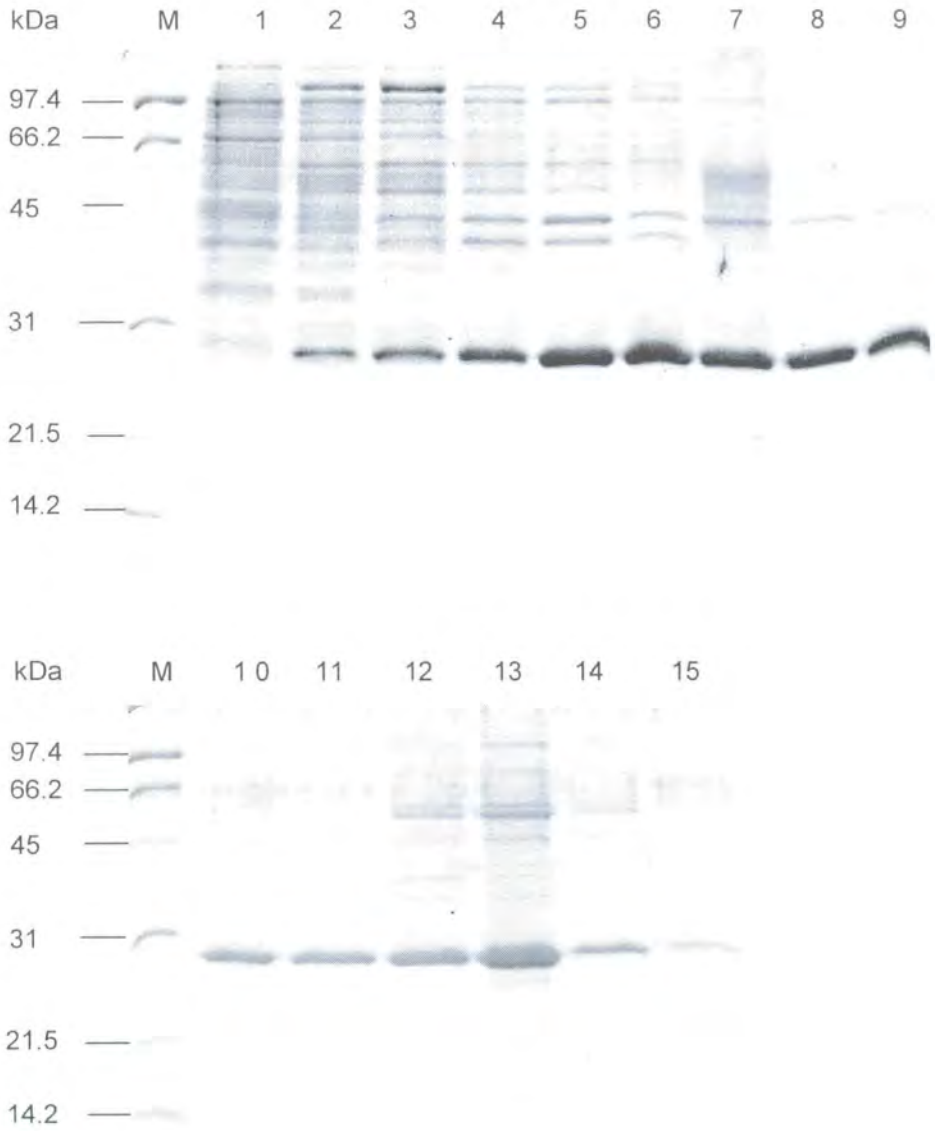

Figure 4.3.5 12.5% SDS PAGE stained with BioRad gel code blue of recombinant *Mg*GSTX1 in fractions eluted from a phenyl sepharose column. Lanes corresponding to the individual fractions associated with the peaks shown in Figure 3.3.4. Fraction 1 = peak one; fraction 2 = peak 2; fractions 3–10 = peak 3; fractions 11-14 = peak 4; fraction 15 = peak 5.

Subsequent purification protocols employed a combination of hydrophobic interaction chromatography using octylsepharose (figure 3.3.6) followed by Q-sepharose anion exchange chromatography. Purification was monitored by SDS PAGE with the purest fractions obtained from the HIC column being pooled and concentrated by further chromatography on a Q-sepharose column (figures 4.3.7 & 4.3.8), thereby removing the need for centrifugation columns.

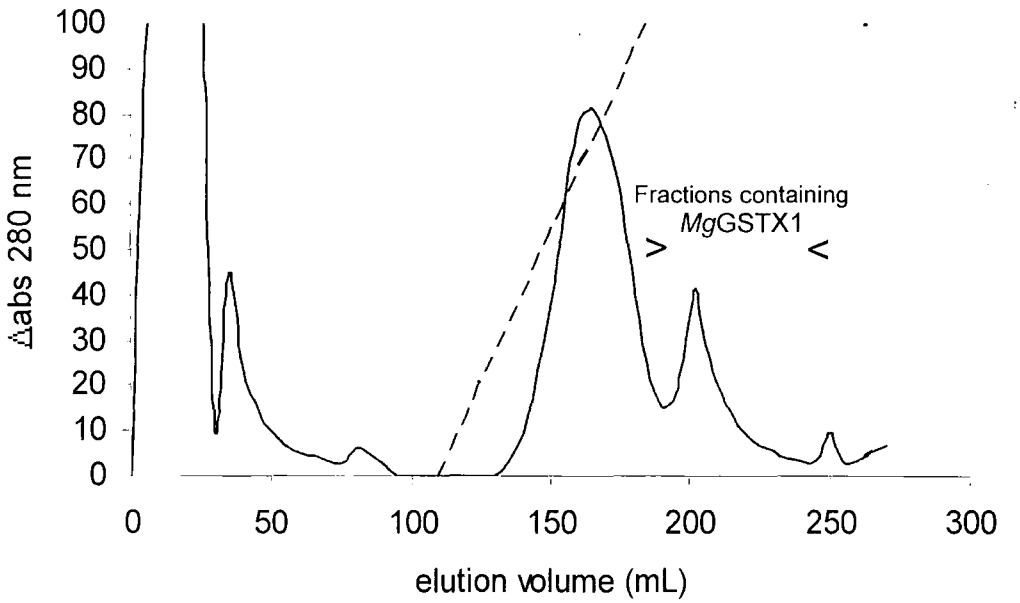

Figure **4.3.6** Hydrophobic interaction chromatography of crude bacterial lysate containing the recombinant *Mg*GSTX1 polypeptide. Protein eluting from the octyl sepharose column was monitored by the change in absorbance at 280 nm (solid line), with decreasing salt concentration (1M $(NH_4)_2SO_4$ to zero $(NH_4)_2SO_4$ dashed line). Purification was monitored by SDS PAGE (overviewed in figure 4.3.8).

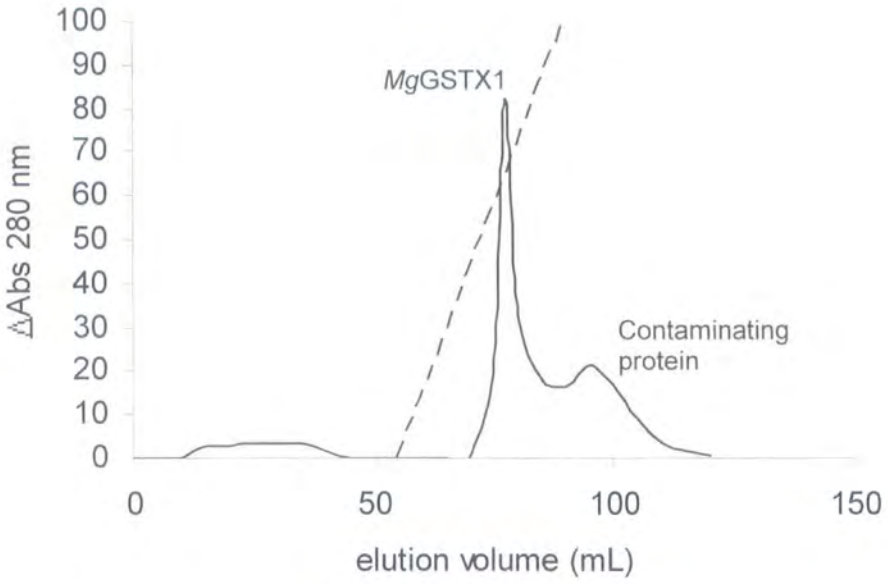

Figure 4.3.7 Anion exchange chromatography of *Mg*GSTX1 following HIC. Protein eluate from the Q-sepharose column was monitored for the change in absorbance at 280 nm (solid line) with increasing salt concentration (zero to 500 mM NaCl dashed line).

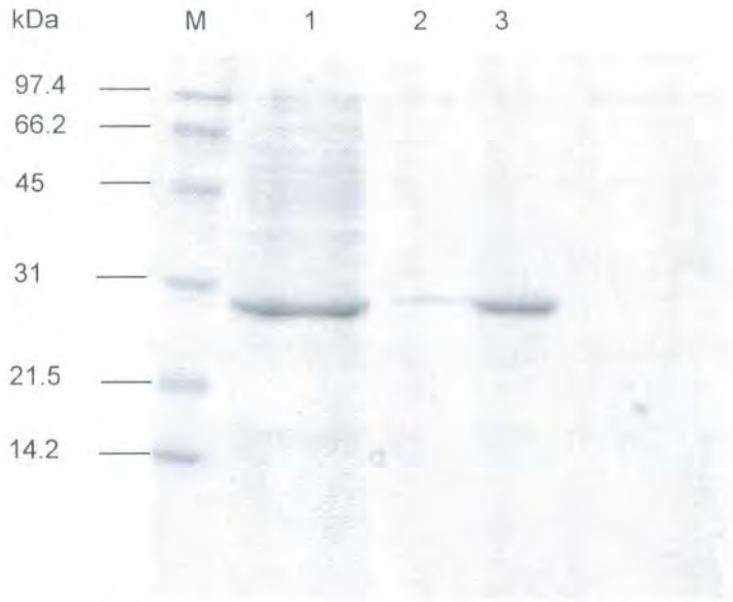

Figure 4.3.8 SDS PAGE overview of *Mg*GSTX1 purification from *E. coli* lysates stained with BioRad gel code blue. 1 = Crude protein; 2 = purified protein from octyl sepharose; 3 = purified protein following further chromatography on Q-sepharose.

4.3.3 Electrospray Ionisation Mass Spectrometry of r*Mg*GSTX1

ESI TOF MS analysis of purified recombinant *Mg*GST1 identified the mass of the recombinant polypeptide to be 28700 Da. The predicted protein mass of the polypeptide was 28829.6 Da as derived from the sequence of *MgGSTX1*. The discrepancy in mass of 130 Da probably corresponded to post translational modification consistent with cleavage of the N-terminal methionine (figure 4.3.9).

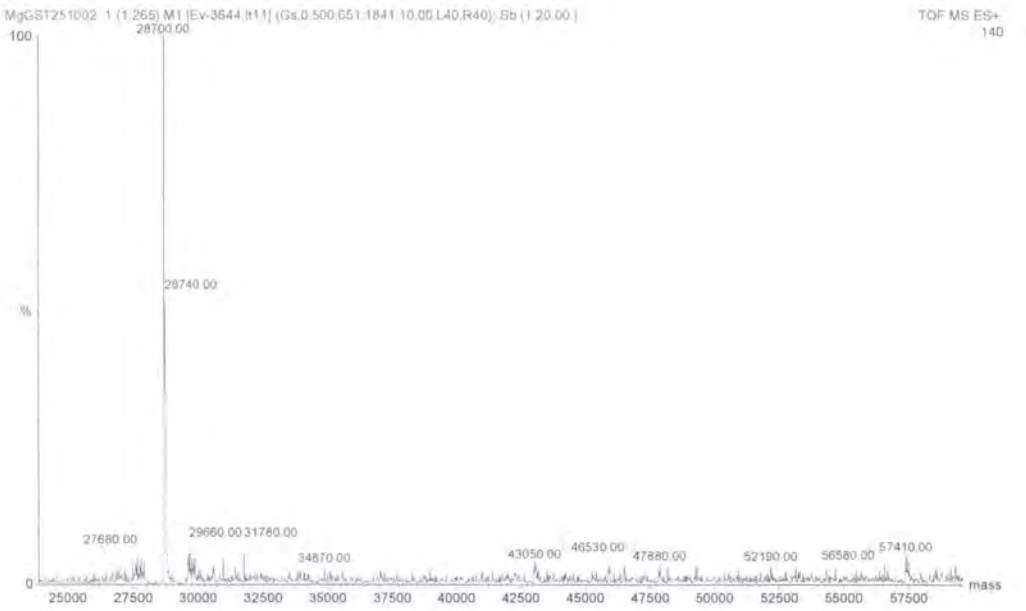

Figure 4.3.9 ESI TOF MS (positive ionisation mode) of purified *Mg*GSTX1 (28700). The predicted mass of *Mg*GSTX1 was 28829.6 Da with the discrepancy in 130 Da probably arising from the cleavage of the N-terminal methionine.

4.3.4 r*Mg*GSTX1 functions as a dimer

To determine the native conformation of the r*Mg*GSTX1 polypeptide, gel filtration was performed to deduce whether the native protein functioned as a monomer or dimer. Gel filtration after calibration with protein standards of BSA, ovalbumin and carbonic anhydrase estimated the native molecular mass of r*Mg*GSTX to be approximately 55 kDa (table 4.3.4). From the subunit mass of 28700 determined by ESI-MS, these data suggest the native enzyme was a dimeric protein, with an actual mass of 57400 Da.

Table 4.3.4 Gel filtration protein calibration curve

		Elution time	
Protein	kDa	minutes	Log
BSA	66	26.404	1.421
Ovalbumin	45	28.61	1.456
Carbonic anhydrase	29	31.09	1.492
Equation for log time minutes	$y = -521.02x + 805.76$ ($R^2 = 0.9923$)		
*Mg*GSTX1-1	27.61	1.441066	54.93558

4.3.5 Thioltransferase activity of r*Mg*GSTX1-1

Assays of recombinant enzyme *MgGSTX1* against a broad spectrum of classic GST substrates (table 4.3.5) revealed that r*Mg*GSTX1 was not active toward pesticides or colorimetric substrates which were acted on by plant GSTs (Chapter 3). Similarly, GST activity toward chromogenic substrates was not detected in protein extracts of *B. cinerea* and *A. nidulans*, (Prins *et al.*, 2000; Fraser *et al.*, 2002) which both contain GST Xi class homologues. Lambda GSTs have been shown to exhibit thioltransferase activity toward the substrate hydroxyethyl disulphide (HED), while being inactive toward many GST substrates such as CDNB (Dixon *et al.*, 2002). As such r*Mg*GST1 was also assayed against HED to determine any potential thioltransferase activity of this enzyme.

Table 3.3.5 Xenobiotic substrates assayed against r*Mg*GSTX1

Pesticide assays
Alachlor
Metalochlor
Atrazine
Ofurace
Fluorodifen
S-ethyl dipropyl thiocarbamate
Fenoxaprop-P-ethyl
Spectrophotometric assays
CDNB (1-chloro-2, 4-dinitrobenzene)
α and β-unsaturated aldehydes
ethacrynic acid
BITC
4-nitrophenyl acetate
cumene hydroperoxide

Thioltransferases (TTases) are monomeric enzymes, which catalyse the reduction of low molecular weight disulphides by utilizing GSH in the presence of NADPH and glutathione reductase (Kim *et al.*, 1999). The substrate hydroxyethyl disulphide (HED) when incubated with GSH forms the mixed disulfide HES-SG and in the presence of a thioltransferase is reduced to HE-SH and GSSG. Purified recombinant dimeric *Mg*GSTX1-1, demonstrated TTase (thioltransferase) activity toward this mixed disulphide substrate. The specific activity of 50.4 ± 3.4 nKat mg^{-1} pure protein, was similar to that of lambda GSTs 1 and 2, from *Arabidopsis* reported by Dixon *et al.*, (2002) (table 4.3.6.). Activity was found to be dependent on protein concentration in the range of 2.5 μg – 17.5 μg r*Mg*GSTX1 (figure 4.3.10).

Table 4.3.6 Thiol transferase activities of recombinant GST like proteins.

Enzyme	Thiol transferase activity nkat mg^{-1} protein
*At*DHAR3	131
*At*DHAR1	116
*At*GSTL2	69
*Mg*GSTX1-1	50.4
*At*GSTL1	41
*At*DHAR2	15

Table adapted from Dixon *et al.*, 2002.

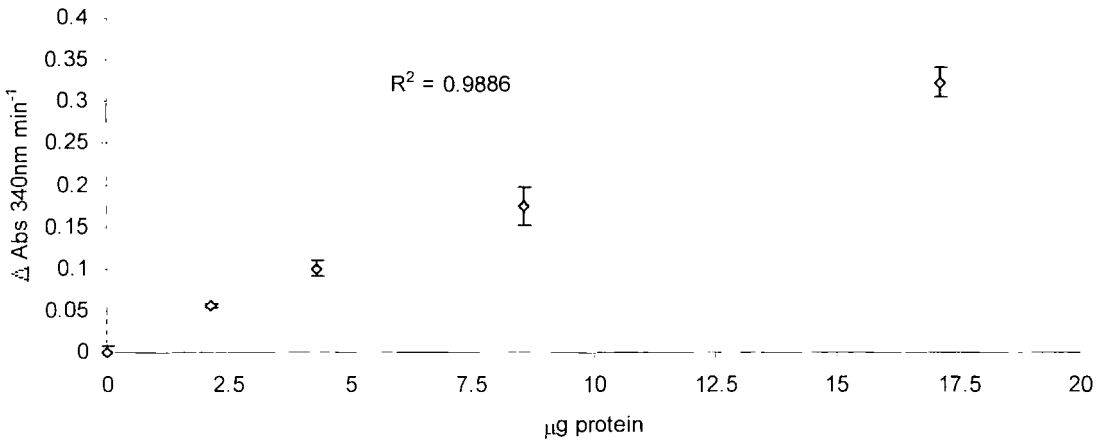

Figure 4.3.10 Enzyme activity of r*Mg*GSTX1-1 toward the substrate HES-SG as a function of protein dependence ranging from 2.5 μg – 17.5 μg recombinant protein.

Glutaredoxins displaying thioltransferase activity contain a conserved binding site for GSH with the active site motif -Cys-Pro-Tyr-Cys (Hoog *et al.*, 1983). However TTase activity is not always restricted to glutatredoxins and thioltransfer has been reported with mammalian and *Arabidopsis* dehydroascorbate reductase, (DHARs) and lambda GSTs (Dixon *et al.*, 2002; Wells *et al.*, 1990). Conversley, GSH conjugating activity toward CDNB has been demonstrated for a thioltransferase in the fission yeast *Schizosaccharomyces pombe* (Kim *et al.*, 1999). The glutaredoxin motif was not present in the r*Mg*GSTX1 protein sequence, but it was possible that cysteine residues 175 and 185 could potentially play a role in thiol transfer (figure 4.2.4). However, incubation for 10 minutes on ice with 1mM iodoacetamide, a thiol modifying reagent, did not inhibit the thioltransferase activity of r*Mg*GSTX1-1 while a similar treatment of *Arabidopsis* DHAR1, reduced thioltransferase activity by 97% (Dixon

et al., 2002). The apparent insensitivity of r*Mg*GSTX1-1 to iodoacetamide and absence of a glutatredoxin-like binding site motif suggested that free cysteines can not be involved in the thioltransferase activity of this enzyme. However, incubation of r*Mg*GSTX1-1 with 1mM N-ethylmaleimide (NEM), an alkylating reagent, which can derivatise cysteines that are disulphide bonded resulted in inhibition of thioltransferase activity, suggesting that if cysteinyl residues took part in catalysis they did so as the respective disulphide.

Paradoxically, neither cysteine was highly conserved within the related Xi GSTs, suggesting that these residues are not part of a catalytically conserved motif. Tryptic digestion and ESMS attempts to identify whether residue 275 or 285 had undergone NEM modification, proved unsuccessful. It was concluded that the loss of activity on NEM treatment was probably due to disulphide bridge disruption, which altered the overall structural conformation and thus catalytic activity of the enzyme. However, the absence of the classic thioltransferase motif (-Cys-Pro-Tyr-Cys) in r*Mg*GSTX1-1 warrants further investigation into the catalytic mechanism of this Xi GST as a thioltransferase.

Chapter 5. Cloning and expression of a recombinant theta class GST from *Phytophthora infestans*.

5.1 Introduction

The Oomycete *Phytophthora infestans* represents a phytopathogen of enormous agronomic importance to solanaceous crops, being able to infect both tomato and potato (Carlisle *et al.*, 2001). It is with regard to the latter crop that *P. infestans* gained infamy during 1840s' Ireland, being the causal agent of late blight of potato leading to famine and subsequent decimation of the Irish population. Understanding the molecular processes occurring during the plant-pathogen infection process may lead to enhanced control measures of this disease.

5.1.2 Oxylipin phytoalexins; a plant defence mechanism

Potato tuber lipoxygenase, 9-LOX (LOX, EC 1.13.11.12), catalyses the formation of the oxylipin hydroperoxides 9(*S*)-HPOD and 9(*S*)-HPOT, derived from the polyenoic unsaturated fatty acids (PUFAs) linoleic and linolenic acid respectively (Gardner, 1991). Rance *et al.*, (1998) highlighted the importance of LOX activity in preventing infection from *Phytophthora* spp., in *Nicotiana tabacum*, by constructing LOX antisense (AS) lines where the wild type were resistant to *Phytophthora parasitica* var. *nicotianae*. The ASLOX antisense lines showed enhanced susceptibility to *P. parasitica* and the fungus *Rhizoctonia solani*. Additionally Kato *et al.*, (1992) have reported that 9(*S*)-HPOT formed *in vitro* by tomato LOX had direct antimicrobial activity toward a variety of plant pathogens (Grechkin, 1998).

5.1.1 Divinyl ether fatty acids

The enzyme divinyl ether synthase (DES) utilises fatty acid hydroperoxides as a substrate with the resulting divinyl ether oxylipins being fungitoxic. Potato tuber

DES is specific toward 9(*S*)-HPOD and 9(*S*)-HPOT and non-active toward 13-hydroperoxides (Galliard & Matthew, 1975). Conversely garlic DES catalyses the conversion of 13-HPOD and 13-HPOT to the respective divinyl ether with no activity being detected toward 9-hydroperoxides (Grechkin, 1998; Grechkin & Hamburg 1996).

Weber *et al.*, (1999), studied the patterns and levels of oxylipins produced in the leaves of potato cultivars infected with *P. infestans*. During colonisation, colnelenic acid (CnA) and colneleic acid (CA) divinyl ether fatty acids, accumulated to a greater extent in the resistant cultivar potato-*P. infestans* pathosystem as opposed to a susceptible system. Application of 150 μM CnA inhibited mycelia growth on agar by 50% after an 18 h period and 30 μM CnA resulted in approximately 95% inhibition of cytospore germination. Colneleic acid was also found to significantly inhibit spore germination by ≈ 70%.

5.1.2 Hydroperoxide lyase and peroxygenase derived phytoalexins

Hydroperoxide lyase catalyses the α cleavage of 9(*S*)-HPOT releasing fungitoxic aldehydes (Blee, 1998) as well as 'traumatin' (12-oxo-10(*E*)-dodecenoic acid), a wound hormone suggested to stimulate cell division and protective callus growth around the site of wounding (Blee, 1998; Vick, 1993). Additionally, hydroxy and epoxy oxylipins derived from 9(*S*)-HPOT via the peroxygenase pathway are believed to be defensive compounds in rice during infection by *Magnaporthe grisea*. Lipid hydroperoxide lyase activity has also been identified in tomato infected with *Verticillum albatrum* and *Phytophthora parasitica* (Blee, 1998; Vernenghi *et al.*, 1985).

Plant lipoxygenases may play dual roles in defence. Initially, the potato 9-LOX acting on linolenic acid can give rise to 9(*S*)-HPOT, which is itself reported to exhibit fungitoxic properties (Kato *et al.*, 1992). In addition, this product can function as a substrate for multiple biochemical pathways associated with defence responses toward pathogen attack (Figure 5.1). PUFAs, such as linole(n)ic acid, having undergone oxidation, are strongly antifungal. In order for host plant colonisation by a fungal pathogen to be successful, the toxic effects of these defences may need to be ameliorated by the fungus. Reported here is the cloning, expression and biochemical characterisation of a theta class GST from *P. infestans*, which can detoxify an oxylipin phytoalexin from potato with roles in plant defence.

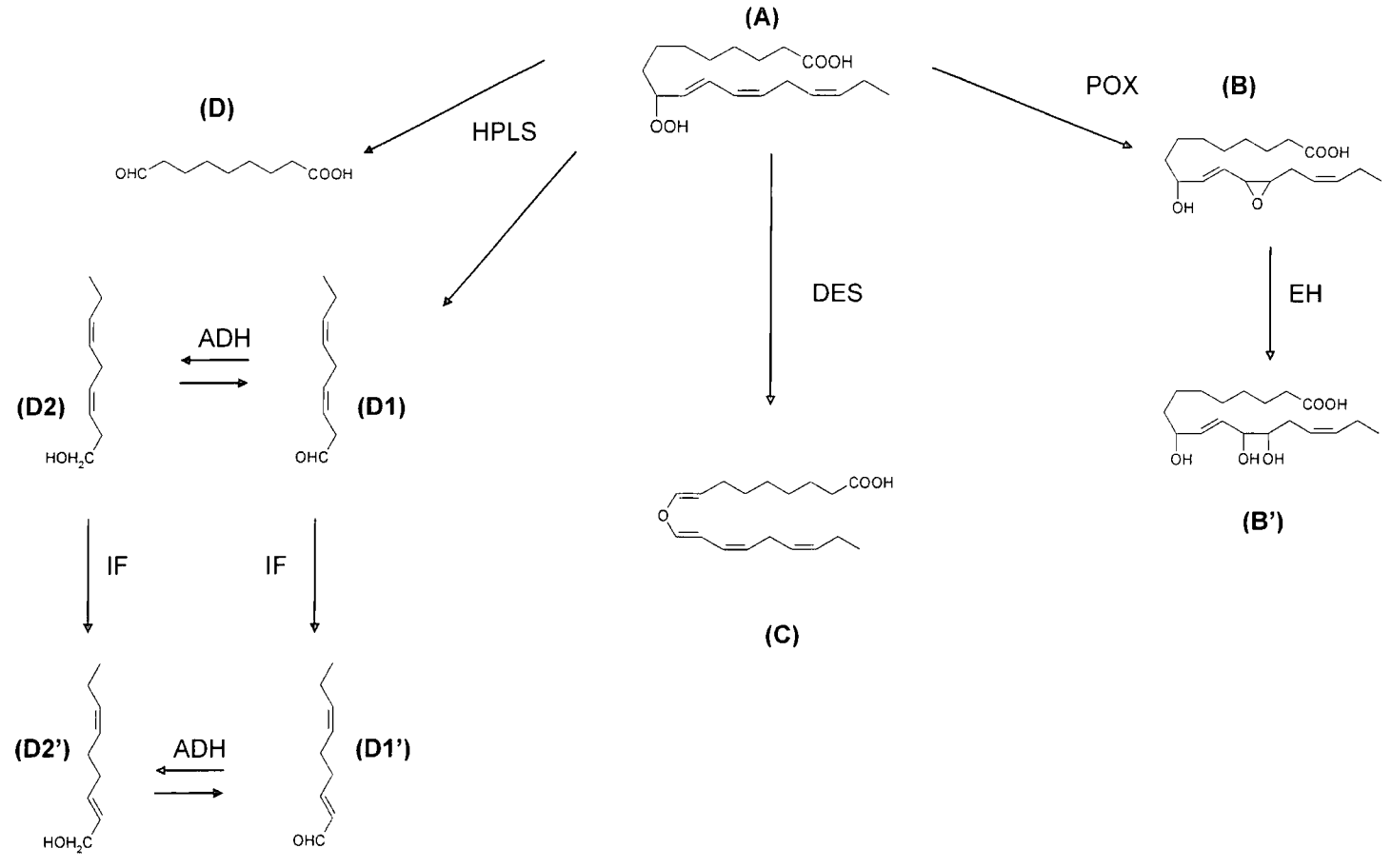

Figure 5.1. Biosynthetic pathways of phytoalexin production derived from the fungi toxic oxylipin 9(*S*)-HPOT. **(A)** 9(S)-HPOT; **(B)** 12,13-Epoxy-9-hydroxy-(9*Z*,11*E*)-octadecdienoic acid; **(B')** 9,12,13-Trihydroxyoctadecdienoic acid; (C) (8*E*,1'*E*,3'*Z*,6'*Z*)-9-(1',3',6'-nonatrienoxy)-8-nonenoic (colnelenic) acid **(D)** 9-oxo-nonanoic acid; **(D1)** (3*Z*),(6*Z*)-nonadienal; **(D2)** (3*Z*),(6*Z*)-nonadienol **(D1')** (2*E*),(6*Z*)-nondienal; **(D2')** (2*E*),(6*Z*)-nonadienol. Peroxygenase, POX; Epoxide Hydrolase, EH; Divinyl Ether Synthase, DES; Hydroperoxide Lyase, HPLS; Alcohol Dehydrogenase, ADH; IF, Isomerisation Factor.

5.2 Cloning of *PiGSTT1* glutathione peroxidase from *P.infestans*

5.2.1 Results and discussion

Following isolation of total RNA from *P. infestans* (Figure 5.2.1) cDNA was synthesised (see 2.7.4) and *PiGSTT1* amplified by touch down PCR (Figure 5.2.1.2). A specific 5' primer PiGST23(2) designed containing an *Nde* 1 restriction site incorporating the start codon of the 5' coding region of the *P.infestans* EST accession Pimy025aC05r from the *Phytophthora* Genome Consortium Database, Primer PiGST(23)2 was used in conjunction with primer OG9 (table 2.7.2), an adapter primer designed to the poly A tail for cDNA synthesis (Dixon *et al.*, 2002) to amplify the entire coding region and 3' UTR of *PiGSTT1*.

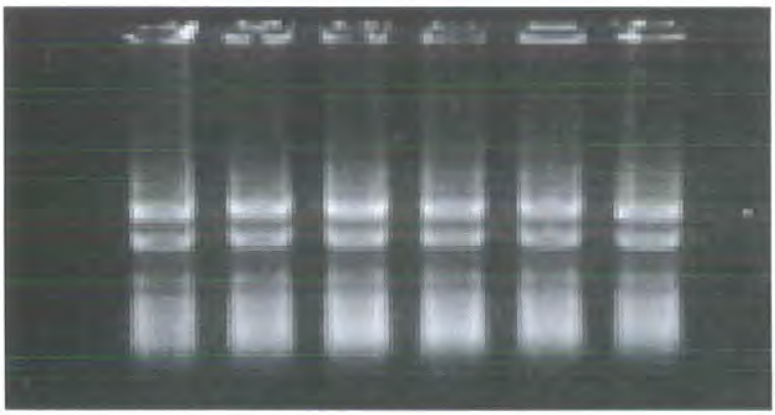

Figure 5.2.1. 1% agarose gel showing total RNA isolated from *Phytophthora infestans* stained with ethidium. Each lane represents an aliquot of RNA recovered from one extraction. Molecular weight markers were not visible due to the absence of ethidium bromide in the loading dye.

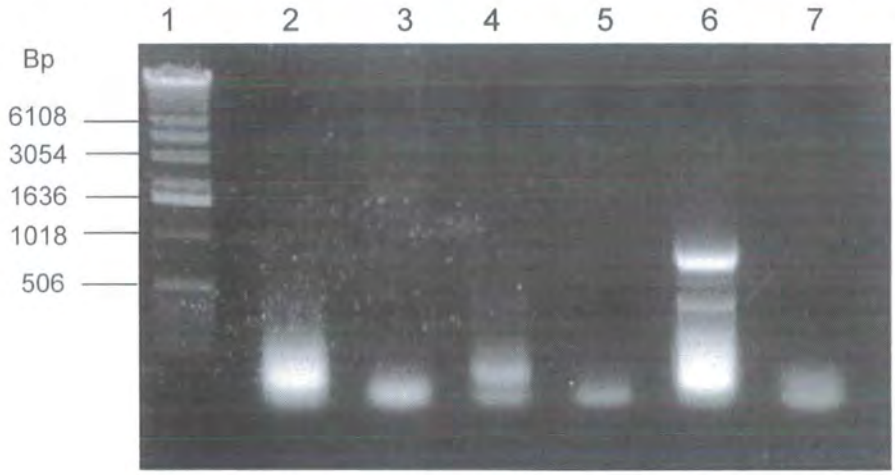

Figure 5.2.1.2. Touch down PCR from cDNA synthesised from total RNA extracted from *P. infestans*.1 = Marker; 2 = OG9 + *Ps*GST8; 3 = RNA control; 4 = OG9 + *Ps*GST23; 5 = RNA negative control; 6 = OG9 + *Pi*GST23(2); 7 = RNA control.

Following excision and purification the 800 kb upper band (Figure 5.2.1.2 lane 6) was ligated into pGEM-T easy vector and transformed into *E. coli* XL-10 Gold with successful transformants being identified by colony PCR using PiGST23(2)and OG9 primers (Figure 5.2.1.3).

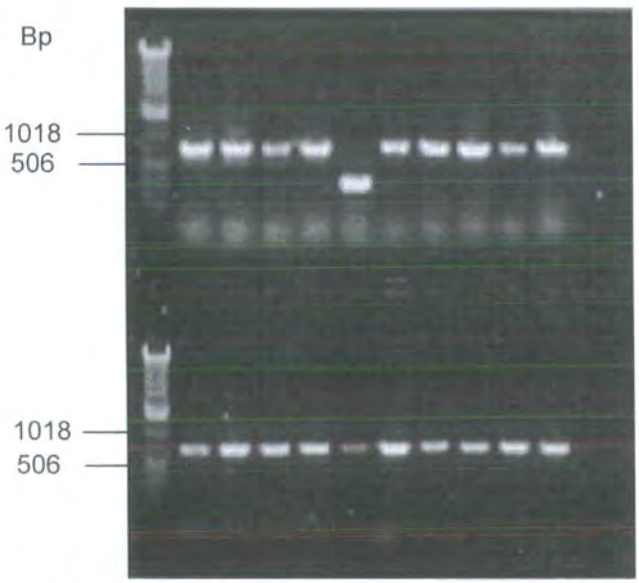

Figure 5.2.1.3. Colony PCR of *PiGSTT1* GST from *E. coli* XL10-gold, pGEMT easy vector.

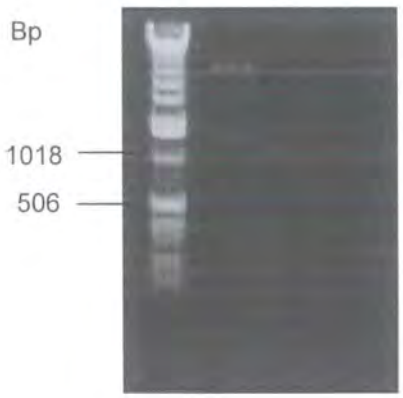

Figure 5.2.1.4. Restriction digest of pET24a using restriction enzymes *Nde*1 and *Xho*1 releasing a 1.5Kb insert, which was barley visible due to low concentration.

The expression vector pET24a was digested using *Nde*1 and *Xho*1 restriction enzymes (Figure 5.2.1.4) and gel purified. The pGEMT easy insert was restricted with the same enzymes and also purified (Figure 5.2.1.5). Following ligation, pET24a containing the *PiGSTT1* insert was transformed *via* electroporation into *E.coli* BL21, with colony PCR screening (Figure 5.2.1.6).

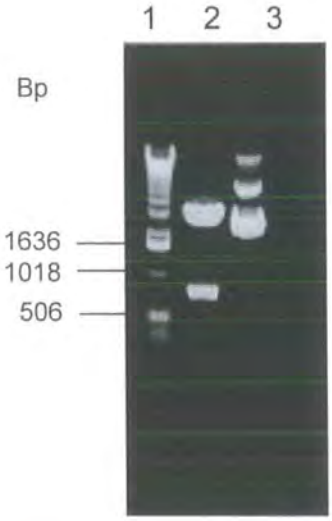

Figure 5.2.1.5. Restriction digest of pGEMT easy using *Nde*1 and *Xho*1 restriction enzymes releasing *PiGSTT1* insert. 1 = molecular marker; 2 = Digestion; 3 = pGEMT easy plasmid.

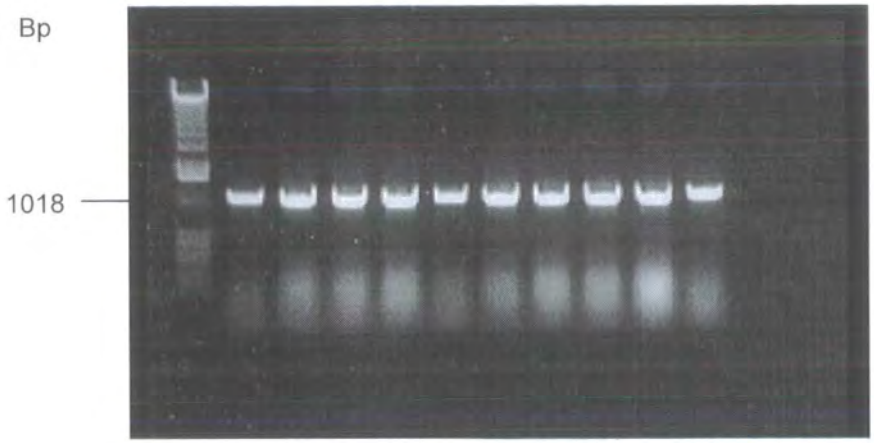

Figure 5.2.1.6. Colony PCR of *E. coli* transformed with *PiGSTT1* in the pET24a plasmid vector.

5.2.2 *PiGSTT1* sequence data

Plasmid preparations were submitted for sequence analysis and from this the full length coding sequence was deduced (figure 5.2.2). From this, the protein molecular mass of the recombinant polypeptide was determined from the predicted amino acid sequence to be 25381.

catATGACCATCAAGCTCTACGCCAACCTCATCAGCCAGCCCAGTCGCGCGGCC
GAGTGGATTTTACGCATTAAGAAGCTGGACCACGAGTTCGTGGCCGCGGAGTT
CGGCGCTCCGATTTTCAAGTCGCCTGAGTTCCTGGCGCTCAACCCGAATGGCC
TCATCCCGGTGTTGCAAGACGGCGACTTCTCGATCTTTGAGGGCAACGCTATCA
TGCAGTACTTGGCCGAGAAGAACGGCTGGACGGACCTCTACCCGGCCGACGC
GCGGGCCCACGCCAAGGTGAACCAATATCTGCACTGGCACCACACGAACGTGC
GTCTCATCACGCCCAAGGTGCTCGTGCCGCTTATGCACACGAAGCAGAACTCG
GCCACCCCGGAGGAAGCCATTATGATCAAGGAGACGCCGGCGCTTCTCACTAA
GCTATCCGAGCTAATGGAGAAGTTCCTGGTCAAGGACTTTGTGGCTGAGACCGA
CCAGCCCACGATCGCCGACATCGCCGCCTACTGCGAGTTCGTGCAGGTGGAGT
ACATGGGCATCTATGATTTTTCCAAGCACCCCAAGCTCGCGGCTTGGCTCAAGC
GTATGAAGTCGGTGCCCCACCACGATGAGATCCAGGCACCTTTGGACCAACTTC
TTACGAGCCTGGAGCTTAAGACCAAGGCCGCGGGTTAAcgcgtaagatcccgaaaagat
actgtacccttctgggttttctctgaaacgtaatacattccgatcggttcgaatttttgngacaaaaaaaaaaaaaaactc
ga

Figure 5.2.2 Full length coding sequence (capitals) of *Pi*GSTT1 cloned from *P. infestans*.

5.2.3 Predicted amino acid sequence

Multiple amino acid sequence alignment of *Pi*GSTT1 with GSTs from different classes revealed homology to plant and mammalian theta class GSTs (Figure 5.3.2). The *P. infestans* glutathione peroxidase shared 26% identity and 49-50% similarity with theta class GSTs from *Arabidopsis*, *Oryza sativa*, *Glycine max* and *Homo sapiens*. The catalytically essential serine 11 (Landi, 2000: Sheehan *et al.*, 2002) formed part of a highly conserved motif (SQPRSA) amongst this class (Figure 5.2.3.1). Theoretical molecular modelling revealed that this motif, part of the glutathione binding domain - G-site, was likely to be found in a pocket of *Pi*GSTT1 (Figure 5.3.2.3). Based on this model, amino acids of the hydrophobic binding domain, H-site, were shown to surround the catalytic cleft (Figure 5.3.2.3).

MTIKLYANLISQPSRAAEWILRIKKLDHEFVAAEFGAPIFKSPEFLALNPNGLIPVLQD
GDFSIFEGNAIMQYLAEKNGWTDLYPADARAHAKVNQYLHWHHTNVRLITPKVLVP
LMHTKQNSATPEEAIMIKETPALLTKLSELMEKFLVKDFVAETDQPTIADIAAYCEFVQ
VEYMGIYDFSKHPKLAAWLKRMKSVPHHDEIQAPLDQLLTSLELKTKAAG

Predicted molecular mass 25381 Da

Figure 5.2.3 The predicited amino acid sequence of the polypeptide encoded by *PiGSTT1*, cloned from *P. infestans*.

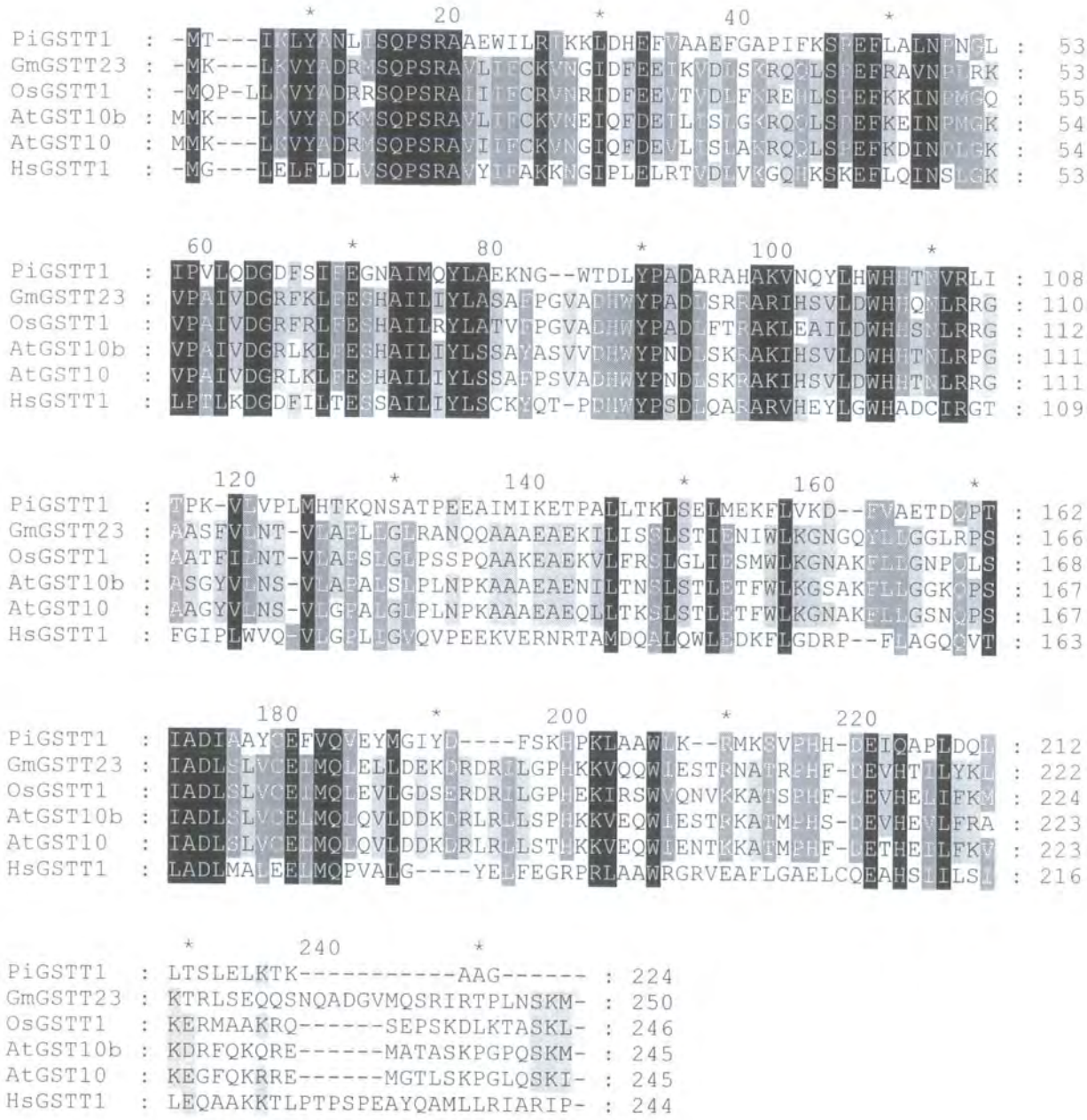

Figure 5.2.3.1 Multiple amino acid sequence alignment of *Pi*GST1 with theta class GSTs from plant and mammalian sources. Homologous regions are highlighted in black, while grey shading regions represent amino acids exhibiting similar physico-chemical properties. Boxed regions represent N and C-terminal domains, with catalytically essential serine 11 forming part of a conserved SQPSRA motif in the GSH binding domain. *Pi* = *Phytophthora infestans*; *At* = *Arabidopsis thaliana*; *Gm* = *Glycine max*; *Os* = *Oryza sativa*; *Hs* = *Homo sapiens*. Alignment was performed in DNA for Windows using ClustalW.

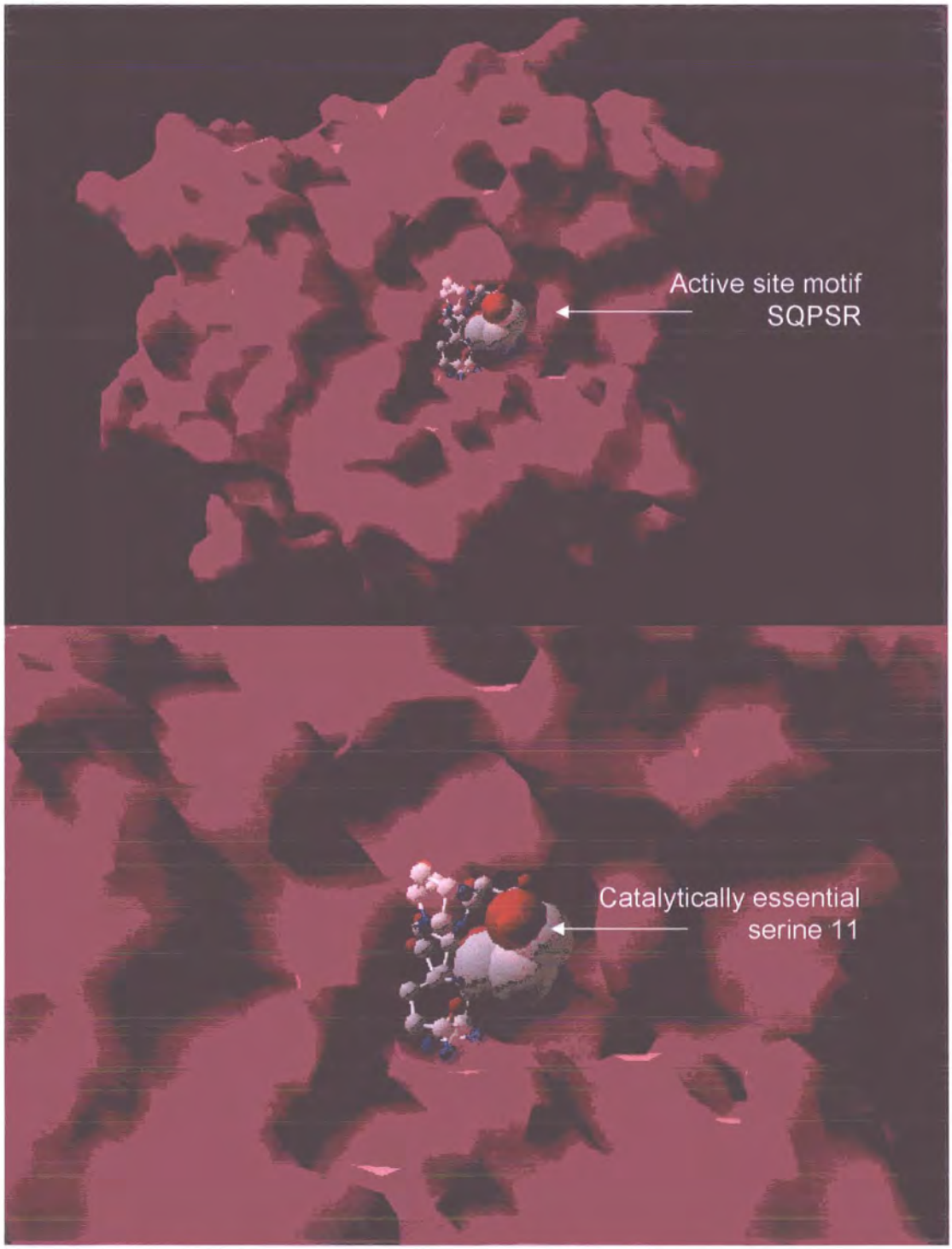

Figure 5.2.3.2 Theoretical model of the *Pi*GSTT1 monomer, full legend over leaf.

Figure 5.2.3.2. (A) Theoretical 3-dimensional model of the molecular surface of the *Pi*GSTT1 polypeptide monomer, detailing the conserved amino acid residues, $S^{11}Q^{12}P^{13}S^{14}R^{15}$, of the active site in the GSH binding domain, located in an apparent pocket (http://www.ebi.ac.uk/interpro/index.html). The catalytically essential serine 11 residue is represented by the large coloured balls showing Van der waals forces, while conserved residues $Q^{12}P^{13}S^{14}R^{15}$ are depicted by the smaller stick and ball model. (B) Close up view of the stick and ball conserved amino acid motif highlighting catalytically essential serine11 with vanderwaals forces as large coloured balls, which appeared to be located in an apparent cleft. Modelling was based on structural co-ordinates of *Hs*GSTT2-2 and *Hs*GSTT in complex with the glutathione conjugate of 1-menaphthyl sulphate performed by Swiss-Model (http://swissmodel.expasy.org/).

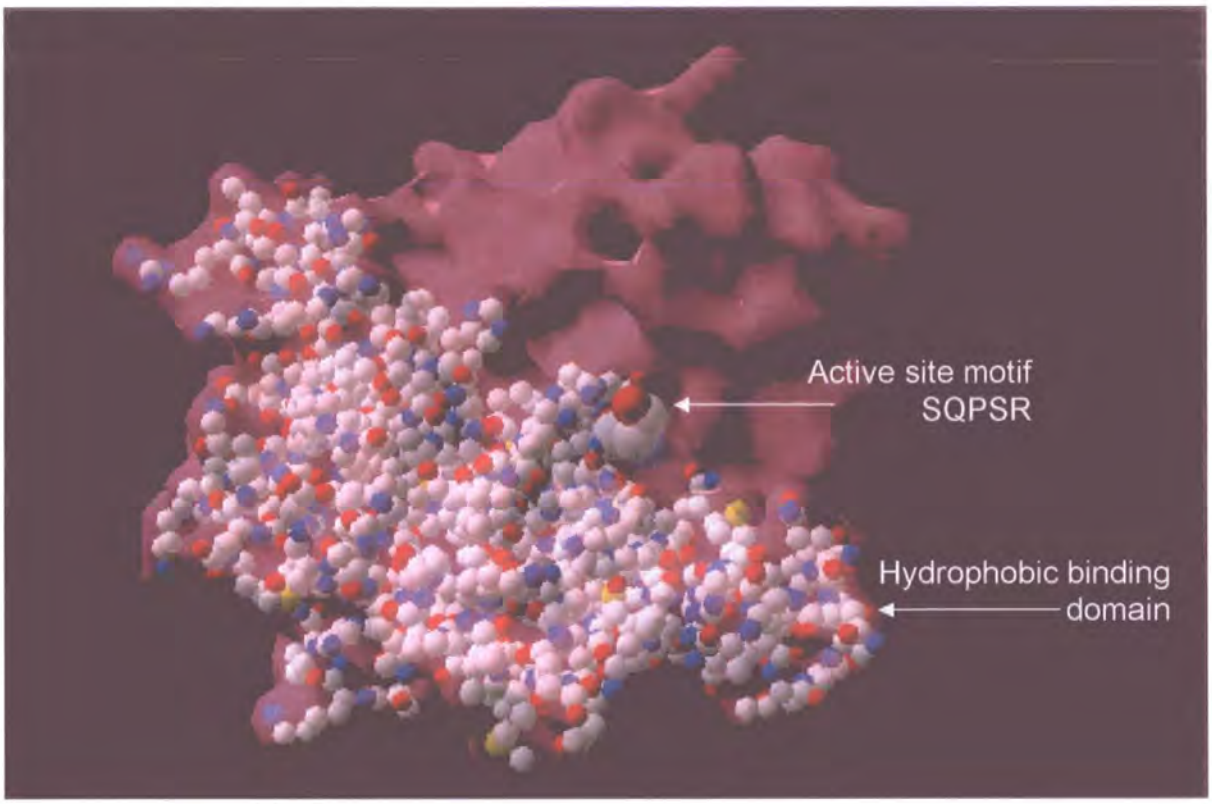

Figure 5.2.3.3. Theoretical 3-dimensional cartoon model of molecular surface *Pi*GSTT1 polypeptide monomer, detailing the conserved amino acid residues, $S^{11}Q^{12}P^{13}S^{14}R^{15}$, of the GSH binding domain located in an apparent cleft and the proximity of residues involved in binding hydrophobic substrates. Catalytically essential serine 11, is represented by larger coloured balls showing van der waals forces Residues 85-200, harbouring the H-site (hydrophobic binding domain), as determined by interpro-scan (http://www.ebi.ac.uk/interpro/index.html), of the C-terminal domain are represented by stick and ball model. Residues involved in binding hydrophobic substrates can be seen to border the apparent cleft harbouring the G-site motif and catalytically active essential serine 11. Modelling was based on structural co-ordinates of *Hs*GSTT2-2 and *Hs*GSTT in complex with the glutathione conjugate of 1-menaphthyl sulphate performed by Swiss-Model (http://swissmodel.expasy.org/).

5.3 Over expression and purification of recombinant *Pi*GSTT1-1

5.3.1 Over expression

Recombinant *Pi*GSTT1 was expressed in *E. coli* strain BL21 using the expression vector pET-24a and induction with 1mM IPTG. Prior to induction only native *E. coli* proteins were observed (Figure 5.3.1).

Following induction, the majority of over expressed recombinant protein was found to be present in the soluble fraction and had a mass of 25 kDa (Figure 5.3.1.2). Experiments were conducted to determine whether temperature had an effect on expression of the recombinant polypeptide in the soluble or insoluble fractions. It was found that varying the temperature had a minimal effect on soluble vs. insoluble protein expression with marginally more soluble protein being produced in cells grown at 37°C. As such, all subsequent cells were grown at 37°C.

5.3.1.1 Enzyme activities of *Pi*GSTT1-1 in bacterial lysate

Following expression of *Pi*GSTT1, bacterial lysates were assayed for GST activity toward CDNB and for glutathione peroxidase (GPOX) activity toward cumene hydroperoxide. Lysates were found to have no measurable GST activity above background, but appreciable GPOX activity (15.8 nKat mg^{-1} protein).

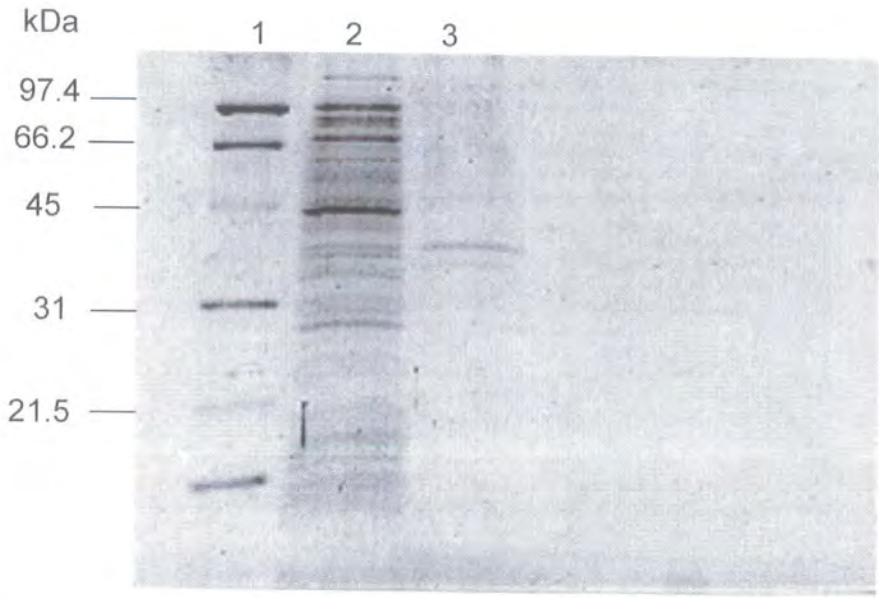

Figure 5.3.1. 12.5% SDS-PAGE with gel code blue staining of *E. coli* BL-21 containing recombinant *PiGSTT1-1* in plasmid pET-24a protein extract prior to induction with 1mM IPTG. 1 = molecular weight marker; 2 = crude soluble; 3 = crude insoluble.

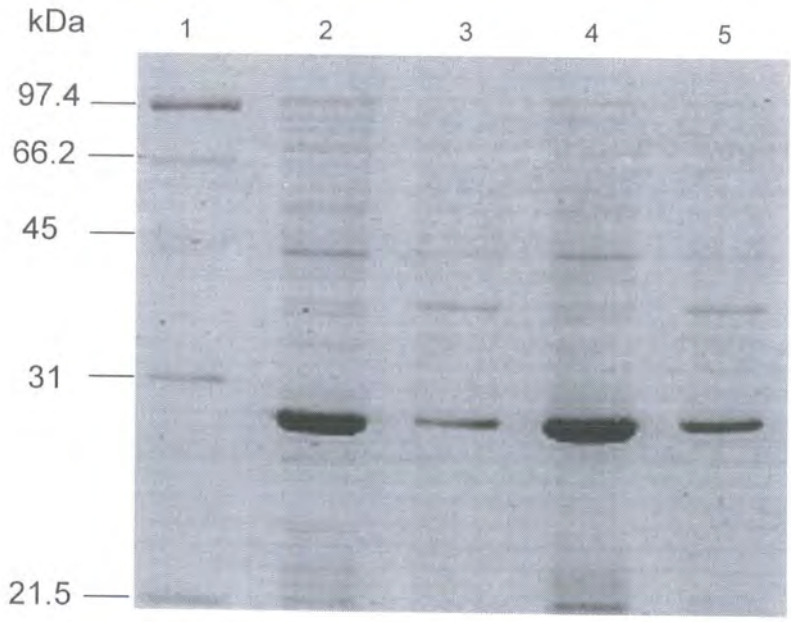

Figure 5.3.1.2. 12.5% SDS-PAGE with gel code blue staining of the effect of temperature at 30 & 37°C on expression of recombinant *PiGSTT1-1* GPOX following induction with 1mM IPTG. M = Molecular weight markers; 2 = 30°C soluble; 3 = 30°C insoluble; 4 = 37°C soluble; 5 = 37°C insoluble.

5.3.2 Purification

Over expressed *Pi*GSTT1-1 was purified by three rounds of chromatography with the activity of the enzyme monitored using a glutathione peroxidase assay with cumene hydroperoxide as the substrate. Combinations of HIC (Hydrophobic Interaction Chromatography) and anion exchange chromatography were employed (Figures 5.3.2 and 5.3.2.1). Purification was monitored by SDS PAGE (Cummins *pers comm.*, 2001) (Figures 5.3.2.2 - 5.3.2.4). The initial round of HIC was performed on a phenyl Sepharose column with elution from high to low salt buffer. Subsequent HIC on octyl-Sepharose improved purification due to the higher hydrophobic binding capacity of octyl-Sepharose. Figure 5.3.2 shows glutathione peroxidase activity eluting in the 50-100% portion of the gradient from the octyl-Sepharose column. In subsequent purifications, the phenyl-Sepharose step was omitted. Homogenous active fractions were pooled, dialysed and concentrated by anion exchange chromatography using Q-Sepharose. Figure 5.3.2 clearly illustrates glutathione peroxidase activity eluting as a single peak along with the UV-absorbing protein peak from the Q-Sepharose column (45-60% eluent).

Polypeptides from each stage of purification were analysed by SDS-PAGE demonstrating that the enzyme was effectively purified to homogeneity (figure 5.3.2.4. Consistently, faint high molecular weight polypeptides were observed throughout the purification at around 66kDa and are attributed to keratin contamination of buffers.

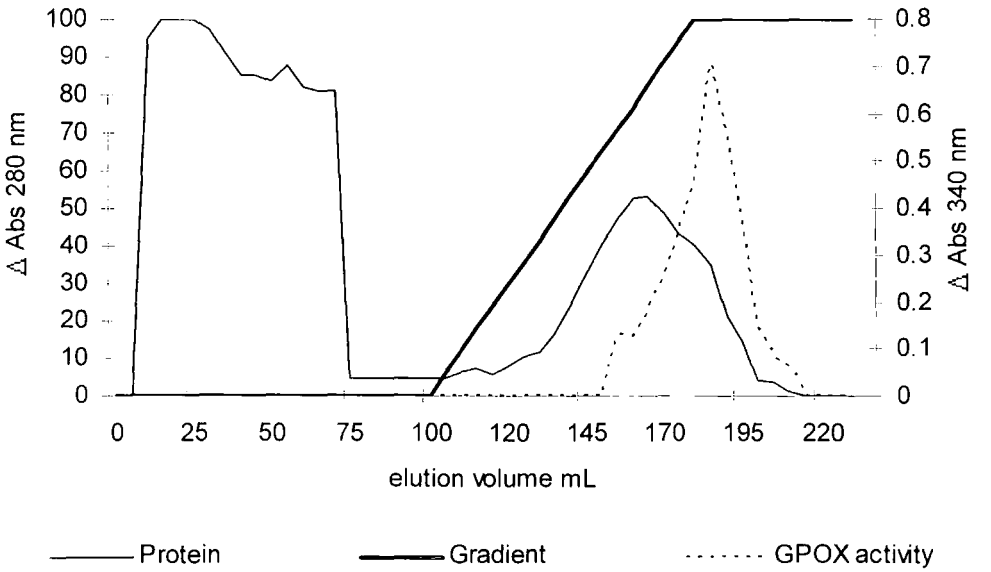

Figure 5.3.2. Octyl sepharose protein purification chromatogram of recombinant *Pi*GSTT1-1 over expressed in *E. coli* BI21. The major peak of glutathione peroxidase activity toward the substrate cumene hydroperoxide, eluted between 160 and 205 mL of elutate, approximately 50-100% of elution buffer. Protein content was monitored from the absorbance of the eluate at 280nm, glutathione peroxidase enzyme activity was monitored as change in absorbance at 340nm min^{-1}.

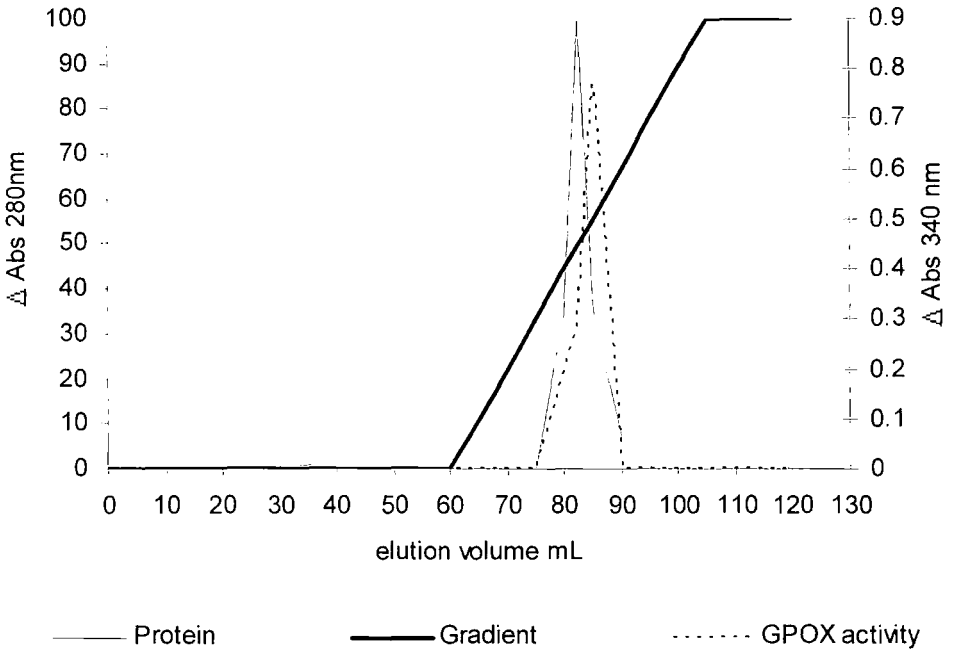

Figure 5.3.2.1. Q-sepharose anion exchange protein purification chromatogram of recombinant *Pi*GSTT1-1 following octyl sepharose chromatography and dialysis. The major protein peak containing glutathione peroxidase activity toward the substrate cumene hydroperoxide, eluted between 75 and 90 mL. Protein content was monitored from the absorbance of the eluate at 280nm, glutathione peroxidase enzyme activity was monitored as change in absorbance at 340nm min^{-1}.

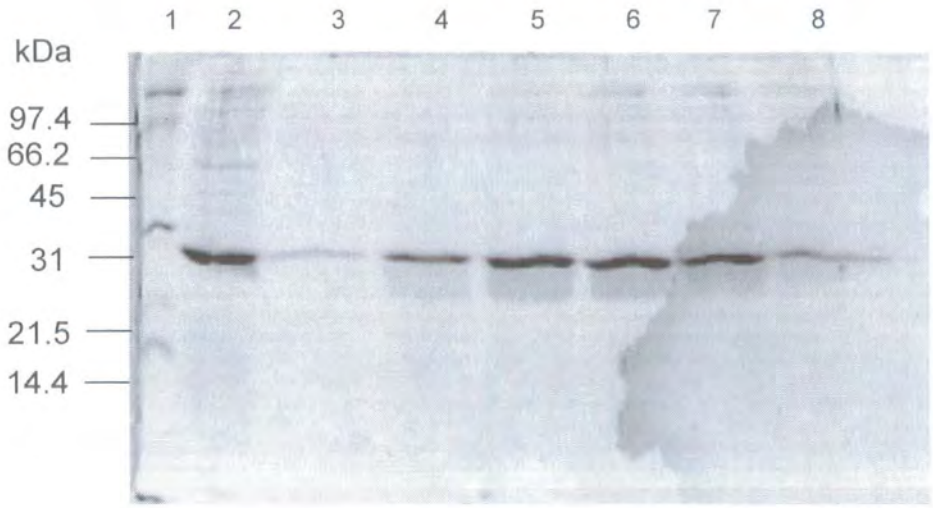

Figure 5.3.2.2. SDS-PAGE with gel code blue staining of fractions exhibiting GPOX activity toward cumene hydroperoxide following phenyl Sepharose hydrophobic interaction chromatography. 1 = molecular weight markers; 2 = Crude extract; 3 – 8 GPOX active fractions.

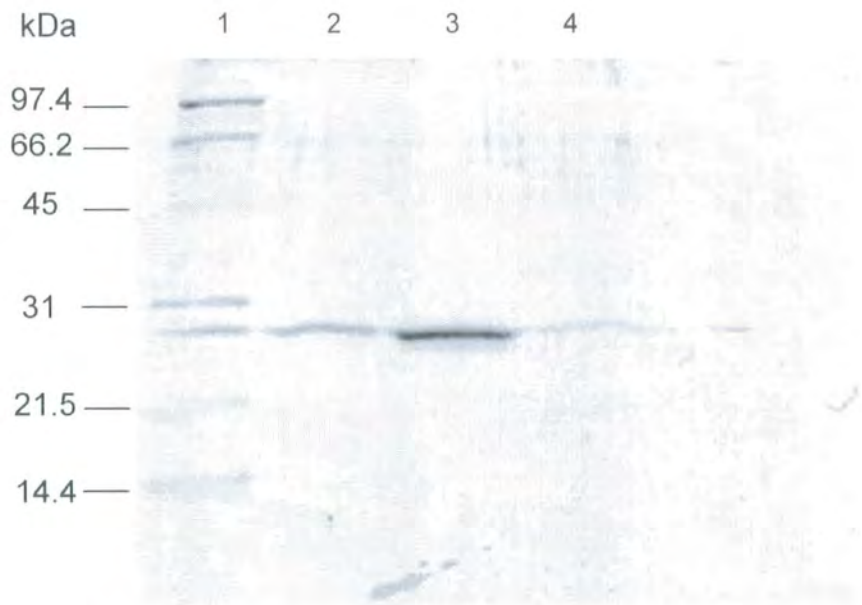

Figure 5.3.2.3. SDS-PAGE with gel code blue staining of fractions exhibiting GPOX activity toward cumene hydroperoxide following Q sepharose anion exchange chromatography. 1 = molecular weight markers; 2 - 5 = GPOX active fractions.

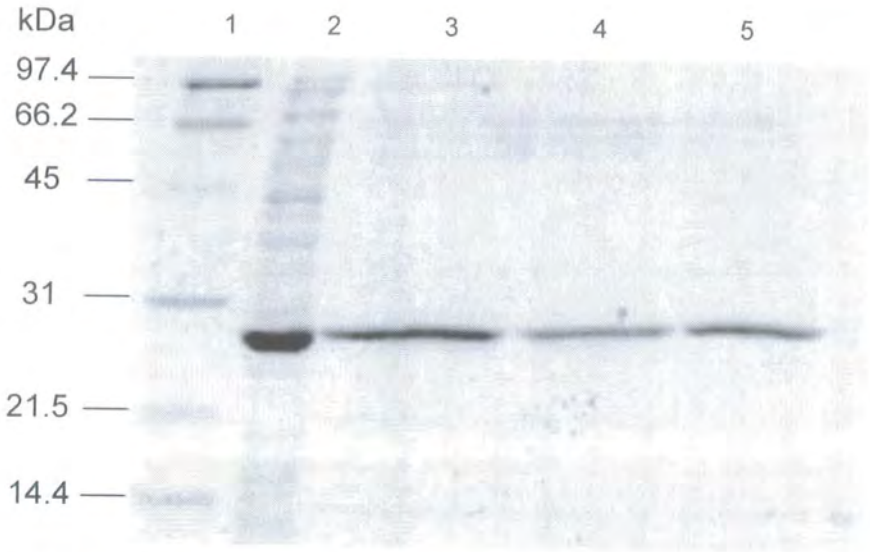

Figure 5.3.2.4. SDS PAGE with gel code blue staining overview of *Pi*GSTT1 GPOX purification. 1= molecular marker; 2 = Crude soluble extract; 3 = phenyl Sepharose hydrophobic interaction chromatography; 4 = Octyl Sepharose chromatography; 5 = Q Sepharose anion exchange chromatography.

5.3.3 Gel filtration

Glutathione *S*-transferases are known, to function in the majority of cases as dimeric proteins. In plants, phytopathogenic fungi and bacteria however, specific GSTs may also function as monomers (Dixon *et al.*, 2002; Dowd and Sheehan, 1993; Ilio *et al.*, 1993). Amino acid sequence analysis of *Pi*GSTT1 revealed homology to theta class GSTs, which are known to function as protein dimers. Gel filtration was performed to determine whether or not the native recombinant protein functioned as a dimer. Using BSA (Bovine Serum Albumin) 66 kDa, ovalbumin 45 kDa and carbonic anhydrase 29 kDa as calibrants, native *Pi*GSTT1-1 was found to function as a dimer with a mass of 46.57 kDa.

5.4 Biochemical characterisation of *Pi*GSTT1-1

5.4.1 Protein dependence of activity

Enzyme activities toward 1.2 mM cumene hydroperoxide with varying protein concentration were determined within the range of 3 – 48 μg pure *Pi*GSTT1-1 per assay (table 5.4). The data revealed a clear linear protein dependence of enzyme activity on enzyme protein content, R^2 0.9975. For routine assays 6 μg of pure protein was used for subsequent biochemical characterisation of the enzyme

5.4.2 Effect of pH on *Pi*GSTT1-1 glutathione peroxidase activity toward cumene hydroperoxide

Enzyme activity towards cumene hydroperoxide was determined between pH 5.8 – 9.2, using potassium phosphate buffer (pH 5.8 – pH 8) and Tris HCl (pH 8.4 – pH 9.2). The data in figure 5.4.2 and table 5.4 show activity was optimal between pH 7.2 – pH 7.4. Background non-enzymic activity followed an exponential increase with respect to increasing pH, due to either the increasing abundance of thiolate anion of glutathione under the oxidation of NADPH under alkaline conditions (figure 5.4.2). Due to the pH dependent chemical activity, it was decided to perform all susbequent assays at pH 7 in order to reduce the background rate of NADP formation.

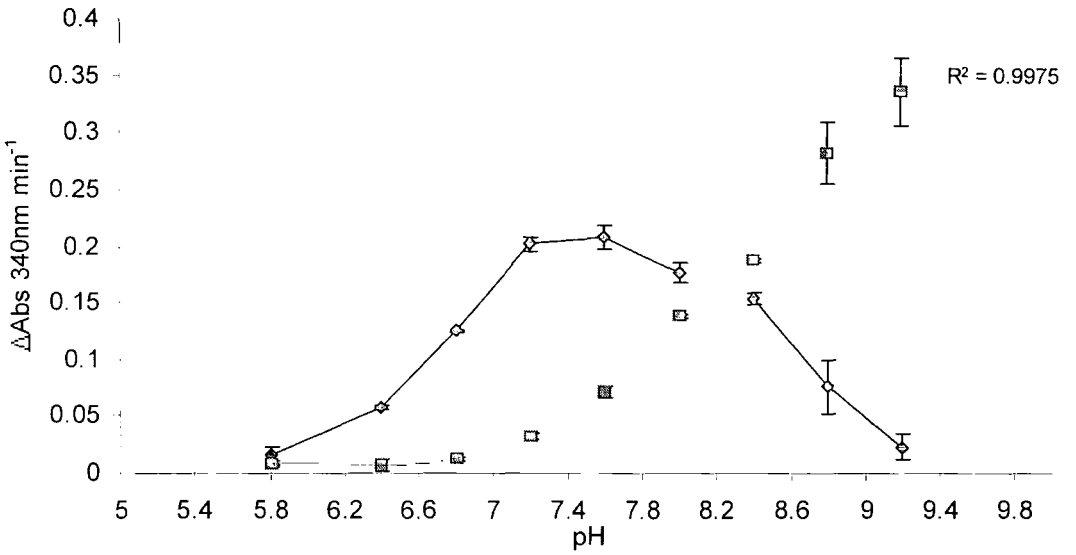

Figure 5.4.2 The effect of varying pH on the net glutathione peroxidase activity of purified *PiGSTT1-1* toward cumene hydroperoxide. Net enzymic activity denoted by diamond, chemical rate represented by squares. Vertical bars represent standard deviation (n=2). The pH range was generated with potassium phosphate buffer pH 5.8 – pH 8, Tris-HCl buffer pH 8.4 – pH 9.2.

5.4.3 Thermotolorance

*Pi*GSTT1-1 was incubated for 10 minutes at 5 different temperature regimes (37°C, 47 °C, 57 °C, 67 °C, and 77°C) to determine the temperature at which the enzyme was fully denatured. As demonstrated previously, boiled enzyme controls are essential in determining activity toward xenobiotic substrates such as herbicides and fungicides, thereby preventing false interpretation of data. The glutathione peroxidase cloned from *Phytophthora infestans* showed no variation in activity when treated at 37–57°C for 10 minutes. Treatment at 67°C and 77°C resulted in complete loss of activity suggesting the enzyme had been fully denatured by 10-minute heating at 67°C (table 5.4).

5.4.4 Enzyme kinetics varying [cumene-hydroperoxide]

V_{max} and K_m values were determined using cumene hydroperoxide as a substrate in the range 0.625 mM – 40 mM. The data in table 5.4 illustrate the observed changes on product formation of *Pi*GSTT1-1 taking into account the non-enzymic reduction rate. Net enzyme activities plateaued at concentrations >20 mM cumene-hydroperoxide suggesting that the enzyme was saturated by substrate. However, the background non-enzymic reaction was seen to follow apparent first order kinetics over the substrate range. The background "activity" may be accounted for by both an increased spontaneous reaction with glutathione due to a concentration effect as well as increasing absorbance due to opalescence, which was observed when adding high concentrations of the hydrophobic substrate to aqueous buffer.

Kinetic constants of net *Pi*GSTT1-1 enzyme activity toward cumene hydroperoxide were determined (table 5.4) giving an apparent K_m value of 14.2 mM. The high K_m value suggests that cumene hydroperoxide was not the most suitable substrate for *Pi*GSTT1-1. This might also suggest potential plant hydroperoxides resembling cumene hydroperoxide in structure, such as caffeic or ferrulic acid hydroperoxides, are not natural substrates for this enzyme.

5.4.5 Enzyme kinetics varying [reduced glutathione]

The data in table 1 demonstrate the effect of varying [GSH] ranging from 0.156 mM to 10 mM on the enzymic velocity of *Pi*GSTT1-1. Background non-enzymic rate was seen to increase linearly with respect to glutathione concentration, whereas enzymic activity was seen to plateau at concentrations above 2.5 mM.

The apparent K_m (glutathione) for *Pi*GSTT1-1 was determined to be 1 mM from these data (table 5.4) and are in stark contrast to the high K_m (cumene-hydroperoxide), showing that the enzyme had a higher affinity for the co-substrate glutathione.

Table 5.4 Biochemical profile of *Pi*GSTT1-1 glutathione peroxidase

pH profile									
pH	5.8	6.4	6.8	7.2	7.6	8	8.4	8.8	9.2
Mean ± S.D	0.015	0.058	0.126	0.202	0.208	0.177	0.154	0.076	0.024
(n = 2)	± 0.008	± -0.001	± 0.001	± 0.006	± 0.011	± 0.009	± 0.006	± -0.024	± -0.012

Enzyme kinetics - cumene hydroperoxide								
Cumene H_2O_2 (mM)	40	20	10	5	2.5	1.25	0.625	V_{max} (mM)
Mean ± S.D	1.302	1.325	0.961	0.637	0.282	0.146	0.024	
(n = 3)	± 0.118	± 0.083	± 0.004	± 0.032	± 0.009	± 0.011	± 0.054	2.294
Km mM	14.2							

Enzyme kinetics - glutathione								
GSH (mM)	10	5	2.5	1.25	0.613	0.312	0.156	V_{max} (mM)
Mean ± S.D	0.151	0.227	0.216	0.161	0.117	0.068	0.037	
(n = 3)	± 0.033	± 0.001	± 0.019	± 0.004	± 0.007	± 0.007	± 0.002	0.3067
Km mM	1							

Protein dependence					
µg pure *Pi*GSTT1-1	48	24	12	6	3
Mean ± S.D	0.58	0.30	0.14	0.07	0.04
(n = 2)	± 0.013	± 0.019	± 0.006	± 0.003	± 0.001

Thermostability (10 minute pre-treatment)					
Temperature °C	37	47	57	67	77
Mean± S.D	0.132	0.136	0.132	0.000	0.000
(n = 2)	± 0.001	± 0.017	± 0.002		

Table 5.4 continued

Gel Filtration				
Protein	BSA	Ovalbumin	Carbonic anhydrase	*Pi*GSTT1-1
Mol.Weight	66	45	29	46.57
Log time (minutes)	1.422	1.456	1.493	1.457

Specific activity toward cumene hydroperoxide and 9(*S*)-hydroperoxytrienoic acid nKat mg^{-1}	
Cumene hydroperoxide	15
(n= 2)	± 1.27
9(S)-HPOT	798.48
(n = 2)	± 12

5.5 Mass spectrometry of recombinant *Pi*GSTT1-1 glutathione peroxidase.

Following mass spectrometry and deconvolution of mass ions between 10-70 kDa, recombinant *Pi*GSTT1-1 was shown to have a sub-unit mass of 25450 Da (Figures 5.5.1 and 5.5.2). The mass of the monomer was found to be in reasonable agreement with the predicted amino acid sequence mass of 25381 Da. The 69 Da difference in mass may possibly be due to artefacts arising during the ionisation process.

5.5.1 Assay for *S*-glutathionylation of GPOX *Pi*GSTT1-1.

Studies with several plant GSTs have shown that these proteins can undergo reversible *S*-glutathionylation (Dixon *et al.*, 2002). It was therefore of interest to determine whether or not *Pi*GSTT1 underwent a similar modification. When incubated in the presence of either 2 mM oxidised glutathione or 2 mM nitrosolated glutathione (GSNO) (courtesy of Dr D. Dixon, University of Durham) the formation of glutathione mixed disulphides with the protein were not observed (Figures 5.5.3 & 5.5.4). Within the *Pi*GSTT1 sequence, only one cysteine residue located at amino acid 170 is present. The failure of this cysteine to form a disulphide bond with glutathione suggests that it may not have been exposed to the external environment within the quaternary protein structure. In accordance with the proposed function of *Pi*GSTT1-1, detoxification of oxidative hydroperoxides, it may be advantageous to enzyme activity not to be modified under oxidative conditions by GSSG and GSNO.

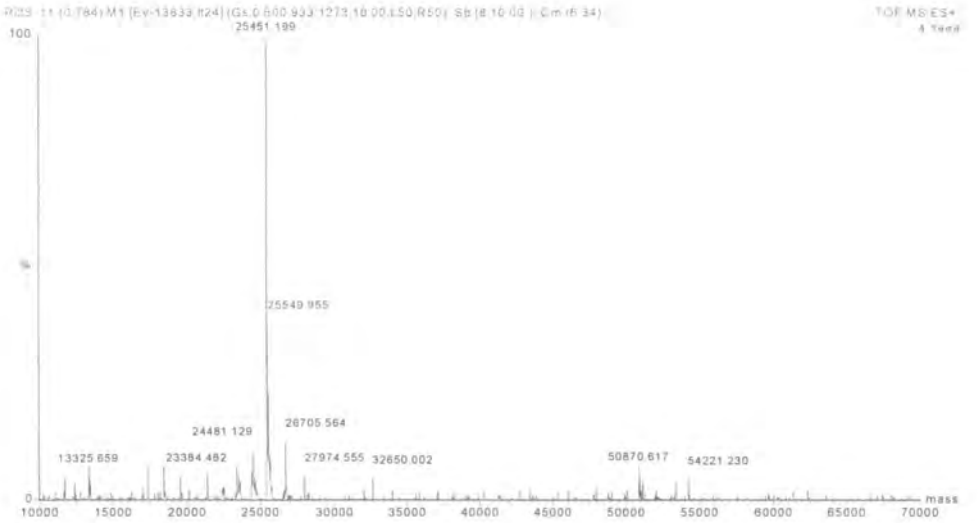

Figure 5.5.1 Positive ionisation ESMS spectra of purified recombinant *Pi*GSTT1 range 10 – 70 kDa functioning at 10 Dalton resolution.

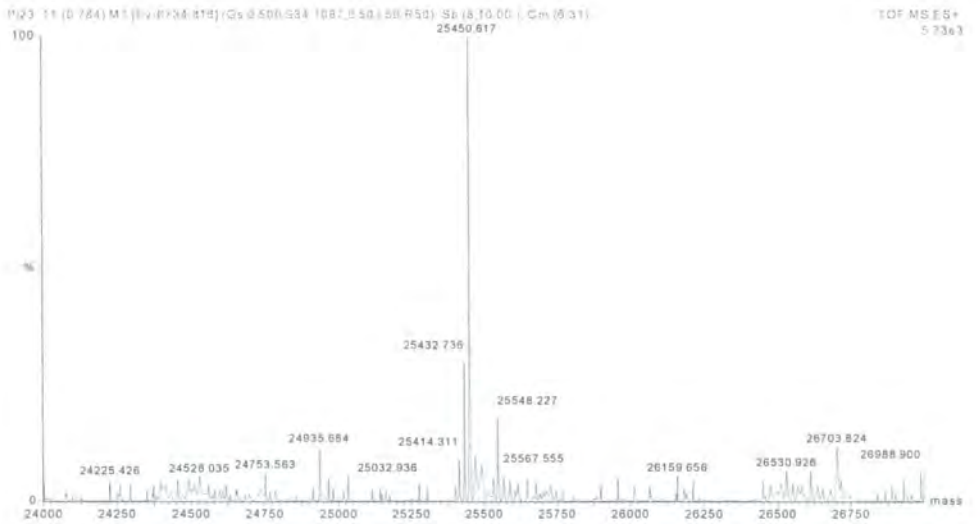

Figure 5.5.2. Positive ionisation ESMS spectra of purified recombinant *Pi*GSTT1 range 24 – 27 kDa functioning at 0.5 Dalton resolution.

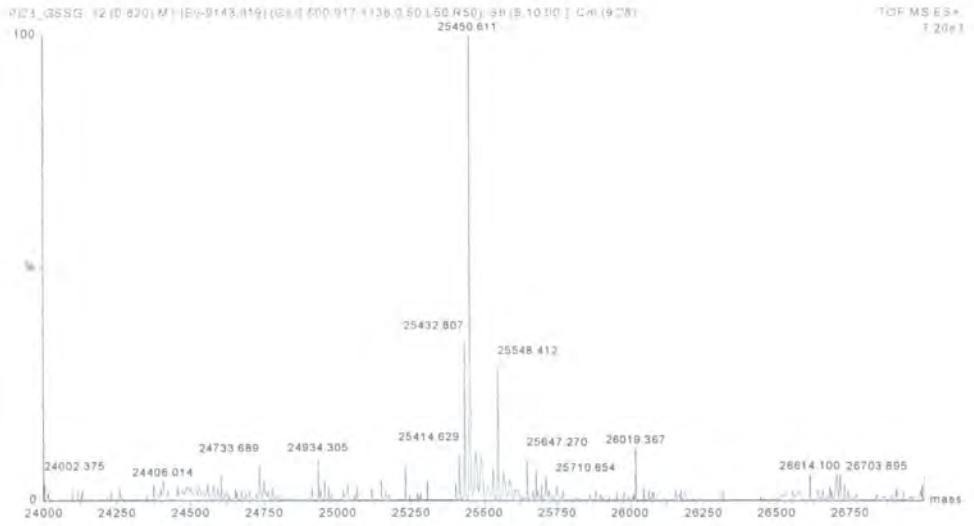

Figure 5.5.3. Positive ionisation ESMS spectra of purified recombinant *Pi*GSTT1 following incubation with 2mM oxidised glutathione (GSSG) functioning at 0.5 Dalton resolution.

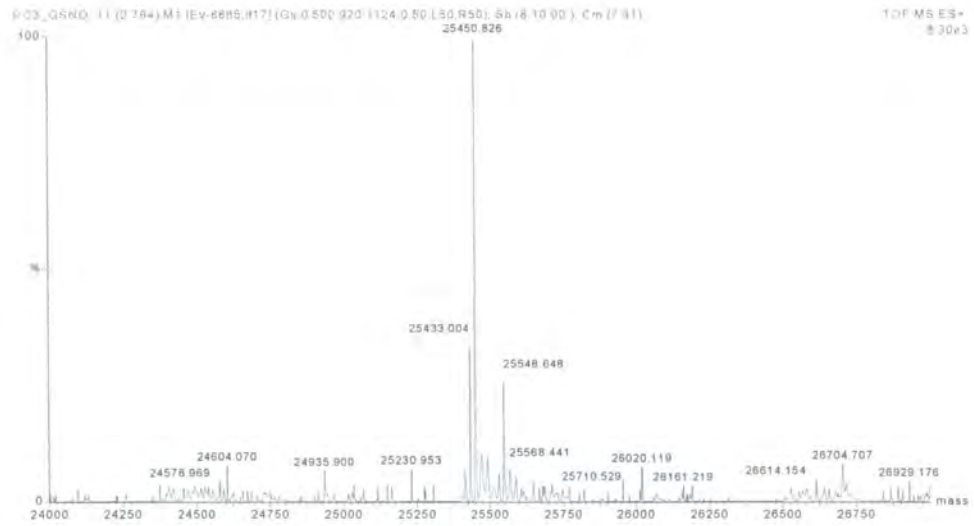

Figure 5.5.4. Positive ionisation ESMS spectra of purified recombinant *Pi*GSTT1 following incubation with 2mM nitrosolated glutathione (GSNO) functioning at 0.5 Dalton resolution.

5.5.1 Western blot analysis of glutathione peroxidase in *P. infestans* grown in culture using anti-sera raised against recombinant *Pi*GSTT1-1.

The recombinant *Pi*GSTT1 was used to raise polyclonal antisera in rabbits. The resulting antibody was seen to be specific for pure recombinant *Pi*GSTT1 and recognised a polypeptide of identical molecular mass in crude preparations taken from cultured *P. infestans*. Analysis of crude total protein (200 ng – 1000 ng) of *P. infestans* by western blot (Figure 5.5.1.1) provided an estimation of *Pi*GSTT1 content of *P. infestans*. Using known amounts of recombinant *Pi*GSTT1 for reference (figure 5.5.1.1, lanes 3 to 5), it was concluded that *Pi*GSTT1 to represent approximately 0.6% of the applied total protein.

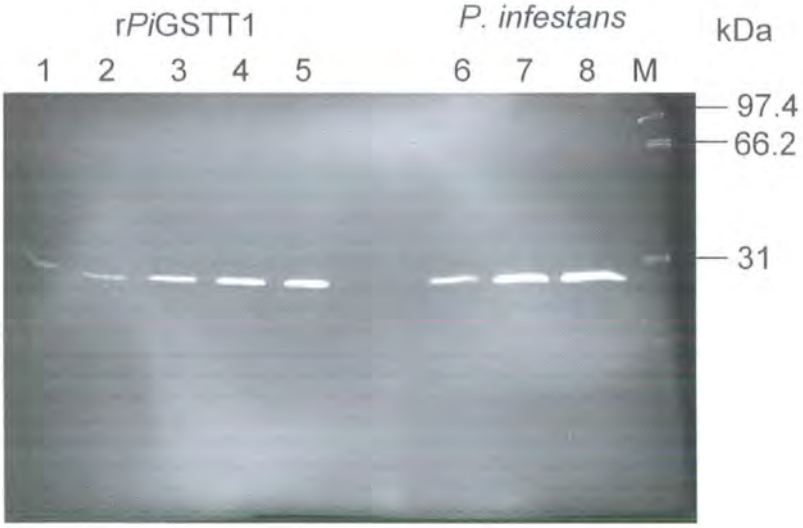

Figure 5.5.1. Negative image of western blot analysis of *Pi*GSTT1 representation in total soluble *P. infestans* protein grown in culture.
1 = 0.61ng, 2 = 1.25 ng, 3 = 2.5 ng, 4 = 5 ng, 5 = 10 ng r*Pi*GSTT1. 6 = 200 ng, 7 = 400 ng, 8 = 10000 ng crude soluble *P.infestans* protein extract.

Two-dimensional western blot analysis revealed that *Pi*GSTT1 appeared to represented 1 major isoform, migrating with pI of around 7 (Figure 5.5.1.2), corresponding to the predicted pI for *Pi*GSTT1 of pH 6.8.

Figure 5.5.1.2 2-Dimensional western blot of 0.2 mg crude soluble protein from cultured *P .infestans* using antisera raised against *Pi*GSTT1.

5.6 Biosynthesis of the fungitoxic oxylipin 9(*S*)-HPOT and subsequent detoxification *via Pi*GSTT1-1

Grechkin (1998) reviewed recent developments in biochemistry of the plant lipoxygenase pathway, noting Kato *et al.*, (1992) had reported the fungitoxic activity of 9(*S*)-HPOT ((10*E*,12*Z*,15*Z*)-9-hydro(pero)xy-10,12,15-octadecatrienoic acid) toward various plant pathogens. Linolenic acid, a major polyenoic fatty acid of seed plants, is the substrate of potato tuber lipoxygenase (LOX, EC 1.13.11.12) an enzyme whose catalytic mechanism is well established (Blee, 1998; Grechkin 1998). Potato LOX converts linolenic acid to HPOT with apparent high yields (Grechkin 1998) with the specificity of conjugation at the 9 chiral atom being pH dependent. Under alkaline conditions, (pH 9), the major product of the reaction is 13(*S*)-HPOT, while at pH 6.4 9(*S*)-HPOT was formed (Grechkin *et al.*, 1991). Here, the specificity of oxygenation was attributed to the carboxylic acid anion being formed at high pH thereby facilitating conjugation at the 13 chiral centre, whereas conjugation at position 9 did not display this specificity.

Since *Pi*GSTT1-1 was able to reduce synthetic organic hydroperoxides, it was hypothesised that this oomycete enzyme, may detoxify specific oxylipin phytoalexins produced by host plants in response to pathogen attack. Figure 5.6 outlines the biosynthesis of linolenic acid hydroperoxide and its hypothesised detoxification by *Pi*GSTT1-1.

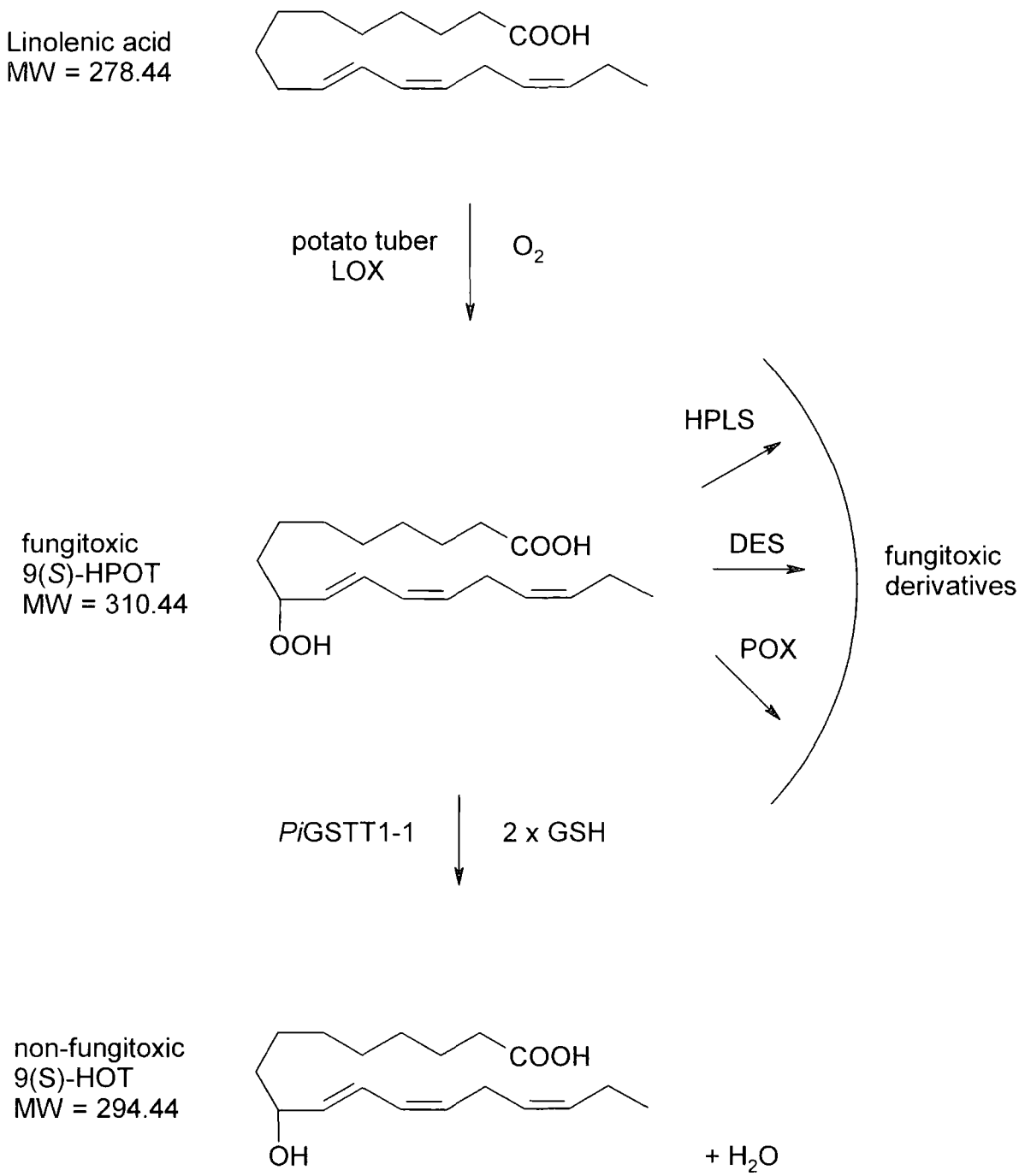

Figure 5.6 Hypothesised overview of the biosynthesis of fungitoxic oxylipin 9(*S*)-HPOT and detoxification *via* *Pi*GSTT1-1 GPOX activity. LOX = lipoxygenase, HPLS = hydroperoxide lyase, DES = divinyl ether synthase, POX = peroxygenase.

LOX activity of crude potato tuber protein extract toward linolenic acid was determined by following the increase in absorbance at 235 nm over 2 minutes (table 5.6) (Cummins *et al.*, 1999).

Table 5.6 Specific activity of crude potato tuber LOX toward linolenic acid at pH 6.4

[Linolenic acid] μM	nKat mg^{-1}
36	7.137

The potato LOX preparation was then incubated with 100 mg of linolenic acid and the oxylipin produced isolated using reversed phase chromatography.

Following purification, a 1:500 v/v diluted solution of the methanolic oxylipin concentrate was scanned 220 – 320 nm (Figure 5.6.1). It was calculated that the 9(*S*)-HPOT was present at 12.42 mM, equal to a 0.5% yield recovery. Absorbance at 267 nm and 280 nm correspond with the synthesis of 9,16(*S*)-diHPOT (di-hydroperoxide) and an intermediate oxylipin respectively (Grechkin *et al.*, 1991).

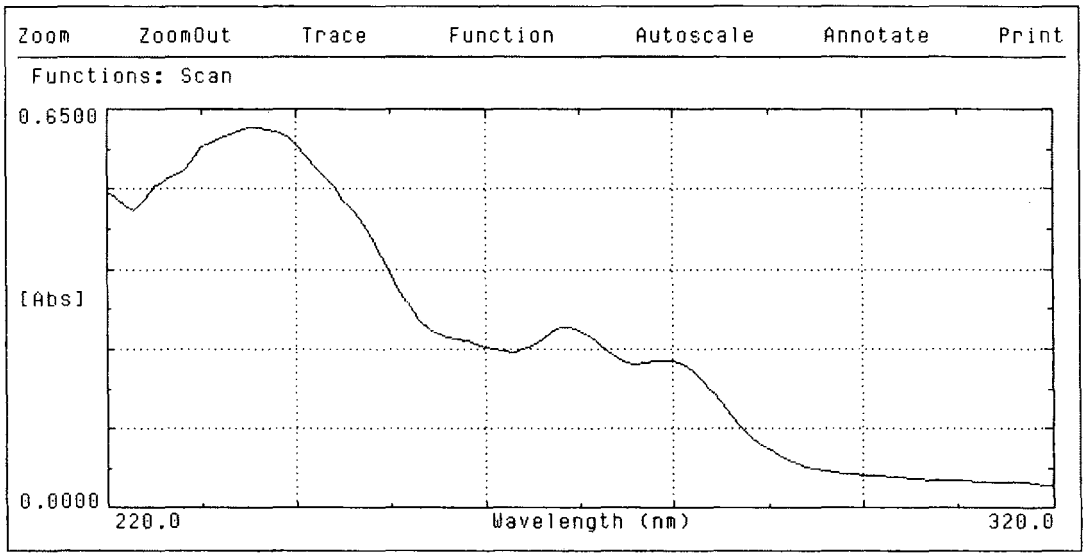

Figure 5.6.1 UV scan of 1:500 dilution of potato tuber LOX reaction products derived from linolenic acid.

5.6.1 LCMS analysis

LCMS of a 20 μL injection of 100 μM oxylipin revealed 4 distinct peaks (Figure 5.6.1). The following mass ions were obtained from the respective ionisation peaks. Linolenic acid 277.269, RT 8.3 min; 9(*S*)-HPOT 309.276, RT 7.71 min; unidentified product 327.294 , RT 6.78 min; 9,16(*S*)-diHPOT 341.285 & UP, RT 0.76 min (Figure 5.6.1). The diHPOT failed to retain on the C4 column and passed through in the injection peak. The mass ion data are however, in good agreement with those of Grechkin *et al.*, (1991) although efficiency of conversion to the hydrperoxide was not as high as those previously reported. In part this may be accounted for by differences in experimental procedure.

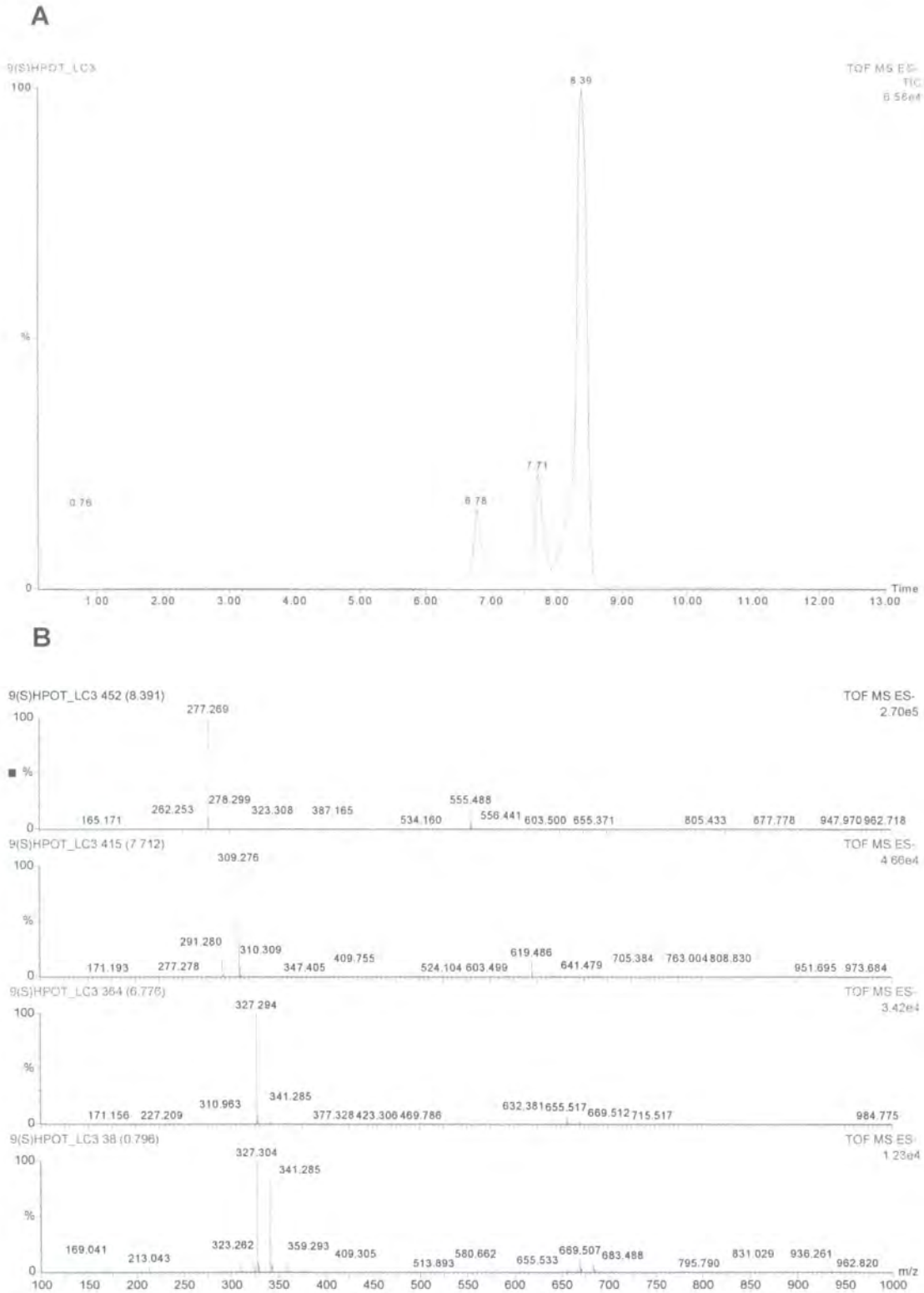

Figure 5.6.1. (A) HPLC negative total ionisation chromatogram of 20 μL injection of 100 μM 9(S)-HPOT synthesised by incubation of potato tuber LOX with Linolenic acid at pH6.4. (B) Accumulated (10sec) mass spectra of respective ionisation peaks. Linolenic acid 277.269, RT 8.3 min; 9(S)-HPOT 309.276, RT 7.71 min; unidentified product 327.294 , RT 6.78 min; 9,16(S)-diHPOT 341.285 & unidentified product, RT 0.76 min.

5.6.2 r*Pi*GSTT1 activity toward fungitoxic oxylipins

*Pi*GSTT1-1 exhibited 70 fold greater glutathione peroxidase activity toward the substrate 9(*S*)-HPOT, 1050.63 nKat mg^{-1}, as compared with cumene hydroperoxide (15 nKat mg^{-1}; figure 5.6.2). These data suggest that the fungitoxic oxylipin 9(*S*)-HPOT was a more suitable substrate for the GST-GPOX cloned from *Phytophthora infestans*. From these data however it could not be determined as to whether activity was solely toward 9(*S*)-HPOT or included the reduction of the di-hydroperoxy product. Therefore it was necessary to follow the reduction of the oxylipin mixture mediated by *Pi*GSTT1-1 using HPLC-MS.

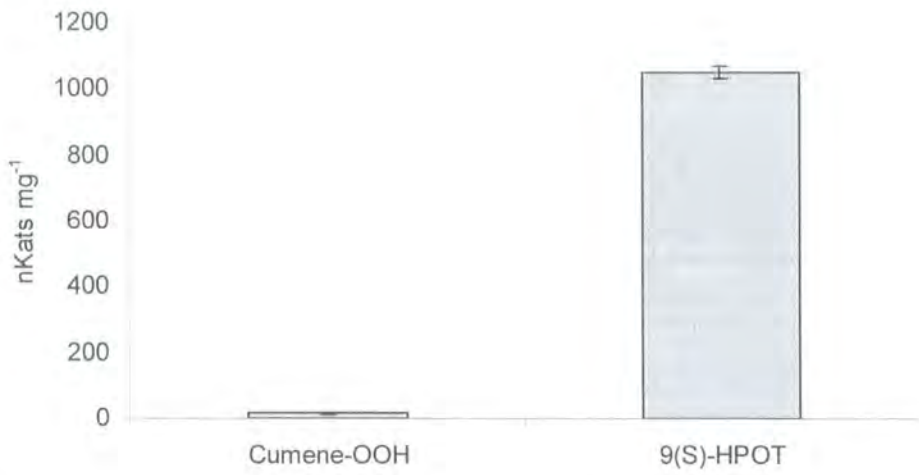

Figure 5.6.2. Specific activity in nKat mg^{-1} *Pi*GSTT1-1 GPOX toward 0.621 mM of the substrates cumene hydroperoxide and 9(*S*)-HPOT in the presence of 1 mM GSH. Vertical bars represent standard deviation (n = 2).

5.6.3 LCMS glutathione peroxidase assay development

Potassium phosphate buffers are incompatible with electrospray ionisation mass spectrometry causing salt precipitation and blockage of the probe capillary. Additionally, in positive mode, excessive quantities of potassium adducts may be observed, with the presence of EDTA and sodium azide in the glutathione peroxidase assay buffer further complicating interpretation of data. As such, it was necessary to use 10 mM ammonium acetate pH 7, an electrospray compatible buffer, in the assays. First, it was concluded that ammonium acetate had no inhibitory effect on the specific activity of *Pi*GSTT1-1 toward 1.2 mM cumene hydroperoxide (Figure 5.6.3).

Figure 5.6.3. Specific activity of *Pi*GSTT1-1 glutathione peroxidase toward 1.2 mM cumene hydroperoxide in 2 different buffer systems at pH7 in the presence of 1 mM GSH. Vertical bars represent standard deviation (n = 2).

5.6.4 Oxylipin substrate specificity

HPLC-MS was used to monitor (Figures 5.6.4 & 5.6.4.1), the interconversion of oxylipin substrates to their respective products, namely the conversion of 9(*S*)-HPOT to 9(*S*)-HOT and 9,16(*S*)-diHPOT to 9(*S*)-HOT,16(*S*)-HPOT (Figures 5.6.4.2 & 5.6.4.3). Using buffer only as a non enzymic control, 83.5% 9(*S*)-HPOT remained as parent substrate, while 16.5% spontaneously converted to the product 9(*S*)-HOT. In the presence of 3 μg *Pi*GSTT1-1, 36.6% of the reaction mix was present as parent substrate and 63.4% as product after 2 minute incubation with *Pi*GSTT1-1. Spontaneous activity toward 9,16(*S*)-diHPOT resulted in 23% conversion to 9(*S*)-HOT,16-HPOT with 77% remaining unconverted. In the presence of *Pi*GSTT1-1 40.8% remained unconverted while 59.2% was converted to the product. Comparison of net enzyme activity toward each oxylipin substrate revealed that detoxification of 9(S)-HPOT to 9(S)-HOT accounted for 76% activity while the remaining 24% was due to the reduction of 9,16(*S*)-diHPOT (Figure 5.6.4.4). Correcting for the activity toward the di-hydroperoxide substrate, the specific activity of *Pi*GSTT1-1 toward 9(*S*)-HPOT can be approximated to 798.48 nKat mg^{-1} protein, while specific activity toward the 9,16(*S*)-diHPOT was estimated to be 252.15 nKat mg^{-1}.

A

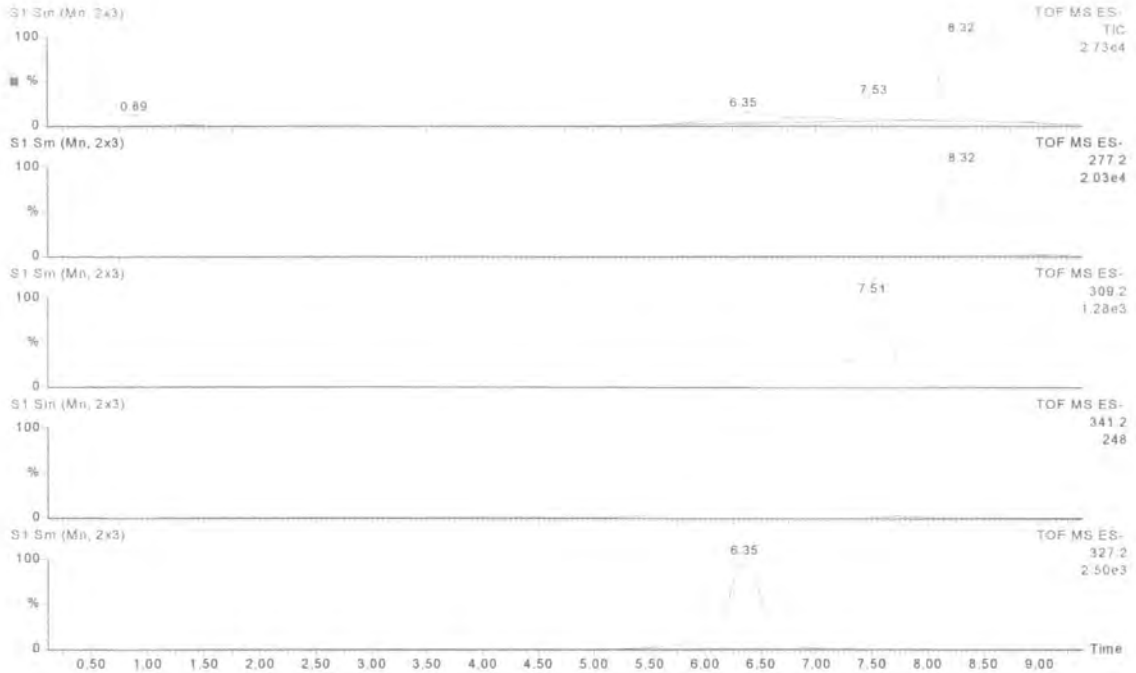

B

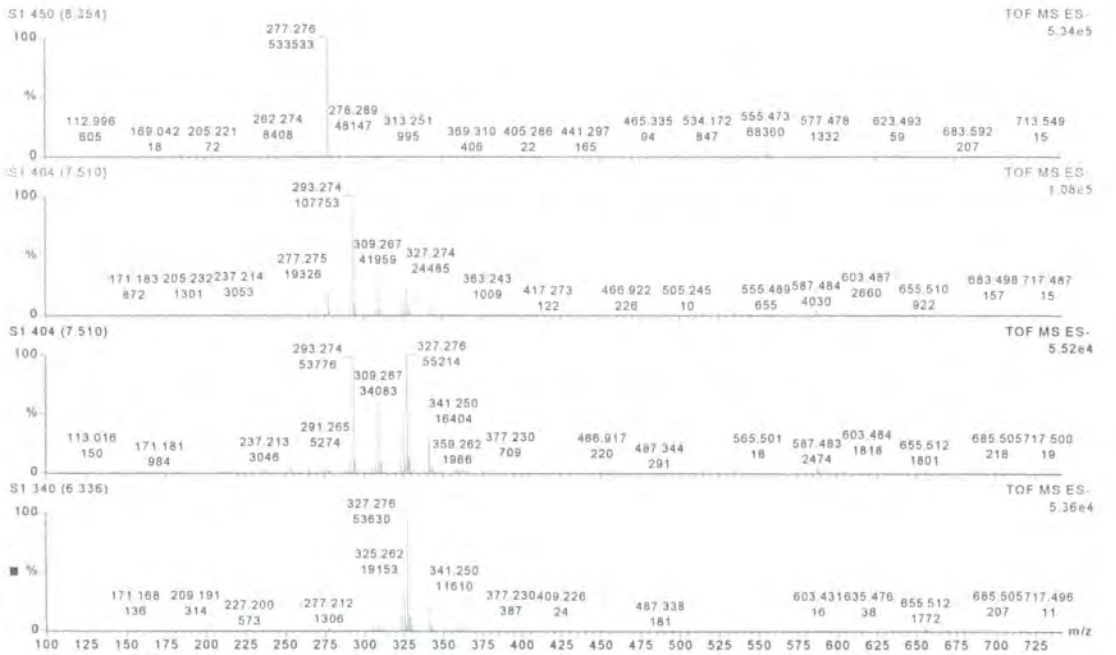

Figure 5.6.4. (A) Integrated negative ionisation chromatogram detailing retention time of α-linolenic acid and distribution of respective oxylipins following incubation with 3 μg *Pi*GSTT1-1 in the presence of 1mM GSH. Linolenic acid, 277.2; 9(S)-HPOT, 309.2; 9,16-diHPOT, 341.2; unknown product (UP), 327.2.

(B) Figure 30. Accumulated negative ionisation spectra of the major integrated peak areas .

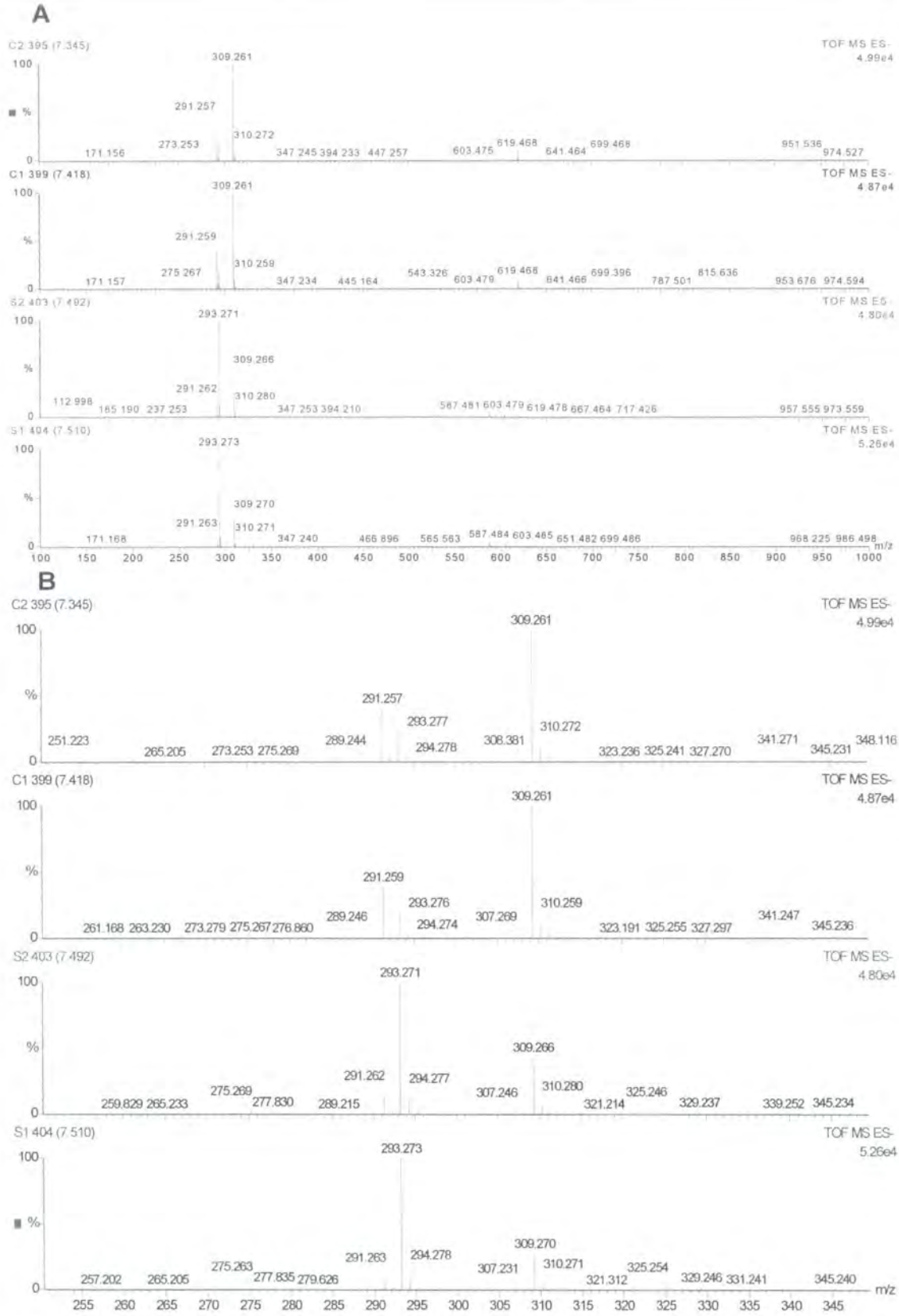

Figure 5.6.4.1. (A)Negative ionisation ESMS spectra scanning 100-100 Daltons (B) 250 - 350 D of peak eluting with a retention time of approximately 7.4 min. C1 and C2 are incubations of 250 μM 9(*S*)-HPOT in the presence of 1 mM GSH. S1 and S2 are incubations of 250 μM 9(*S*)-HPOT in the presence of 1 mM GSH and 3 μg *Pi*GSTT1-1 glutathione peroxidase.

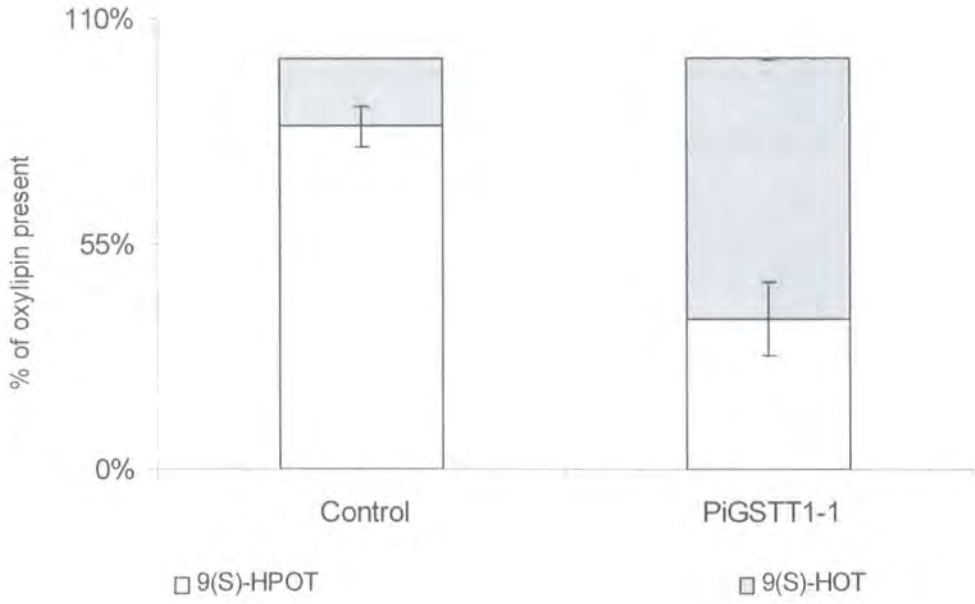

Figure 5.6.4.2. Reduction of 9(*S*)-HPOT (white) to 9(*S*)-HOT, (grey shading), following 2 minute incubation in the presence of 1mM GSH ± *Pi*GSTT1-1 cloned from *Phytophthora infestans*. After 2 minute incubation without enzyme 16% of the hydroperoxide (white) was reduced to 9(*S*)-HOT (grey shading). In the presence of *Pi*GSTT1-1 63% of the hydroperoxde was reduced to 9(*S*)-HOT (grey shading). Control samples were performed in the presence of boiled *Pi*GSTT1-1 as a denatured protein source. Vertical bars represent standard deviation (n=2).

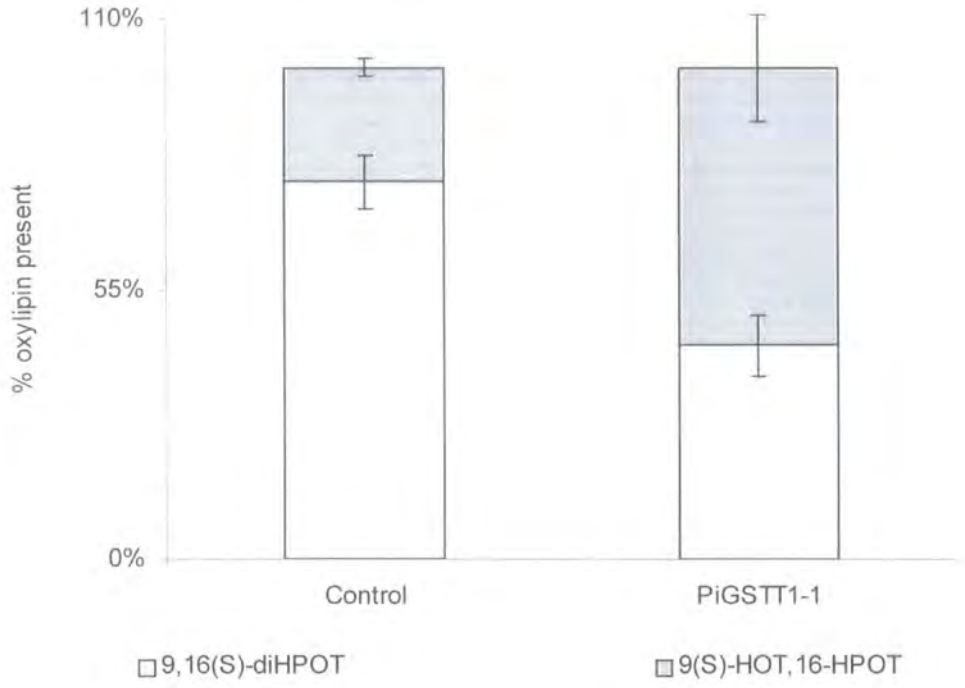

Figure 5.6.4.3. Reduction of 9,16(*S*)-diHPOT to 9(*S*)-HOT,16-HPOT, grey shading following 2 minute incubation in the presence of 1mM GSH ± *PiGSTT1-1* glutathione peroxidase cloned from *Phytophthora infestans*. After 2 minute incubation without enzyme 16% of the di-hydroperoxide (white) was reduced to 9(*S*)-HOT,16-HPOT (grey shading). In the presence of *Pi*GSTT1-1 63% of the di-hydroperoxde was reduced white to 9(*S*)-HOT,16-HPOT (grey shading). Control samples were performed in the presence of boiled *Pi*GSTT1-1 as a denatured protein source. Vertical bars represent standard deviation (n=2).

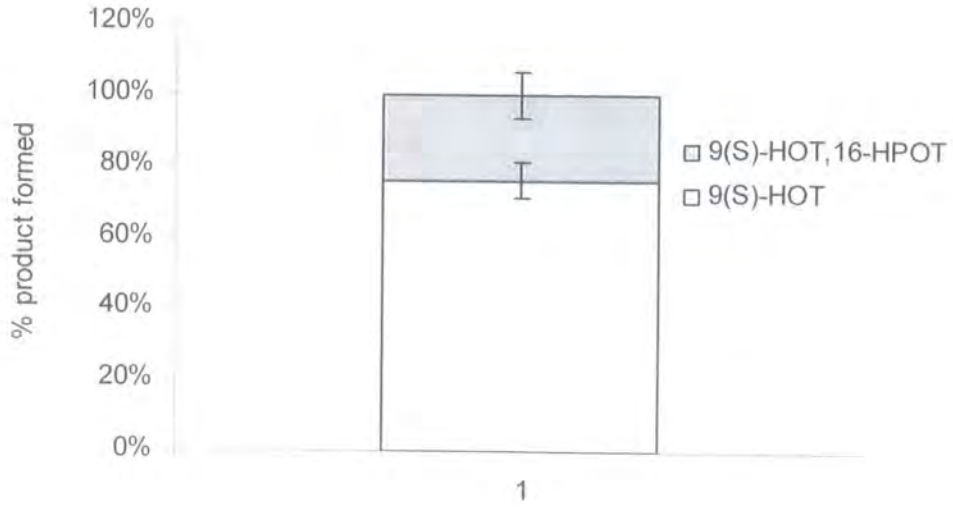

Figure 5.6.4.4. Net activity of *Pi*GSTT1-1 GPOX toward the substrates 9(*S*)-HPOT and 9(*S*)-HPOT,16-HPOT expressed as negative ion intensity of product formation. White and grey bars represent total (*S*)-HOT and 9(*S*)-HOT-16(*S*)-HPOT product formed respectively after correcting for non-enzymic reduction. Vertical bars represent standard deviation (n = 2).

5.7. Expression of *Pi*GSTT1-1 during *Phytopthora infestans* colonisation of *Solanaceae tuberosum* Var. *Bintje.*

Potentially *Pi*GSTT1-1 may play an important role in detoxification of fatty acid hydroperoxides produced by potato as a defence response to colonistation by phytopathogens. Expression of *Pi*GSTT1-1 in *P. infestans* during host plant colonisation would provide further evidence to support this hypothesis. *P. infestans*-*S. tuberosum* Var. *Bintje* pathosystems established at Bayer Crop Science, Lyon were used to monitor colonisation over 7 days (Figures 5.7– 5.7.1). At 5 day post inoculation, the disease can be seen to have taken effect with wilting and a reduction in growth evident in the haulm and water soaked leaves, with necrotic leisions evident on the leaf underside, whilst the control plants remained healthy (Figure 5.7.2). Following a 7 day infection, potato plant structure was completely lost, with a complete break down in leaf cellular structure and function with leaves only evident as a darkened necrotic mass with hypahe present (Figure 5.7.3).

Protein extracts from the infected plants were analysed by SDS PAGE and western blot analysis (Figure 5.7.4a). All protein samples were standardised and polypetide bands (50 kDa & 14.4 kDa) were seen to be more intense in control plants than those observed 5 and 7 days post infection. The decrease in plant derived protein with an increase in infection time in each total protein extract applied to the gel, indicated a concomittant increase in protein derived from *P. infestans*. Thus the major plant polypeptide visible (50 kDa figure 5.7.4a), was absent by day 7 as were polypeptides at 14.4 kDa. Immuno detection using antibodies raised to recombinant *Pi*GSTT1-1 revealed the expression of an immuno-reactive polypeptide, which was recognised by the anti-*Pi*GSTT1 serum during the infection process (Figure 5.7.4b). In contrast, *Pi*GSTT1 could not be dectected in control plants, which were not

infected with *P. infestans*. After 5 days of infection, an immunoreactive band corresponding to *Pi*GSTT1 was observed, accumulating maximally at day 7.

These data reveal that during infection *Phytophthora infestans* expresses *Pi*GSTT1, which may be capable of detoxifying fatty acid hydroperoxides produced by host plants in response to pathogen challenge. Expression of this protein in *P. infestans* may be part of a sophisticated mechanism, which has evolved to counter plant defence pathways through the production of oxylipin phytoalexins. As discussed in chapter 1, GSTs from several plants have been shown to be upregulated during fungal infection or treatment with fungal elicitors (Mauch & Dudler, 1993; Martini *et al.*, 1993; Beyer *et al.*, 2001; Yu & Facchini, 2000). However, the possibility that the observed immuno-reactive polypeptides (Figure 5.7.4b) originated from potato in response to infection as opposed to *Phytophthora,* seemed unlikely, with SDS PAGE analysis showing a decrease in plant protein content during infection (figure 5.7.4a). Thus, expression of the immunoreactive polypeptide coincided with the progress of infection (figures 5.7-5.7.3) The most intense immuno-reactive polypeptide (figure 5.7.4b) was observed at day 7, at this stage leaf structure and function was observed to collapse (Figures 5.7.1 & 5.7.3). Furthermore, molecular analysis of potato mRNA up regulated during infection by *Phytophthora* (Beyer, 2001; Martini *et al.*, 1993) revealed tau rather than theta class GSTs accumulated during infection and theta class GSTs have not been shown to be up-regulated in response to pathogen challenge in any plant species (Wagner *et al.*, 2002). It was concluded that the immuno-reactive bands (figure 5.7.4b) originated from *Phytophthora infestans* and that *Pi*GSTT1-1 may play a major protective role in this organism during infection.

Figure 5.7 uninfected control potato plants

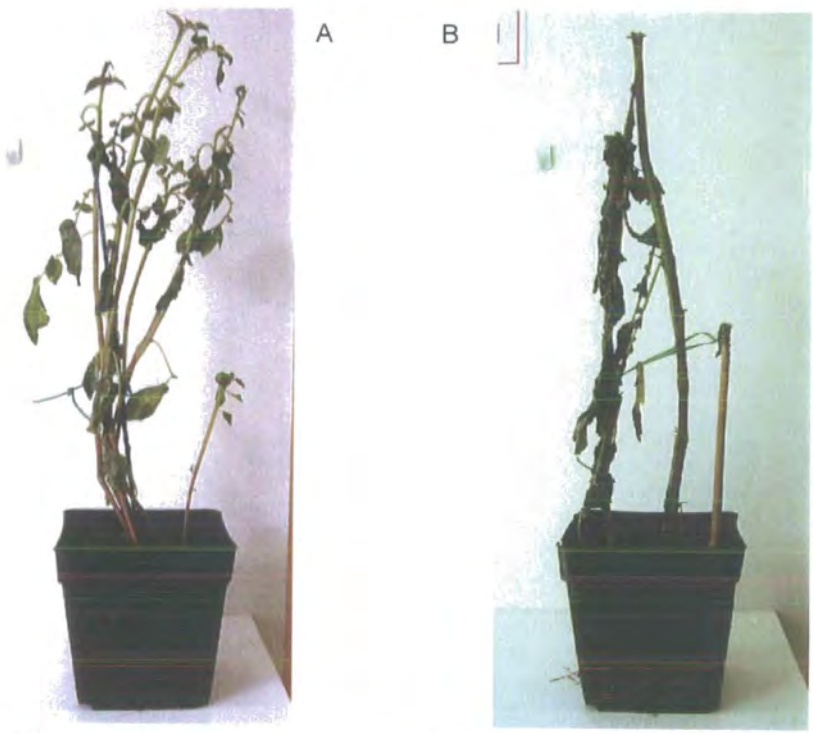

Figure 5.7.1. Potato plants 5 (A) and 7 days (B) post inoculation with 40,000 *P. infestans* sporocysts mL^{-1}.

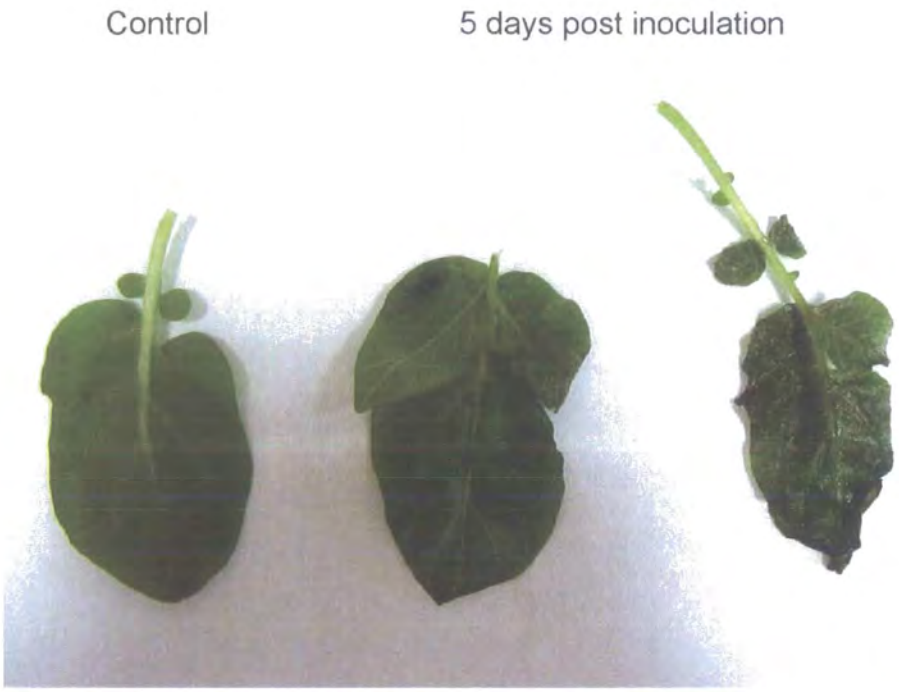

Figure 5.7.2 Comparison of leaf under surface between control and 5 day *P. infestans* infected potato leaves.

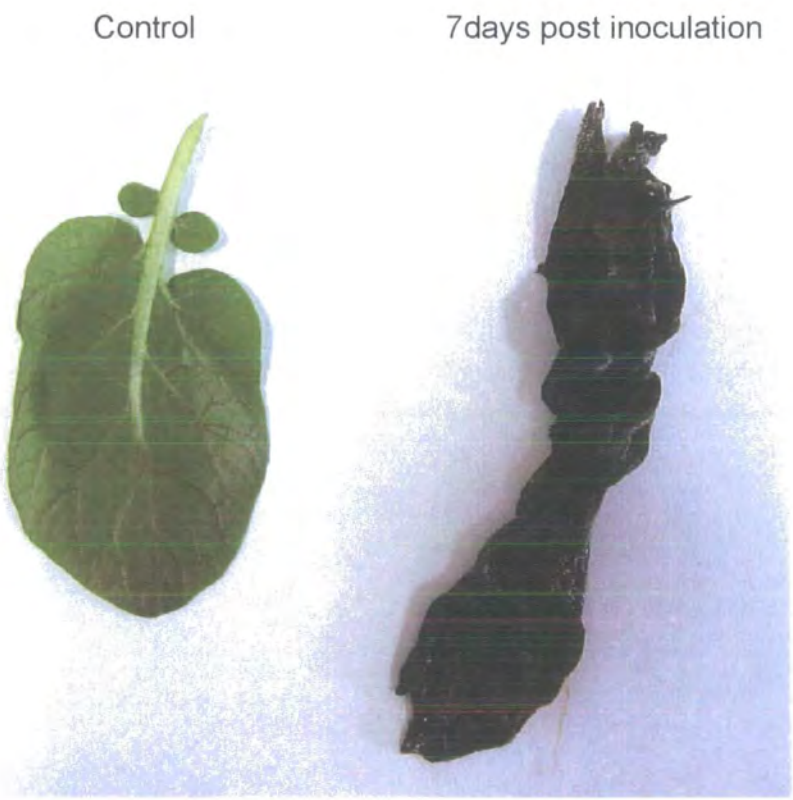

Figure 5.7.3 Comparison of leaf under surface between control and 7 day *P. infestans* infected potato leaves.

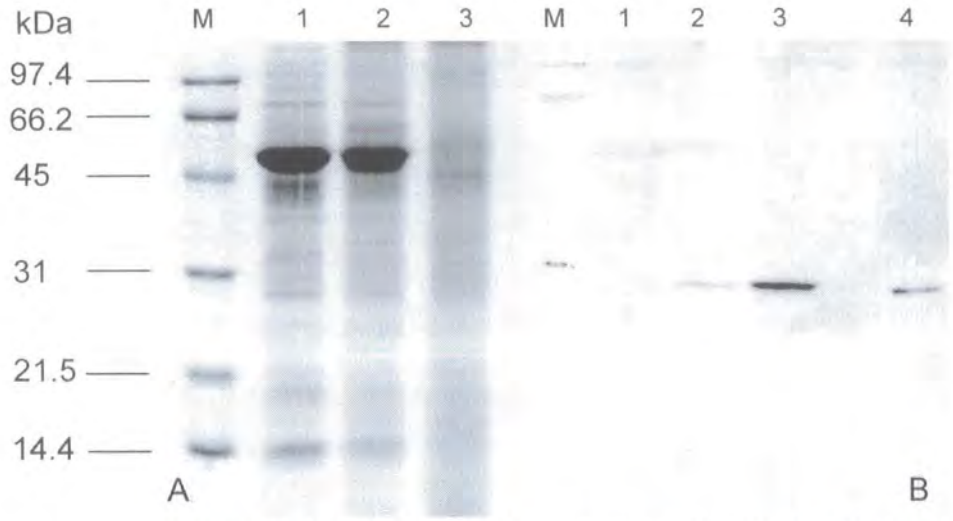

Figure 5.7.4. SDS PAGE gel stained with BioRad gel code blue (A) and western blot (B) of uninfected potato leaf protein (1), potato leaf protein 5 days post infection with *P. infestans* (2) and potato leaf protein 7 days post infection with *P. infestans* (3). All protein samples were normalised and lanes 1 - 3 contained 26.9 µg protein (4) 0.6 ng recombinant *Pi*GSTT1-1. M = molecular weight markers.

5.8 Glutathione peroxidases *of Phytophthora infestans*; implications for pathogen defence

The plant lipoxygenase pathway has been shown to be a mechanism vital to the role plant defence during pathogen attack (Webber e*t al.*, 1998). Biosynthesis of 9(*S*)-HPOT not only results in production of a fungitoxic oxylipin (Kato *et al.*, 1992), but additionally serves as the substrate precursor for 3 biosynthetic pathways of fatty acid derived phytoalexins (Blee 1998; Grechkin 1998; Howe and Schilmiller, 2002, Weichert *et al.*, 2002;).

Enzymatic reduction of 9(*S*)-HPOT to 9(*S*)-HOT mediated by *Pi*GSTT1-1 prevents the formation of antifungal compounds resulting from the action of DES, hydroperoxide lyase and peroxygenase. As such the action of *Pi*GSTT1-1 effectively prevents a cascade of synthesis of antifungal oxylipins by the host. The prevention of accumulation of the oxylipins divinyl ether and 9,12,13-trihydroxyoctadecanoic acid would counter their functions as fungistatic compounds. Colnelenic acid, for example is a potent inhibitor of cytospore germination and mycelial growth of *P. infestans* (Weber *et al.*, 1999). Tolerance of CnA, by *Phytophthera infestans* would therefore facilitate dispersal and propagation of the pathogen on susceptible species. Alternatively the role of *Pi*GSTT1-1 would be to directly counter the fungitoxicity of 9(*S*)-HPOT once inside the mycelia.

It seems evident that production of 9(*S*)-HPOT from linolenic acid via the lipoxygenase pathway is a vital step in the production of 3 anti fungal compounds derived from this organic hydroperoxide (Figure 5.1). The presence of a GST in *Phytophthera infestans* capable of detoxifying this oxylipin suggests expression may play a role in pathogen protection during host plant colonisation.

5.9 Lipid peroxidation of *P. infestans*; potential endogenous substrates of *Pi*GSTT1-1.

5.9.1 Fatty acid composition of *Phytophthora infestans*

Griffith *et al.*, (1992) note the unusual fatty acid composition of oomycetes as compared with that of true fungi. The ability to synthesise lipids such as γ-linolenic acids and long chain polyunsaturated fatty acids is uncommon in higher fungal species. In *Phytophthora infestans* however, only trace quantities of γ-linolenic acid have been detected. Table 5.9 outlines the total fatty acid composition of *P. infestans* reviewed by Wassef (1977).

Table 5.9 Fatty acid composition of *P. infestans*

	Carbon number and degree of desaturation								
	14:0	16:0	16:1	18:0	18:1	18:2	18:3	20:3	20:4
% fatty acid	23.5	12	3.4	2.1	31.2	4.5	tr.	10.2	7.7

tr = trace quantities. Table adapted from Wassef (1977)

Within *P. infestans* the main polyunsaturated fatty acids to be found include arachidonic acid, 20:4; 7.7% and the 20:3; 10.2% lipids. It is known that tomato and potato tuber lipoxygenase 5 can introduce a hydroperoxy group at the fifth carbon in arachidonic acid, which is released by *P. infestans* during infection, thereby converting it to 5-*S*-HPETE (Ricker & Bostock, 1992). Thus 5-*S*-HPETE is a putative substrate for the glutathione peroxidase *Pi*GSTT1-1 of *P. infestans*. The possible detoxification of this oxylipin by *Pi*GST1-1 was of particular interest, as the 5(*S*)-HPETE has been reported to induce phytoalexins from potato tuber (Castoria *et al.*, 1992). However, attempts to biosynthesise 5-*S*-HPETE from arachidonic acid using

potato tuber lipoxygenase proved unsuccessful. Future biosynthesis of lipoxin hydroperoxides derived from endogenous fatty acids of *P. infestans* may reveal additional substrate specificities of *Pi*GSTT1-1 toward substrates of fungal origin.

5.10 Amelioration of fungicide cytotoxicity invoked by lipid peroxidation

Enzyme assays using the substrates fenoxaprop-P-ethyl and zoxamide revealed *Pi*GSTT1-1 did not exhibit GSH conjugating activity toward any of the pesticides tested. In accordance with the known absence of glutathione conjugating activity of theta class GSTs, these data suggest that this enzyme would play no direct role in fungicide detoxification. However it is possible that *Pi*GSTT1-1 may contribute to resistance to fungicides through its GPOX activity. For instance cells treated with dicarboximide fungicides (DCOFs) have been shown to undergo drastic morphological alterations with hyphal collapse and pronounced changes of ultrastructure, in particular the endoplasmic reticulum and mitochondria. It has been suggested that these effects indicate a complex mode of action on several cellular compartments and metabolic processes (Edlich & Lyr, 1992; Edlich & Lyr, 1987; Lyr, 1987). One such mechanism of toxicity is the induction of lipid peroxidation, which if uncontrolled, can be a pathological process. Removal of a hydrogen atom from a PUFA, generates a free radical capable of reacting with molecular oxygen with subsequent conversion to peroxy radical. Continuation of this process, if left unchecked can lead to a cascade of dismutation of hydroperoxides resulting in structural and functional damage of lipid membranes and loss of membrane bound proteins. Most of the morphological events in hyphal death caused by exposure DCOFs (dicarboximide fungicides) appear to be explained by these events (Edlich & Lyr, 1992). Constitutive expression of the endogenous *Pi*GSTT1-1 capable of

detoxifying fatty acid derived hydroperoxides may afford *P. infestans* a protective mechanism detoxifying organic hydroperoxides induced on exposure to fungicides such as DCOFs. Glutathione peroxidase activity has been shown to contribute toward pesticide resistance in weeds (Cummins *et al.*, 1999) and insects (Hemmingway, 2002). Interestingly, exposure of *B. cinerea* to the DCOF vinclozolin was found to strongly stimulate lipid peroxidation whilst in *P. infestans*, an insensitive species, lipid peroxidation was not observed. The cause of selectivity between each species was not believed to be due to differences in PUFA levels as *P. infestans* was found to have higher polyunsaturated fatty acid levels than DCOF-sensitive *B. cinerea* (Edlich & Lyr, 1992; Dorobek and Lyr, 1987). It may be possible that lipid peroxides in *P. infestans*, generated from exposure to vinclozolin, were reduced by constitutive, endogenous expression of *Pi*GSTT1-1. The presence of a constitutive *Pi*GSTT1-1 homologue in *Botrytis* has not been reported.

Sudden oxidative stress, such as DCOF application, may exceed the capability of basal enzyme levels, such as catalase and superoxide dismutase, which are central in suppressing lipid peroxidation in facualtive aerobic organisms. Edlich & Lyr, (1992) speculated that both glutathione and glutathione dependent peroxidases are also integrative parts of the fungal antioxidant protective system. However, the exact role of glutathione peroxidase activity with respect to fungicide resistance in *P. infestans* remains unclear. Non-DCOF fungicides, etridiazole, chloroneb and dimethoporph, which are toxic to *P. infestans* also produce lipid peroxides as part of their mode of action (Edlich & Lyr, 1992). In this respect, investigation of transgenic *P. infestans* lines, harbouring over expressing and RNAi constructs of *PiGSTT1*, may provide new insights into the role of glutathione dependent enzymes functioning within fungicide resistant mechanisms in this problematic species.

6.0 Fungal GST classification, main conclusions, and future work.

6.1 Fungal GST classification

Among the glutathione *S*-transferase super-family as many as 28 independent GST classes have been proposed to exist (Pemble and Taylor, 1992). Of these 28, 14 classes have been described in published papers (Blocki *et al.*, 1994; Chelvanayagam *et al.*, 2001; Thomson *et al.*, 1998; Cummins *et al.*, 1999; Dixon *et al.*, 2000; Droog, 1997; Awasthi *et al.*, 2001; Hansson *et al.*, 1999; Wolf *et al.*, 2001; Rossjohn *et al.*, 1998; Board *et al.* 2001; Pemble *et al.*, 1996; Dixon *et al.,* 2002). The most recent inclusion has been the fungal gamma class GSTs (Cha *et al.*, 2002). Fungal GSTs have been proposed to have arisen from the theta-class GSTs (Pemble and Taylor, 1992), which are believed to be the progenitor of all eukaryotic GSTs (Edwards *et al.*, 2000; Wagner *et al.*, 2002). The saprophyte *Aspergillus nidulans,* contains a zeta class GST, however, most of the sequence and enzymic data available on recombinant fungal GSTs has come from those cloned from *Cunninghamella elegans* (Cha *et al.*, 2002), *Saccharomysces cerevisiae* (Choi *et al.*, 1998), *Schizosacharomyces pombe* (Shin *et al.*, 2002; Kim *et al.*, 2001) and *Issatchenkia orientalis* (Tamaki *et al.*, 1999; Tamaki *et al.*, 1991) with information on GSTs in phytopathogenic fungi being scant.

The first GST of a fungal phytopathogen was identified in *Botrytis cinerea*, *BcGST*, (Prins *et al.*, 1999) with the homologue identified in *A. nidulans*, *GSTA*, being assigned as a theta-class GST (Fraser *et al.*, 2002). However, the homologue of *GSTA* and *BcGST* cloned from *Magnaporthe grisea* bore only weak homology to theta class GSTs, although sharing 61% and 65% identity at the amino acid level with *GSTA* and *BcGST* respectively. Due to the lack of sequence data available the classification of fungal GSTs has not been easily defined. Fungal sequences have been previously assigned to the theta class GSTs based on incomplete sequence

analysis and the absence of GST catalytic activity toward the substrate CDNB (Pemble and Taylor, 1992; Tamaki *et al.*, 1999; Fraser *et al.*, 2002). However, with the advent of genome sequencing projects of both saprophytic and phytopathogenic fungi, advances have been made in the classification of fungal GSTs including their possible relationship to extant GST classes.

Based on multiple sequence alignment and phylogenetic analysis, the amino acid sequences of *GSTA* and *BcGST* were found to represent members of a new discrete grouping, which for classification purposes have been assigned the Greek letter ξ (Xi) (figure 6.1). Xi class GSTs were situated on a well supported branch, which also contained 2 other new GST classes, bacterial specific Xi' (ξ') and epsilon (ε), all of whom appeared to share a common branch point with phi class GSTs. Recombinant *Mg*GSTX1-1 has demonstrated glutaredoxin activity being able to reduce mixed disulfides in the presence of GSH, indicating that Xi class GSTs may function in thiol transfer as well as conferring tolerance toward heavy metals and xenobiotics (Fraser *et al.*, 2002).

Within this study six new GST classes were identified, iota (ι), xi (ξ), xi' (ξ'), epsilon (ε), nu (η) and rho' (ρ'). As discussed in chapter 1, the nomenclature for the classification of GSTs centres upon the use of a Greek letter for each class, coupled with the species initials and a numbering system relating to the order of discovery and subunit composition of the respective enzyme (see 1.4.2). Chelvanayagam *et al.*, (2001), suggested that due to the limited number of Greek alphabet letters available and the presence of phylum or species specific GSTs, such as a mammalian alpha, mu and pi class GSTs, plant specific phi, bacterial specific beta and insect specific delta class GSTs, modifications to the existing nomenclature may be necessary. Furthermore, genome-wide sequencing projects of a diverse range of organisms

have contributed GST like sequences to the databases at a rate surpassing the capability of biochemical characterisation of the respective enzymes. As discussed previously (see 1.4.1), sequence similarity alone has been proposed to be insufficient criteria for GST classification (Edwards *et al.*, 2000). Therefore on this basis, it is suggested that putative GST like sequences identified in databases, which form classes based on sequence identity but have not yet been biochemically analysed for GST activity or function, should be assigned the integer prime (') following a putative GST classification. The aim of this modification to the existing nomenclature is to separate proteins known to exhibit GST related activities, from similar sequences, which are not known to use GSH catalytically and may have diverged to fulfil alternative functions

One such example of a putative class was the bacterial specific Xi' GSTs diverging from Xi class GSTs on a well supported branch (figure 6.1), which were found to share 37% - 40% identity at the amino acid level with *Mg*GSTX1. However, neither endogenous function nor GSH-dependent catalytic activity of xi' GSTs has been demonstrated. Thus, these bacterial sequences were assigned as xi' class GSTs, due to their relatedness to the xi class GSTs and absence of biochemical or functional characterisation.

Epsilon class GSTs *Sp*GSTE1 and *Sp*GSTE2GSTs cloned from *Schizosaccharomyces pombe* (Kim *et al.*, 2001), clustered closely to the Ure2p polypeptides of *Saccharomyces cerevisiae* (Coshigano and Magasank, 1991) and other fungi. The crystal structure of *S. cerevisiae* Ure2p revealed a fold resembling the active site of bacterial β-class GSTs (Bousset *et al.*, 2001), however Ure2p is not a catalytically active GST and functions in regulating nitrogen catabolism. Coshigano and Magasank (1991) speculated that Ure2p may *S*-glutathionylate an active site cysteine of glutamine synthase, thereby inhibiting glutamine synthetase activity.

However, it has been demonstrated that nitrogen catabolism in *S. cerevisiae* is regulated by Ure2p binding to the transcription factor Gln3p thereby down regulating gene expression by inactivating the transcriptional function of Gln3p (Blinder *et al.*, 1996).

Over expression of *Sp*GSTE2 in *S. pombe*, *S. cervisiae* and *E. coli* has been shown to increase GST activity toward CDNB 2.59, 1.92 and 1.67 fold respectively (Kim *et al.*, 2001). The amino acid sequence of *N. crassa Nc*GST was present in the database as a hypothetical protein; as such information regarding enzyme activity of this putative polypeptide was not present.

Fungal and bacterial classes xi, xi', Ure2p and epsilon class GSTs all clustered together on a well supported branch related to the theta class GSTs (figure 6.1). It is interesting that the Ure2p GST-like polypeptides that are non-catalytic with GSH were found to contain a fold in the 3-dimensional structure, which closely resembled the active site of bacterial specific beta class GSTs (Bousset *et al.*, 2001). The observation of this seemingly evolutionary artefact and the well supported position of Xi, bacterial-specific Xi' Ure2p and epsilon classes may suggest that these sequences evolved from beta class GSTs and not theta, as has been proposed for all fungal GSTs (Pemble and Taylor, 1992). These GST classes now fulfil different cellular roles, with proteins such as Ure2p no longer functioning as GSTs, having evolved to regulate gene expression (Blinder *et al.*, 1996). Xi class GSTs have demonstrated thioltransferase activity and maintain a role in cellular detoxification of heavy metals and xenobiotics (Fraser *et al.*, 2002), although direct conjugation of GSH to xenobiotics by Xi class GSTs has not been demonstrated, with epsilon GSTs demonstrating the ability to conjugate xenobiotics with GSH (Kim *et al.*, 2001).

Of the bacterial GST sequences identified to date only those belonging to beta have been classified. However, 3 new groupings, which have been classified as xi'

(ξ'), rho' (ρ') and nu' (η') containing bacterial GSTs were apparent in the databases. Within GST class nu, expressed sequences tags of the fungal phytopathogens *Bulmeria graminis* and *Septoria tritici,* revealed GST like sequences found to cluster closely with *Xanthomonas campestris, X. axonopodis, Bradyrhizobium japonicum, Caulobacter crescentus* along with 2 sequences of *S.cerevisiae*. The presence of a branch point with low significance supporting the bacterial and fungal data sets may have resulted from analysing partial *S. tritici* and *B. graminis* sequences. GSH conjugating activity of both *Sp*GSTN1 and *Sc*GSTN1 toward CDNB as a substrate has been confirmed and the sub-cellular localisation of *Sc*GSTN1 found to be membrane associated (Choi *et al.*, 1998; Shin *et al.*, 2002). On the basis of these sequences clustering on a well supported branch they have been assigned the GST classification of nu (η). However, due to the branching pattern observed within this GST class and GST activity only having been identified in *Sc*GSTN1 and *Sp*GSTN1, several members have also been assigned the prime integer. Subsequent studies may reveal nu to be a heterogenous class, which similar to theta class may give rise to new GST classes.

The new gamma class of fungal GST, identified in *Cunninghamella elegans* (Cha *et al.*, 2002) were located on the well supported clade containing α, μ, π and σ class GSTs. Demonstrating GST activity toward CDNB, gamma class GSTs were considered to have evolved from α, μ and π class GSTs following early divergence from theta class (Cha *et al.*, 2002; Pemble & Taylor, 1992).

Interestingly, expressed sequence tags of *Phytophthora infestans* (*Pi*GSTS and *Pi*GSTS2) and of the unicellular green algae *Chlamydomonas reinhardtii* (*Cr*GSTS) were found to cluster with sigma GSTs. Sigma GSTs have been shown to catalyse the glutathione dependent formation of prostaglandin D_2, PGD_2, derived

from arachidonic acid (Thomson *et al.*, 1998). Considering that arachidonic acid is a major fatty acid of *P. infestans*, these GSTs may have evolved to function in the regulation of metabolic derivatives of this polyunsaturated fatty acid. Furthermore, the identification of a putative sigma GST in the algae *C. reinhardtii* was of interest as sigma class GSTs have not been shown to occur in plant species or been observed in this well supported clade (Snyder and Maddison, 1997). *P. infestans* is not a member of true fungi and belongs to the kingdom Chromista, having been found to be more closely related to diatoms and algae than true fungi (Judelson, 1997). Full length polypeptide sequence analysis of *Pi*GSTS, *Pi*GSTS2 and *Cr*GSTS may confirm or refute the classification of these sequences.

GST contigs derived from *Candida albicans* were found to cluster with GSTs of *Issatchenkia orientalis*, where the respective proteins have been shown to be capable of conjugating CDNB with GSH (Tamaki *et al.*, 1989) and act to detoxify xenobiotics *in vivo* (Tamaki *et al.*, 1999; Tamaki *et al.*, 1991). Previously suggested to belong to theta class (Tamaki *et al.*, 1999; Pemble and Taylor, 1992), these *Io*GSTs were not found to cluster with theta class GSTs. Thus, these sequences were termed iota (ι) class GSTs. Although closely positioned to theta and delta class GSTs the common branch supporting all three classes was not found to be significant (figure 6.1). *Io*GSTI1 and I2 of *I. orientalis* have been found to metabolise the xenobiotics *o*-DNB and CDNB, with the processed cysteinyl derivative of the *o*-DNB-GSH conjugate being excreted into the media (Tamaki *et al.*, 1991). In this respect the presence of putative iota class GSTs in the human pathogen *C. albicans* is of considerable interest, as only a few classes of drugs used to treat this infectious agent are effective (http://www-sequence.stanford.edu/group/candida/). It may be possible that expression of iota GSTs in *C. albicans* contributes to the drug resistance of this pathogen. Thus cloning and expression of recombinant *Ca*GSTI1

and I2 proteins, may uncover new information regarding drug detoxification in this pathogenic fungi.

Glutathione *S*-transferases from the true fungi were not found to cluster with theta class GSTs. However, the *Pi*GSTT1 polypeptide of *P. infestans* was related to the theta class GSTs, which may be attributed to oomycetes being taxonomically more closely related to diatoms and algae than to true fungi (Judelson, 1997). However, within this class *Pi*GSTT1 did not cluster closely with mammalian and plant theta GSTs, which may have been the result of evolving unique functions related to the ability to detoxify specific fatty acid derived phytoalexins as opposed to maintaining general lipid membrane integrity following oxidative stress. By way of analogy, the insect specific delta class GSTs, were originally classed as theta but have now been shown to form a distinct class (Chelvaningham *et al.*, 2001). It may be possible that theta class GSTs of oomycete origin may yet form a distinct sub-grouping within this class, as has been proposed for a nematode specific sub-grouping of sigma GSTs (Campbell *et al.*, 2002). However, further GST sequences form other oomycetes would be required to confirm the presence of a sub-class. On the basis of sequence similarity, the presence of the conserved amino acid sequence among theta class GSTs, SQPRS, incorporating the catalytically essential serine 11, structural modelling to *Hs*GST1 and 2 theta class GSTs (see 5.2.3) and phylogenetic analysis *Pi*GSTT1 can be classed as a theta GST.

The ability to conjugate GSH to CDNB has been demonstrated for fungal GST members of iota, gamma, nu and epsilon (Cha *et al.*, 2002; Kim *et al.*, 2001; Choi *et al.*, 1998; Shin *et al.*, 2002) with Xi class GSTs also being capable of using GSH catalytically in thiol transfer. With the advent of fungal genome sequencing projects it has been possible to establish a more complete picture of GST classification incorporating GSTs of pathogenic, saprophytic and phytopathogenic fungi. However,

there remain some anomalies at present, such as HPAJ3294 of *Pitchia angusta*, and *Sc*GST2 of *S. cerevisiae*, the sequences of which to do not cluster with each other or within any GST class. Tantalisingly, an EST of *Septoria tritici* was found to cluster with tau class GSTs, which are known to detoxify herbicides by conjugation with glutathione in wheat (Thom *et al.*, 2002). The diversity seen among GSTs of fungal origin suggests arbitrary assignment as theta class GSTs is inadequate for incorporation into the established GST nomenclature. As with the majority of GST classes the endogenous roles performed by fungal GSTs yet remain to be elucidated. However, theta class *Pi*GSTT1 is the first example of a GST identified in a phytopathogen that is capable of detoxifying anti-microbial phytoalexins induced in plants in response to pathogen challenge.

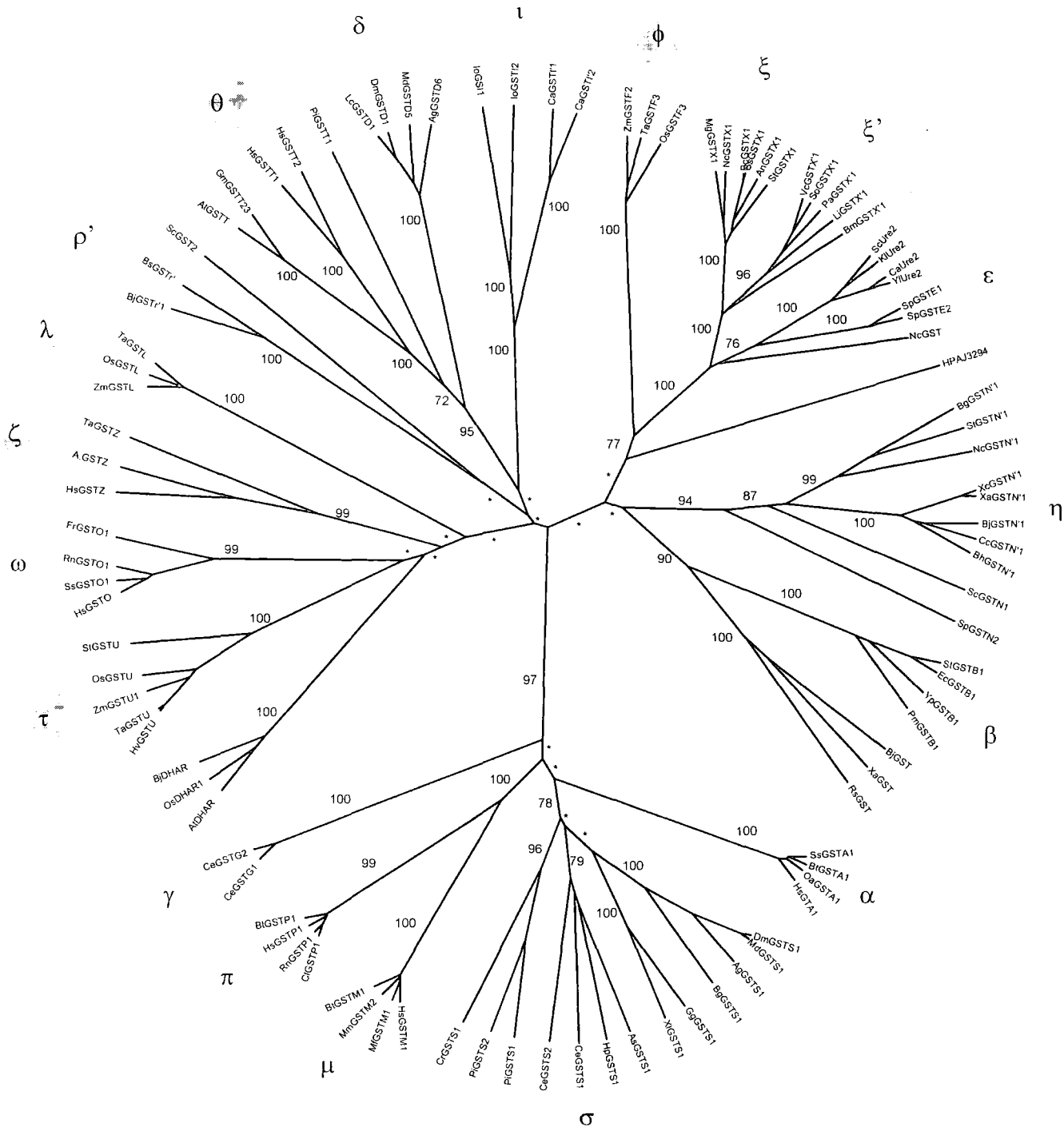

Figure 6.1 Bootstrapped dendogram of GST classes based on amino acid analysis including GSTs of saprophytic and phytopathogenic fungi. Numbers represent branch node confidence, * indicates branch nodes of low confidence (n = 100) with GST classes found to occur in plants being distinguished by grey shading. Full legend annotation over leaf.

Figure 6.1 Bootstrapped dendogram of GST classes

*At*DHAR, *Arabidopsis thaliana* Q8LB28; *Os*DHAR1, *Oryza sativa* AB037970; *Hs*GTA1, *Homo sapiens* P08263; *Ss*GSTA, *Sus scrofa* Q29057; *Oa*GSTA, *Ovis aries* Q9XS30, *Bt*GSTA, *Bos taurus*, Q28035; *Hs*GTM1, *H.sapiens* P09488; *Mf*GSTM, *Macca fascicularis* Q9TSM5; *Bt*GSTM *B.taurus* Q9NOV4; *Mm*GSTM2, *Mus musculus* P15626; *Bt*GSTP1, *B.taurus* P28801; *Hs*GSTP *H.sapiens* P09211; *Cl*GSTP1 *Cricetulus longicaudatus* P46424; *Rn*GSTP1 *Rattus norvegicus* P04906; *Hs*GSTO, *H.sapiens* U90313; *Rn*GSTO1, *Rattus norvegicus* Q9Z339; *Ss*GSTO1, *S.scrofa* Q9N1F5; *Fr*GSTO1, *Fugu rubripes* Q90XY6; *Zm*GSTL, *Zea mays* X58573; *Os*GSTL, *O.sativa* Q9M578; *Ta*GSTL, *Triticum aestivum* CAD29476; *Ta*GSTZ, *T.aestivum* O04437; *Hs*GSTZ, *H.sapiens* O43708; *Zm*GSTF2, *Z.mays* P46420; *Ta*GSTF3, *T.aestivum* CAD2946; *Oa*GSTF3 *O.sativa* Q9FUE0; *Zm*GSTU1, *Z.mays* O24595; *Hv*GSTU; *Hordeum vulgare*, Q9SES7; *Ta*GSTU, *T.aestivum* Q8RW02; *Os*GSTU, *O.sativa* O65032; *At*GSTT; *A.thaliana* AB010072; *Hs*GSTT1, *H.sapiens* P30711; *Hs*GSTT2, *H.sapiens* Q9HD76; *Gm*GSTT23, Q9FQD5; *Ag*GSTS, *Anopheles gambia* P46428; *Gg*GSTS, *Gallus gallus* O73888; *Cr*GSTS, *Chlamydomnas reinhardti* BQ825815; *Dm*GSTS1, *Drosophilla melongaster* Q9V7Y4; *As*GSTS *Ascarius sum* P46436; *Md*GSTS1, *Musca domestica* P46437; *Xl*GSTS, *Xenopus laevis* Q8JHA7; *Bg*GSTS *Blattella germanica* O18598; *Ce*GSTS, *Caenorhabditis elegans* CE14870; *Ce*GSTS2, *C.elegans* CE07825; *Hp.b*GSTS, Heligmosomoides polygyrus. Bakeri AF128959; *Pm*GSTB1, *Proteus mirabilis* U38482; *Yp*GSTB1, *Yersinia pestis* AAM85534; *St*GSTB, *Salmonella typhi* Q8Z6Q4; *Ec*GSTB, *Escherichia coli* P39100; *Md*GST5, *M.domestica* Q254450; *Lc*GSTD1, *Lucila cuprina* P42860; *Ag*GSTD6, *A.gambia* Q93113.*Bc*GSTX1 = *Botrytis cinerea* Q9HF89; *St*GSTX1 = *Mycosphaerella graminicola* mg0656; *Ss*GSTX1 = *Sclerotinium sclerotia* AR123147; *An*GSTX1 = *Aspergillus nidulans* AF425746; *Nc*GSTX = *Neurospora crassa* AL807366; *Vc*GSTX' = *Vibrio cholerae* AE004389; *Li*GSTX' = *Leptospira interrogans* AAN50554; *So*GSTX' = *Shewanella oneidensis* AAN54633; *Pa*GSTX' = *Pseudomonas aeruginosa* Q9I399; *Bm*GSTX' = *Brucella melitensis* biovar Suis AAN29555; *Sc*GSTN1 = *Saccharomyces cereviseae* P40582; *Sc*GST2 = *S.cerevisiae* Q12390; *Bg*GSTN1 = *Blumeria graminis* bga1228f; *St*GSTN1 = *M.graminicola* mg[0278]; *Xc*GSTN'1 = *Xanthomonas campestris* Q8P8F6; *Xa*GSTN'1 = *Xanthomonas axonopodis* (pv. citri) Q8PJY3; *Nc*GSTN'1 = *N.crassa* EAA33832; *Bh*GSTN'1 = *Bradyrhizobium japonicum* AP005937; ScURE2 = *S.cerevisiae* AAA35201; *Ca*URE2 = *Candida albicans* AF260777; *Kl*URE2 = *Kluyveromyces lactis* AF260776; *Yl*URE2 = *Yarrowia lipolytica* AF525171; *Sp*GSTN2 = *Schizosaccharomyces pombe* QP6M1; *Cc*GSTN'1 = *Caulobacter crescentus* AE005950; *Io*GSTI'1 = *Issatchenkia orientalis* AB021655; *Io*GSTXI'1 = *I.orientalis* X57957; *Sp*GSTE1 = *S.pombe* O59827; *Sp*GSTE2 = *S.pombe* Q9Y7Q2; *Ca*GSTI'1 = *C.albicans* contig 6-2235 bp7966-8553; *Ca*GSTI'2 = contig6-2235 bp6689-7485; *Nc*GST = *N.crassa* XP_325635; *Bj*GST = *B.japonicum* Q89WU3; *Bj*GSTR'1 = *B.japonicum* Q89WH2; *Bj*GSTR'2 = *B.japonicum* Q89WB2; *Bs*GST = *Brucella suis* AAN34211; *Xa*GST = *X.axonopodis* (pv. citri) Q8PMX6; RsGST = *Ralstonia solanacearum* Q8Y1T2.

6.2 Main conclusions

6.2.1 Herbicide and fungicide metabolism in wheat

Two routes of thiol mediated herbicide detoxification in wheat has been demonstrated through the identification of HmGSH conjugates of fenoxaprop-P-ethyl in addition to the more commonly determined glutathione conjugates. Involvement of HmGSH in xenobiotic detoxification in wheat has not been reported before, having potentially been overlooked resulting from the inability of equine liver GST to utilise HmGSH as a co-substrate (Klapheck *et al.*, 1992). However, GST catalysed conjugation of HmGSH to fenoxaprop-P-ethyl could not be concluded. In fact the ratio of GS- to HmGS-conjugates was such that it closely mirrored the relative abundance of the two thiols, which would be more consistent with non-enzymic conjugation. However this does not take into account the relative ratios of processing of the two tripeptide derivatives, which makes it impossible to judge the initial ratios of formation of the GSH and HmGSH derivatives. HmGSH conjugates of fenoxaprop-P-ethyl were not detected in herbicide resistant or susceptible black grass biotypes, indicating that HmGSH was not involved in the detoxification of fenoxaprop in black-grass despite HmGSH being present.

Enzymic processing of conjugated fenoxaprop was found to occur in both wheat and black grass with 4 catabolites being identified, initiated by phytochelatin synthase carboxypeptidase activity giving rise to the γ-glu-cys derivative. Wheat shoot metabolism of the GSH/HmGSH fenoxaprop conjugates by phytochelatin synthase was very rapid as compared with either black-grass biotype, with the Fe-γ-glu-cys derivative being the major metabolite derived from detoxification of this herbicide in wheat. In contrast, the GSH conjugate was the major metabolite identified in both black-grass biotypes.

Both wheat and black grass were capable of processing either the GSH and/or HmGSH conjugates of fenoxaprop-P-ethyl through to final highly polar, cysteinyl, glucosyl and malonyl derivatives. The cysteinyl conjugate underwent subsequent *N*-glycosylation of the cysteine residue amine, followed by malonylation of the sugar group. The identification of HmGSH conjugates along with *N*-glucosyl and malonyl conjugated catabolites has extended the known route of detoxification of fenoxaprop-P-ethyl in both wheat and black-grass.

Conversely, wheat GST mediated conjugation of the fungicide fluquinconazole to GSH did not occur either *in vitro* or *in vivo* in wheat. The slow rate of conjugation of GSH to fluquinconazole *in vitro* was brought about by spontaneous chemical substitution of the triazole moiety with GSH, which was elevated in the presence of non-catalytic protein and negligible spontaneous conjugation of this fungicide to GSH occurred *in vivo*. Thus it was concluded, that conjugation of fluquinconazole to GSH was not a route of fungicide detoxification in wheat. Similarly, conjugation of zoxamide, quinoxyfen, cyazofamid and chorothalinil to GSH was not mediated by wheat GSTs, even though it was possible to synthesise glutathione conjugates of these fungicides chemically at non-physiological pH.

6.2.2 GSTs cloned from the phytopathogens *Magnaporthe grisea* and *Phytophthora infestans*.

Purified recombinant Xi class GST, *Mg*GSTX1-1, cloned from the fungal pathogen *Magnaporthe grisea* functioned as a glutaredoxin, with the recombinant homo-dimeric protein being capable of reducing the mixed disulphide of glutathione and hydroxyethyl disulphide. Thioltransferase activity was dependent on the presence of a mixed disulphide bond between cysteines 175 and 185 and the amino

acid sequence did not contain the catalytic motif -Cys-Pro-Tyr-Cys, common to glutaredoxins. The catalytic residues involved in the reduction of mixed disulphides in this recombinant protein are unknown and as such represent a novel mechanism for thiol transfer among enzymes with glutaredoxin activity. Of the xenobiotic and pesticide substrates tested *Mg*GSTX1-1 did not display glutathione conjugating catalytic activity and does not directly detoxify pesticides through conjugation to GSH.

Taken together the cloning, expression and biochemical characterisation of theta class *Pi*GSTT1 GST from *P. infestans* represents the first such work undertaken on a phytopathogenic oomycete. The purified recombinant polypeptide forms a homo-dimeric protein capable of detoxifing organic hydroperoxides through GSH dependent reduction to their corresponding alcohols. Recombinant *Pi*GSTT1-1 readily detoxifies the fungitoxic oxylipin 9(*S*)-HPOT biosynthesised from arachidonic by potato lipoxygenase in response to infection, with the endogenous protein of *P. infestans* being expressed constitutively both *in vitro* and *in planta* during host plant colonisation. Thus it was concluded that activity of this enzyme offered *P. infestans* a major protective role in detoxification of fungitoxic oxylipins during the infection process.

6.3 Future areas of investigation

6.3.1 Metabolism of fenoxaprop-P-ethyl in wheat

The identification of fenoxaprop-P-ethyl conjugated with HmGSH in wheat has demonstrated an alternative thiol mediated route of detoxification of this herbicide, runs parallel with GSH conjugation in wheat. The relative importance of the parallel HmGSH route of fenoxaprop-P-ethyl detoxification in this major crop needs to be

addressed, along with the identification of wheat GSTs capable of using HmGSH as a co-substrate for conjugation to herbicide. Cloning and expression of recombinant HmGSH synthetase from wheat would facilitate *in vitro* synthesis of HmGSH to be tested for use as a substrate by wheat GSTs. Comparative analysis of both pure recombinant and crude wheat GSTs with HmGSH and GSH as co-substrates, should enable the relative merit of each thiol for *in vitro* conjugation to fenoxaprop to be determined. Additionally, synthesis of authentic HmGSH conjugates of fenoxaprop would facilitate quantification of both conjugates formed in wheat as would the biochemical synthesis of the *N*-glucosyl and *N*-glucosyl-malonyl derivatives.

Further *in vivo* metabolism studies of chlorinated herbicides in wheat analysed by LC-MS, should enable a more complete biochemical pathway of pesticide metabolism in this major crop to be constructed. Additionally, from the derived metabolite knowledge, substrates could be synthesised aiding the purification of the respective enzymes and subsequent cloning from the deduced nucleic acid sequence via proteomic techniques.

6.3.2 *Mg*GSTX1

Due to the novel glutaredoxin mechanism of thiol transfer of *Mg*GSTX1, MALDI-TOF tryptic digest of this protein following with treatment with NEM would confirm which cysteine residue became alkylated. It would be interesting to crystallise the recombinant Xi class GST polypeptide of *Magnaporthe grisea* to compare active site folds with those of beta class GSTs and the Ure2P prion like proteins, thereby establishing any conservation at the tertiary level. Identification of the active site of this GST may provide clues to possible function and relationship to other GST classes.

6.3.3 *Pi*GSTT1

Generation of RNAi *PiGSTT1* mutants of *Phytophthora infestans* should help determine the extent of protection afforded to this phytopathogen by *Pi*GSTT1-1 during the infection process. In addition such lines may establish whether *Pi*GSTT1-1 has a protective role in *P. infestans* on exposure to the DCOFs such as vinclozolin through stabilizing lipid membranes under oxidative stress. Over expressing lines may provide an indication whether gene duplication of *PiGSTT1* would facilitate tolerance toward multiple fungicides. In this respect, questions regarding the forced evolution of fungicide tolerance from fungicide exposure may be addressed and control measures for this major agronomic disease be improved.

Literature cited

Allocati N., Favaloro B., Masulli M., Tamburro A., Rotilio D. and Di Ilio C. (2001) *In vivo* effect of xenobiotics compounds on the *Proteus mirabilis* glutathione transferase B1-1. *Chemico-Biological Interactions* **133**: 261-264.

Anders M.W., Anderson W.B., Tzeng H-F., and Board P.G. (2001) Glutathione transferase zeta; novel xenobiotic substrates and enzyme inactivation. *Chemico-Biological Interactions* **133**: 201-216.

Anderson M.P and Gronwald J.W. (1991) Atrazine resistance in a velvetleaf (*Abutilon-theophrasti*) biotype due to enhanced glutathione S-transferase activity. *Plant Physiology* **96**, (1):104-109.

Awasthi Sanjay., Cheng J., Singhal S.S., Zhao T., Saini M.K., Pandaya U., Clark-Wronski J., Ziminiak P. and Awasthi Y.C. (2001) Physiological substrates of Glutathione *S*-transferases. *Chemico-Biological Interactions* **133**: 217 – 223.

Azerad R (2000) Microbial models for drug metabolism. In *Biotransformations*. Ed. Faber K., Springer-Verlag, Berlin, Heidleberg, New York.

Baez S., Segura-Aguilar J., Widersten M., Johansson A.-S and Mannervik B. (1997) Glutathione transferases catalyse the detoxication of oxidized metabolites (*o*-quinones) of catecholamines and may serve as an antioxidant system preventing degenerative cellular processes. *Biochemical Journal* **324**: 25–28.

Bartsch H. (1996) DNA adducts in human carcinogenesis: etiologial relevance and structure–activity relationship. *Mutation Research* **340**: 67–79.

Beck A., Ledzian L., Oven M., Christmann A. and Grill E., (2003) Phytochelatin synthase catalyses key step in the turnover of glutathione conjugates. *Phytochemistry* **62**: 423-431.

Beyer K., Binder A., Boller T. and Collinge M. (2001) Identification of potato genes induced during colonization by *Phytophthora infestans*. *Molecular Plant Pathology* **2,** (3): 125-134.

Blée E. (1998) Phytooxylipins and plant defense reactions. *Progress in Lipid Research* **37,** (1): 33-72.

Blinder D., Coschigano P. and Magasanik B. (1996) Interaction of the GATA factor Gln3p with the nitrogen regulator Ure2p in *Saccharomyces cerevisiae*. *Journal of Bacteriology* **178**: 4734–4736.

Blocki F.A., Logan M.S., Baoli C. and Wackett L.P. (1994) Reaction of rat liver glutathione *S*-transferases and bacterial dichloromethane dehalogenase with dihalomethanes. *Journal of Biological Chemistry* **269**: 8826-30.

Board P.G., Coggan M., Chelvanayagam G., Easteal S., Jermiin L.S., Schulte G.K., Danley D.E., Hoth L.R., Griffor M.C., Kamath A.V., Rosner M.H., Chrunyk B. A., Perregaux D.E., Gabel C.A., Geoghhegan K.F. and Pandit J. (2000) Identification, characterization, and crystal structure of the Omega class glutathione transferases. *Journal of Biological Chemistry* **275**: 24798-24806.

Board P.G., Coggan. M., Chelvanayagam G., Eastal S., Jermiin L.S., Schulte G.K., Danley D.E., Hoth L.R., Griffir M.C., Kamath A.V., Rosner M.H., Chrunyk B.A., Perregaux D.E., Gabel C.A., Geoghegan K.F., and Pandit J. (2001) Characterisation of the Omega class glutathione transferases. *Chemico-Biological Interactions* **133**: 204 – 206.

Bousset L., Belrhali H., Janin J., Melki R., and Morera S. (2001) Structure of the globular region of the prion protein Ure2 from the yeast *Saccharomyces cerevisiae*. *Structure* **9**: 39-46.

Briggs G. (2001) Aventis crop science, Lyon, France. *Personal communication.*

Burnett J.H. (1987) In: Evolutionary biology of the fungi. (A.D.M Rayner, C.M. Brasier and D. Moore, eds.) p1. Cambridge University Press, Cambridge.

Caccuri A.M., Giovanni A., Board P.G., Porker M.W., Nicotara M., Lo Bello M., Fedrici G. and Ricci G. (1999) Proton release on binding of glutathione to alpha, mu, pi and delta class glutathione transferases. *Biochemical Journal* **344**: 419-425.

Campbell A.M., Teesdale-spittle P.H., Barrett J., Liebau., Jefferies J.R. and Brophy P.M. (2002) A common class of nematode glutathione *S*–transferase (GST) revealed by the theoretical proteome of the model organism *Caenorhabditis elegans*. *Comparative Biochemistry and Physiology part B* **128**: 701 – 708.

Carlile M.J., Watkinson S.C. and Gooday G.W. (2001) The fungi. Second edition. Academic Press. London.

Castoria R., Fanelli C., Fabbri A.A. and Passi S. (1992) Metabolism of arachidonic acid involved in its eliciting activity in potato tuber. *Physiological and Molecular Plant Pathology* **41**: 127–137.

Cha C.J., Kim S., Stingley R. and Cerlniglia C.E. (2002) Molecular clonining, expression and characterisation of a novel class glutathione *S*-transferase from the fungus *Cunninghamella elegans*. *Biochemical Journal*. **368**: 589 – 595.

Chelvanayagam G., Parker M.W., and Board P.G. (2001) Fly fishing for GSTs: a unified nomenclature for mammalian and insect glutathione transferases. *Chemico-Biological Interactions* **133**: 256 – 260.

Chen W. and Singh K.B. (1999)The auxin, hydrogen peroxide and salicylic acid induced expression of the Arabidopsis GST6 promoter is mediated in part by an ocs element. *Plant Journal* **19**: 667-677.

Choi J.H., Lou W., and Vancura A. (1998) A novel membrane bound glutathione *S*-transferase functions in the stationary phase of the yeast *Saccharomyces cerevisiae*. *The Journal of Biological Chemistry* **273**, (45): 29915 – 29922.

Cohen E., Gamliel A. and Katan J. (1986) Glutathione and glutathione *S*-transferase in fungi: effect of pentachloronitrobenzene and 1-chloro-2,4-dinitrobenzene; Purification and characterisation of the transferase from *Fusarium*. *Pesticide Biochemistry and Physiology* **26**: 1-9.

Cole D. and Edwards R. (2000) Secondary metabolism of agrochemicals in plants. In *Metabolism of agrochemicals in plants*. Ed. Roberts T. John Wiley and sons.

Coleman J.O.D., Mechteeld M.A., Blake-Kaliff. and Emyr Davies T.G. (1997). Detoxification of xenobiotics by plants: chemical modification and vacuolar compartmentation. *Trends in Plant Science* **2** (4): 144-151.

Coshigano P.M. and Magasanik B. (1991). The URE2 gene product of *Saccharomyces cereviseae* plays an important role in the cellular response to the nitrogen source and has homology to glutathione *S*-transferases. *Molecular and Cellular Biology* **11**, (2): 822 – 832.

Cummins I., Cole D.J. and Edwards R. (1999) A role for glutathione transferases functioning as glutathione peroxidases in resistance to multiple herbicides in black-grass. *The Plant Journal* **18** (3): 285-292.

Cummins I., Cole D.J., and Edwards R., (1997) Purification of multiple glutathione transferases involved in herbicide detoxification from wheat (*Triticum aestivum* L.) treated with the safener fenchlorazole-ethyl. *Pesticide Biochemistry and Physiology* **59**: 35-49.

Datta J. and Samanta T.B. (1992). Characterisation of a novel microsomal glutathione *S*-transferase produced by *Aspergillus ochraceus* TS. *Molecular and Cellular Biochemistry* **118**: 31-38.

Datta J., Dutta T.K and Samanta T.B. (1994) Microsomal glutathione *S*-transferase (GST) isozymes in *Aspergillus ochraceus* TS: induction by 3 methyl-cholanthrene. *Biochemical and Biophysical Research Communications* **203**, (3): 1508-1514.

Davies J. and Caseley J.C. (1999) Herbicide safeners: a review. *Pesticide Science.* **55**:1043-1058.

Dean J.V. and Devarenne TP (1997) Peroxidase-mediated conjugation of glutathione to unsaturated phenylpropanoids. Evidence against glutathione *S*-transferase involvement. *Physiologia Plantarum* **99** (2): 271-278.

Detlef D., Yuri L., Eugene I. W., Koonin V. and Aravind L. (2002) Classification and Evolution of P-loop GTPases and Related ATPases *Journal of Molecular Biology* **317**, (1): 41-72.

Di Ilio C., Aceto A., Allocati N., Piccolomini R., Bucciarelli T., Dragani B., Faraone A., Sacchetta P., Petruzzelli R. and Federici G. (1993) Characterisation of glutathione *S*-transferase from *Xanthamonas campestris*. *Archives of Biochemistry and Biophysics* **305**, (1): 110-114.

Dixon D.P., Cole D.J. and Edwards R. (1999) Dimerisation of maize glutathione transferases in recombinant bacteria. *Plant Molecular Biology* **40**: 997 –1008.

Dixon D.P., Cole D.J. and Edwards R. (2001) Probing plant GST activity using heterodimers and domain swapping. *Chemico-Biological interactions* **133**: 37 – 39.

Dixon D.P., Cole D.J., and Edwards R. (2001) Cloning and characterisation of plant theta and zeta class GSTs: Implications for plant GST classification. *Chemico-Biological Interactions* **133**: 33 – 36.

Dixon D.P., Lapthorn A. and Edwards R. (2002) Plant glutathione transferases. *Genome Biology* **3**, (3): reviews 3004.1 – 3004.10.

Dixon D.P., Davis B.G. Edwards R. (2002) Functional divergence in the glutathione transferase superfamily in plants - Identification of two classes with putative functions in redox homeostasis in *Arabidopsis thaliana. Journal of Biological Chemistry* **277**, (34): 30859 – 30869.

Dorobek F. and Lyr H. (1987) Determination of unsaturated fatty acid levels in mitochondria from various fungal species with lipoxygenase. *Tagungsber. Akad. Landwirtschaftswiss. DDR.* 253, 345.

Dowd C.A and Sheehan D. (1993) Purification of glutathione *S*-transferase from the fungus *Alternaria alternata. Biochemical Society Transactions* **22**: 58S.

Dowd C.A., Buckley C.M. and Sheehan D. (1997) Glutathione *S*-transferases from the white rot fungus *Phanerochaete chryosprium. Biochemical Journal* **324**: 243-248.

Droog F. (1997) Plant glutathione *S*-transferases, a tale of theta and tau. *Journal of Plant Growth Regulation* **16**: 95 – 107.

Drotar A-M. and Fall R. (1985) *Experientia* **41**: 762-764.

Dutton G. (1978) Phase II metabolic reactions in man. In *Drug metabolism in man.* Ed. Gorrod J.W. and Beckett A.H.Taylor and Francis (printers) Ltd.

Edlich W. and Lyr H. (1992) Target sites of fungicides with primary effects on lipid peroxidation. In *Target sites of fungicide action.* Ed Koller. 69-100. 54-68.

Edlich W. and Lyr H. (1987) Mechanism of action of dicarboxamide fungicides, in Modern *selective fungicides – Properties, application and mechanism of action*, Lyr H., Ed., Gustav Fischer Verlag, Jena, 107.

Edwards R, and Dixon R.A. (1991) Glutathione *S*-cinnamoyl transferases in plants. *Phytochemistry*. **30** (1): 79-84.

Edwards R. and Cole D., (1996) Glutathione transferases in wheat (*Triticum*) species with activity toward fenoxaprop-ethyl and other herbicides. *Pesticide Biochemistry and Physiology* **54**: 96-104.

Edwards R. (1996) Characterisation of Glutathione transferases and glutathione peroxidases in pea (*Pisum sativum*). *Physiologia Plantarum* **98**: 594-604.

Edwards R. (1999) Department of Biological and Biomedical Sciences, University of Durham, Durham, DH1 3LE, UK. *Personal communication*.

Edwards R., Andrews C.J. and Jepson I. (2001) Engineering herbicide tolerance with glutathione transferases. *In:* Agrochemical discovery; insect, wood and fungal control (Eds D. R. Baker and N. K. Umetsu) *American Chemical Society Symposium* Series No 774. ACS, Washington, USA pp. 133-141.

Edwards R., Dixon D.P. and Walbot V. (2000) Plant glutathione S-transferases: enzymes with multiple functions in sickness and in health. *Trends in Plant Science* **5**, (5): 193-198.

Eulgem T., Rushton PJ., Schmelzer E., Hahlbrock K. (1999) Early nuclear events in plant defence signalling: rapid gene activation by WRKY transcription factors. *EMBO Journal* **18**: 4689-99.

Felsenstein J. (1991-2002) SEQBOOT -- Bootstrap, Jackknife, or Permutation Resampling of Molecular Sequence, Restriction Site, Gene Frequency or Character Data. *University of Washington*.

Felsenstein J. (1985) Confidence limits on phylogenies: an approach using the bootstrap. *Evolution* **39**: 783-791.

Fernández-Cañón J.M. and Peñalva M.A. (1998) Charcterization of a fungal maleylacetoacetate isomerase gene and identification of its human homologue. *Journal of Biological Chemistry* **273**: 329–337.

Fraser J.A., Davis M.A. and Hynes M.J. (2002) A gene from *Aspergillus nidulans* with similarity to URE2 of *Saccharomyces cerevisiae* encodes a glutathione *S*-transferase which contributes to heavy metal and xenobiotic resistance. *Applied and Environmental Microbiology* **68**, (6): 2802 – 2808.

Frear D. S. and Swanson H. R. (1970) Biosynthesis of *S*-(4-ethylamino-6-isopropylamino- 2-*s*-triazino) glutathione: Partial purification and properties of a glutathione *S*-transferase from corn. *Phytochemistry* **9**, (10): 2123-2132.

Galliard T. and Matthew J.A. (1975) Enzymic reactions of fatty acid hydroperoxides in extracts of potato tuber. I. Comparison of 9D- and 13L-hydroperoxy-octadecadienoic acids as substrates for the formation of a divinyl ether derivative. *Biochimica et Biophysica Acta* **398**:1-9.

Gardner H.W. (1991) Recent investigations into the lipoxygenase pathway of plants. *Biochimica et Biophysica Acta* **1084**: 221-39

Grechkin A. (1998) Recent developments in biochemistry of the plant lipoxygenase pathway. *Progress in Lipid Research* **37**:317-52.

Grechkin A.N., Kuramshin R.A., Safonova E.Y., Yefremov Y.J., Latypov S.K., Ilyasov A.V., and Tarchevsky I.A. (1991) Double hydroperoxidation of alpha-linolenic acid by potato tuber lipoxygenase. *Biochimica et Biophysica Acta.* **1081**:79-84.

Griffith J., Davis A.J., and Grant B.R. (1992)Target sites of fungicides to control oomycetes. in *Target sites of fungicide action*. Ed Koller. CRC Press Inc. 69-100.

Guex N. and Peitsch M.C. (1997) SWISS-MODEL and the Swiss-PdbViewer: An environment for comparative protein modeling. *Electrophoresis* **18**: 2714-2723.

Gurr S.J. and McPherson M.J. (1992) Nucleic acid isolation and hybridization techniques. In *Molecular plant pathology. Volume 1. A practical approach*. Ed. Gurr S.J., McPherson M.J. and Bowles D.J. Oxford University Press, New York.

Habig W.H., Pabst M.J. and Jakoby W.B. (1974). Glutathione *S*-transferases; The first enzymatic step in mercapturic acid formation. *The Journal of Biochemistry* **249**, (22): 7130 7139.

Hall C.J., Wickenden S. and Yau K.Y.F.M (2001). Biochemical conjugation of pesticides in plants and micro-organisms. An overview of similarities and divergences. In *Pesticide biotransformation in plants and micro organisms. Similarities and divergences*. Ed. Hall C.J., Hoagland R.E., and Zablotowicz R.M. American Chemical Society, Washington, DC.

Hall L. M., Mossand S. R. and Powles S. B. (1997) Mechanisms of Resistance to Aryloxyphenoxypropionate Herbicides in Two Resistant Biotypes of*Alopecurus myosuroides*(blackgrass): Herbicide Metabolism as a Cross-Resistance Mechanism. *Pesticide Biochemistry and Physiology* **57**, (2): 87-98

Hamid K., and Strange R.N. (2000) Phytotoxicity of solanopyrones A and B produced by the chickpea pathogen *Asochyta rabiei* (Pass.) *Labr.* and the

apparent metabolism of solanapyrone A by chickpea tissues. *Physiological and Molceular Plant Pathology* **56**: 235-244.

Hansson L O., Bolton-Grob R., Massoud T. and Mannervik B. (1999) Evolution of differential substrate specificities in Mu class glutathione transferases probed by DNA shuffling. *Journal of Molecular Biology* **287**, (2): 265-276.

Hatton P.J., Cole D.J. and Edwards R. (1996) Influence of plant age on glutathione levels and glutathione transferases involved in herbicide detoxification in corn (*Zea mays* L.) and giant foxtail (*Seratia faberi* Herrm). *Pesticide Biochemistry and Physiology* **54**: 199-209.

Hatton P.J., Cummins I., Cole D.J. and Edwards R. (1999) Glutathione transferases involved in herbicide detoxification in the leaves of *Seratia faberi* (giant foxtail). *Physiologia Plantarum* **105**: 9-16.

Hatton P.J., Cummins I., Price L.J., Cole D.J. and Edwards R. (1998) Glutathione transferases and herbicide detoxification in suspension cells of giant foxtail (*Seratia faberi*). *Pesticide Science* **53**: 209-216.

Hemingway J. (2000) The molecular basis of two contrasting metabolic mechanisms of insecticide resistance. *Insect Biochemistry and Molecular Biology* **30**: 1009–1015.

Hemingway J., Field L. and Vontas J. (2002) An Overview of Insecticide Resistance. *Science* **298**: 96-97.

Hemingway J., Miyamoto J., Herath P.R.J. (1991). A possible novel link between organophosphorus and DDT insecticide resistance genes in *Anopheles*: supporting evidence from fenitrothion metabolism studies. *Pesticide Biochemistry and Physiology* **39**, 49–56.

Henderson C. J., Smith A.G., Ure J., Brown K., E. Bacon J., and Wolf C. R. (1998) Increased skin tumorigenesis in mice lacking pi class glutathione *S*-transferases. *Proceedings of the National Acadamy of Sciences USA* **95**: 5275-5280.

Henderson C.J., McLaren A.W., Moffat G.J., Bacon E.J. and Wolf C.R. (2001) *Chemical-Biological Interactions* **111-112**: 69 – 82.

Hershey H.P and Stoner T.D. (1991) Isolation and characterization of cDNA clones for RNA species induced by substituted benzenesulfonamides in corn. *Plant Molecular Biology* **17**: 679-90.

Höög J.O., Jörnvall H., Holmgren A., Carlquist M. and Persson M. (1983) The primary structure of *Escherichia coli* glutaredoxin. Distant homology with thioredoxins in a superfamily of small proteins with a redox-active cystine disulfide/cysteine dithiol. *European Journal of Biochemistry* **136**: 223–232.

Howe G.A. and Schilmiller A.L. (2002) Oxylipin metabolism in response to stress. *Current Opinion in Plant Biology* **5**: 230-6.

Ingram D. S. (1981) In: *The downey mildews* (D.M. Spencer, ed.) p. 143, Academic Press, London.

Ji X.H., Vonrosenvinge E.C., Johnson W.W., Tomarev S.I., Piatigorsky J., Armstrong R.N. and Glliand G.L. (1995) Three-dimensional structure, catalytic properties, and evolution of a sigma class glutathione transferase from squid, a progenitor of the lens *S*-crystallins of cephalopods. *Biochemistry* **34**: 5317-5328.

Ji X.H., Zhang P.H., Armstrong R.N., and Gilliard G.L. (1992) The three-dimensional structure of a glutathione *S*-transferase from the mu gene class. Structural

analysis of the binary complex of isoenzyme 3-3 and glutathione at 2.2-A resolution. *Biochemistry* **31**: 5317-10184.

Jirajaroenrat K., Pongjaroenkit S., Krittanai C., Prapanthadara L., and Ketterman A.J. (2001) Heterologous expression and characterization of alternatively spliced glutathione *S*-transferases from a single *Anopheles* gene. *Insect Biochemistry and Molecular Biology* **31**: 867–875.

Jones D. T., W. R. Taylor and J. M. Thornton. (1992) The rapid generation of mutation data matrices from protein sequences. *Computer Applications in the Biosciences (CABIOS)* **8**: 275-282.

Judelson H. (1997). The genetics and biology of *Phytopthora infestans*: Modern approaches to a historical challenge. *Fungal Genetics and Biology* **22**: 65-76.

Kampranis S.C., Damianova R., Atallah M., Toby G., Kondi G., Tsichlis P.N. and Makris A.M. (2000) A novel plant glutathione S-transferase/peroxidase suppresses Bax lethality in yeast. *Journal of Biological Chemistry* **275**: 29207-16.

Kato T., Maeda Y., Hirukawa T., Namai T. and Yoshioka N. (1992) Lipoxygenase Activity Increment in Infected Tomato Leaves and Oxidation Product of Linolenic Acid by Its In Vitro Enzyme Reaction. *Bioscience Biotechnology and Biochemistry* **56**: 373-375.

Ketterer B. (2001) A birds eye view of the glutathione transferase field. *Chemico-Biological Interactions* **138**: 27–42.

Kim H-G., Park E-H. and Lim C-J. (1999). A second thioltransferase of *Schizosaccharomyces pombe* contains Glutathione *S*-transferase activity. *J. Biochemistry and Molecular Biology* **32**, (6): 535 – 540.

Kim H-G., Park K-N., Cho Y-W., Park E-H., Fuchs J.A. and Lim C-J (2001) Characterisation and regulation of glutathione *S*-transferase gene from *Schizosaccharomyces pombe*. *Biochimica et Biophysica Acta* **1520**: 179–185.

Klapheck S., Chrost B., Starke J. and Zimmermann H. (1992). Gamma-glutamylcysteinylserine – A new homologue of glutathione in plants of the family *Poaceae*. *Botanica Acta* **105**, (3): 174-179.

Klapheck S., Fliegner W. and Zimmer I. (1994) Hydroxymethyl-phytochelatins [γ-(glutamylcysteine)$_n$-serine] are metal-induced peptides of the Poaceae. *Plant Physiology* **104**:1325–1332.

Klein M., Martinoia E., Hoffmann-Thoma G. and Weissenbock G. A membrane dependent ABC like transporter mediates the vacuolar uptake of rye flavone glucuronides: regulation of glucuronide uptake by glutathione and its conjugates. *The Plant Journal* **21**, (3): 289-304.

Kolm R.H., Danielson U.H., Zhang Y., Talalay P. and Mannervik B. (1995) Isothiocyanates as substrates for human glutathione transferases: structure-activity studies. *Biochemical Journal* **311** (2):453-9.

Kreuz K., Tommasini R. and Martinoia E. (1996) Old enymes for a new job. Herbicide detoxification in plants. *Plant Physiology* **111**: 349-353.

Kumagai H., Tamaki H., Koshino Y., Suzuki H. and Tochikura T. (1988) Distribution, formation and stabilization of yeast glutathione *S*-transferase. *Agricultural and Biological Chemistry* **52**, (6): 1377-1382.

Laemmli U.K. (1970) Cleavage of structural proteins during the assembly of the head of bacteriophage T4. *Nature* **227**, (259): 680-5.

Landi S. (2000). Mammalian class theta GST and diferential susceptability to carcinogens: a review. *Mutation Research* **463**: 247 – 283.

Lebel E., Heifetz P., Thorne L., Uknes S., Ryals J. and Ward E (1998) Functional analysis of regulatory sequences controlling *PR-1* gene expression in *Arabidopsis*. *Plant Journal* **16**: 223-233.

Lefsrud C. and Hall J.C. (1989) Basis for sensitivity differences among crab grass, oat, and wheat to fenoxaprop ethyl. *Pesticide Biochemistry and Physiology* **34**: 218-227.

Li Z.S., Alfennito M., Rea P. A., Walbott V. and Dixon R. (1997) Vacuolar uptake of the phytoalexin by the glutathione conjugate pump. *Phytochemistry* **45**, (4): 689-693.

Lyr H. (1987) Mechanism of action of aromatic hydrocarbon fungicides, in Modern *selective fungicides – Properties, application and mechanism of action*, Ed., Lyr H., Gustav Fischer Verlag, Jena, 75.

Margush T. and McMorris F. R. (1981) Consensus n-trees. *Bulletin of Mathematical Biology* **43**: 239-244.

Marrs K.A. (1996) The functions and regulation of glutathione *S*-transferses in plants. *Annual Review of Plant Physiology and Plant Molecular Biology* **47**: 127-58.

Martin M.N. and Slovin J.P. (2000) Purified gamma-glutamyl transpeptidases from tomato exhibit high affinity for glutathione and glutathione S-conjugates. *Plant Physiolology* **122**: 1417-26

Martini N., Egen M., Runtz I. and Strittmatter G. (1993) Promoter sequences of a potato pathogenesis-related gene mediate transcriptional activation selectively upon fungal infection. *Molecular and General Genetics* **236**: 179-186.

Matthies A., Walker F. and Buchenauer H. (1999) Interference of selected fungicides, plant growth retardants as well as piperonyl butoxide and 1-aminobenzotriazole in trichothecene production of *Fusarium graminearum* (strain 4528) *in vitro*. *Zeitschrift fur Pflanzenkrankheiten und Pflanzenschutz - Journal of Plant Diseases and Protection* **106,** (2): 198-212.

Mauch F. and Dudler R. (1993) Differential induction of distinct glutathione *S*-transferases of wheat by xenobiotics and by pathogen attack. *Plant Physiology* **102**: 1193-1201.

McGonigle B, Keeler SJ, Lau SM, Koeppe MK, O'Keefe DP (2000) A genomics approach to the comprehensive analysis of the glutathione *S*-transferase gene family in soybean and maize. *Plant Physiology* **124**:1105-20.

Mctigue M.A., Williams D.R., and Tainer J.A. (1995) Crystal Structures of a Schistosomal Drug and Vaccine Target: Glutathione *S*-Transferase from *Schistosoma japonica* and its Complex with the Leading Antischistomal Drug Praziquantel. *Journal of Molecular Biology* **246**: 21-27.

Mullis K., Faloona F., Scharf S., Saiki R., Horn G. and Erlich H. (1986) Specific enzymatic amplification of DNA *in vitro*: The polymerase chain reaction. *Cold Spring Harbour Symposium. Quant. Biol.* **51**: 263.

Mullis K.B. and Faloona F. (1987) Specific synthesis of DNA *in vitro* via a polymerase-catalyzed chain reaction. *Methods in Enzymology* **155**: 335.

Nehls U., Beguiristain T., Ditengou F., Lapeyrie F. and Martin F. (1998) The expression of a symbiosis regulated gene in eucalypt roots is regulated by auxins and hypaphorine, the tryptophan betaine of the ectomycorrhizal baisidomycete *Pisolithus tinctorius*. *Planta* **207**: 296-302.

Neuefeind T., Huber R., Reinemer P., Knablein J., Prade L., Mann K. and Bieseler B. (1997) Cloning, sequencing, crystallisation and X-ray structure of glutathione *Zea mays* var. *mutin:* A leading enzyme in detoxification of Maize herbicides. *Journal of Molecular Biology.* **274**: 577-587.

Newbold R.F. and Brookes P. (1976) Exceptional mutagenicity of a benzo[*a*]pyrene diolepoxide in cultured mammalian cells. *Nature* **261**, pp. 52–54.

Nichloas K.B. and Nicholas H.B. (1997) GeneDoc: A tool for editing and annotating multiple sequence alignments. *Distributed by author.* www.psc.edu/biomed/genedoc.

Niitsu Y., Takayama T., Miyanishi K., Nobuoka A., Hayashi T., Nakakima T., Miyake S., Henderson C.J. and Wolf R. (2001). Implication of GST-pi expression in colon carcinogenesis. *Chemico-Biological Interactions* **133**: 287 – 290.

Nishida M., Harada S., Noguchi S., Satow Y., Inoue H. and Takahashi K. (1998) Three-dimensional structure of *Escherichia coli* glutathione *S*-transferase complexed with glutathione sulfonate: catalytic roles of Cys10 and His106. *Journal of Molecular Biology* **281**: 135-147.

Nishida M., Harada S., Noguchi S., Satow Y., Inoue H., and Takashaki K. (1998) Three-dimensional structure of *Escherichia coli* glutathione *S*-transferase complexed with glutathione sulfonate: catalytic roles of Cys10 and His106. *Journal of Molecular Biology* **281**: 135-147.

O'Neil E. (2001) Aventis crop science, Lyon, France. *Personal communication.*

Oros G. and Komives T. (1991) Effects of phenylamide pesticides on the GSH-conjugation system of *Phytophthora* spp. Fungi. *Verlag der Zeitschrift fur Naturforschung* **46c**: 866-874.

Oros G., Ersek T. and Viranyi F. (1988) *Acta Phytopathol. Entomol.* Hung. **23**,: 11-19.

Pemble S.E., Wardle A.F. and Taylor J.B (1996) Glutathione S-transferase class Kappa: characterization by the cloning of rat mitochondrial GST and identification of a human homologue. *Biochemical Journal* **319**: 749–754.

Pemble S.E. and Taylor J.B. (1992) An evolutionary perspective on glutathione transferases inferred from class-theta glutathione transferase cDNA sequences. *Biochemical Journal* **287**: 957–963.

Pflugmacher S. and Sandermann H. (1998a) Cytochrome P450 mono-oxygenases for fatty acids and xenobiotics in marine macroalgae. *Plant Physiology* **117**: 123-128.

Pflugmacher S. and Sandermann H. (1998b) Taxanomic distribution of plant glucosyltransferases acting on xenobiotics. *Phytochemistry* **49**: 507-511.

Pflugmacher S., Schroder P. and Sandermann Jr. H. (2000). Taxanomic distribution of plant glutathione *S*-transferases acting on xenobiotics. *Phytochemistry* **54**: 267-273.

Prapanthadara L.A., Hemingway J., Ketterman, A.J. (1993) Partial Purification and Characterization of Glutathione *S*-Transferases Involved in DDT Resistance from the Mosquito *Anopheles gambiae. Pesticide Biochemistry and Physiology* **47**, (2): 119-133.

Prapanthadara, L., Ketterman, A.J., Hemingway, J., 1995. DDT-resistance in *Anopheles gambiae* Giles from Zanzibar Tanzania based on increased DDT-dehydrochlorinase activity of glutathione *S*-transferases. *Bulletin of Entomological Research* **85**: 267–274.

Prins T.W., Wagemakers L., Schouten A. and Van Kan J.A.L. (2000) Cloning and characterisation of a glutathione *S*-transferase from the plant pathogenic fungus *Botrytis cinerea*. *Molecular Plant Pathology* **1**, (3): 169-178.

Ramma R. (2002) Bayer crop science, Lyon, France. *Personal communication.*

Rance I., Fournier J. and Esquerre-Tugaye M-T. (1998) The incompatible interaction between *Phytophthora parasitica* Var. *nicotianae* race 0 and tobacco is suppressed in transgenic plants expressing antisense lipoxygenase sequences. *Proceedings of the National Academy of Sciences USA* **95**: 6554 – 6559.

Ranson H., Collins F. and Hemmingway J. (1998) The role of alternative mRNA splicing in generating heterogeneity within *Anopheles gambia* class I glutathione trasnferase family. *Proceedings of the National Academy of Sciences USA* **95**: 14284 – 14289.

Rea P.A., Li Z.S., Lu Y.P. and Drozdowicz (1998) From vacuolar GS-X pumps to multispecific ABC transporters. *Annual Reviews of Plant Molecular Biology* **49**: 727-60.

Reade P.H. and Cobb A.H. Purification. (1999). Characterisation and comparison of glutathione *S*-transferase from black-grass (*Alopecurus myosuroides* Huds) biotypes. *Pesticide Science* **55**: 993-999.

Reichers D.E., Yang K., Irzyk G.P., Jones S.S. and Fuerst P. (1996) Variability of glutathione *S*-transferase levels and dimthenamid tolerance in safener treated wheat and wheat relatives. *Pesticide Biochemistry and Physiology* **56**: 88-101.

Reinemer P., Dirr H.W., Ladenstein R., Schaffer J., Gallay O. and Huber R. (1991) The three-dimensional structure of class pi glutathione *S*-transferase in

complex with glutathione sulfonate at 2.3 A resolution. *EMBO Journal* **10**: 10997-2005.

Reinemer P., Prade L., Hof P., Neufeind T., Huber R., Zettl R., Palme K., Schell J., Koelln I., Bartunik H.D. and Bieseler B. (1996) Three-dimensional Structure of Glutathione *S*-transferase from *Arabidopsis thaliana* at 2.2 Å Resolution: Structural Characterization of Herbicide-conjugating Plant Glutathione *S*-transferases and a Novel Active Site Architecture. *Journal of Molecular Biol*ogy **225**: 289-309.

Ricker K.E. and Bostock R.M. (1992) Evidence for release of the elicitor arachidonic acid and its metabolites from sporangia of *Phytophthora infestans* during infection of potato. *Physiological and Molecular Plant Pathology* **41**: 61–72.

Roberts T. and Huston D.H (1998) Metabolic pathways of agrochemicals. Part 1: Herbicides and plant growth regulators. The Royal Society of Chemistry, Cambridge.

Roberts T. and Huston D.H (1999) Metabolic pathways of agrochemicals. Part 2: Fungicides and insecticides. The Royal Society of Chemistry, Cambridge.

Romano M.L., Stephenson G.R., Tal A. and Hall C.J. (1993). The effect of monooxygenase and glutathione *S*-transferase inhibitors of diclofop-methyl and fenoxaprop-ethyl in barley and wheat. *Pesticide Biochemistry and Physiology* **46**:181-189.

Rossjohn J., Polekhina G., Feil S.C., Allocati N., Masulli M., De Illio C. and Parker M.W., (1998) A mixed disulfide bond in bacterial glutathione transferase: functional and evolutionary implications. *Structure* **6**: 721-734.

Rossjohn J., McKinstry W.J., Oakley A.J., Verger D., Flanagan J., Chelvanayagam G., Tan K.L, Board P.G. and Parker M.W. (1998) Human theta class

glutathione transferase: the crystal structure reveals a sulfate-binding pocket within a buried active site. *Structure* **6**: 309-322.

Rushmore T.H., King R.G., Paulson K.E. and Pickett C.B. (1990) Regulation of glutathione *S*-transferase Ya subunit gene exprsseion: identification of a unique xenobiotic responsive elament controlling inducible expression by planar aromatic compounds. *Proceedings of the National Academy of Sciences USA* **87**: 3826-3830.

Rushmore T.H., Morton M.R. and Pickett C.B. (1991) The antioxidant responsive element. Activation by oxidative stress and identification of the DNA consensus sequence required for functional activity. *Journal of Biological Chemistry* **266**: 11632-11639.

Sambrook J., Fritsch E.F. and Maniatis T. (1989) Molecular cloning a laboratory manual. 2nd edition. Cold Spring Harbour Laboratory Press, USA.

Sandermann H. Jr. (1992) Plant metabolism of xenobiotics. *Trends in Biochemical Science* **17**: 82-84.

Sansome E.R. (1987) In: *Evolutionary biology of the fungi.* Eds. A.D.M Rayner, C.M. Brasier and D. Moore. p97. Cambridge University Press, Cambridge.

Schnabel G. and Parisi L. (1997) Sensitivity of *Venturia inaequalis* to five DMI fungicides, including the new triazole fluquinconazole and to pyrimenthanil. *Zeitschrift fur Pflanzenkrankheiten und Pflanzenschutz* **104**, (1): 36-46.

Schroder P., and Stampfl A. (1999). Visualisation of glutathione conjugation and the inducibility of glutahione *S*-transferases in onion (*Allium cepa* L.) epidermal tissue. *Zeitschrift Naturforsch* **54c**: 1033-1041.

Segura-Aguilar J., Baez S., Widersten M., Welch C. and Mannervik B. (1997) Human class mu glutathione transferases, in particular isoenzyme M2-2,

catalyze detoxification of the dopamine metabolite aminochrome. *Journal of Biological Chemistry* **272**: 5727–5731.

Sheehan D. and Casey J.P. (1992) Microbial glutathione *S*-transferases. *Comparative Biochemistry and Physiology* **104B**, (1): 1-6.

Sheehan D., Meade G., Foley V.M. and Dowd A. (2001) Structure, function and evolution of glutathione transferases: Implications for classification of non-mammalian members of an ancient enzyme super family. *Biochemical Journal* **360**: 1-16.

Shimuzu T., Hashimoto N., Nakayama I., Nakao T., Mizutani H., Unai T., Yamaguchi M. and Abe H. (1995) A novel isourazole herbicide, fluthiacet-methyl, is a potent inhibitor of protophyrinogen oxidase after isomerization by glutathione *S*-transferase. *Plant Cell Physiology* **36**: 625-32.

Shin Y.H., Park E.H., Fuchs J.A., Lim C.J. (2002) Characterization, expression and regulation of a third gene encoding glutathione S-transferase from the fission yeast. *Biochimica et Biophysica Acta* **1577**:164-70.

Singh K.B., Foley R.C. and Oñate-Sánchez L. (2002) Transcription factors in plant defense and stress responses. *Current Opinion in Plant Biology* **5**:430–436.

Sinning I., Kleywegt G.T., Cowan S.W., Reinmer P., Dirr H.W., Huber R., Gillilan G.L., Armstromg R.N., Ji. X.H., Board P.G., Olin B., Mannervik B., and Jones T.A. (1993) Structure determination and refinement of human alpha class glutathione transferase A1-1, and a comparison with the mu and pi class enzymes. *Journal of Molecular Biology* **232**: 192-212.

Skipsey M. (2000) Department of Biological and Biomedical Sciences, University of Durham, Durham, DH1 3EA, UK. *Personal communication.*

Skipsey M., Andrews C.J., Townson J.K., Jepson I. and Edwards R. (1997) Substrate and thiol specificity of a stress-inducible glutathione transferase from soybean. *FEBS Letters*. **409**, (3): 370-374.

Smith A.D. (2000) Oxford dictionary of biochemistry and molecular biology. Oxford University Press Inc. New york.

Snyder M.J. and Maddison D.R. (1997) Molecular Phylogeny of Glutathione S-Transferases. *DNA and Cell Biology* **16**, (11): 1373-1384.

Steyn P.S. and Stander M.A . (1999) Mycotoxins as causal factors of diseases in humans. *Journal of Toxicology-Toxin reviews* **18** (3-4): 229-243.

Syvanen M., Zhou Z., Wharton J., Goldsbury C. and Clark A.G. (1996) Heterogeneity of the glutathione transferase genes encoding enzymes responsible for insecticide degradation in the housefly. *Journal of Molecular Evolution* **43**: 236–240.

Tal A., Romano L., Stephenson G.R., Schwann A.L. and Hall J.C. (1993) Glutathione conjugation: A detoxification pathway for fenoxprop-ethyl in barley, crabgrass, oat and wheat. *Pesticide Biochemistry and Physiology* **46**: 190-199.

Talbot N.J. (2003) On the trail of a cereal killer: Exploring the Biology of *Magnaporthe grisea*. *Annual Review of Microbiology* **57**: 177-202.

Talbot NJ (1995) Having a blast: exploring the pathogenicity of *Magnaporthe grisea*. *Trends Microbiology* **3**: 9-16.

Tamaki H., Kumagai H. and Tochikura T. (1991) Nucleotide sequence of the yeast glutathione *S*-transferase cDNA. *Biochimica et Biophysica Acta* **1089**: 276-279.

Tamaki H., Yamamoto K. and Hidehiko K. (1999) Expression of two glutathione *S*-transferase genes in the yeast *Issatchenkia orientalis* is induced by *o*-dinitrobenzene during cell growth arrest. *Journal of Bacteriology* **181**, (9): 2958-2962.

Tamaki H, Kumagai H and Tochikura T (1989) Purification and properties of glutathione transferase from *Issatchenkia orientalis*. *Journal of Bacteriology* **171**:1173-7.

Tamaki, H, Kumagai, H, Shimada, Y, Kashima, T, Obata, H, (1991) Detoxification and metabolism of o-Dinitrobenzene by the yeast *Issatchenkia orientalis* *Agricultural and Biological Chemistry* **55**, (4): 951-956.

Taylor J.L., Fritzemeier K-H., Hauser I., Kombrink E., Rohwer F., Schroder M., Strittmatter G. and Hahlbrock K. (1990) Structural analysis and activation by fungal infection of a gene encoding a pathogenesis-related protein in potato. *Molecular Plant-Microbe Interactions* **2**: 72-77.

Theodoulou F.L. (2000) Plant ABC transporters. *Biochimica et Biophysica Acta.* **1465**: 79-83.

Thom R., Cummins I., Dixon D.P., Edwards R., Cole D.J., and Lapthorn A.J. (2002) Structure of a tau class glutathione *S*-transferase from wheat active in herbicide detoxification. *Biochemistry* **41**: 7008-7020.

Thom R., Dixon D.P., Edwards R., Cole D.J. and lapthorn L.J. (2001) The structure of a zeta class glutathione *S*-transferase from *Arabidopsis thaliana*: characterisation of a GST with novel active-site architecture and a putative role in tyrosine catabolism. *Journal of Molecular Biology* **308**: 949-962.

Thompson, J.D., Higgins, D.G. and Gibson, T.J. (1994) CLUSTAL W: improving the sensitivity of progressive multiple sequence alignment through sequence

weighting, positions-specific gap penalties and weight matrix choice. *Nucleic Acids Research* **22**: 4673-4680.

Thomson A.M., Meyer D.J. and Hayes J.D. (1998) Sequence catalytic properties and expression of chicken glutathione dependent prostaglandin D2 synthase, a novel class sigma glutathione *S*-transferase. *Biochemical Journal* **333**: 317–325.

Tolstikov V.V. and Fiehn O. (2002) Analysis of highly polar compounds of plant origin: Combination of hydrophilic interaction chromatography and electrospray ion trap mass spectrometry. *Analytical Biochemistry* **301**: 298-307.

Tommasini R., Vogt E., Fromenteau M., Hörtensteiner S., Matile P., Amrhein N. and Martinoia E. (1998) An ABC-transporter of *Arabidopsis thaliana* has both glutathione-conjugate and chlorophyll catabolite transport activity. *Plant Journal.* **13**:773-80.

Tommasini R., Vogt E., Schmid J., Fromentau M., Amrhein N., Martinoia E. (1997) Differential expression of genes coding for ABC transporters after treatment of *Arabidopsis thaliana* with xenobiotics. *FEBS Letters* **411**: 206-10.

Ueno Y., Yabe T., Hashimoto H., Sekijama M., Masuda T., Kim D.J., Hasegawa R. and Ito N. (1992) Enhancement of GST-P-Positive liver-cell foci development by nivalenol, a trichothecene mycotoxin. *Carcinogenesis* **13**, (5): 787-791.

Van Bladeren P.J. (2001) Glutathione conjugation as a bioactivation reaction. *Chemico-Biological Reactions* **133**: 61-76.

Van der Zaal E.J., Droog F.N., Boot C.J., Hensgens L.A., Hoge J.H., Schilperoort R.A., and Libbenga K.R. (1991). Promoters of auxin-induced

genes from tobacco can lead to auxin-inducible and root tip-specific expression. *Plant Molecular Biology* **16**: 983-98

Verneghi A., Einhorn J., Kunesch G., Malosse C., Raiandrasoa F. and Ravise A. (1985) *Canadian Journal of Botany* **64**: 973 – 982.

Vick B.A. (1993) in *Lipid metabolism in plants*, ed. T.S. Moore. CRC Press, Boca Raton, Ann Arbor, London, Tokyo, pp167-191.

Vontas J.G., Small G.J and Hemmingway J. (2001) Glutathione *S*-transferases as antioxidant defence agents confer pyrethroid resistance in *Nilaparvata lugens* *Biochemical Journal* **357**: 65-72.

Wackett L.P. and Gibson D.T. (1982) Metabolism of xenobiotic compounds by enzymes in the cell extracts of the fungus *Cunninghamella elegans*. *Archives of Biochemistry and Biophysics* **186**: 121-127.

Wagner U, Edwards R, Dixon DP, Mauch F (2002) Probing the diversity of the *Arabidopsis* glutathione *S*-transferase gene family. *Plant Molecular Biology* **49**: 515-32.

Walczak H.A. and Dean J.V. (2000) Vacuolar transport of the glutathione conjugate of trans-cinnamic acid. *Phytochemistry* **53**, (4): 441-446.

Wassef M.K. (1977) Fungal lipids. *Advances in Lipid Research*. **15**: 159-232.

Weber H., Chételat A., Caldelari D. and Farmer E.E. (1999) Divinyl ether fatty acid synthesis in late blight-diseased potato leaves. *Plant Cell* **11**: 485-94.

Wei SH, Clark AG, Syvanen M, (2001) Identification and cloning of a key insecticide-metabolizing glutathione *S*-transferase (MdGST-6A) from a hyper insecticide-resistant strain of the housefly *Musca domestica*. *Insect Biochemistry and Molecular Biology* **31**:1145-53.

Weichert H., Kolbe A., Kraus A., Wasternack C. and Feussner I. (2002) Metabolic profiling of oxylipins in germinating cucumber seedlings – lipoxygenase-dependent degradation of triacylglycerols and biosynthesis of volatile aldehydes. *Planta* **215**: 612-9.

Wells W.W., Xu D.P., Yang Y. and Rocque P.A., (1990) Mammalian thioltransferase (glutaredoxin) and protein disulpihide isomerase have dehydroascorbate reductase activity. *Journal of Biological Chemistry* **265**: 15361 – 15364.

Wilce M.C.J., Board P.G., Feil S.C. and Parker M.W. (1995) Crystal structure of a theta-class glutathione transferase. *EMBO Journal* **14**, 2133-2143.

Wolf A.E., Dietz K.J. and Schroder P. (1996) Degradation of glutathione *S*-conjugates by a carboxypeptidase in the plant vacuole. *FEBS letters* **384**: 31-34.

Wolf C.R., Park K.B., Kitteringham N., Otto D. and Henderson C.H. (2001) Functional and genetic analysis of glutathione *S*-transferase π. *Chemico-Biological Interactions* **133**: 280 – 284.

Yoder O.C., Turgeon B.G. (2001) Fungal genomics and pathogenicity. Current Opinion in Plant Biology **4**, (4): 315-21.

Yu M., and Facchini P.J. (2000) Molecular cloning and characterisation of a type III glutathione *S*-transferase from cell suspension cultures of opium poppy treated with a fungal elicitor. *Physiologia Plantarum* **108**: 101-109.

Zeigler, R.S., S.A. Leong, and P.S. Teng, (1994). Rice Blast Disease. In *Rice Blast Disease*, pp. 1-626. Cab International, Wallingford

Zhang D., Yang Y., Leaky J.E.A. and Cerniglia C.E. (1996) Phase I and Phase II enzymes produced by *Cunninghamella elegans* for the metabolism of xenobiotics. *FEMS Microbiological letters* **138**: 221-226.

Zhou Z.H. and Syvanen M. (1997) A complex glutathione transferase gene family in the housefly *Musca domestica*. *Molecular and General Genetics* **256**: 187 – 194.

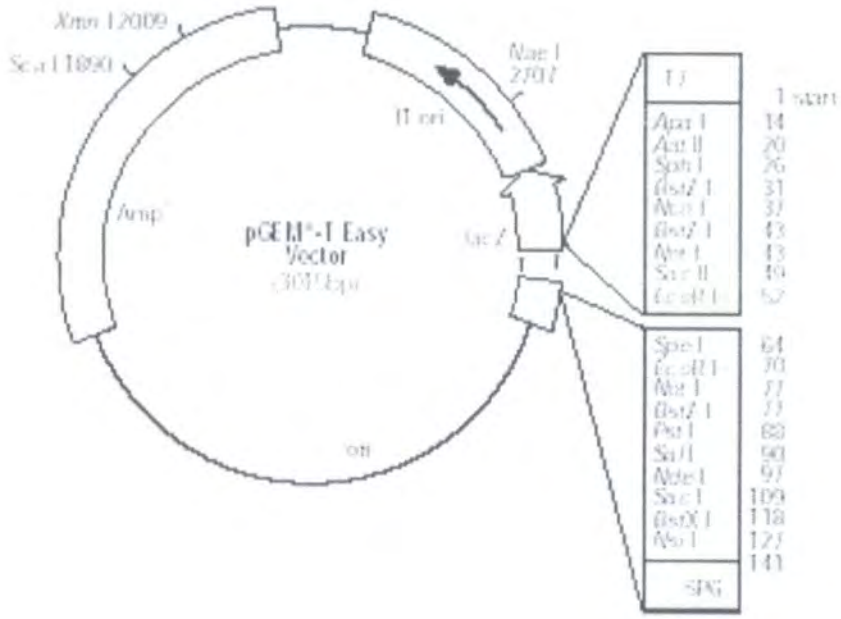

Appendix A. Sequence and reference points of the Promega pGEM®-T Easy vector map.

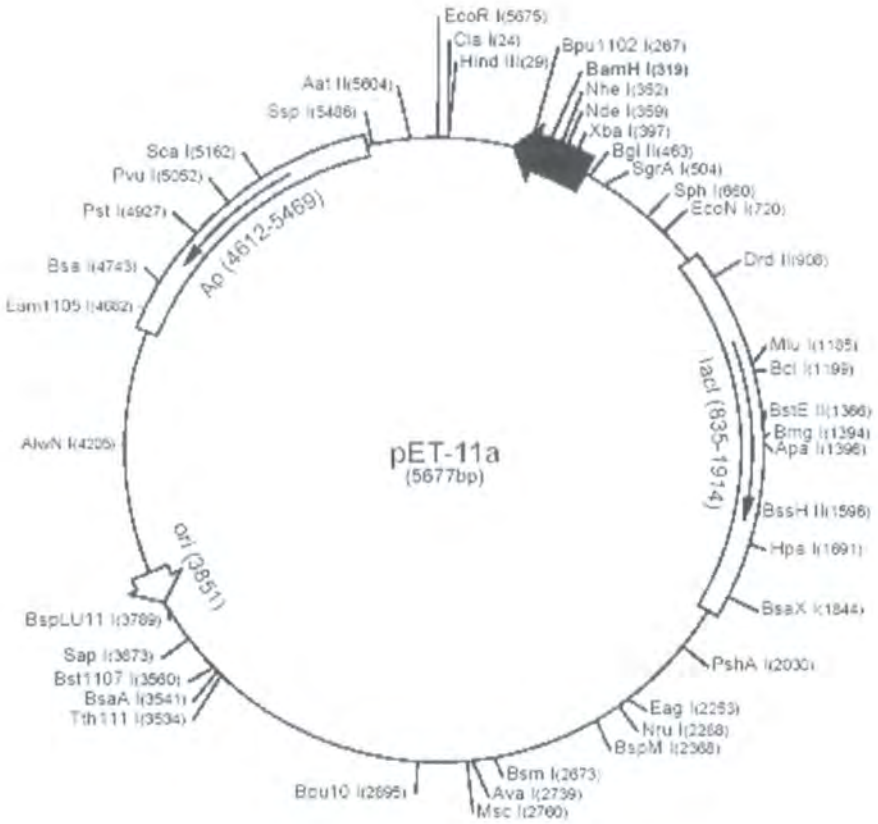

Appendix B. Sequence and reference points of the Novagen pET-11d vector.

The maps for pET-11b, pET-11c and pET-11d are the same as pET-11a (shown) with the following exceptions: pET-11b is a 5676bp plasmid; subtract 1bp from each site beyond *Bam*H I at 319. pET-11c is a 5675bp plasmid; subtract 2bp from each site beyond *Bam*H I at 319. pET-11d is a 5674bp plasmid;the *Bam*H I site is in the same reading frame as in pET-11c. An *Nco* I site is substituted for the *Nde* I site with a net 1bp deletion at position 359 of pET-11c. As a result, *Nco* I cuts pET-11d at 355. For the rest of the sites, subtract 3bp from each site beyond position 360 in pET-11a. *Nde* I does not cut pET-11d.

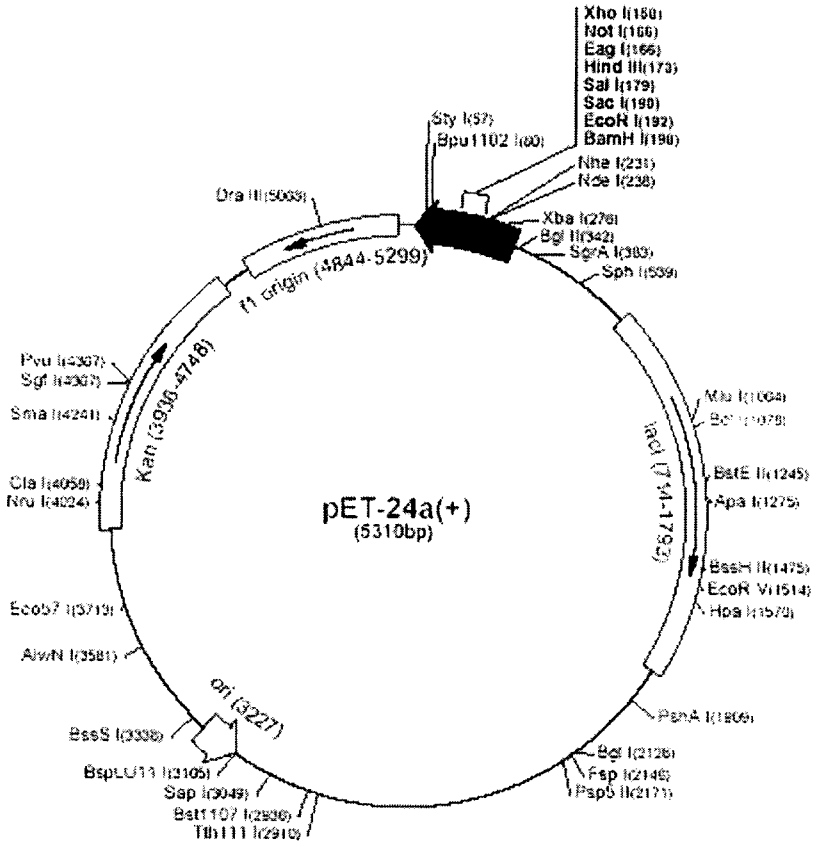

Appendix C. Sequence and reference points of the pET-24a vector map. T7 promoter 311-327, T7 transcription start 310, T7 Tag coding sequence 207-239, Multiple cloning sites (*Bam*H I - *Xho* I) 158-203, His Tag coding sequence 140-157, T7 terminator 26-72, *lacI* coding sequence 714-1793, pBR322 origin 3227, Kan coding sequence 3936-4748, f1 origin 4844-5299.